

A RECONNAISSANCE OF ORGANIC MATURATION AND PETROLEUM
SOURCE POTENTIAL OF PHANEROZOIC STRATA IN NORTHERN YUKON
AND NORTHWESTERN DISTRICT OF MACKENZIE

by

CHRISTINE MARIE LINK

B.Sc., Biology, The University of British Columbia, 1977

B.Sc., Geology, The University of Calgary, 1984

A THESIS SUBMITTED IN PARTIAL FULFILMENT OF
THE REQUIREMENTS FOR THE DEGREE OF
MASTER OF SCIENCE

in

THE FACULTY OF GRADUATE STUDIES

Department of Geological Sciences

We accept this thesis as conforming
to the required standard

THE UNIVERSITY OF BRITISH COLUMBIA

MARCH 1988

© CHRISTINE MARIE LINK, 1988

In presenting this thesis in partial fulfilment of the requirements for an advanced degree at the University of British Columbia, I agree that the Library shall make it freely available for reference and study. I further agree that permission for extensive copying of this thesis for scholarly purposes may be granted by the head of my department or by his or her representatives. It is understood that copying or publication of this thesis for financial gain shall not be allowed without my written permission.

Department of *Biological Sciences*

The University of British Columbia
1956 Main Mall
Vancouver, Canada
V6T 1Y3

Date 88-03-12

ABSTRACT

The level of organic maturation, thermal history and petroleum source potential of Phanerozoic strata in northern Yukon and northwestern District of Mackenzie have been investigated by measurement of vitrinite (% Rorand) and graptolite (% Romax) reflectance, conodont alteration index (CAI) and Rock-Eval pyrolysis. The strata in general have lower maturity levels in southern Mackenzie Delta, Peel Plateau and Eagle Plain than in the Richardson and Ogilvie Mountains.

The level of maturation varies from graptolite reflectance values of 4.0% to 6.5% Romax and CAI values of 3.5 to 5 in Upper Cambrian to Lower Devonian strata whereas vitrinite reflectance ranging from 0.2% to 3.75% Rorand occur in Middle Devonian to Upper Cretaceous strata. Time-averaged numerical modelling of measured maturation gradients (0.10 to 0.32 log Rorand/km) suggest paleogeothermal gradients on the order of 20 to 45°C/km in southern Mackenzie Delta and Peel Plateau, from 10 to 20°C/km in central Eagle Plain and from 20 to 45°C/km adjacent the Richardson and Ogilvie Mountains. The higher maturity levels in mountainous areas reflect higher maturation gradients and, in the Richardson Mountains, deeper burial due to rapid subsidence caused by the foundering of grabens within the Richardson Fault Array. Anomalously high maturation values (0.92% to 1.60% Rorand) measured in Lower Cretaceous strata on the Campbell Uplift are interpreted to reflect high paleoheat flow associated with basement uplift.

Average TOC contents are generally low to moderate (0.1 to 2.0%) but

organic-rich intervals occur throughout the studied succession. TOC values up to 14.5% are present in the Upper Cretaceous Eagle Plain Group, values up to 9.5% occur in the Middle Devonian Canol Formation and Upper Cambrian to Lower Devonian Road River Group and values up to 5.0% are present in the Lower Cretaceous map unit Kwr and Mount Goodenough Formation, the Lower Cretaceous and Jurassic Husky Formation, the Jurassic Porcupine River Formation and the Upper Carboniferous Blackie and Hart River Formations and the Ford Lake Shale. The organic matter (OM) is dominantly type III except for minor amounts of type I and II in Lower Paleozoic strata and a mixture of type II and III in parts of Middle Devonian, Carboniferous, Jurassic and Lower Cretaceous strata.

The quality of organic matter varies significantly (QOM; 0.01 to 6.1 mg HC/g Corg) as a result of variation in organic maturity, the type of OM and, in some cases, migration. Average QOM values are generally low to moderate (0.01 to 1.5 mg HC/g Corg) and, along with low to moderate Hydrogen Index values (<300 mg HC/g Corg), suggest poor to moderate petroleum source potential. Relatively few examples of potential oil prone source rocks occur, but these include parts of the Road River Group, the Hare Indian, Canol, Hart River, Blackie, Mount Goodenough and Arctic Red River Formations, the Ford Lake Shale, unnamed Carboniferous unit and map unit Kwr. Gas prone source rocks comprise parts of the Blackie, Porcupine River, Husky, Mount Goodenough and Arctic Red River Formations and the Bug Creek and Eagle Plain Groups and map unit Kwr. With respect to petroleum generation, Upper Cretaceous strata are generally immature. Lower Cretaceous to Permian strata are immature to

mature, Carboniferous strata are immature to overmature, and Devonian and older rocks are mature to overmature. The timing of hydrocarbon generation from source rocks in the study area varied substantially both laterally and stratigraphically as a result of variations in the timing and magnitude of the maximum depths of burial.

The variation in source rock quality appears to closely reflect the interpreted depositional environment of some of the strata which facilitates the interpretation of regional extent of potential hydrocarbon source rocks.

A correlation of graptolite and vitrinite reflectance, calibrated by conodonts, shows that a graptolite reflectance range of 5% to 6.5% R_{max} (CAI=5) corresponds to a vitrinite reflectance of 4.0% R_{max} . Graptolite organic remains appear to behave similar to bitumen with increasing depth of burial; at higher levels of thermal maturity, graptolite reflectance increases more rapidly than vitrinite reflectance.

TABLE OF CONTENTS

ABSTRACT	ii
LIST OF TABLES	vii
LIST OF FIGURES	ix
ACKNOWLEDGMENT	xvi
I. INTRODUCTION	1
II. REGIONAL GEOLOGY	3
A. TECTONIC ELEMENTS	3
B. STRATIGRAPHY	4
III. PART I. ORGANIC MATURATION OF PHANEROZOIC STRATA IN NORTHERN YUKON AND NORTHWESTERN DISTRICT OF MACKENZIE	12
A. ABSTRACT	12
B. INTRODUCTION	14
C. METHODS	15
1. Vitrinite reflectance	15
2. Conodont alteration index	16
3. Correlation of Thermal Maturity Indicators	17
D. RESULTS	18
1. Stratigraphic (Vertical) Variation in Organic Maturity	18
2. Lateral Variation in Organic Maturity	18
3. Time-temperature Modelling	39
a. Paleogeothermal Gradients	40
b. Thickness of Eroded Section	58
E. DISCUSSION	62
1. Interpretation of Paleogeothermal Gradients	62
2. Interpretation of Maturation Levels	63
3. Anomalous Maturation Levels	64
a. Richardson Mountains	64
b. Campbell Uplift	66
4. Hydrocarbon Generation Models	67
a. Regional Variation in Maturation Levels with Respect to Hydrocarbon Generation	67
b. Timing of Hydrocarbon Generation	72
F. SUMMARY AND CONCLUSIONS	74
IV. REFERENCES	78
V. PART II. PETROLEUM SOURCE POTENTIAL OF PHANEROZOIC STRATA IN NORTHERN YUKON AND NORTHWESTERN DISTRICT OF MACKENZIE	87
A. ABSTRACT	87
B. INTRODUCTION	89

LIST OF TABLES

- TABLE I. Formations and groups comprising the tectono-stratigraphic assemblages in the study area. p. 11
- TABLE II. Comparison of calculated thickness of eroded section using sedimentation rates based on the preserved section, to the amount of eroded section calculated by extrapolation of measured maturation gradients. p. 61
- TABLE III. Measured and calculated parameters derived from Rock-Eval/TOC analysis. p. 92
- TABLE IV. Classification and maturation of various stratigraphic units in the study area. p. 116-130
- TABLE V. Graptolite-bearing samples collected from northern Yukon. p. 200
- TABLE VI. Measured graptolite reflectance in samples collected from measured section of Road River Group, along James River, northern Yukon. p. 213-214
- TABLE VII. Measured graptolite reflectance in samples collected from Road River Group in northern Yukon. p. 215
- TABLE VIII. Measured bitumen reflectance in sections cut perpendicular to bedding. p. 216

TABLE IX. Measured vitrinite reflectance in samples collected from measured section of Canol Formation, along James River in northern Yukon.

p. 217

TABLE X. Conodont alteration index (CAI) determined for samples collected from Road River Group and Canol Formation.

p. 225

LIST OF FIGURES

- FIGURE 1. Index map and physiographic divisions in the area of study. p. 5
- FIGURE 2. Tectonic elements. p. 6-7
- FIGURE 3. Stratigraphic correlation of Cambrian to Tertiary strata in the area of study. p. 8
- FIGURE 4. Maturation gradients for 12 wells in the area of study. p. 19-22
- FIGURE 5. Regional variation in measured maturation gradients in the study area. p. 23
- FIGURE 6. Representative levels of organic maturity at the surface in study area. p. 26-27
- FIGURE 7. Regional maturation patterns of Upper Cambrian to Upper Cretaceous strata. p. 28-38
- FIGURE 8. Burial and maturation history and calculated and measured gradients for strata in Southern Mackenzie Delta. p. 46
- FIGURE 9. Burial and maturation history and calculated and measured gradients for strata in Eastern Peel Plateau. p. 47

- FIGURE 10. Burial and maturation history and calculated and measured gradients for strata in Western Peel Plateau. p. 48
- FIGURE 11. Burial and maturation history and calculated and measured gradients for strata in North-central Eagle Plain. p. 49
- FIGURE 12. Burial and maturation history and calculated and measured gradients for strata in Northwestern Eagle Plain. p. 50
- FIGURE 13. Burial and maturation history and calculated and measured gradients for strata in Eastern Eagle Plain. p. 51
- FIGURE 14. Burial and maturation history and calculated and measured gradients for strata in Southeastern Eagle Plain. p. 52
- FIGURE 15. Burial and maturation history and calculated and measured gradients for strata in Central Eagle Plain. p. 53
- FIGURE 16. Burial and maturation history and calculated and measured gradients for strata in Central Eagle Plain. p. 54
- FIGURE 17. Burial and maturation history and calculated and measured gradients for strata in Central Eagle Plain. p. 55
- FIGURE 18. Burial and maturation history and calculated and measured

- gradients for strata in Northern Eagle Plain. p. 56
- FIGURE 19. Burial and maturation history and calculated and measured gradients for strata in Western Eagle Plain. p. 57
- FIGURE 20. Cross-section through northern Yukon and northwestern District of Mackenzie showing regional maturation pattern with respect to hydrocarbon generation. p. 70
- FIGURE 21. Depth to oil window. p. 71
- FIGURE 22. Rock-Eval logs for 12 wells examined in the study area. p. 96-108
- FIGURE 23. Histograms of total organic carbon (TOC) content of some formations and groups examined in study area. p. 109-112
- FIGURE 24. Modified van Krevelen diagrams (Hydrogen Index (HI) versus Oxygen Index (OI)) for some formations and groups examined in study area. p.113-115
- FIGURE 25. Regional distribution of the average TOC content, the average HC potential and quality of organic matter (QOM), and the degree of organic maturity (DOM) for Road River Group. p. 132-133
- FIGURE 26. Regional distribution of the average TOC content, the average HC

potential and quality of organic matter (QOM), and the degree of organic maturity (DOM) for Ogilvie and Hume Formations.

p. 134-135

FIGURE 27. Regional distribution of the average TOC content, the average HC potential and quality of organic matter (QOM), and the degree of organic maturity (DOM) for Canol Formation.

p. 136-137

FIGURE 28. Regional distribution of the average TOC content, the average HC potential and quality of organic matter (QOM), and the degree of organic maturity (DOM) for Imperial Formation.

p. 138-139

FIGURE 29. Regional distribution of the average TOC content, the average HC potential and quality of organic matter (QOM), and the degree of organic maturity (DOM) for Ford Lake Shale.

p. 140-141

FIGURE 30. Regional distribution of the average TOC content, the average HC potential and quality of organic matter (QOM), and the degree of organic maturity (DOM) for Hart River Formation.

p. 142-143

FIGURE 31. Regional distribution of the average TOC content, the average HC potential and quality of organic matter (QOM), and the degree of organic maturity (DOM) for Mount Goodenough Formation.

p. 144-145

FIGURE 32. Regional distribution of the average TOC content, the average HC potential and quality of organic matter (QOM), and the degree of organic

- maturity (DOM) for Rat River Formation. p. 146-147
- FIGURE 33. Regional distribution of the average TOC content, the average HC potential and quality of organic matter (QOM), and the degree of organic maturity (DOM) for Albian strata (Arctic Red River and Horton River Formations and map unit Kwr). p. 148-149
- FIGURE 34. Regional distribution of the average TOC content, the average HC potential and quality of organic matter (QOM), and the degree of organic maturity (DOM) for Eagle Plain Group. p. 150-151
- FIGURE 35. Present day maturity map of Phanerozoic strata in the study area. p. 153
- FIGURE 36. Locality map, Romax values of graptolites, vitrinite and CAI values of the Road River Group and Canol Formation. p. 197
- FIGURE 37. Measured section along James River, Yukon Territory, $66^{\circ}55'N$, $136^{\circ}15'W$. p. 198-199
- FIGURE 38. Structural features of the graptolite rhabdosome. p. 203
- FIGURE 39. Fragments of graptolites in Road River Group samples, polished surfaces, oil immersion. Sections cut normal to bedding, plane polarized light. p. 204-205

- FIGURE 40. Fragments of graptolites from the Road River Group in sections cut and polished parallel to bedding. p. 206-207
- FIGURE 41. Fragments of Tasmanites in section cut and polished normal to bedding. p. 211
- FIGURE 42. Bitumen in sections cut and polished parallel to bedding. p. 212
- FIGURE 43. Principal reflectance axes measured in graptolites. p. 219
- FIGURE 44. Maturation gradients for stratigraphic sections through the Road River Group and Canol Formation. p. 222
- FIGURE 45. Conodonts recovered from the Road River Group, CAI of 5. p. 226-227
- FIGURE 46. Maximum reflectance in oil of graptolites versus CAI. p. 230
- FIGURE 47. Arrhenius plot of the experimental data of Epstein et al. (1977) and maximum and minimum temperature ranges of conodont samples from the Road River Group in the study area. p. 239
- FIGURE 48. Diagram of thermal history calibrated with maximum vitrinite reflectance in oil. p. 243
- FIGURE 49. Plot of maximum versus minimum reflectance in oil for coal to

graphite, heat affected coal, graptolites and bitumen.

p. 244

ACKNOWLEDGMENT

The author is grateful to the thesis supervisor Dr. R.M. Bustin for direction, advice, support and patience throughout this study. Financial support for this thesis was received from an NSERC grant (A7337) and an EMR research grant to Dr. R.M. Bustin. The author gratefully acknowledges the technical support of the Geological Survey of Canada which provided the use of a petrographic microscope, Rock-Eval instrument and computing facilities and the support of Shell Canada Limited which prepared pellets for vitrinite reflectance measurements. Thanks are also due to Dr. M.A. Barnes and Dr. W.C. Barnes of the University of British Columbia and to Dr. J. Dixon, Dr. F. Goodarzi, Dr. L. Snowdon and many other staff at the Institute of Sedimentary and Petroleum Geology for consultation.

I. INTRODUCTION

Organic geochemical evaluation of sedimentary basins requires identification of potential petroleum source rocks and establishing the degree of organic maturation (DOM). The organic maturation and petroleum source potential of the Phanerozoic succession in the northern Yukon and northwestern District of Mackenzie have been alluded to previously (Hume and Link, 1945; Tassonyi, 1969; Graham, 1973; Martin, 1973; Kunst, 1973; Coté et al., 1975; Pugh, 1983; A.W. Norris, 1985; and D.K. Norris, 1985) but little or no models of thermal history or geochemical data have accompanied these discussions. The present investigation is the first systematic attempt to determine the areal and vertical variation in the degree of organic maturity (DOM), the abundance and type of organic matter, and the petroleum source potential of the Phanerozoic succession in the northern Yukon and northwestern District of Mackenzie.

Microscopic examination of samples combined with organic geochemical analysis can be utilized to assess the origin and hydrocarbon source potential of organic-rich sediments (Espatilié et al., 1977; Hunt, 1979; Durand, 1980; Waples, 1980; Tissot and Welte, 1984; Bustin et al., 1985; and many others). In this study, organic petrography and Rock-Eval pyrolysis are used to determine the DOM and to identify and quantify petroleum source rocks. The regional extent of possible hydrocarbon source rocks and organic facies are determined and, combined with thermal maturity data, to delineate areas of potential hydrocarbon generation. The variation in source rock quality appears to closely reflect the interpreted depositional environment of some of the strata and thus help define

the regional extent of potential hydrocarbon source rocks.

This thesis is divided into three parts. In the first part, the level of organic maturation and thermal history of Phanerozoic strata in the study area are described as determined by measurement of vitrinite reflectance (% Rorand and conodont alteration index (CAI). In the second part, Rock-Eval pyrolysis and organic petrography are used to evaluate the petroleum source rock potential of Phanerozoic strata. In the third part, the utility of graptolites as a measure of thermal maturity in the Lower Paleozoic Road River Group is evaluated by measuring maximum, minimum and random reflectance.

II. REGIONAL GEOLOGY

The study area approximately encompasses the area covered by Operation Porcupine (see Geological Survey of Canada, Map 10-1963) between latitudes 65° N and 69° N and between longitudes 132° W and 139° W (Fig. 1). The regional geology of the area has been summarized by Lerand (1973), Miall (1973) and Balkwill et al. (1983). In addition, the maps of Norris (1981 (a-f); 1982 (a;b)) provide comprehensive summaries of the regional stratigraphy and geology. Depositional environments have been interpreted by various authors (Pugh, 1983; A.W. Norris, 1985; Dixon, 1986; and many others referenced in later sections of this paper) and represent current ideas of regional geology of Phanerozoic strata. Below, the tectonic elements and stratigraphy are briefly summarized.

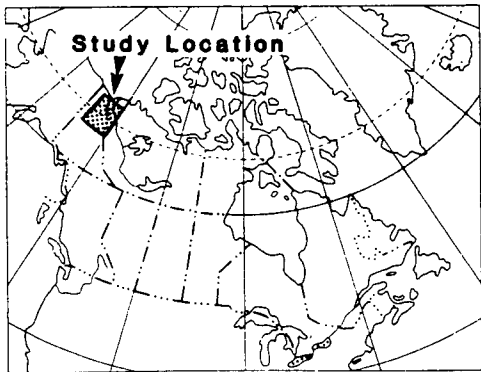
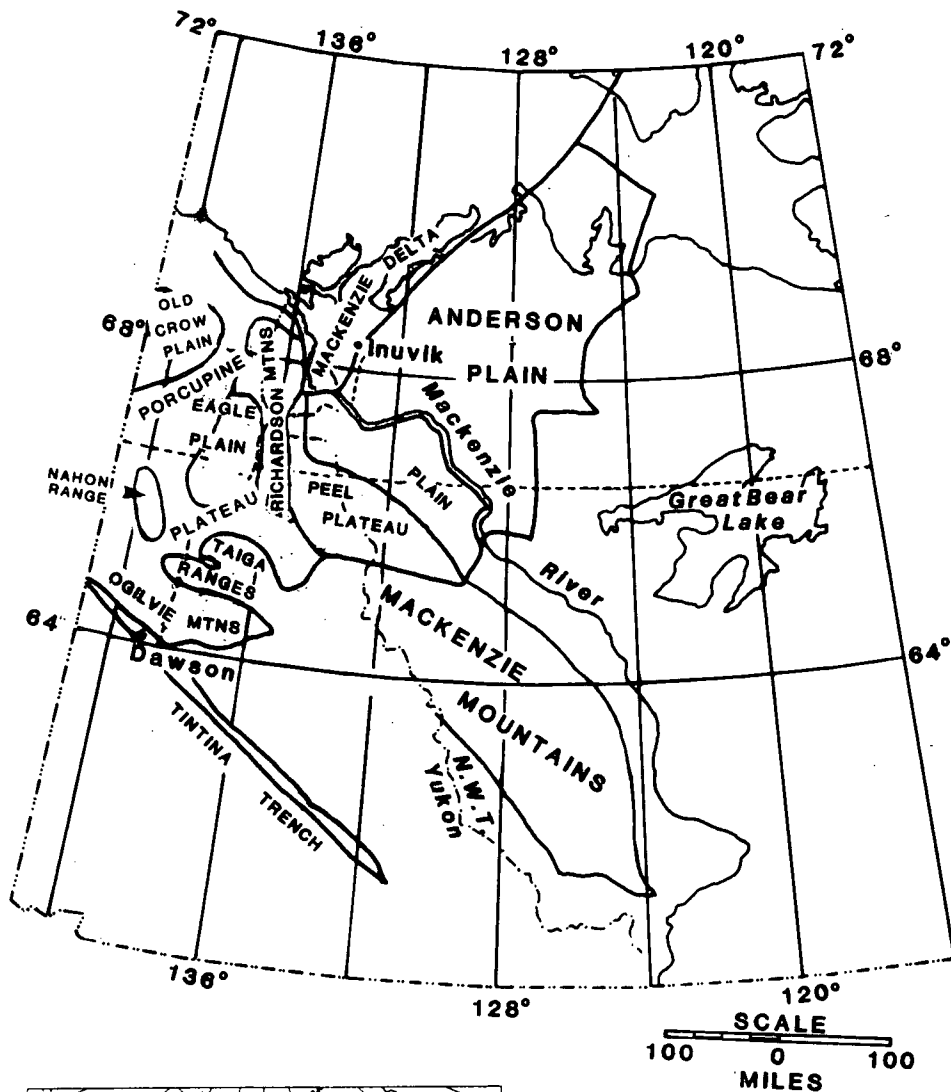
A. TECTONIC ELEMENTS

The study area covers a variety of physiographic divisions (Fig. 1) which roughly coincide with major tectonic elements comprising the Interior Platform and northern Cordilleran Orogenic System (Norris, 1980; Fig. 2). The distribution of pre-Mesozoic and Mesozoic-Tertiary elements reflects an increase in tectonic complexity from east to west and to the southwest (Fig. 2). Many unconformities are present in the stratigraphic succession and attest to prolonged and intermittent tectonic activity (Norris and Yorath, 1981). The Late Devonian to Early Mississippian Ellesmerian orogeny resulted in a regional unconformity at the base of the Mississippian (Norris and Yorath, 1981). The second regional

unconformity in the sedimentary succession represents the Early Cretaceous (Hauterivian) Columbian orogeny (D.K. Norris, 1985). Source areas and depositional basins were redistributed during the Columbian orogeny, which climaxed with the Late Cretaceous to Early Tertiary Laramide orogeny (D.K. Norris, 1985; Dixon, 1986). The Laramide orogeny resulted in major thrust faults and folding in the Ogilvie Mountains as well as normal faulting in the Richardson Mountains and thrusting and folding in the Eagle Fold Belt. The Laramide orogeny in part overprinted and/or rejuvenated older tectonic elements in many areas (Norris and Yorath, 1981).

B. STRATIGRAPHY

The stratigraphic succession in the northern Yukon and northwestern District of Mackenzie comprises an eastward tapering and northward truncated sedimentary wedge. It has an estimated thickness of 7 km at the eastern margin of the Cordilleran region and is more than twice this thickness within the orogen (D.K. Norris, 1985). The stratigraphic correlation of Cambrian to Pleistocene strata in the study area is summarized in figure 3. Pre-Mesozoic stratigraphy has been described by Hume (1954), Tassonyi (1969), Bamber and Waterhouse (1971), Martin (1972), Pugh (1983) and D.K. Norris (1985). Mesozoic and Cenozoic stratigraphy of the study area has been published by Jeletsky (1958, 1960, 1961, 1967, 1972, 1974, 1975), Mountjoy (1967), Mountjoy and Chamney (1969), Young (1971, 1975a, 1975b, 1977, 1978), Young et al. (1976), Sweet (1978) and Dixon (1986).



INDEX MAP

Figure 1. Index map and physiographic divisions in the area of study. Dempster Highway is shown as dashed line. (modified from Norris, 1980.)

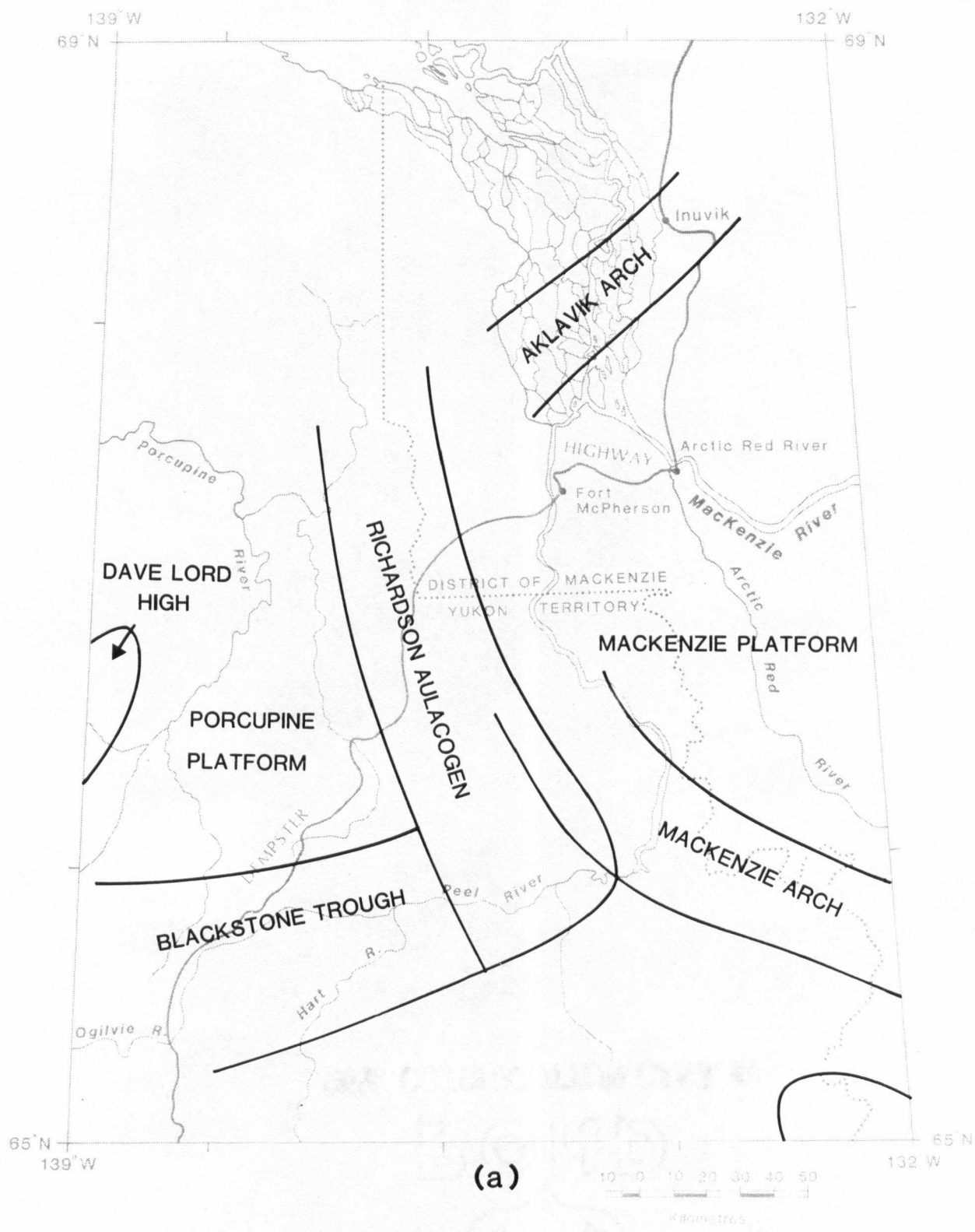
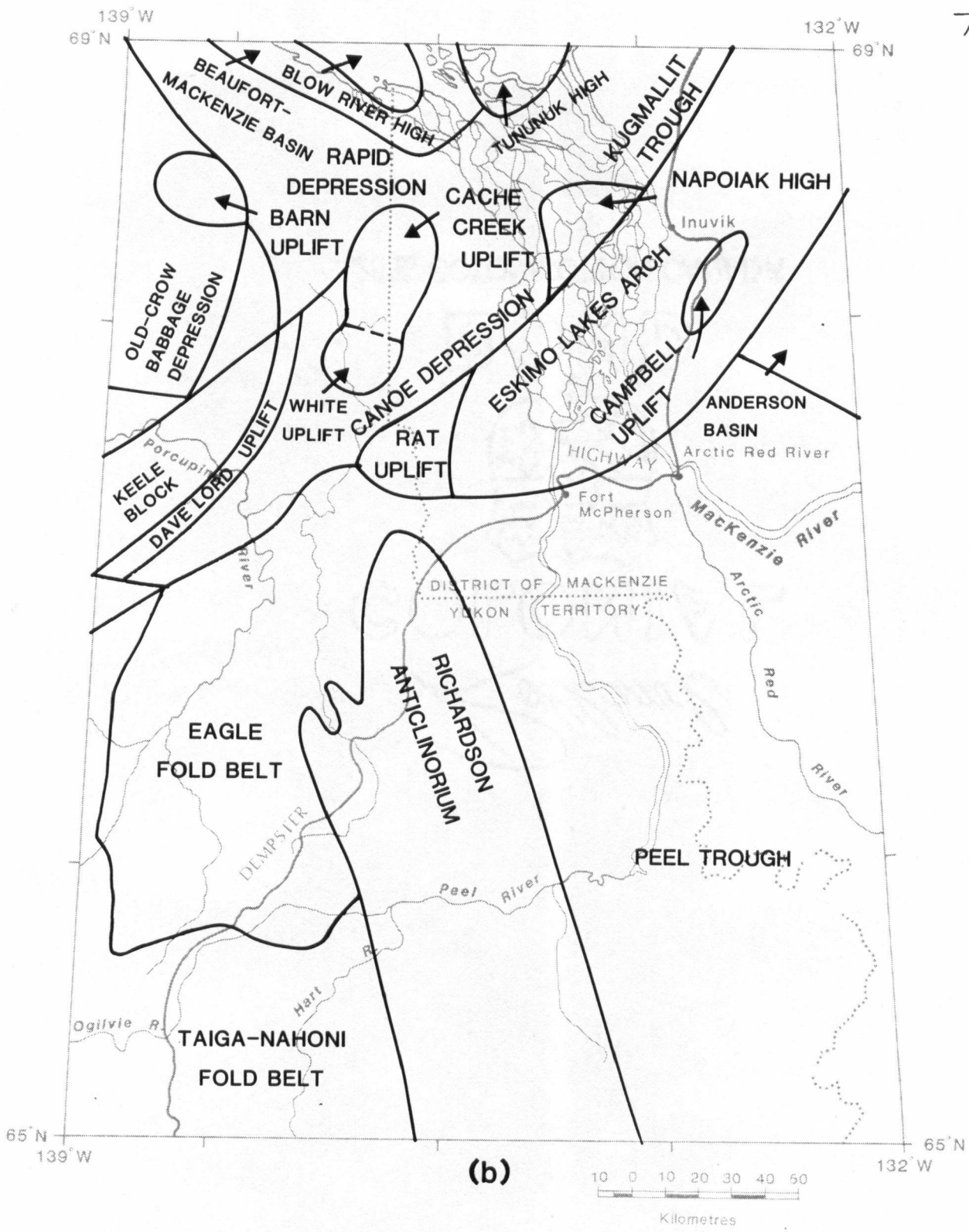


Figure 2. Tectonic elements: a) Pre-Mesozoic tectonic elements (modified from Pugh, 1983.)



b) Mesozoic and Tertiary tectonic elements. (modified from Yorath and Cook, 1981; Norris, 1983.)

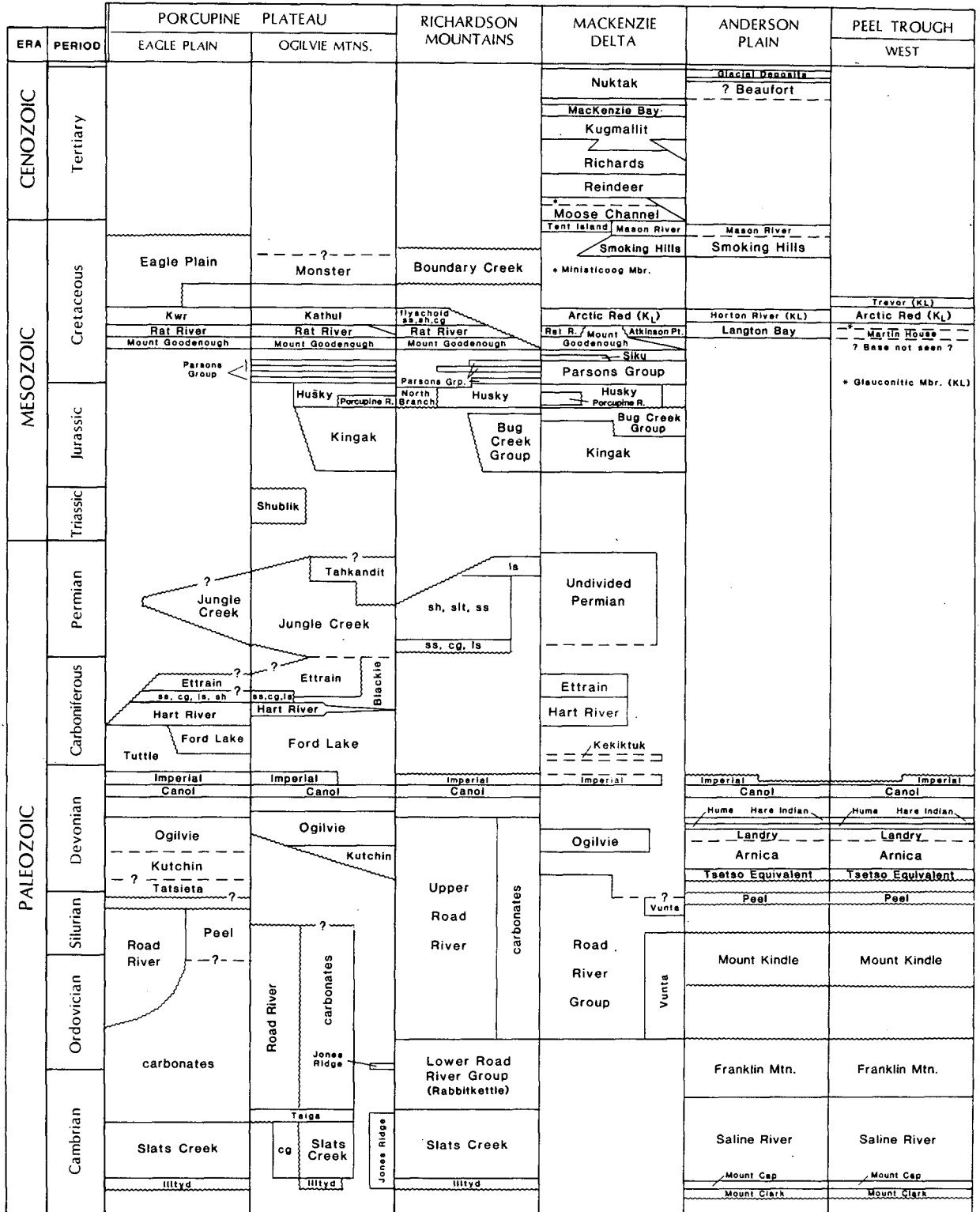


Figure 3. Stratigraphic correlation of Cambrian to Tertiary strata in the area of study. Tectonic divisions correspond to tectonic elements indicated in figure 2. (modified from Norris, 1983; Pugh, 1983; Dixon, 1986; Yorath, unpublished.)

The stratigraphic succession in the northern Yukon and northwestern District of Mackenzie is best described on a regional scale by tectono-stratigraphic assemblages (Table I) because the stratigraphic nomenclature is both complicated and the study area encompasses several tectonic elements. The oldest sequence examined in this study is the Upper Cambrian to Lower Devonian EDM assemblage. The carbonate platform of the EDM sequence is interrupted in the Richardson anticlinorium by the north-trending Richardson Trough (D.K. Norris, 1985) and, in the Ogilvie Mountains, by the west- and southwest-trending Blackstone Trough (A.W. Norris, 1985). These troughs mark the site of shale and limestone deposition from Late Cambrian to Early Devonian (Richardson Trough) and from late Early or early Mid-Ordovician to Early Devonian (Blackstone Trough). The DJF assemblage (Table I) includes the Middle Devonian to Upper Jurassic succession consisting of shelf carbonates with associated clastics in the lower part of the sequence (Devonian, Carboniferous and Permian). Epicontinental clastic rocks predominate in the Jurassic part of the sequence. The DJF assemblage is conformably overlain by Lower Cretaceous strata of the JKK assemblage, which consists primarily of clastic shelf deposits. The regional unconformity in the middle of the JKK assemblage represents the Columbian orogeny (D.K. Norris, 1985). The JKK assemblage is in turn unconformably overlain by Upper Cretaceous strata of the KA assemblage, which mark the beginning of gradual northward progradation of shoreline-delta sediments from Late Cretaceous to Recent. By Maastrichtian time, most sedimentation in the northern Yukon and northwest District of Mackenzie was limited to the Beaufort Sea continental margin (Dixon, 1986). The absence of significant Tertiary sedimentation in southern parts of the study area is important for interpretation

of maturation levels and paleogeothermal gradients as discussed later.

Table I. Formations and groups comprising the tectono-stratigraphic assemblages in the study area. Assemblages after Geological Survey of Canada, Map 1505A (Tipper et al., 1981).

EDM: Hare Indian, Hume, Ogilvie, Arnica, Landry, Gossage, Tatsieta, Tsetso-equivalent, Peel, Mount Kindle, Franklin Mountain, Road River Group, Vunta, Taiga, Jones Ridge, Slats Creek, Iltyd.

DJF: Bug Creek Group, Kingak, Husky, North Branch, Shublik, Tahkandit, Jungle Creek, Ettrain, Blackie, Hart River, Ford Lake Shale, Tuttle, Kekiktuk, Imperial, Canol.

JKK: unit Kwr (Eagle Plain Formation), Arctic Red River, Kathul, Horton River, Langton Bay, Martin House, Sans Sault, Trevor, Rat River, Mount Goodenough, Parsons Group.

KA: Monster, Boundary Creek, Smoking Hills, Mason River, Moose Channel, Tent Island, Eagle Plain.

III. PART I. ORGANIC MATURATION OF PHANEROZOIC STRATA IN NORTHERN YUKON AND NORTHWESTERN DISTRICT OF MACKENZIE

A. ABSTRACT

The level of organic maturation and thermal history of the Phanerozoic sedimentary sequence in the northern Yukon and northwestern District of Mackenzie has been investigated by measurement of vitrinite reflectance (% Rorand) and conodont alteration index (CAI). Maturity in coeval strata is generally lower in southern Mackenzie Delta, Peel Plateau and Eagle Plain than in the Richardson and Ogilvie Mountains. The strata are immature to overmature and maturation increases laterally with structural complexity.

Upper Cambrian to Middle Devonian strata have CAI values of 3.5 to 5 in the Richardson and Ogilvie Mountains. The degree of organic maturity (DOM) at the base of Middle Devonian (Givetian) strata varies laterally from 0.79% to 3.75% Rorand whereas the regional variation in DOM at the base of Upper Devonian strata ranges from 0.80% to 2.13% Rorand. Reflectance values vary laterally from 0.50% to 1.69% Rorand at the base of Carboniferous strata and range from 0.24% to 1.39% Rorand at the base of Lower Cretaceous strata. In Eagle Plain, the DOM of Upper Cretaceous strata ranges regionally from 0.38% to 0.53% Rorand. The higher maturity levels in mountainous areas reflect higher maturation gradients and, in the Richardson Mountains, deeper burial due to rapid subsidence caused by the foundering of grabens within the Richardson Fault Array. Anomalously high maturation values (0.92% to 1.60% Rorand) measured

in Lower Cretaceous strata on the Campbell Uplift are interpreted to reflect high paleoheat flow associated with basement uplift.

Time-averaged numerical modelling of the measured maturation gradients suggest paleogeothermal gradients on the order of 20 to 45°C/km in southern Mackenzie Delta and Peel Plateau, from 10 to 20°C/km in central and western Eagle Plain and 20 to 45°C/km towards the Richardson and Ogilvie Mountains. The low paleogeothermal gradients calculated from parts of Eagle Plain are considered to reflect low paleoheat flow and/or rapid Late Cretaceous sedimentation and uplift such that an equilibrium geothermal gradient never existed. The thickness of eroded section in the study area varies from 0.7 to 4.7 km based on interpretation of measured maturation gradients. Such values are consistent with rates of subsidence and uplift estimated from the ages and thicknesses of preserved section in the study area. In Peel Plateau, approximately 1.7 km of post-Upper Devonian section has been eroded. In eastern Eagle Plain, 2.6 to 2.8 km of post-Carboniferous overburden has been removed whereas in western Eagle Plain, up to 4.7 km of coeval strata has been eroded. In northwestern Eagle Plain, about 3.5 km of post mid-Cretaceous section has been eroded which is almost three times the amount of post mid-Cretaceous overburden which has been removed in southern Mackenzie Delta (1.1 km). Estimates of the eroded Upper Cretaceous section vary significantly from central to northern Eagle Plain (0.7 to 3.4 km).

Interpretation of burial and thermal history diagrams indicates the DOM required for hydrocarbon generation for Devonian strata was attained in the Late

Devonian to Early Carboniferous in Peel Plateau but not until Late Carboniferous to Permian in Eagle Plain. Devonian strata left the oil window during the Carboniferous to Early Tertiary in most parts of the study area. Carboniferous and Permian strata entered the oil window in Late Carboniferous to Triassic time in southern Eagle Plain but not until the Late Cretaceous to Early Tertiary in northwestern and eastern Eagle Plain. In western Eagle Plain, the Carboniferous sequence exited the oil window during the Late Cretaceous. Carboniferous and Permian strata are immature with respect to hydrocarbon generation in the central Eagle Plain, due to low paleogeothermal gradients and shallow burial depths. Lower and Upper Cretaceous strata in southern Mackenzie Delta, Peel Plateau and most of Eagle Plain generally have not entered the oil window whereas in the northwestern Eagle Plain, Lower Cretaceous strata entered the oil window in Late Cretaceous to Early Tertiary time during or just after they reached their maximum depth of burial.

B. INTRODUCTION

Knowledge of the degree and timing of maturation of organic matter is important in hydrocarbon exploration. In particular, modelling of thermal history provides details of the timing of hydrocarbon generation relative to the tectonic evolution of a sedimentary succession. In the northern Yukon and northwestern District of Mackenzie a thick sequence of Upper Cambrian to Upper Cretaceous strata is preserved. These strata crop out along the Dempster Highway and occur at depths greater than 3100 m. Aside from hydrocarbon exploration in the early 1920's (Hume and Link, 1945; Tassonyi, 1969) and renewed interest in the

1960's (Graham, 1973; Martin, 1973; Kunst, 1973), the area has received little study. The present investigation is the first systematic attempt to determine the areal and vertical variation in the degree of organic maturity (DOM) of the Phanerozoic succession in the northern Yukon and northwestern District of Mackenzie. In this study, a regional framework of maturity data is established, incorporating some 240 field and 818 well cuttings samples.

This study must be considered reconnaissance in nature because it is the first attempt to investigate the thermal maturation of Phanerozoic strata in the study area, and because of the large geographic area, complex geologic history and various tectonic elements. It is hoped that this research will provide working models that can be modified as further study warrants.

C. METHODS

Vitrinite reflectance and conodont alteration index (CAI) were determined from 818 well cuttings samples collected from 12 wells and from 240 outcrop samples along the Dempster Highway.

1. Vitrinite reflectance

The DOM of all post-late Silurian samples in this study was determined by vitrinite reflectance methods (I.C.C.P., 1971). Cuttings samples were sieved and the < 2 mm (10 mesh) portion was washed to remove water-soluble drilling mud contaminants prior to crushing. Outcrop and well cuttings samples were crushed and pulverized with a centrifugal grinding mill to approximately 170 μm

(80 mesh) sized particles. A portion of the pulverized sample was used to prepare organic concentrates for vitrinite reflectance measurements. Pellets were prepared from whole-rock samples and demineralized samples from outcrop while only demineralized samples were utilized from well cuttings. Both whole-rock samples and organic concentrates were mounted in cold-setting polyester resin, covered with protective plastic caps and stored in argon gas to prevent oxidation prior to analysis.

The mean random reflectance in oil ($n=1.518$ at 546 nm, polarizer out) was measured and recorded with a computerized Leitz® microscope (orthoplan M.P.V. II). The mean random reflectance (% Rorand) was measured rather than the mean maximum reflectance (% Romax) because: a) the Rorand method is faster inasmuch as rotation of the stage is not required; and b) smaller particles can be measured because accurate stage centring is not required (see Davis, 1978 for a discussion of these methods). Other studies (e.g., England and Bustin, 1986) have shown no significant difference between Rorand and Romax for vitrinite with a level of thermal maturity less than 3% Rorand.

Mean random reflectance was established by averaging up to 50 readings. Each sample data set was analyzed statistically.

2. Conodont alteration index

Conodont alteration index (CAI) is a useful thermal maturity indicator for Pre-Devonian rocks and in post-Late Silurian to Triassic carbonates where

vitritine is rare or absent (Epstein et al., 1977; Harris, 1979). Eighty outcrop samples were collected from Cambrian to Permian strata for conodont extraction. Samples were sieved and the > 0.71 mm (+24 mesh) portion was weighed. Samples ranging in weight from 70 to 2000 grams were dissolved in dilute (10%) acetic or formic acid, depending on the lithology. Conodonts were isolated from the 74 to 2000 μm (-10 to +200 mesh) fraction of the residues by standard tetrabromoethane heavy-liquid and hand picking techniques. The conodont color was then established by using a standard binocular microscope in conjunction with a visual color comparison (Epstein et al., 1977) with a set of standards.

3. Correlation of Thermal Maturity Indicators

In order to relate the maturity measurements made using vitritine reflectance and CAI, maturity boundaries with respect to hydrocarbon generation (immature, mature and overmature) are utilized to describe the DOM. The limits for maturity boundaries are adopted from the summary of Bustin et al. (1985). Immature conditions are defined by vitritine reflectance values $< 0.61\%$ Rorand and CAI < 1.5 whereas the mature stage is defined by vitritine reflectance values ranging from 0.61% to 1.35% Rorand and CAIs ranging from 1.5 to 3. Reflectance values $> 1.35\%$ Rorand and CAI values > 3 indicate overmature conditions.

D. RESULTS

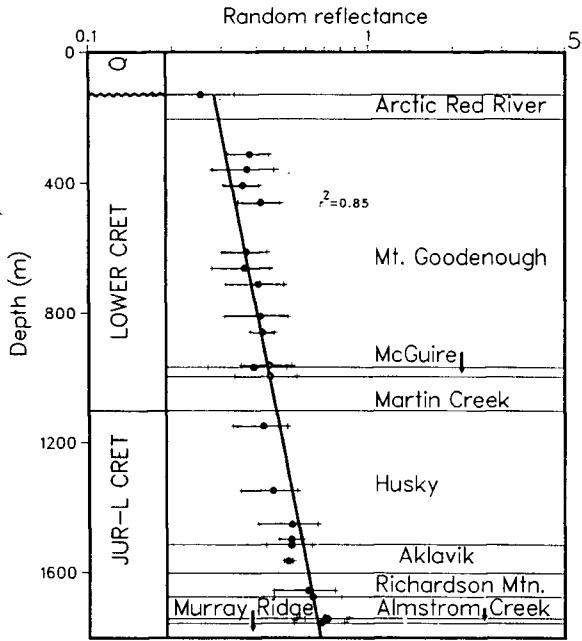
1. Stratigraphic (Vertical) Variation in Organic Maturity

The vertical variation in maturity was determined for 9 wells in Eagle Plain, 2 wells in Peel Plateau and one well in southern Mackenzie Delta. Maturity gradients were not determined from outcrop data due to the lack of stratigraphically thick continuous exposures. The measured maturation gradients best fit a log (reflectance) linear (depth) relationship (Fig. 4). Maturation gradients determined from the first order regression line drawn for each profile vary from 0.10 log Rorand/km to 0.29 log Rorand/km in Eagle Plain (Fig. 5). In Peel Plateau, the measured gradients are about 0.32 log Rorand/km whereas in southern Mackenzie Delta, a slightly lower gradient (0.23 log Rorand/km) was obtained (Fig. 5). A maturation gradient measured at the I-50 well on the west side of Peel Plateau (Fig. 4c) is composed of two segments, an upper shallower gradient and a steeper lower segment. A gradient could not, however, be calculated for the upper segment due to a poor fit of the regression line ($r^2 = 0.47$).

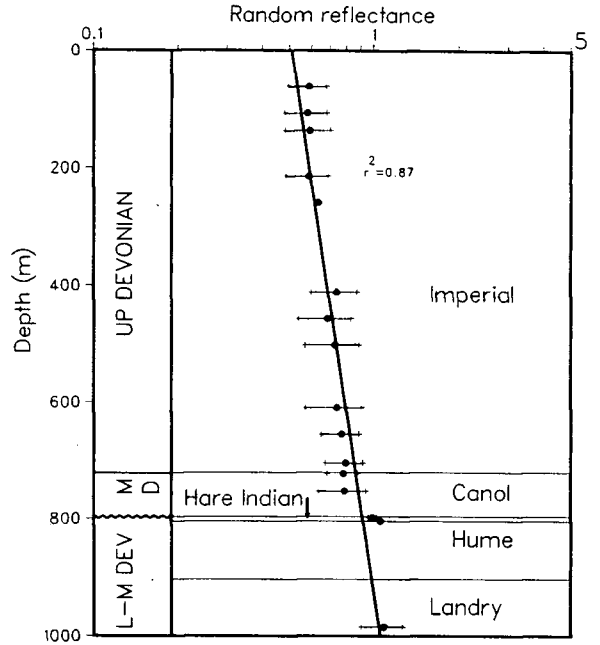
2. Lateral Variation in Organic Maturity

In this section the lateral variation in organic maturity for specific stratigraphic horizons are documented.

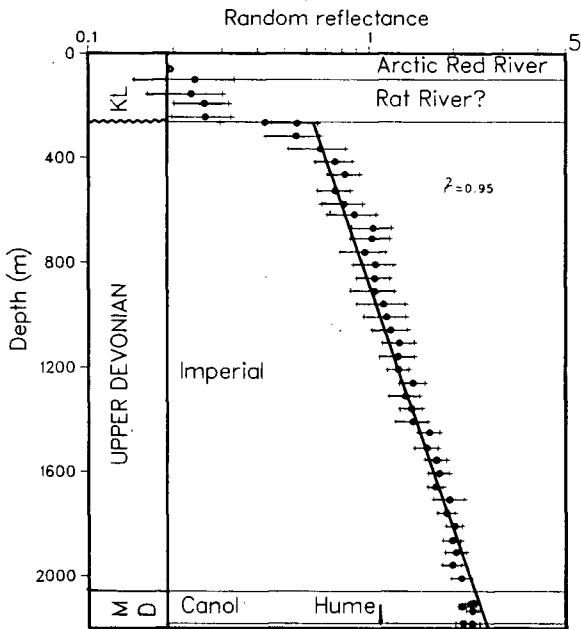
Figure 4. Maturation gradients for 12 wells in the area of study. Location of wells are shown in figure 6 and well names are identified on each plot. Regression lines: $\log R_{orand}/km$. r^2 value is goodness of fit of regression line. Standard deviation bar is shown for samples for which more than one reflectance measurement was made. Abbreviations for ages of strata: Q=Quaternary; CRET=Cretaceous; KL=Early Cretaceous; J, JUR=Jurassic; P=Permian; C, CAR= Carboniferous; D, DEV=Devonian; CAM=Cambrian; L, LWR=Lower; L-M=Lower to Middle; M=Middle; UP=Upper; KL (Albian) is equivalent to map unit Kwr.



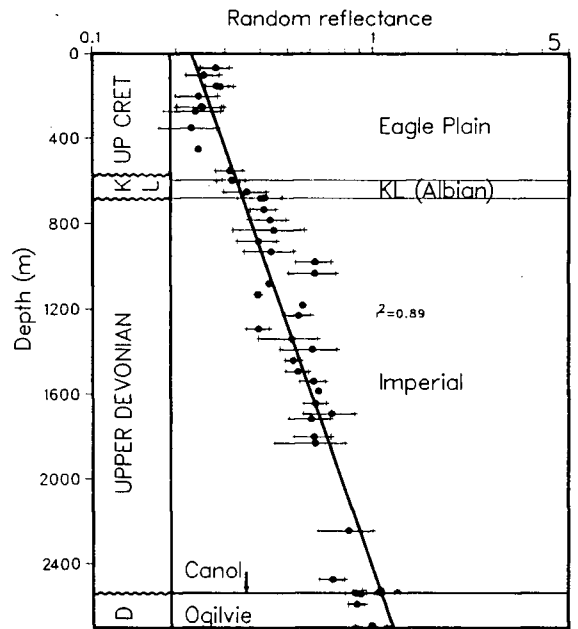
Shell Aklavik A-37 (a)
 Depth=4408(log Ro)+2559



Shell Tree River E. H-57 (b)
 Depth=3147(log Ro)+923

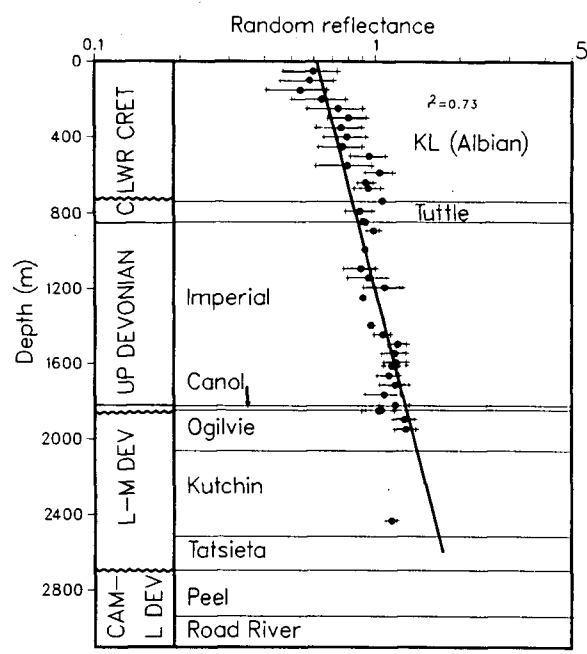


IOE Stony I-50 (c)
 Depth=3096(log Ro)+895

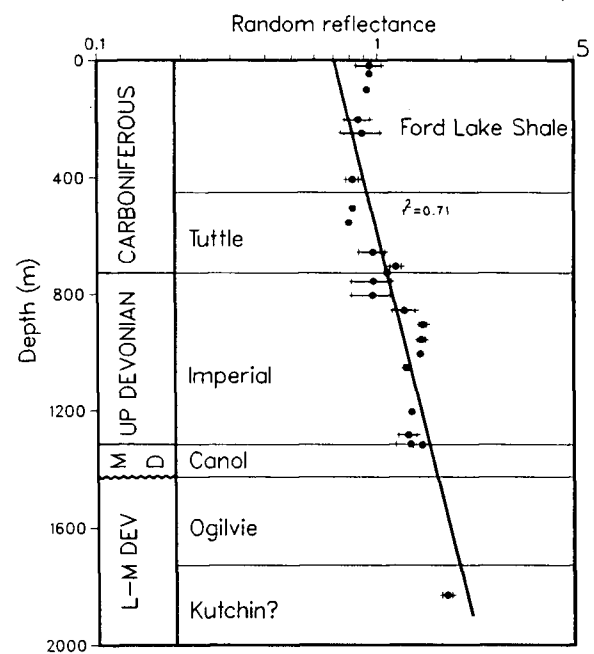


SOBC Shaeffer Creek 0-22 (d)
 Depth=3754(log Ro)+2420

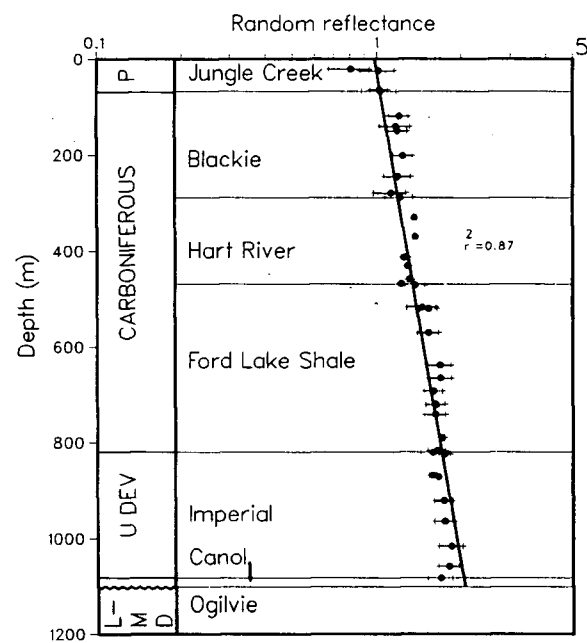
- a) Southern Mackenzie Delta.
- b) Eastern Peel Plateau.
- c) Western Peel Plateau.
- d) North-central Eagle Plain.



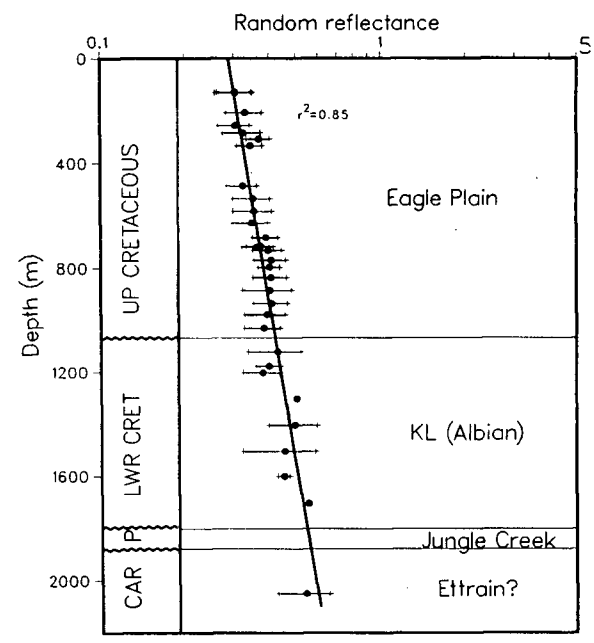
Western Minerals N. Hope N-53
 Depth=5686(log Ro)+1205 (e)



Socony Mobil WM S. Tuttle N-05
 Depth=3883(log Ro)+592 (f)

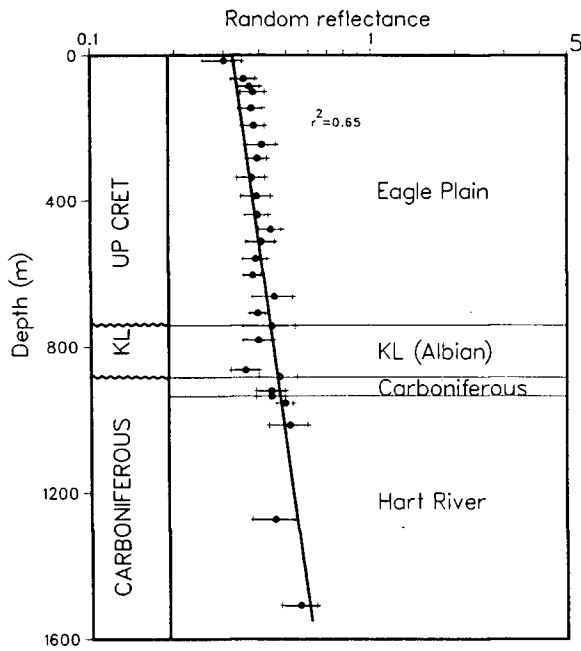


SOBC Blackstone YT D-77
 Depth=3403(log Ro)+31 (g)

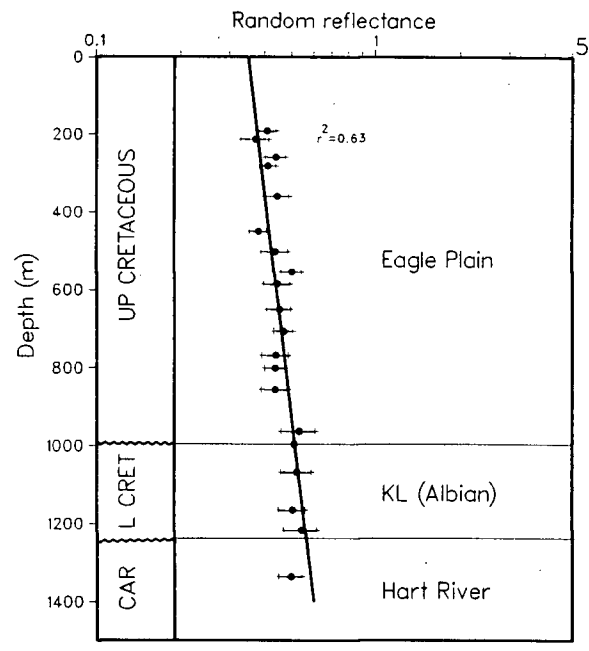


Murphy Mesa BP S. Whitestone N-58
 Depth=6494(log Ro)+3508 (h)

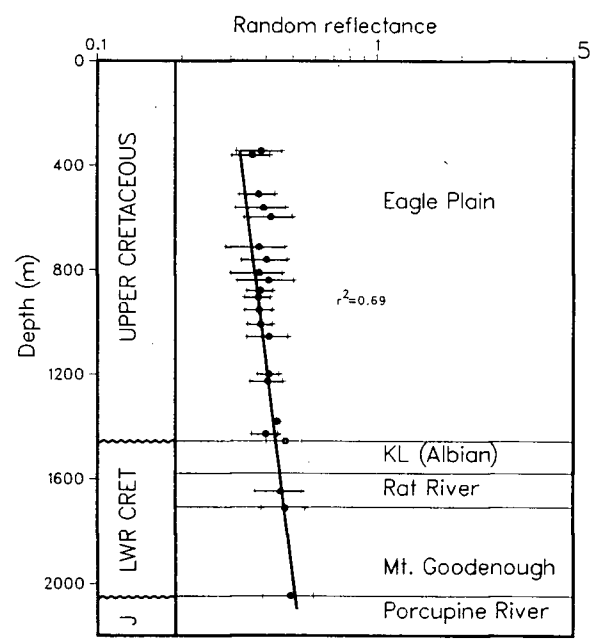
- e) Northwestern Eagle Plain.
- f) Eastern Eagle Plain. The interval indicated by the Ford Lake Shale and Tuttle Formation is now considered to be part of the Imperial Formation (Snowdon, 1987).
- g) Southeastern Eagle Plain.
- h) Central Eagle Plain.



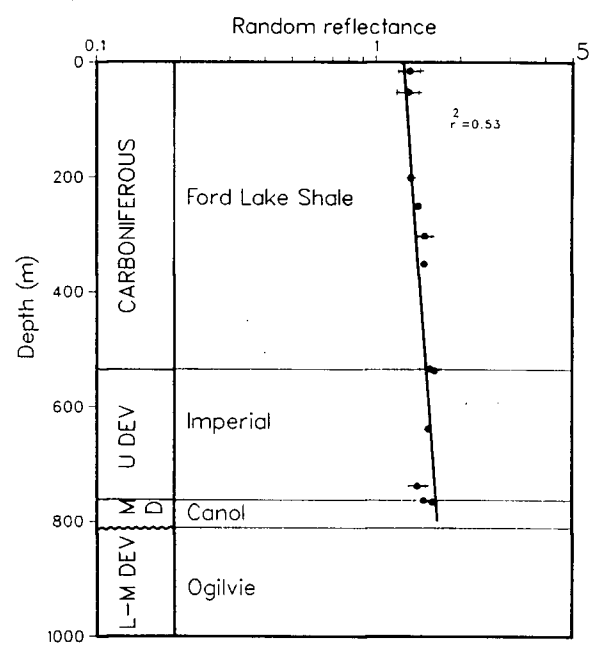
Canoe River E. Chance C-18
 Depth=5591(log Ro)+2751 (i)



Canoe River Chance J-19
 Depth=5898(log Ro)+2705 (j)



Chevron SOBC Whitefish J-70
 Depth=10294(log Ro)+5046 (k)



Socony Mobil WM N. Cathedral B-62
 Depth=6488(log Ro)-636 (l)

- i) Central Eagle Plain.
- j) Central Eagle Plain.
- k) Northern Eagle Plain.
- l) Western Eagle Plain.

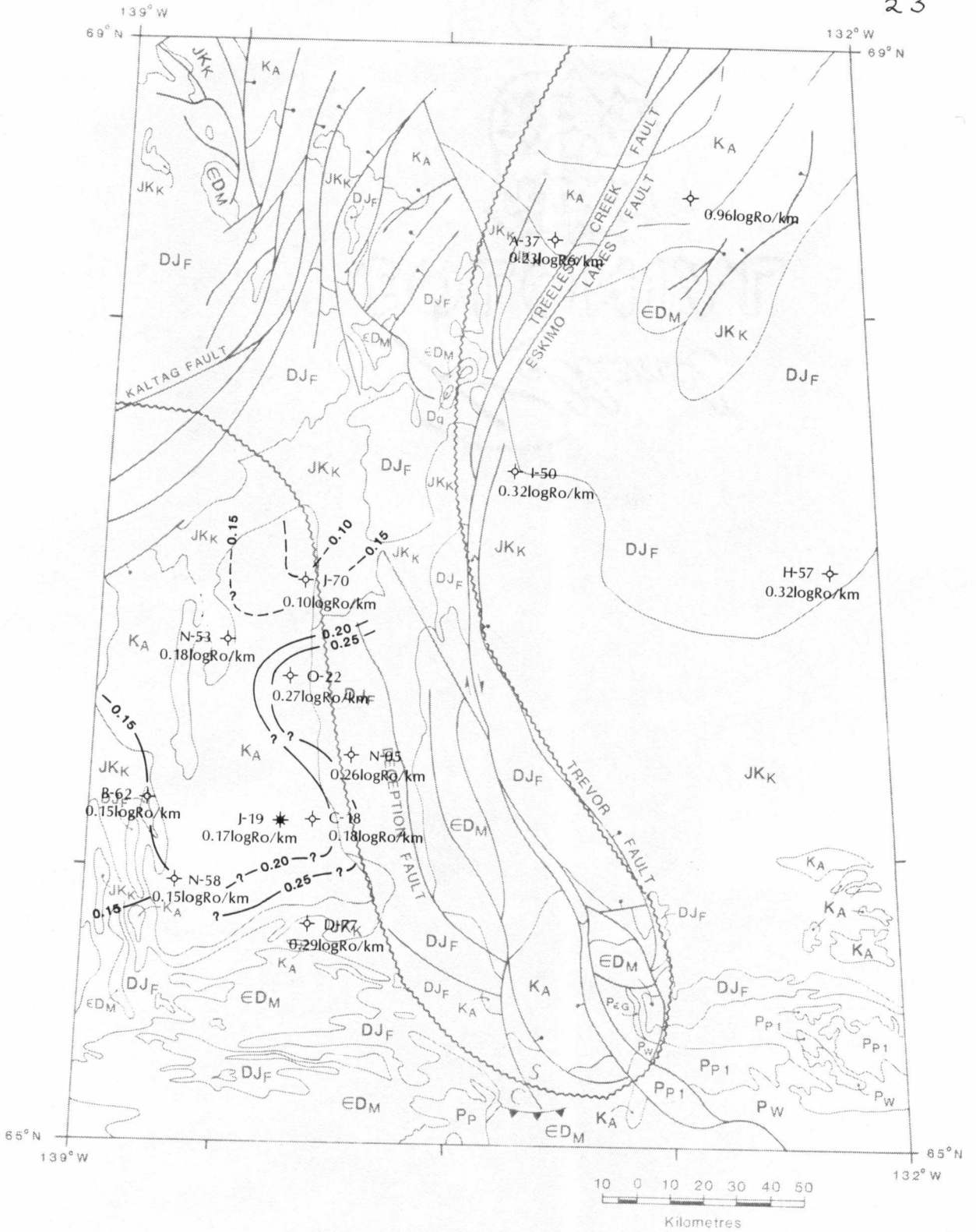


Figure 5. Regional variation in measured maturation gradients in the study area. Contour interval=0.05 log Rorand/km.

Because the northern Cordilleran Orogen is characterized by a limited lateral continuity of stratigraphic units and structural elements, it is difficult to interpret maturation patterns laterally over any distance, especially where sample density is low. Thus, it must be emphasized that the interpretations presented here are based on limited data and the isomuration lines may change significantly as more data become available.

In figures 6 and 7 representative DOMs in the study area are plotted. For additional control, the calculated maturation gradients (Fig. 4) were used to predict maturation levels. Appendix A (on file in geology department, UBC) summarizes sample descriptions for each outcrop location and Appendix B (on file in geology department, UBC) contains CAI measurements and histograms and statistical data for reflectance measurements made on each sample.

The oldest strata examined in the study area, the Upper Cambrian to Lower Devonian Road River Group, are overmature (CAI values ranging from 4.5 to 5) in the Richardson and Ogilvie Mountains (Fig. 7a). The DOM at the base of the Road River Group calculated from maturation gradients (Fig. 4) indicates an increase in maturation from north (2.22% Rorand) to south (6.01% Rorand) in Eagle Plain. The Road River Group is less mature (1.01% Rorand) in southern Mackenzie Delta, based on the maturation gradient measured at the A-37 well.

The DOM of Devonian strata (Hume, Canol and Imperial Formations) increases from east to west in Peel Plateau (e.g., 0.80% to 2.13% Rorand for the Imperial Formation; Figs. 7b-d). The DOM of the Canol and Imperial Formations

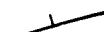
progressively increases from the central part of Eagle Plain to the east, west and south (Figs. 7c and d). Both the Canol and Imperial Formations are overmature in the Richardson and Ogilvie Mountains (1.76% to 3.75% Rorand, CAI=5). CAI values of 4.5 to 5 were measured in the Middle Devonian Gossage Formation which crops out on the Campbell Uplift in the northwestern corner of Anderson Plain (Fig. 7b). In Eagle Plain, the DOM of the Early to Middle Devonian Ogilvie Formation increases from north to south (0.99% to 2.30% Rorand) and towards the Ogilvie Mountains (CAI=3.5 to 5; Fig. 7b).

The DOM of Carboniferous strata of the Ford Lake Shale (0.88% to 1.69% Rorand; Fig. 7e) and Hart River (0.50% to 1.22% Rorand; Fig. 7f) Formations increases from north to south in Eagle Plain.

The DOM of Lower Cretaceous strata of the Mount Goodenough, Rat River and Arctic Red River Formations increases from east to west in Peel Plateau, based on the limited data available (e.g., 0.44% to 0.73% Rorand for the Mount Goodenough Formation; Figs. 7g, h and i). In the Richardson Mountains, the DOM increases rapidly west of the Treeless Creek Fault (e.g., 0.45% to 1.39% Rorand for Rat River Formation). In Eagle Plain, the DOM of Albian strata increases from east to west (Fig. 7i) with reflectance values ranging from 0.41% to 1.10% Rorand at the base of the Albian succession.

Figure 6. Representative levels of organic maturity at the surface in study area. Maturation data from published literature are plotted for comparison. Sources: a. Uyeno (Read, in press); b. Nowlan (Read, in press); c. Goodarzi and Norford (1985); d. Norris and Cameron (1986); e. Utting (Read, in press); f. Ricketts (1985); g. Cameron et al. (1986); h. Young (1975a). Base map modified from Tipper et al. (1981). Formations and groups comprising tectono-assemblages (e.g. EDM) are summarized in table I. Line A-B denotes line of section of figure 20. Scale is the same as figure 5.

LEGEND

-  Assemblage contact (approx.)
-  Fault with downthrown side indicated by solid circle
-  Dextral transcurrent fault (approx., assumed)
-  Late Ordovician–Early Silurian carbonate (C)–shale (S) boundary
-  Borehole (dry and abandoned, suspended oil and gas)

Data from this study	Published data
5 ■ Conodont alteration index	3.0 □ C.A.I.
1.2 ◆ Vitrinite reflectance (random)	0.7 ◇ Vitrinite reflectance
5.6 ▲ Graptolite reflectance	2 * Thermal Alteration Index

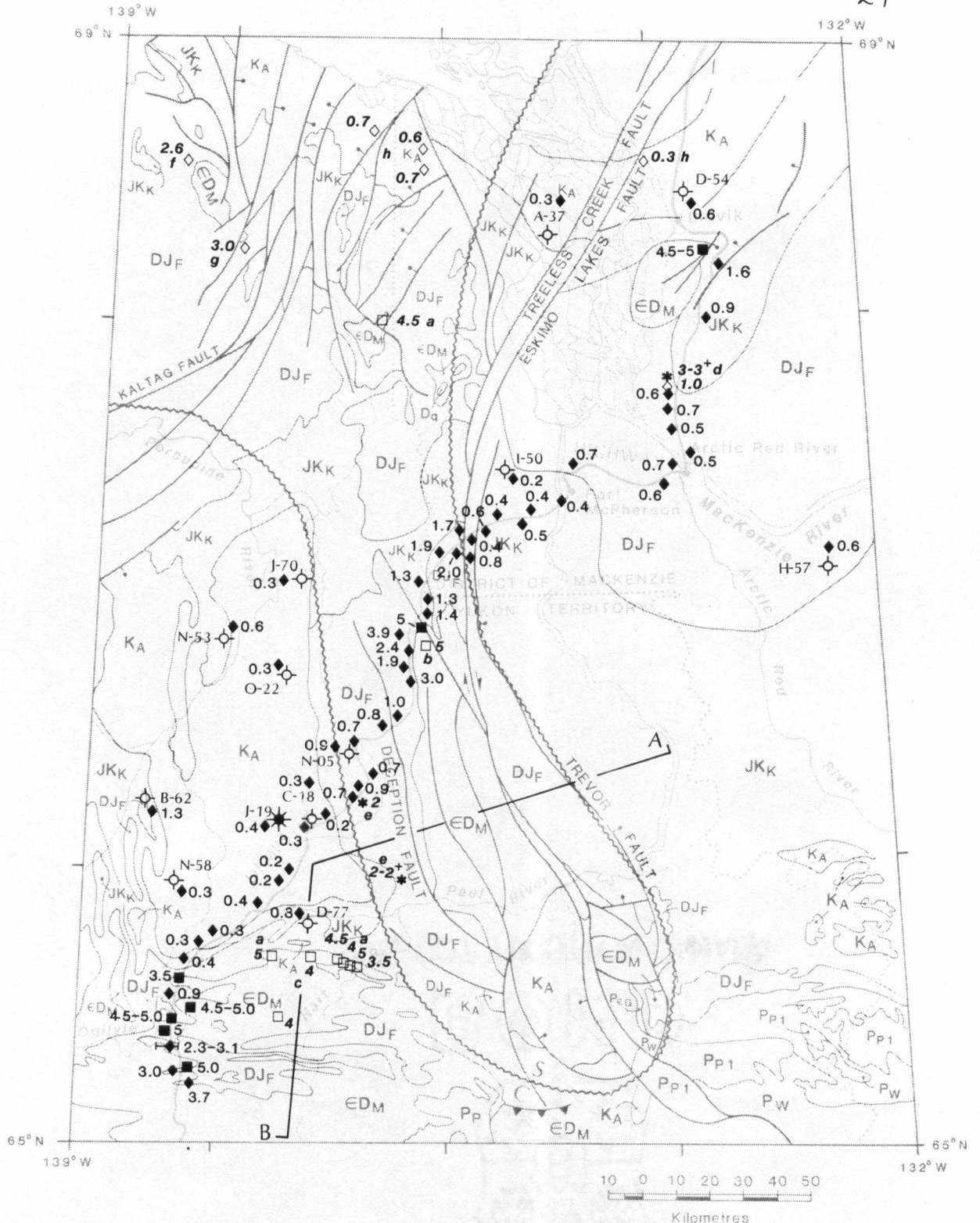
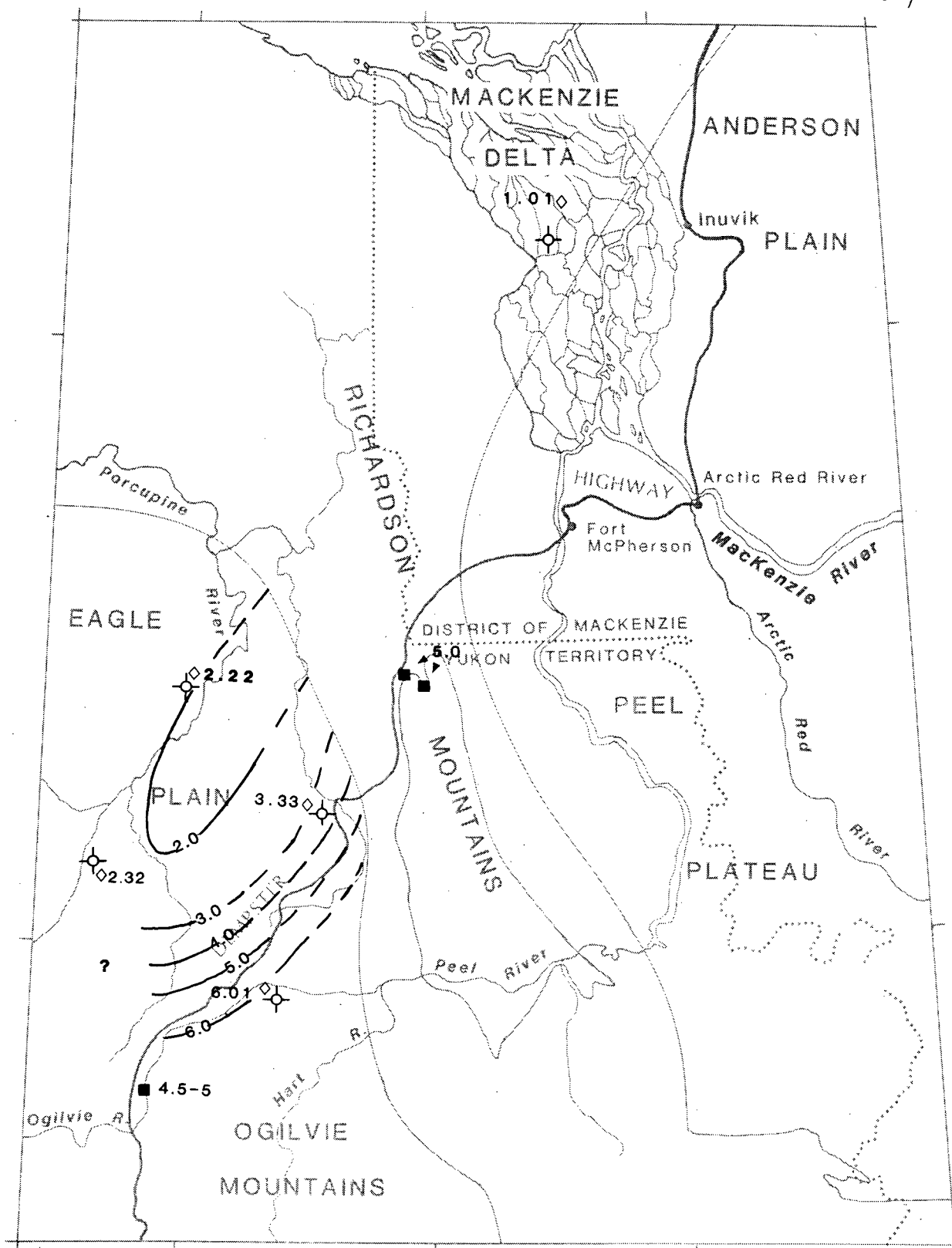
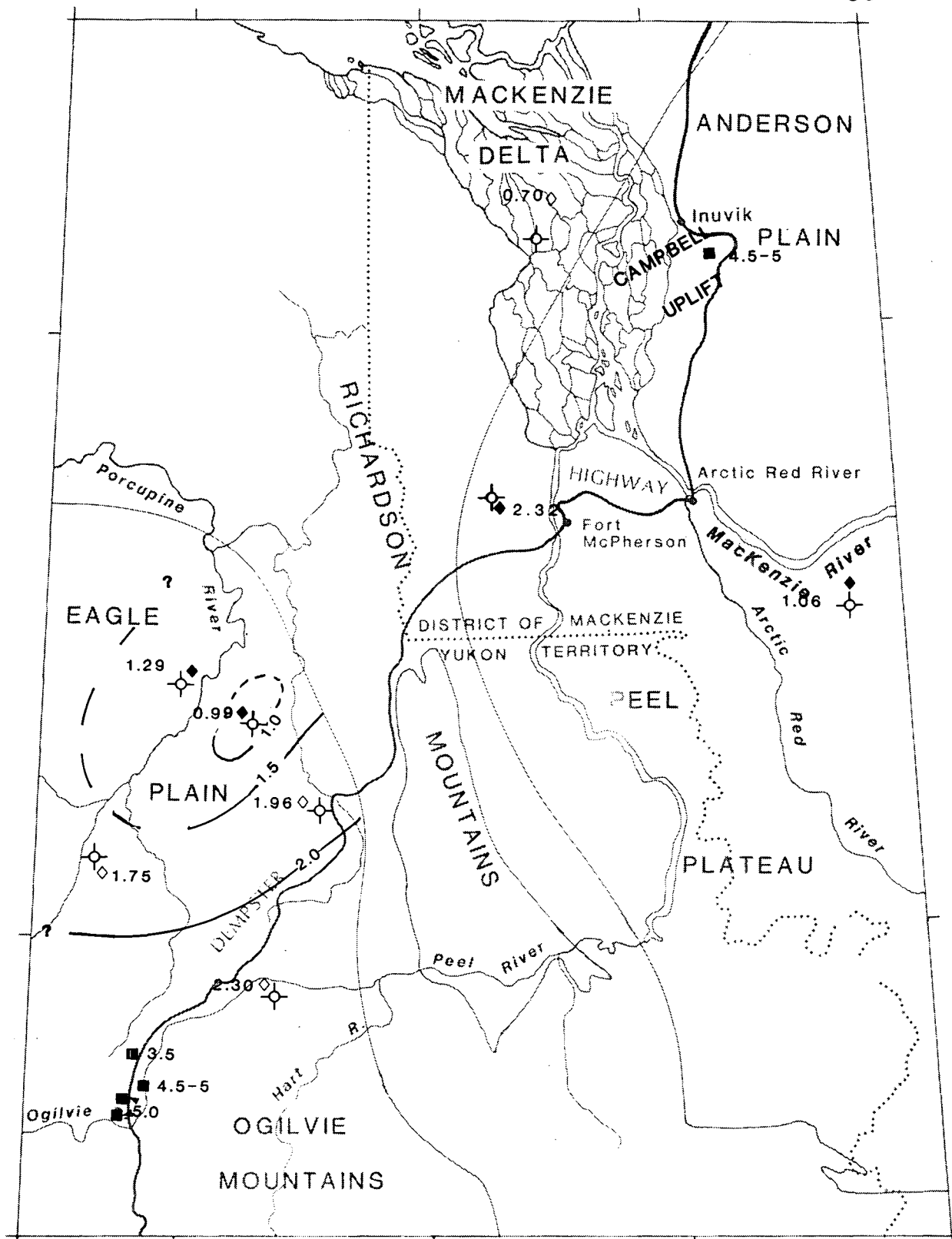


Figure 6.

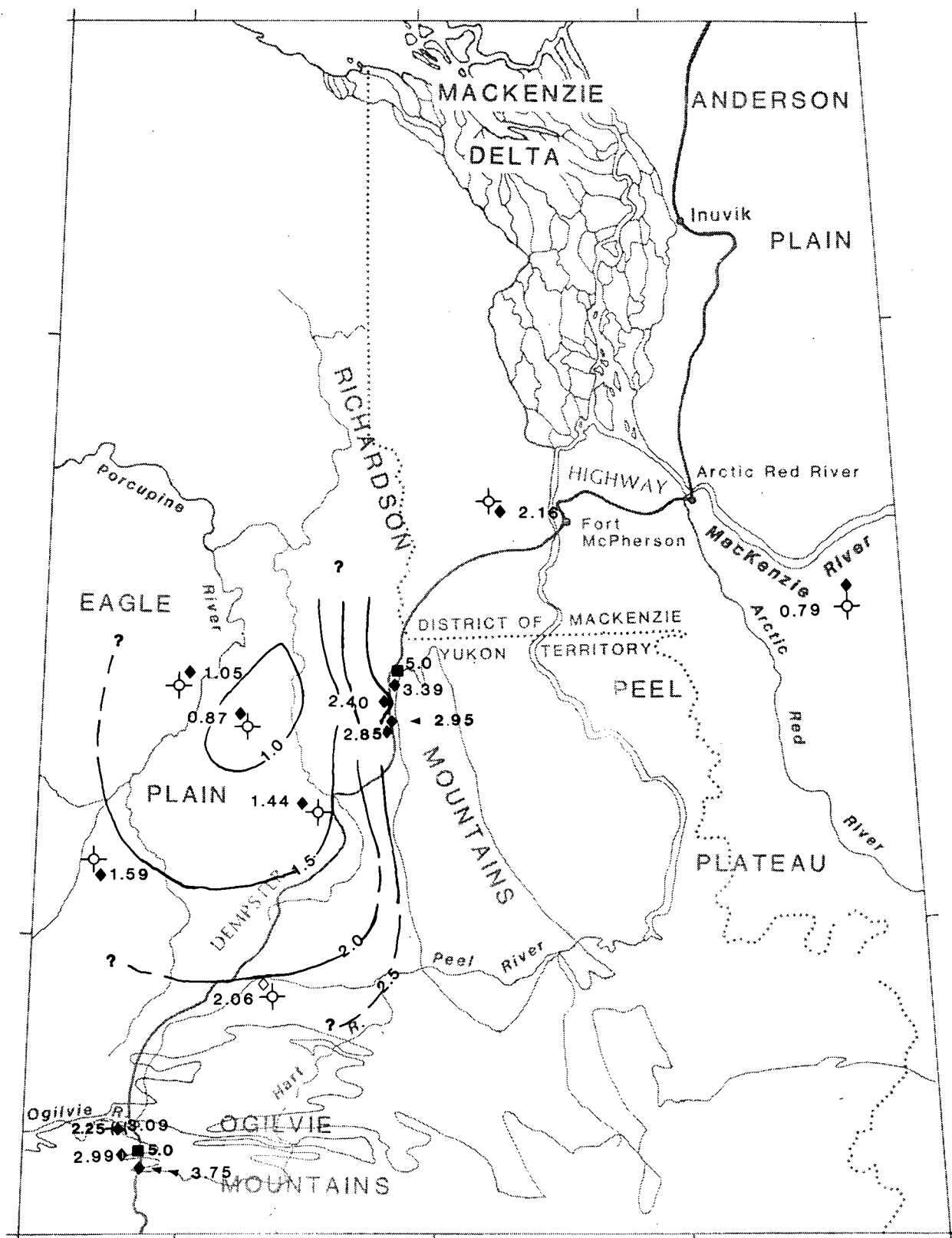
Figure 7. Regional maturation patterns of Upper Cambrian to Upper Cretaceous strata. Representative levels of organic maturity (% Rorand and CAI) at or near the base of each formation or group are plotted. '◇' denotes reflectance value calculated using line of best fit in figure 4. Scale is the same as figure 5.



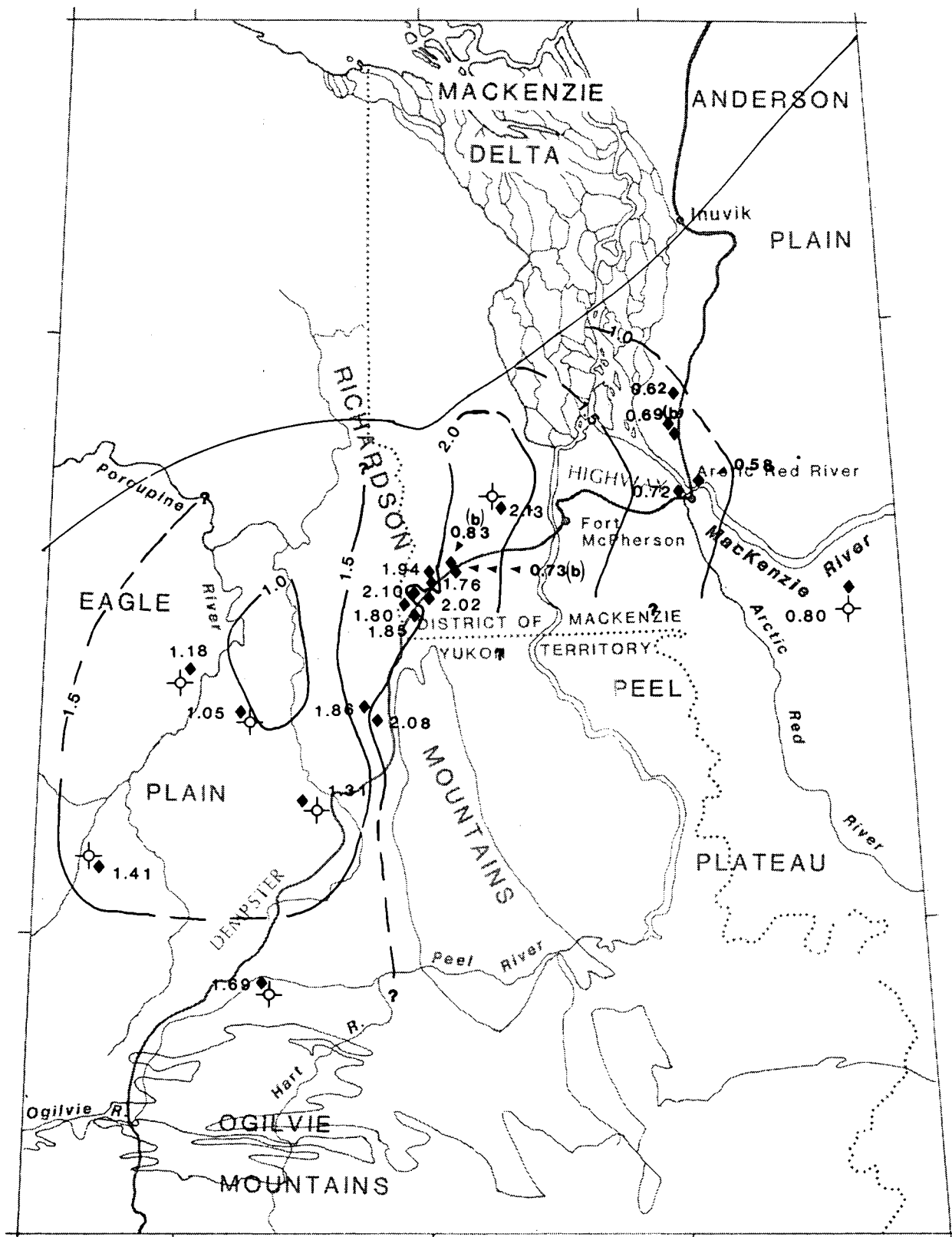
a) Road River Group. Contour interval = 1.0% Rorand. Boundaries of paleogeographic elements (modified from A.W. Norris, 1985) and the erosional edge of the EDM assemblage in the Richardson Mountains are shown.



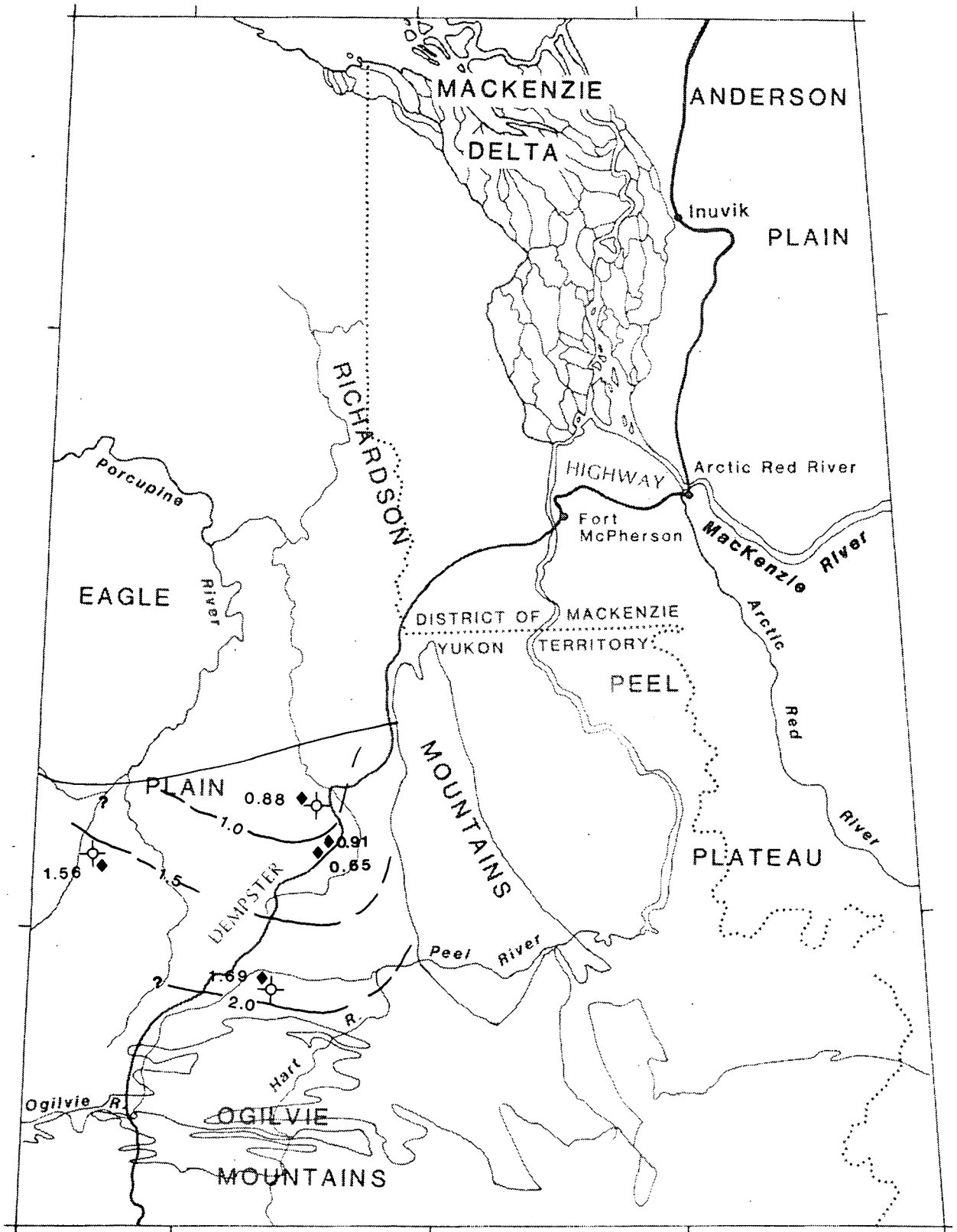
b) Ogilvie Formation (in Eagle Plain and southern Mackenzie Delta); Gossage and Hume Formations (in Peel Plateau). Contour interval=0.5% Rorand. Boundaries of paleogeographic elements (modified from A.W. Norris, 1985) and the erosional edge of the EDM assemblage in the Richardson Mountains are shown.



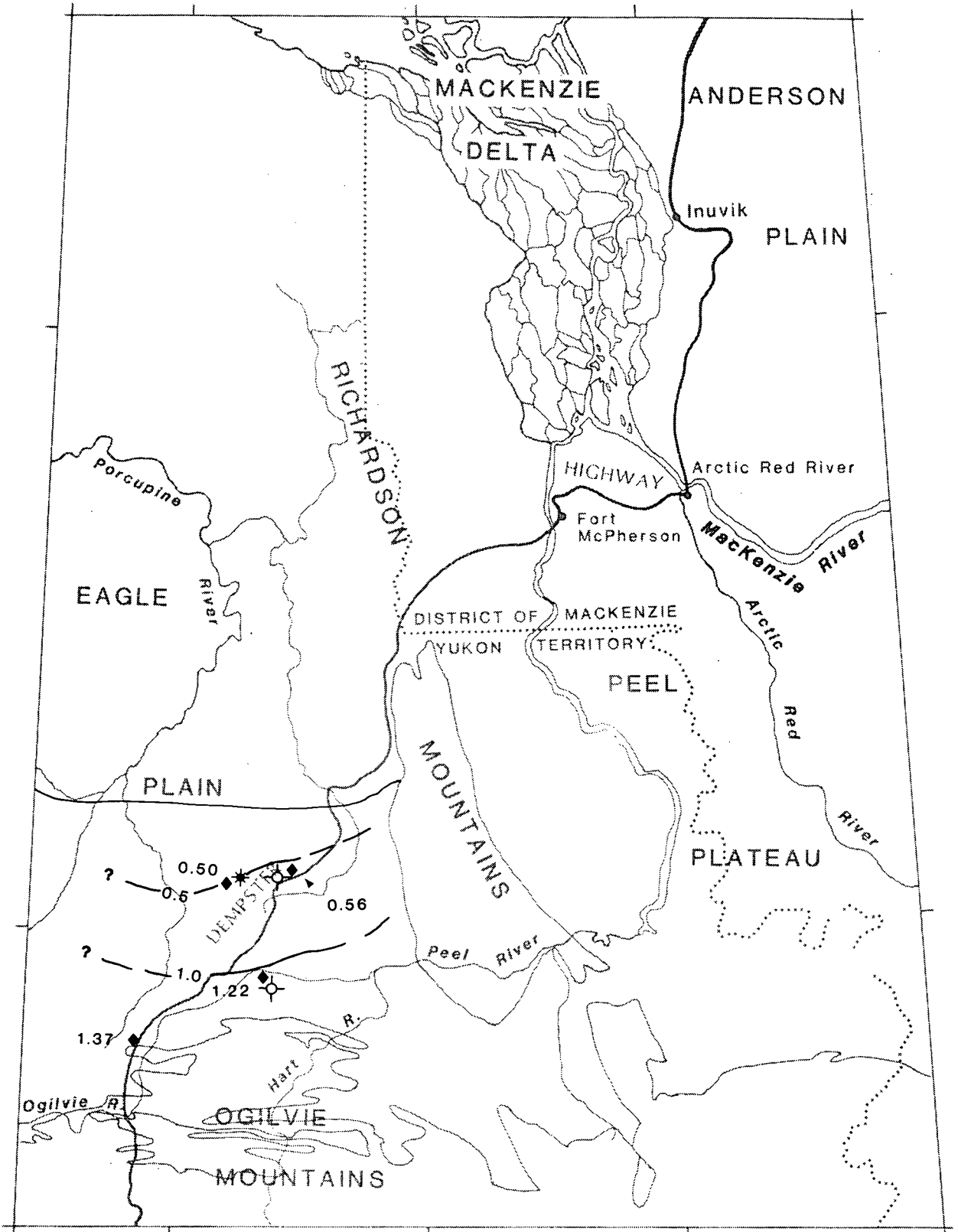
c) Canol Formation. Contour interval = 0.5% Rorand. '2.25 \blacklozenge 3.09' denotes reflectance at top and bottom, respectively, of a 200 m section. The erosional and/or depositional edge of the DJF assemblage is shown.



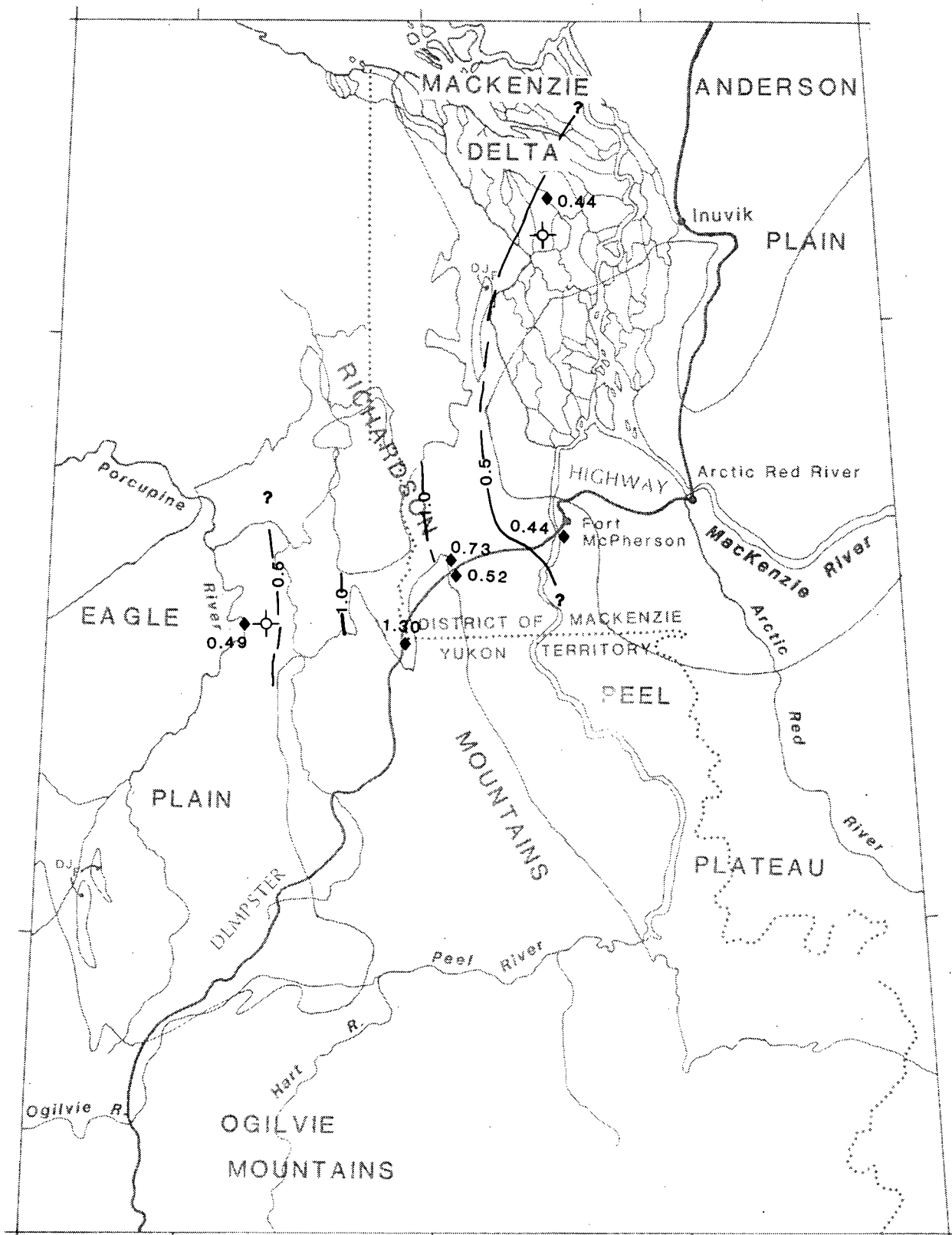
d) Imperial Formation. Contour interval=0.5% Rorand. '(b)' denotes reflectance of bitumen (albertite). Reflectance values for outcrop samples in Peel Plateau from near the top of the Formation are included to illustrate the maturity pattern. The erosional and/or depositional edge of the DJF assemblage is shown. Northern erosional edge modified from Pugh (1983).



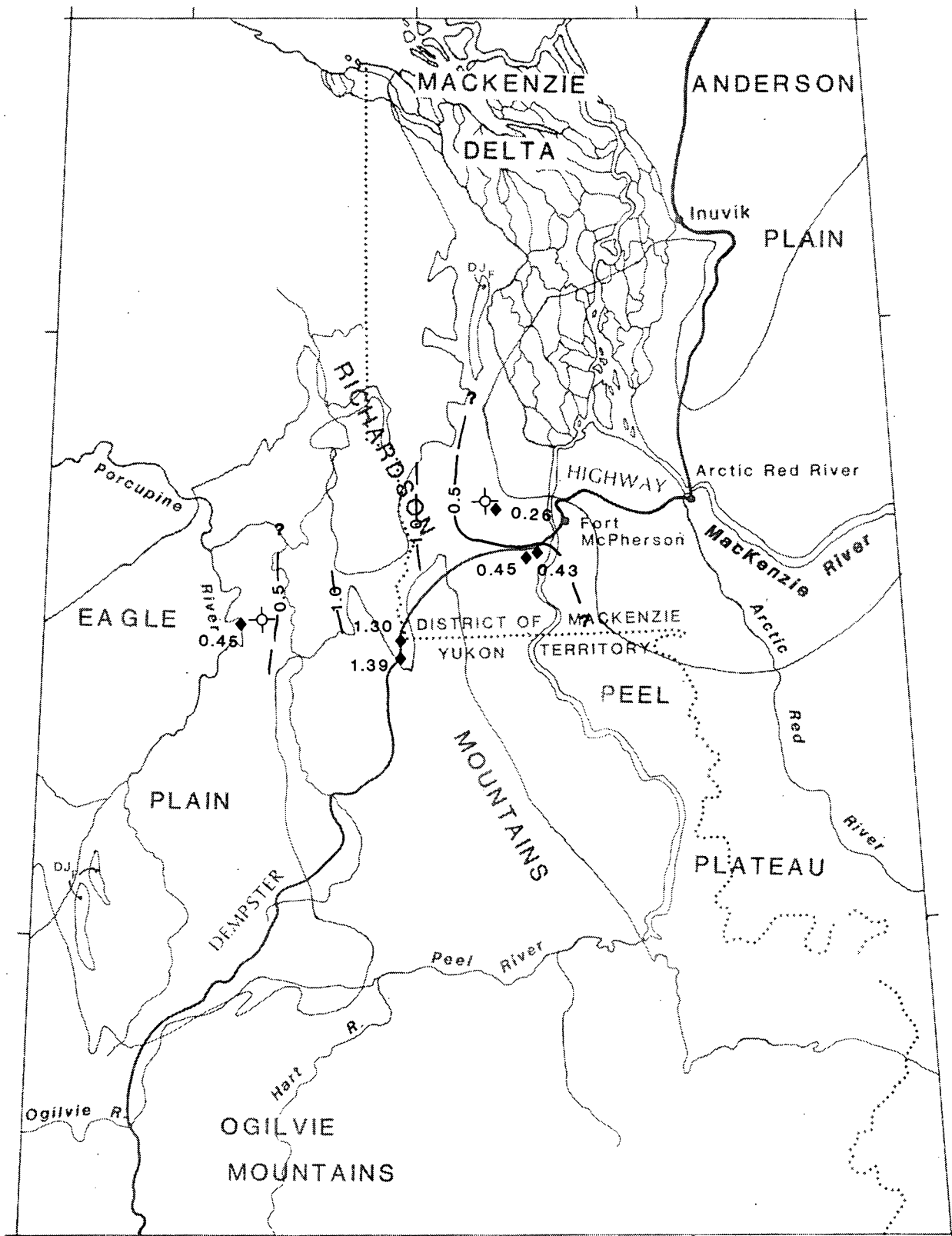
e) Ford Lake Shale. Contour interval=0.5% Rorand. Reflectance values for outcrop samples from near the top of the Formation are included to illustrate the maturity pattern. The erosional and/or depositional edge of the DJF assemblage is shown. Northern erosional edge modified from Pugh (1983).



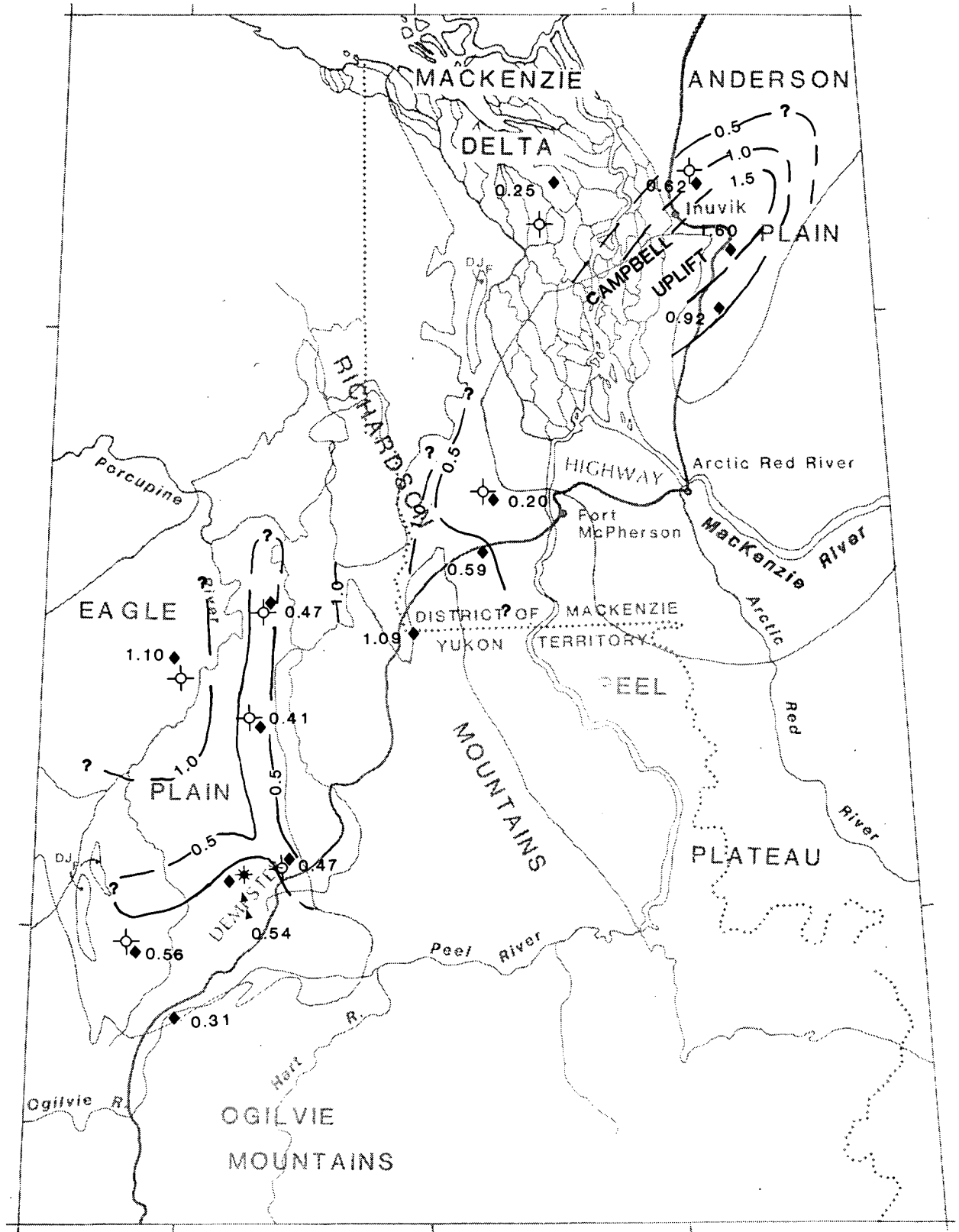
f) Hart River Formation. Contour interval=0.5% Rorand. The erosional and/or depositional edge of the DJF assemblage is shown. Northern erosional edge modified from Pugh (1983).



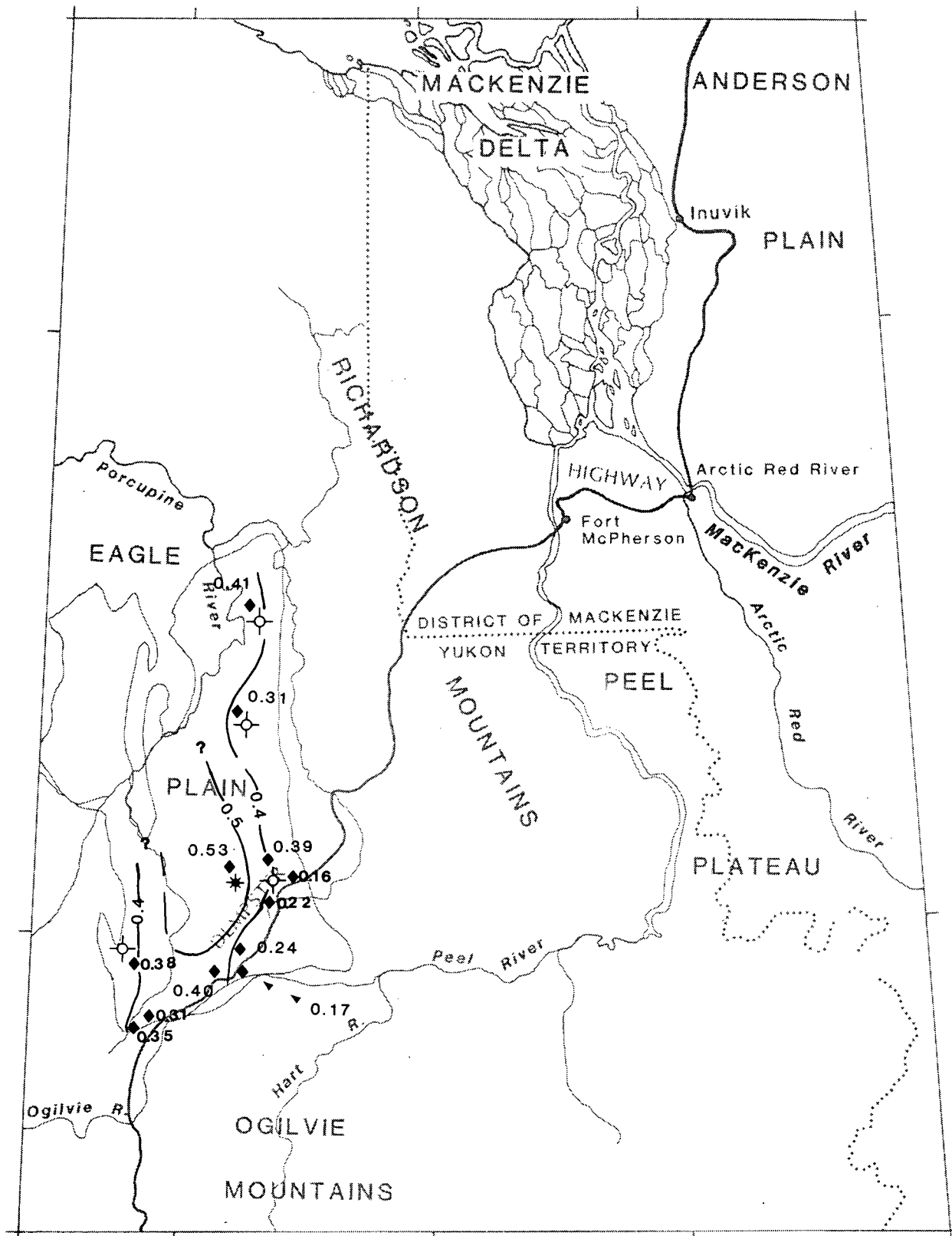
g) Mount Goodenough Formation. Contour interval=0.5% Rorand. Reflectance values plotted in Peel Plateau from near the top of the Formation are included to illustrate the maturity pattern. The erosional and/or depositional edge of the JKK assemblage is shown.



h) Rat River Formation. Contour interval = 0.5% Rorand. Reflectance values for outcrop samples in Peel Plateau from near the top of the Formation are included to illustrate the maturity pattern. The erosional and/or depositional edge of the JKK assemblage is shown.



i) Albian strata (Arctic Red River and Horton River Formations and map unit Kwr). Contour interval=0.5% Rorand. Reflectance values for outcrop samples in Peel Plateau and Eagle Plain from near the top of the Formations and map unit Kwr are included to illustrate the maturity pattern. The erosional and/or depositional edge of the JKK assemblage is shown.



j) Eagle Plain Group. Contour interval=0.1% Rorand. Reflectance values for outcrop samples from near the top of the Group are included to illustrate the maturity pattern. The erosional and/or depositional edge of the KA assemblage is shown.

Anomalously high reflectance values (up to 1.60% Rorand) were obtained from Albian samples of the Horton River Formation exposed on the Campbell Uplift. The DOM of Albian strata decreases from the crest of the uplift (1.60% Rorand) to the south (0.92% Rorand) and to the northwest (0.62 %Rorand; Fig. 7i). In southern Mackenzie Delta, Lower Cretaceous (Upper Hauterivian to Barremian and Albian) strata are less mature (0.25% to 0.44% Rorand; Figs. 7g and i) than coeval strata on the Campbell Uplift.

The DOM of Upper Cretaceous strata at or near the base of Eagle Plain Group (new name; Dixon, in press) is nearly constant apart from a slight increase (0.31% to 0.53% Rorand) towards the central part of Eagle Plain (Fig. 7j).

3. Time-temperature Modelling

It is well documented that the degree of organic maturity is related to the thermal history (Karweil, 1956; Lopatin, 1971; Bostick, 1973; Hood et al., 1975; Waples, 1980; Bustin, 1984; England and Bustin, 1986; and many others). Numerical models have been developed to predict thermal maturation of organic matter as a function of time and temperature (e.g., see summaries by Waples, 1983; Bustin et al., 1985). In this study, a 'Lopatin-Waples' type model is used to estimate paleogeothermal gradients and thickness of eroded section, based on maturation levels measured at each of the 12 wells examined in the study area.

a. Paleogeothermal Gradients

Paleogeothermal gradients were approximated by modelling the measured maturation gradients using an integral form of the Lopatin equation (McKenzie, 1981; Bustin et al., 1985; Bustin, 1986). The model used iteratively solves for maturation gradients using a burial history based on geological history and varying geothermal gradient. The calculated gradients are then compared to the measured gradient in order to estimate the paleogeothermal gradient. In this respect, the maturation gradient is modelled rather than a single point and is thus independent of the absolute DOM (Bustin, 1986). The model assumes a constant activation energy (as opposed to increasing activation energies with increasing DOM) and does not model changes in thickness as a result of compaction but models compacted rock thickness. Because subsidence and uplift rates are assumed to be uniform throughout, and heat flow, thermal conductivity and surface temperature are held constant, the model represents a time-averaging of the actual, more complicated depositional and thermal history. Neither the precision of the model nor the maturity measurements and gradients warrant consideration of these possible variables.

(i) Burial Histories

The burial history of several stratigraphic horizons at each well location were reconstructed based on time stratigraphy and estimates of the amount and timing of erosion derived from well-log evaluation and published sources. Ages and thicknesses of strata used to reconstruct the depositional and tectonic histories

(Figs. 8a to 19a) are not firmly constrained by the available geologic data; hence the numbers are considered a best estimate at present. Estimates of the amount of eroded section of Jurassic to mid-Hauterivian strata, used for the purpose of modelling, are hypothetical in Eagle Plain because these strata were completely eroded accompanying Valanginian to mid-Hauterivian (Jeletsky, 1975; 1980) or mid to late Hauterivian (Dixon, 1986) orogenesis. Differences in estimates of the amount of eroded overburden have a significant influence on estimates of maximum depth of burial and maximum temperatures attained. The thermal and burial histories presented in this study represent working models that will undoubtedly be modified as more data becomes available.

Southern Mackenzie Delta

In southern Mackenzie Delta (Fig. 8a), Jurassic strata (Bug Creek Group) were deposited about 205 Ma (Dixon, 1982) and subsided below Lower Cretaceous strata (Parsons Group and Mount Goodenough and Arctic Red River Formations) to about 100 Ma, with minor erosion and uplift at the end of the Berriasian and in the mid to late Hauterivian (Dixon, 1986; Fig. 8a). A major phase of uplift and erosion at the end of Albian time (90 Ma) was followed by burial beneath Upper Cretaceous strata (Boundary Creek or Smoking Hills Formations) and later by a period of minor erosion and/or non-deposition. Upper Cretaceous to early Tertiary sedimentation resulted in maximum burial at about 45 Ma. A mid-Eocene unconformity (Hea et al., 1980; Dixon, 1986) provides evidence for a major pulse of uplift and erosion culminating with erosion of the entire Upper Cretaceous to Tertiary sequence. Burial beneath Quaternary deposits resulted in

present day burial depths in southern Mackenzie Delta.

Peel Plateau

In Peel Plateau (Figs. 9a and 10a), Middle Devonian strata (Hume Formation) were deposited about 390 Ma (A.W. Norris, 1985); subsidence continued to about 380 Ma when a phase of epeiorogenic uplift (Kunst, 1973) or a period of non-deposition (Pugh, 1983) occurred. Rapid subsidence in Middle to Late Devonian was culminated by the Ellesmerian orogeny which resulted in a long period of uplift and erosion (Kunst, 1973; Pugh, 1983). The Peel Plateau remained emergent from Carboniferous to Berriasian time according to some authors (Miall, 1973; Poulton, 1982; Pugh, 1983) but others (Jeletsky, 1980; Dixon, 1986) suggest sedimentation continued from Late Jurassic to Berriasian time in Peel Plateau. In the present study, the burial history in Peel Plateau area (Figs. 9a and 10a) was modelled assuming deposition of Upper Jurassic to Berriasian strata, based on data from Jeletsky (1980) and Dixon (1986). Sedimentation resumed in Peel Plateau about 125 Ma and continued to about 90 Ma when Lower to Upper Cretaceous strata (Rat River, Arctic Red River and Trevor Formations) were deposited (Dixon, 1986). The Trevor Formation is the youngest unit in northwestern Peel Plateau, although it is possible that younger rocks were deposited and subsequently removed by erosion (Yorath and Cook, 1981). Minor uplift and erosion in early to mid Coniacian followed by Laramide deformation in Late Cretaceous to early Tertiary (Norris and Yorath, 1981) uplifted the strata to their present position.

Eagle Plain

A different tectonic and depositional history was modelled for each well (Figs. 11a to 19a) in Eagle Plain, based on geologic data and subsurface formation tops supplied by various published sources in addition to unpublished data supplied by the Geological Survey of Canada (Dixon and Hamblin, pers. comm., 1986). Upper Silurian strata (Tatsieta Formation) were deposited about 415 Ma (A.W. Norris, 1985) and subsided to about 380 Ma. A minor period of uplift and erosion and/or a period of non-deposition lasted until about 375 Ma (Martin, 1973; Pugh, 1983). Sedimentation in Eagle Plain was uninterrupted until about 355 Ma when the Ellesmerian orogeny uplifted most of Eagle Plain (Martin, 1973) with the exception of southern portion (Figs. 14a and 19a) where Carboniferous strata conformably overly Devonian strata (Pugh, 1983). Most of the Eagle Plain was emergent during the Carboniferous or Permian to Early Jurassic (Martin, 1973; Jeletsky, 1975 and 1980). Sedimentation resumed in the western Eagle Plain about 205 Ma (Bug Creek Formation of Jeletsky, 1975) and may have continued to about 135 Ma (Valanginian to mid-Hauterivian orogeny; Jeletsky, 1980) or to about 130 Ma (mid to late Hauterivian orogeny; Dixon, 1986) when Early Cretaceous orogenesis resulted in erosion of most or all of the Jurassic to mid-Hauterivian sequence in Eagle Plain (Figs. 12a to 17a). Sedimentation resumed in late Hauterivian time and continued until Aptian time in most areas. All of Eagle Plain except the northern portion (Fig. 18a) was emergent during the Aptian (Dixon, 1986). Sedimentation continued in Albian time (Dixon, 1986), followed by a major period of uplift and erosion about 105 Ma which was succeeded about 95 Ma with deposition of Upper Cretaceous strata

(Eagle Plain Group). Sedimentation ended about 75 Ma in Eagle Plain when Laramide tectonism uplifted and folded Eagle Plain (Dixon, 1986).

(ii) Maturation histories

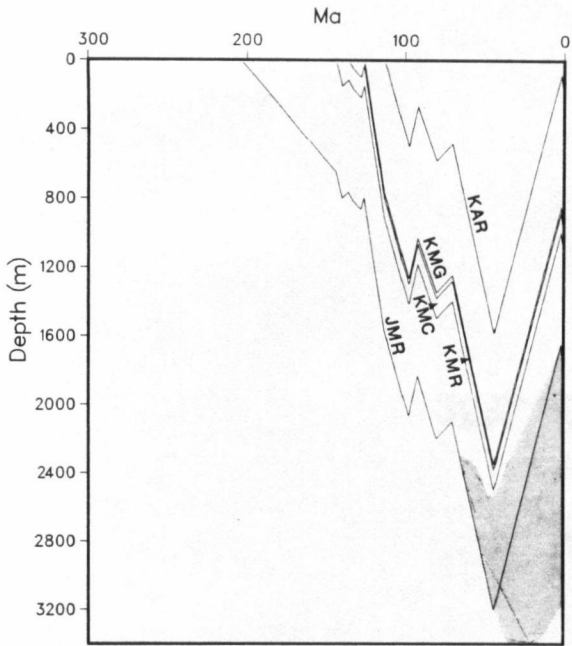
In figures 8b to 19b the calculated DOMs of the oldest stratigraphic horizon modelled at each well are plotted, assuming geothermal gradients of 10 to 50°C/km. In figures 8c to 19c the calculated paleogeothermal gradients are compared to the measured maturation gradients.

Comparison of the measured and calculated gradients suggests that the paleogeothermal gradients in southern Mackenzie Delta, Peel Plateau and north-central, northwestern, eastern and southeastern Eagle Plain range from 20 to 45°C/km (Figs. 8c to 14c). The models suggest low paleogeothermal gradients (10 to 20°C/km) for the central, most northern and western Eagle Plain (Figs. 15c to 19c). Paleogeothermal gradients decrease from the eastern margin (35 to 40°C/km) of Eagle Plain to the west (15 to 20°C/km) and to the north (10°C/km; Fig. 5).

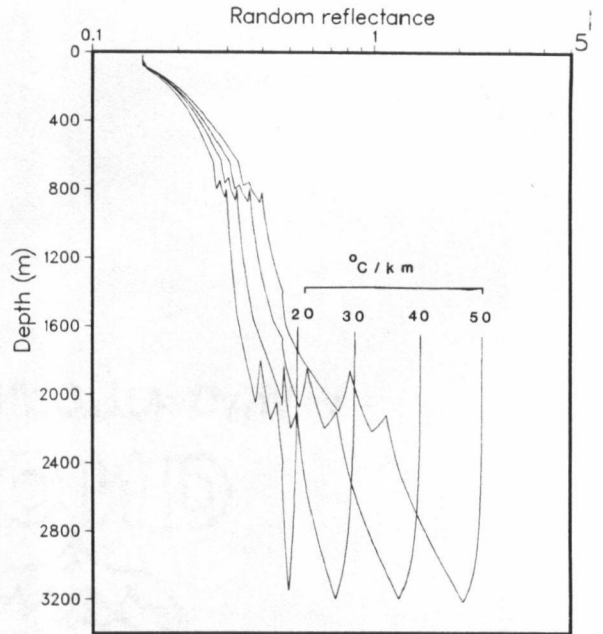
Figures 8 to 19. a) Interpretation of burial histories of several stratigraphic horizons at each of 12 wells in the study area. The burial histories were determined by assuming uniform rates of uplift and subsidence. The small 'kinks' in several of the plots represent minor erosion and uplift, based on geologic evidence derived from various authors cited (see text). These unconformities are included to show the complex burial history of strata in the study area, although they have little effect on the maturation history (compare to Figs. 8b to 19b). In figures 9a and 10a, '?' denotes burial beneath Late Jurassic to Early Cretaceous strata which are missing in Peel Plateau whereas are preserved in Richardson Mountains (900 m, Jeletsky, 1980). In figures 12a to 17a and 19a, '?' denotes burial beneath Early Jurassic to mid-Hauterivian strata which are missing in Eagle Plain whereas are preserved in the Richardson Mountains (up to 930 m, Jeletsky, 1974). Abbreviation for horizons (groups and/or formations) modelled: KEPN=Eagle Plain Group; Kwr=Albian map unit; KAR=Arctic Red River; KRR=Rat River; KMG=Mount Goodenough; JMR=Murray Ridge (base of Parsons Group); PJC=Jungle Creek; CE=Ettrain; un. Carb.=unnamed Carboniferous strata overlying Hart River Formation; CHR=Hart River; CF=Ford Lake Shale; CT=Tuttle; DI=Imperial; DCA=Canol; DO=Ogilvie; DHU=Hume; KUT=Kutchin; TAT=Tatsieta.

b) Maturation history for a single horizon (the oldest horizon) at each well assuming various paleogeothermal gradients and a surface temperature of 20°C. Each of the stratigraphic horizons in figures 8a to 19a were so modelled in order to calculate curves shown in figures 8c to 19c.

c) Calculated and measured maturation gradients for 12 wells in the area of study. The gradients have all been plotted through the origin (0.15% Rorand) to facilitate comparison of slopes. The heavy line is the measured maturation gradient and light lines are calculated paleogeothermal gradients.

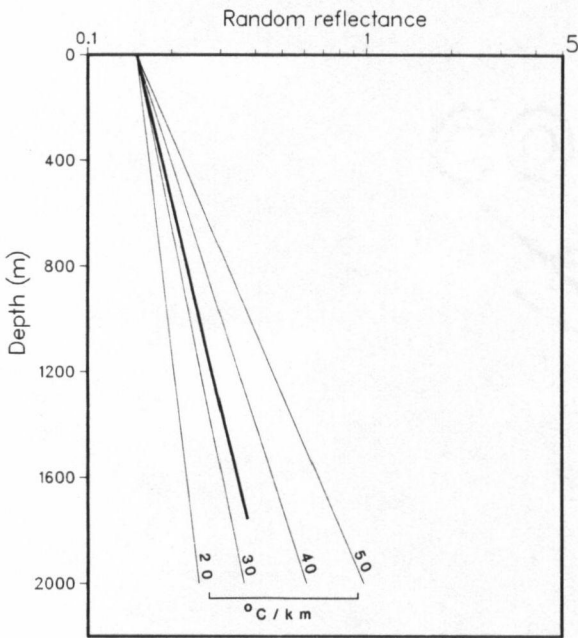


(a)



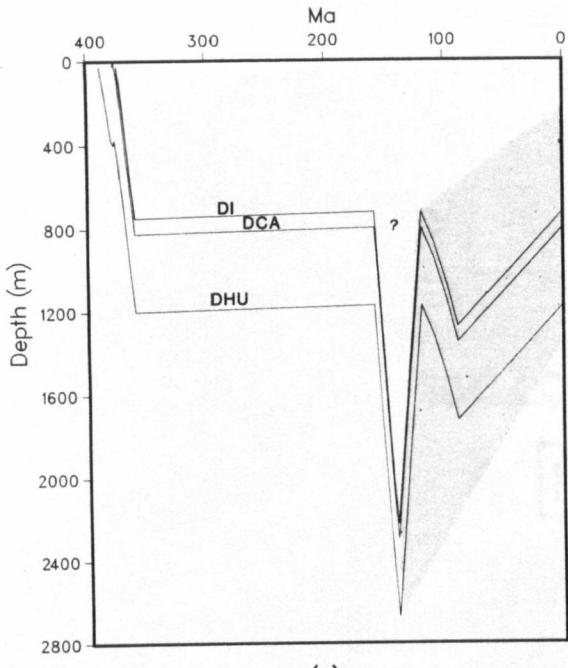
Shell Aklavik A-37
Murray Ridge Formation

(b)

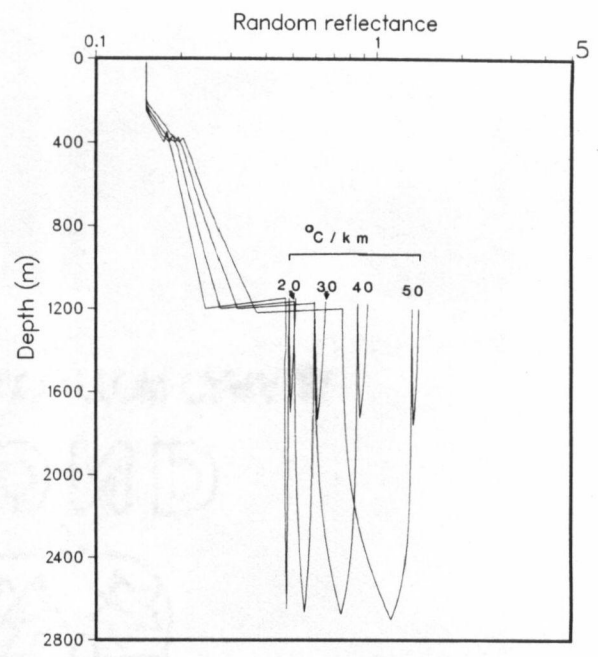


(c)

Figures 8 a), b), c) Southern Mackenzie Delta. Jurassic strata (Bug Creek Group) entered the oil window in Late Cretaceous to Early Tertiary whereas Upper Jurassic to Lower Cretaceous strata (Husky Formation, middle and upper Parsons Group, Mount Goodenough and Arctic Red River Formations) have not entered the oil window.

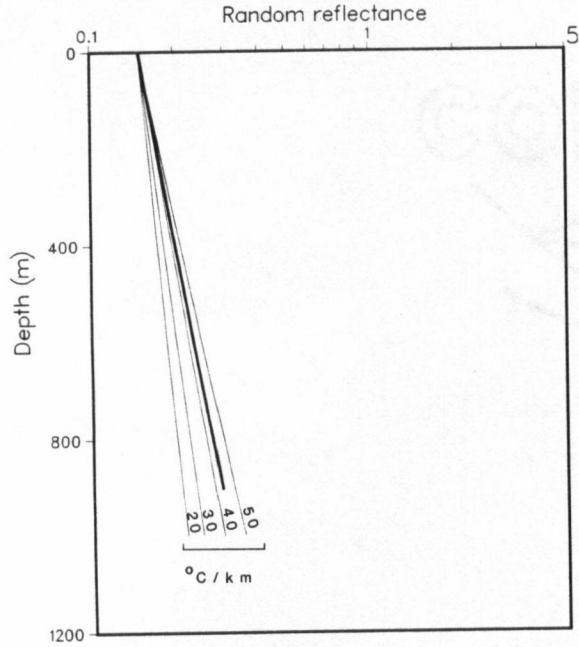


(a)



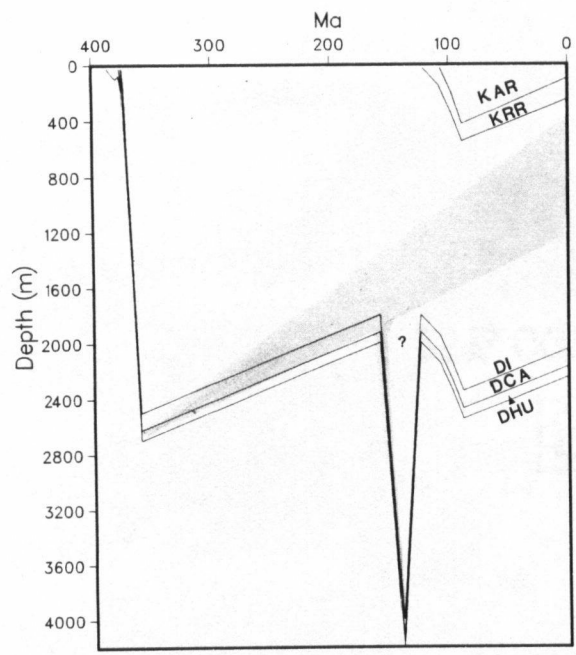
Shell Tree River E. H-57
Hume Formation

(b)

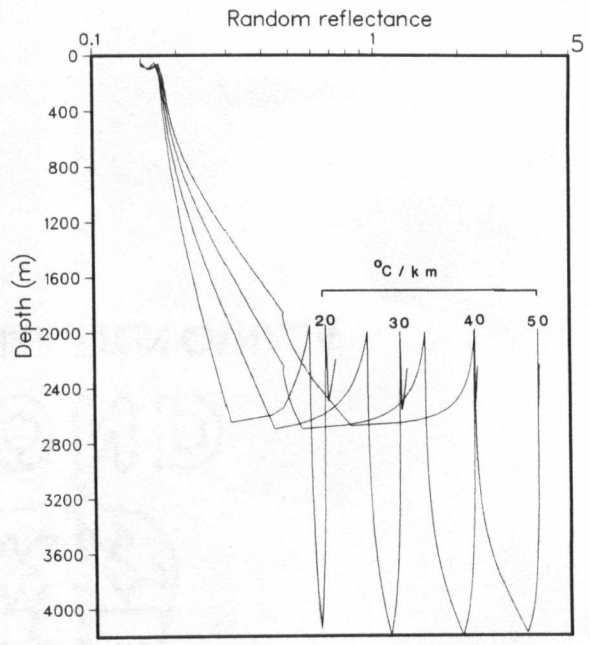


(c)

Figures 9 a), b), c) Eastern Peel Plateau. Devonian strata (Hume, Canol and Imperial Formations) entered the oil window in Late Jurassic to Early Cretaceous time and are presently mature.

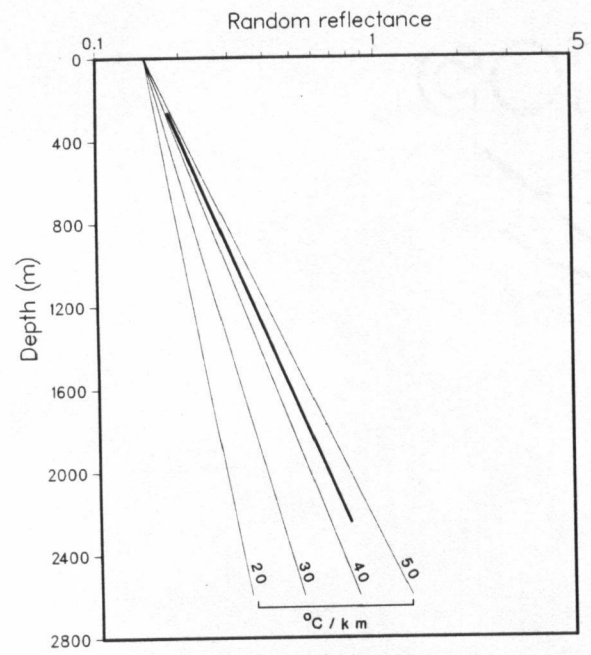


(a)



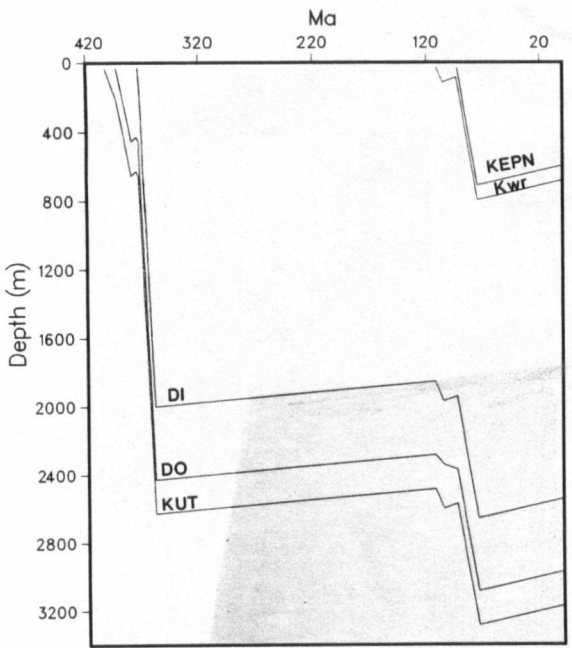
IOE Stony I-50
Hume Formation

(b)

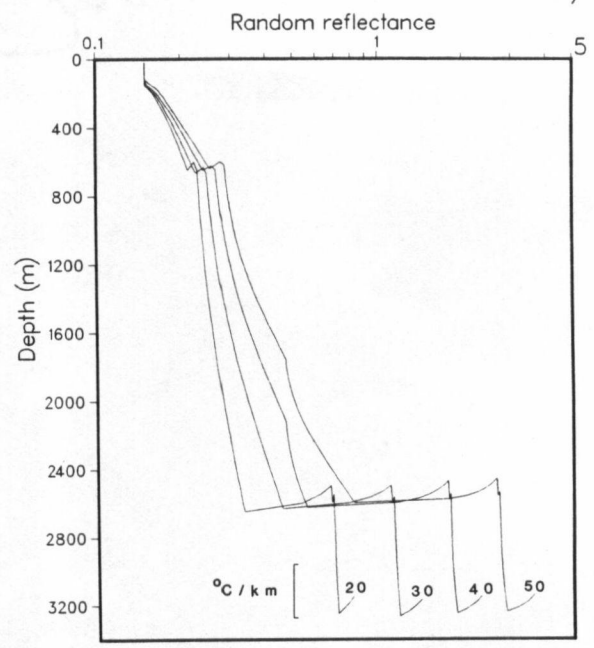


(c)

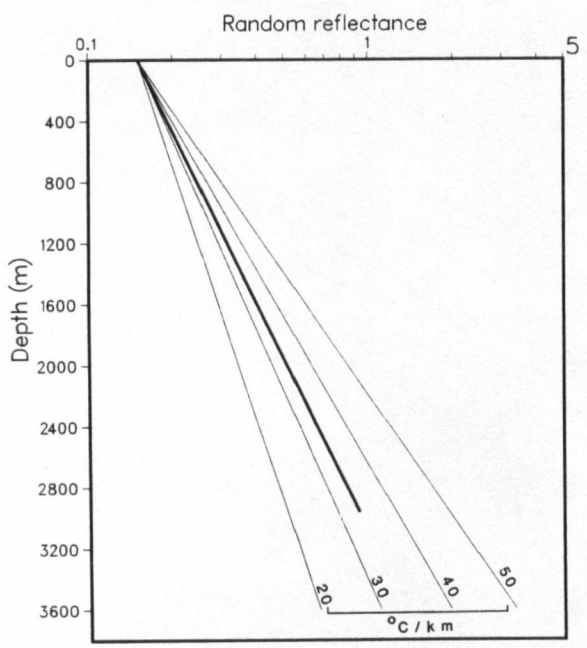
Figures 10 a), b), c) Western Peel Plateau. Devonian strata (Hume, Canol and Imperial Formations) entered the oil window in the Late Devonian to Early Carboniferous whereas exited the oil generation zone in Early Permian to Late Jurassic time.



(a)

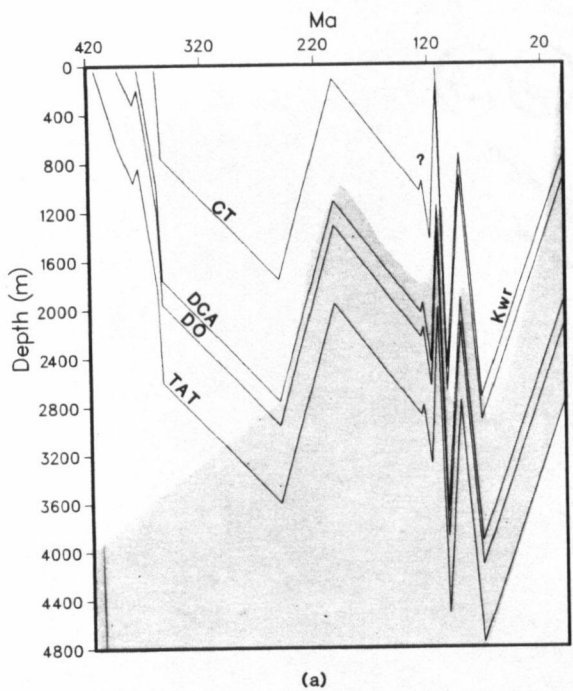


SOBC Shaeffer Creek 0-22
Kutchin Formation
(b)

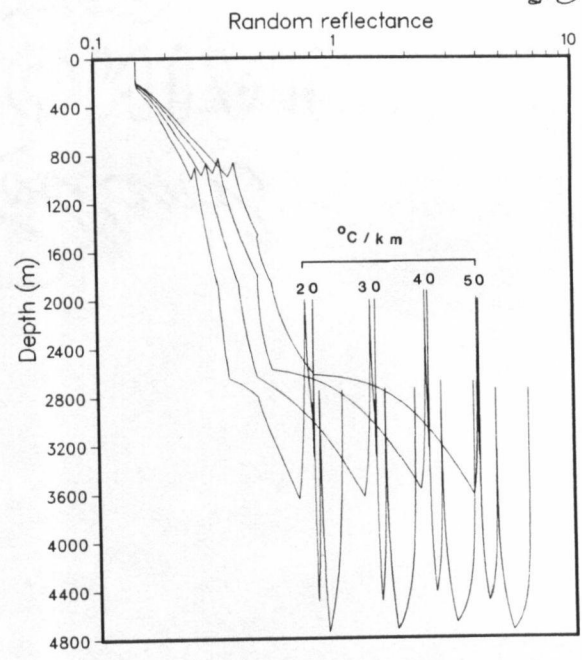


(c)

Figures 11 a), b), c) North-central Eagle Plain. Devonian strata (Kutchin, Ogilvie, Canol and Imperial Formations) entered the oil window in Late Carboniferous time whereas Lower and Upper Cretaceous strata (map unit Kwr and Eagle Plain Group) have never entered the oil window.

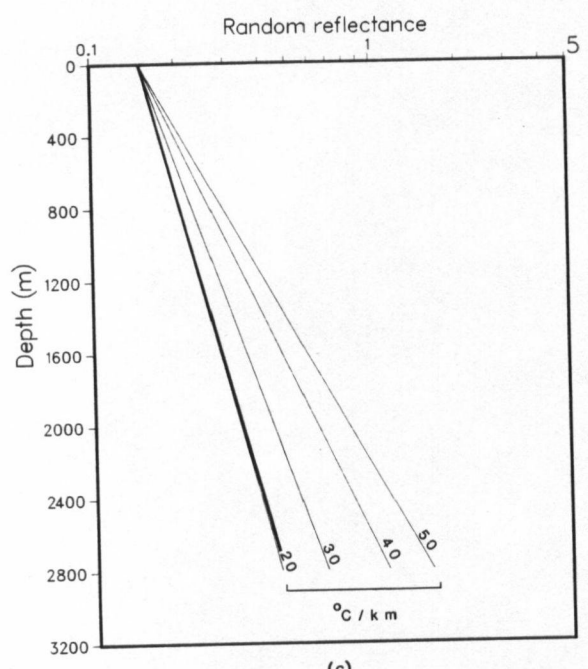


(a)



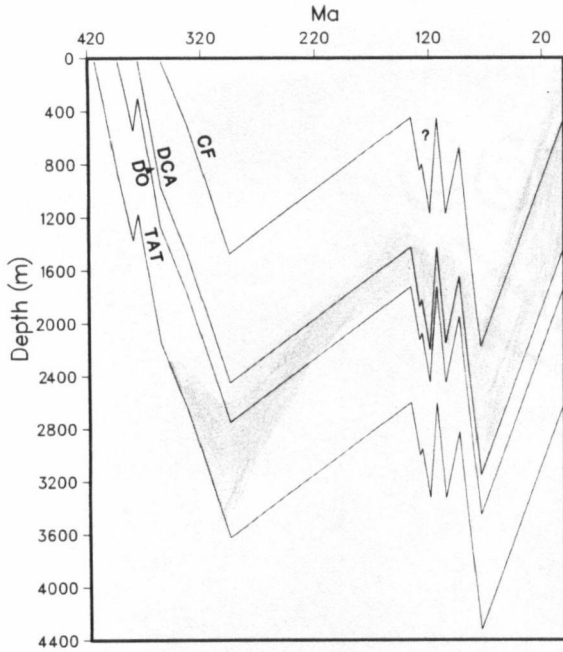
Western Minerals N. Hope N-53
Tatsieta Formation

(b)

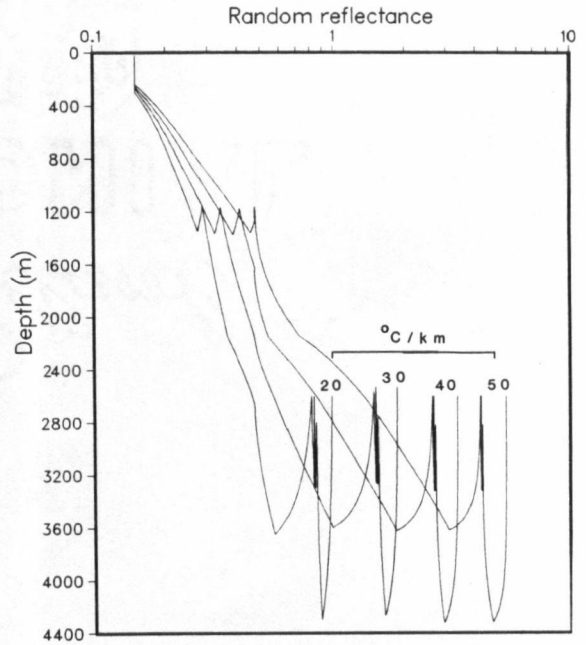


(c)

Figures 12 a), b), c) Northwestern Eagle Plain. Devonian strata (Tatsieta, Ogilvie, Canol and Imperial Formations) entered the oil window in Late Carboniferous to Permian time whereas Carboniferous (Tuttle Formation) and Lower Cretaceous (map unit Kwr) strata did not enter the oil window until Tertiary time. The Early Devonian Tatsieta Formation exited the oil window in Late Cretaceous to Early Tertiary time whereas younger strata are still within the oil window.



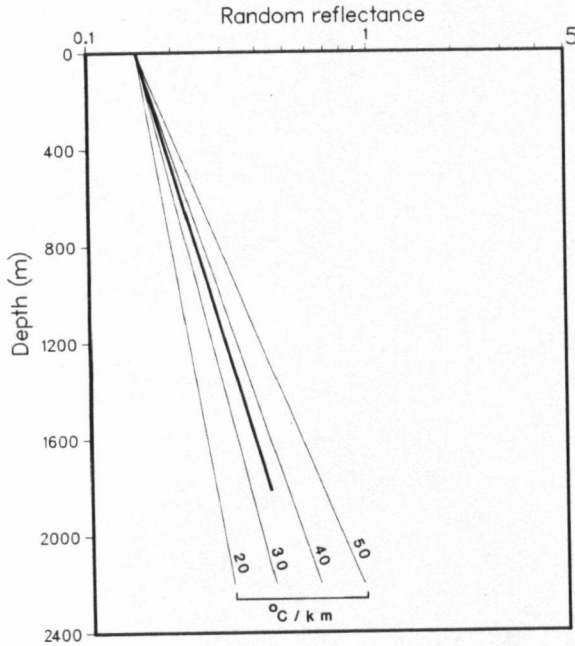
(a)



Socony Mobil WM S. Tuttle N-05

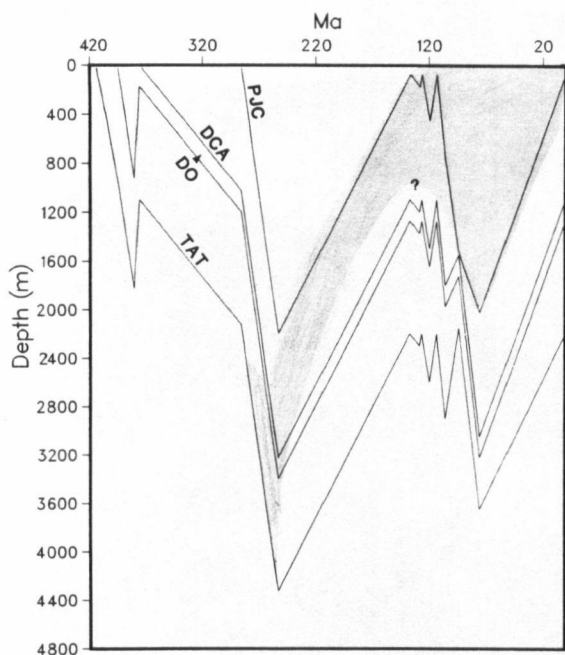
Tatsieta Formation

(b)

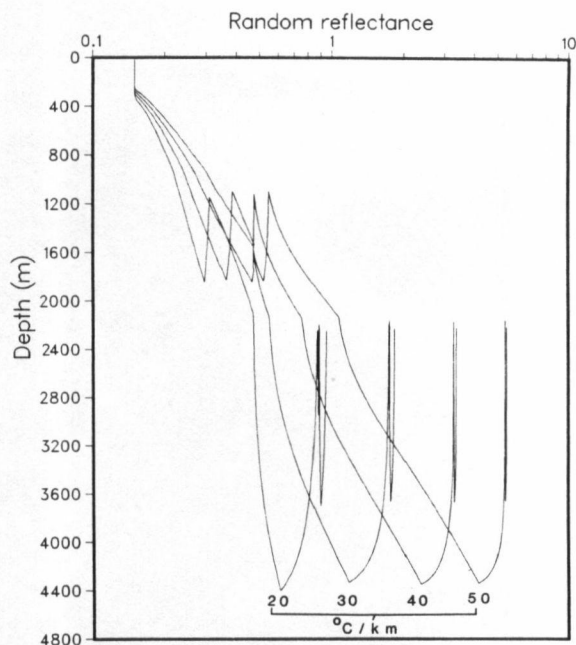


(c)

Figures 13 a), b), c) Eastern Eagle Plain. Devonian strata (Tatsieta, Ogilvie, Canol and Imperial Formations) entered the oil window in the Carboniferous. Carboniferous strata did not enter the oil window until Late Cretaceous time. The Early Devonian Tatsieta Formation exited the oil window in Late Carboniferous time; the Middle and Upper Devonian sequence left the oil window in Triassic to Late Cretaceous time whereas Carboniferous strata are presently mature.



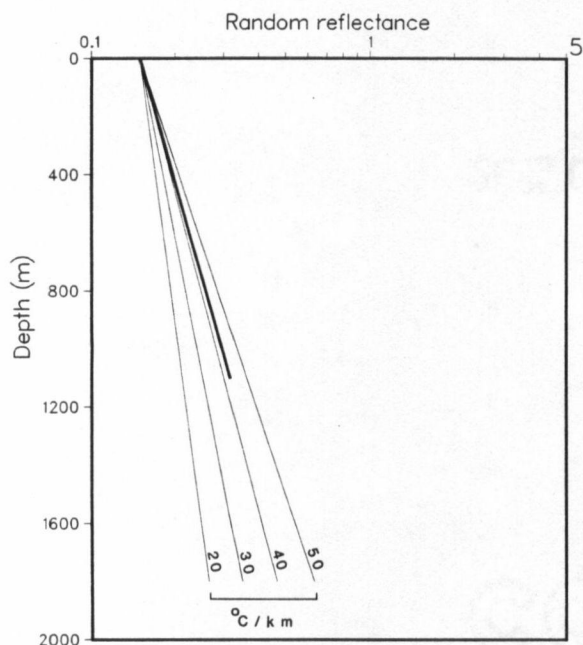
(a)



SOBC Blackstone D-77

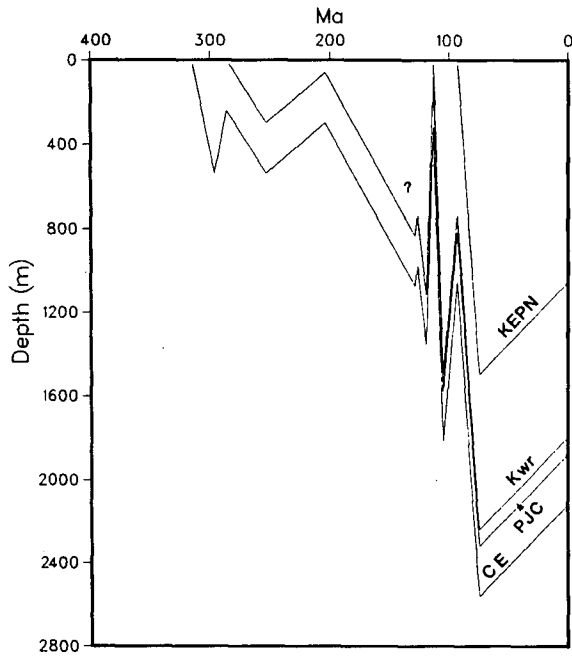
Tatsieta Formation

(b)

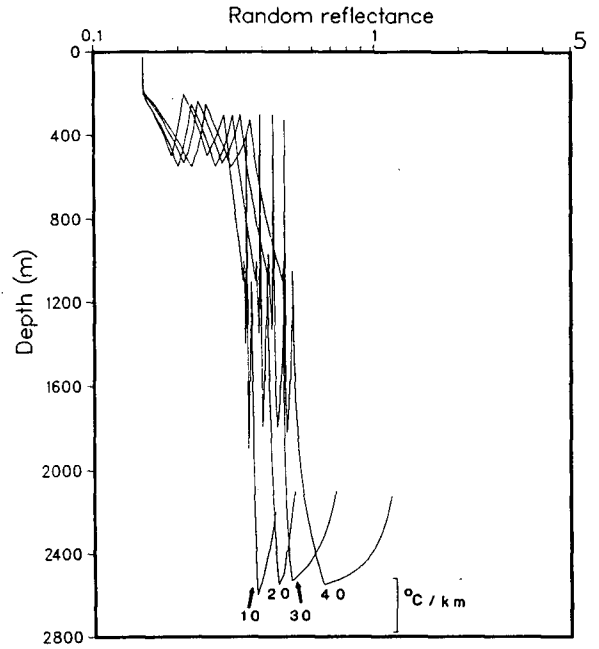


(c)

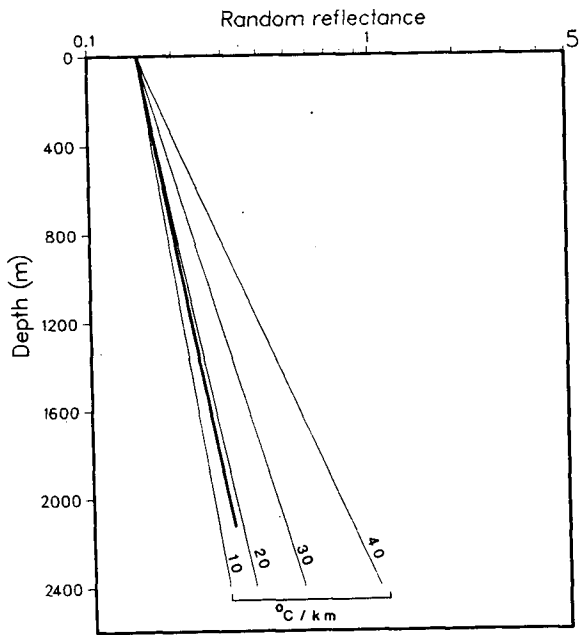
Figures 14 a), b), c) Southeastern Eagle Plain. Devonian strata (Tatsieta, Ogilvie, Canol and Imperial Formations) entered the oil window in Carboniferous to Permian time during deep burial whereas Carboniferous and Permian strata (Ford Lake Shale and Hart River, Blackie and Jungle Creek Formations) did not enter the oil window until Triassic time. The Devonian and Lower Carboniferous sequence exited the oil window in Permian to Early Jurassic time; Upper Carboniferous and Permian strata are still within the oil window.



(a)

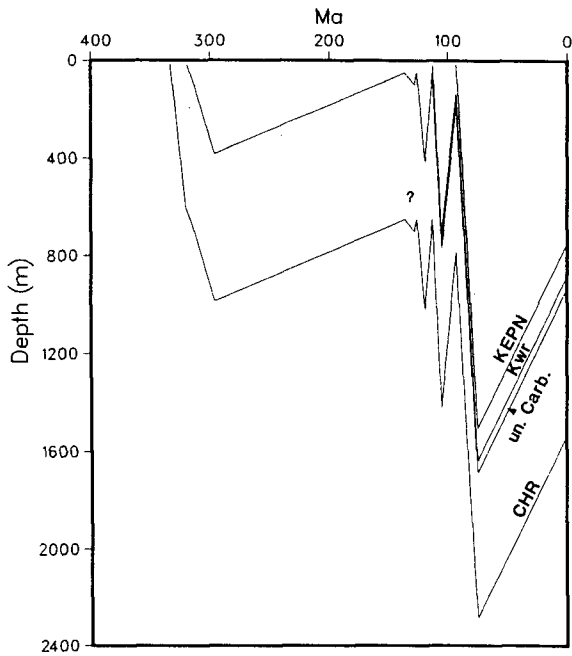


Murphy Mesa BP S. Whitestone N-58
Ettrain Formation
(b)

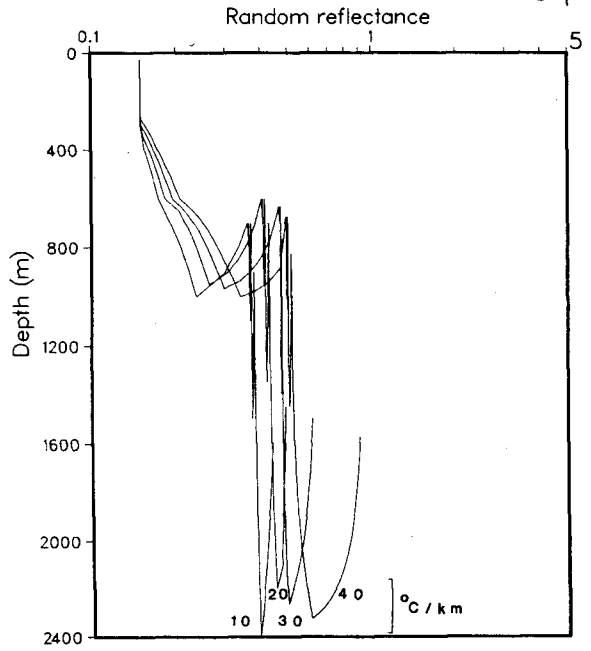


(c)

Figures 15 a), b), c) Central Eagle Plain. Carboniferous to Upper Cretaceous strata (Ettrain, Jungle Creek Formations, map unit Kwr and Eagle Plain Group) have never entered the oil window.

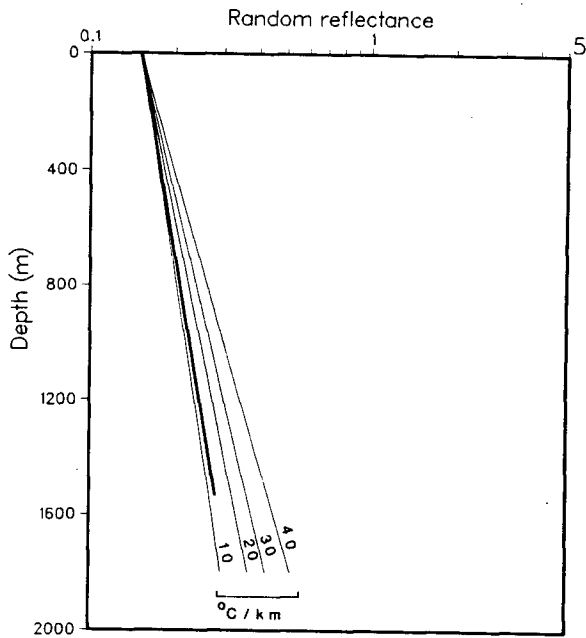


(a)



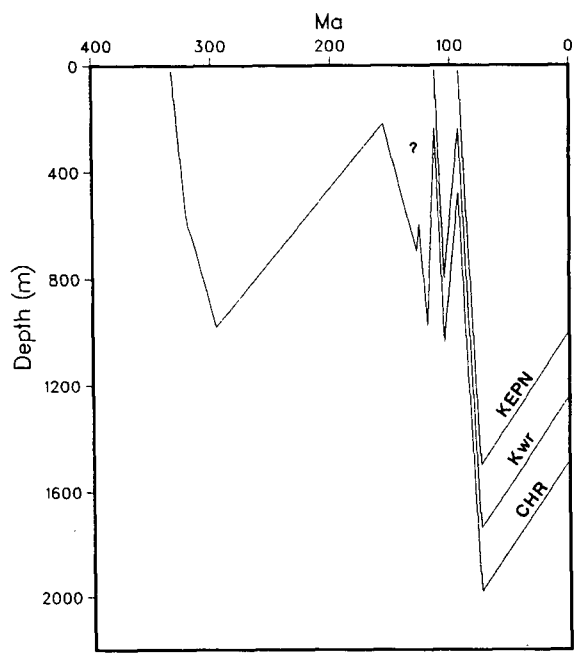
Canoe River E. Chance C-18
Hart River Formation

(b)

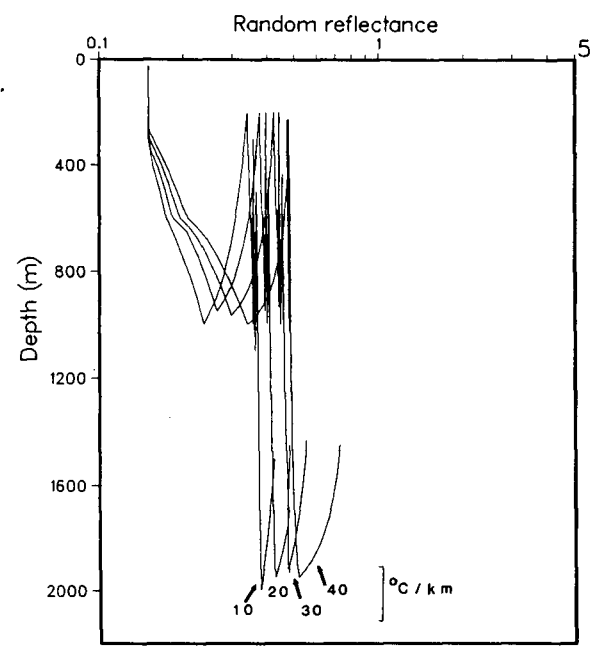


(c)

Figures 16 a), b), c) Central Eagle Plain. Carboniferous to Upper Cretaceous strata (Hart River Formation, unnamed Carboniferous unit, map unit Kwr and Eagle Plain Group) have never entered the oil window.

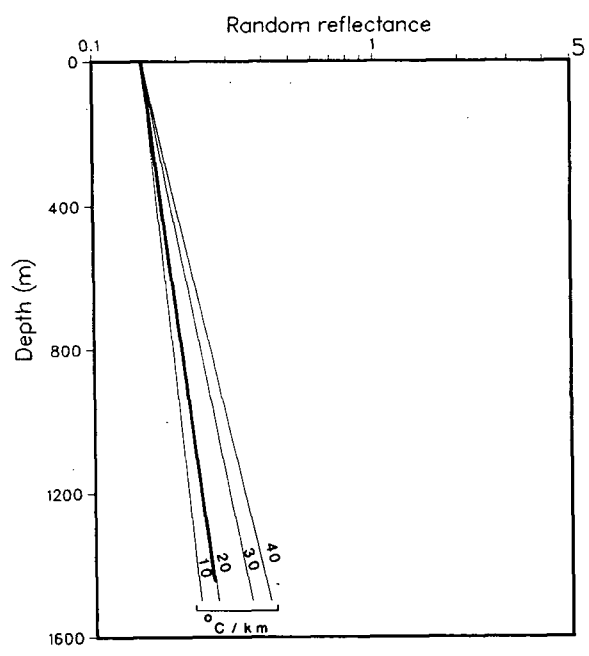


(a)



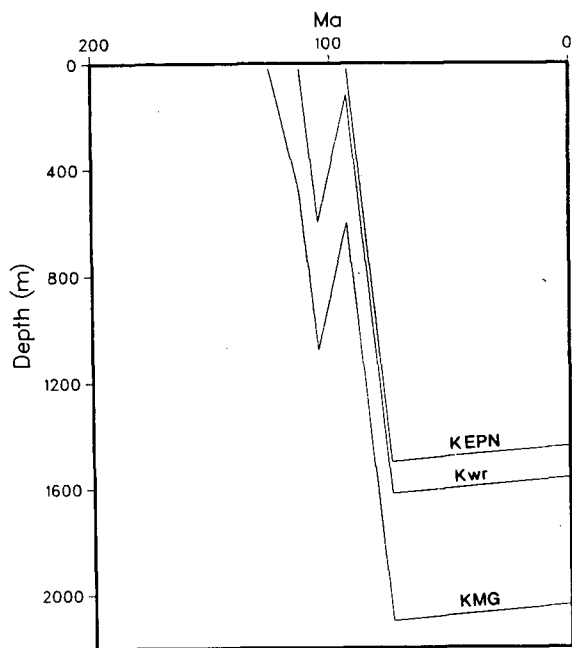
Canoe River Chance J-19
Hart River Formation

(b)

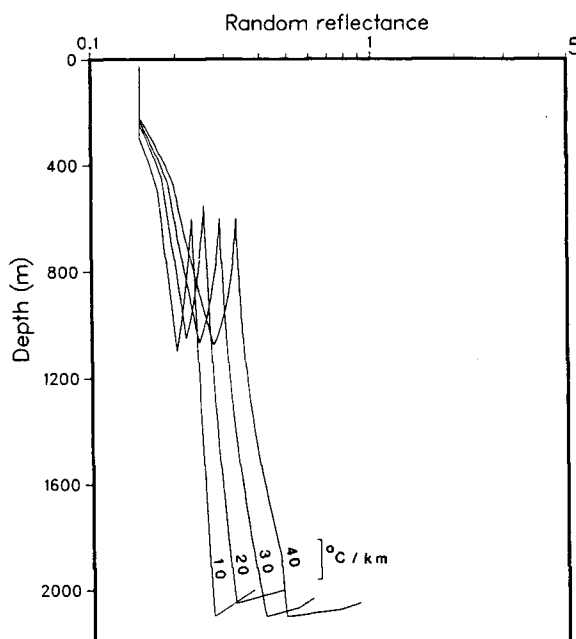


(c)

Figures 17 a), b), c) Central Eagle Plain. Carboniferous to Upper Cretaceous strata (Hart River Formation, map unit Kwr and Eagle Plain Group) have never entered the oil window.

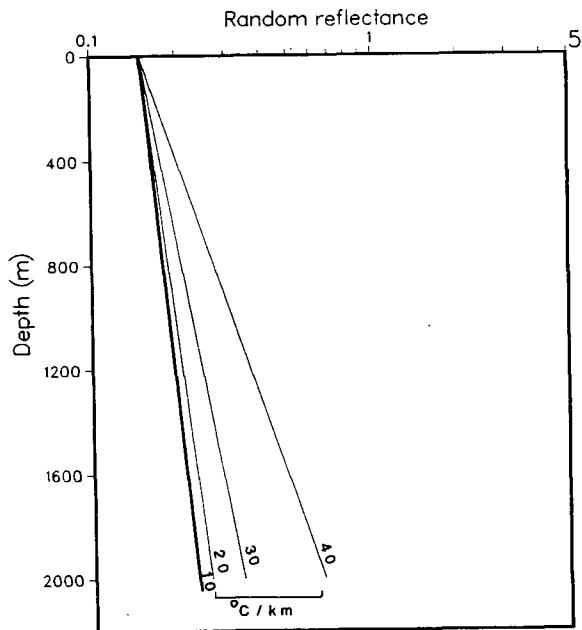


(a)



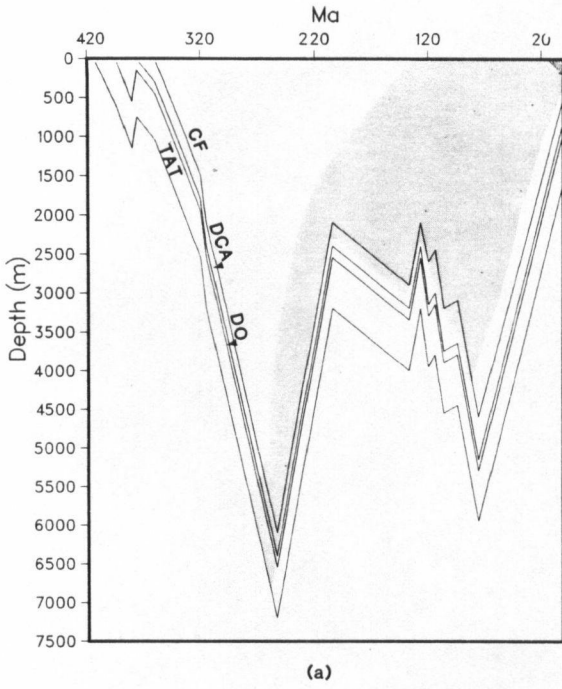
Chevron SOBC Whitefish J-70
Mount Goodenough Formation

(b)

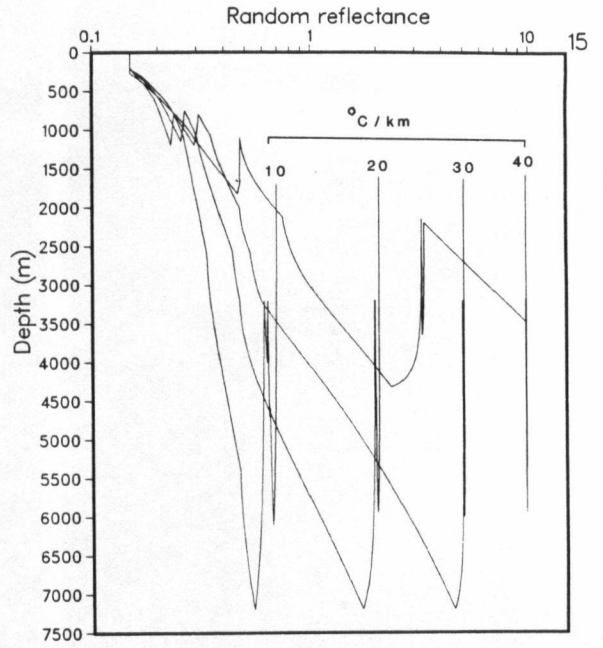


(c)

Figures 18 a), b), c) Northern Eagle Plain. Lower and Upper Cretaceous strata (Mount Goodenough Formation, map unit Kwr and Eagle Plain Group) have never entered the oil window.



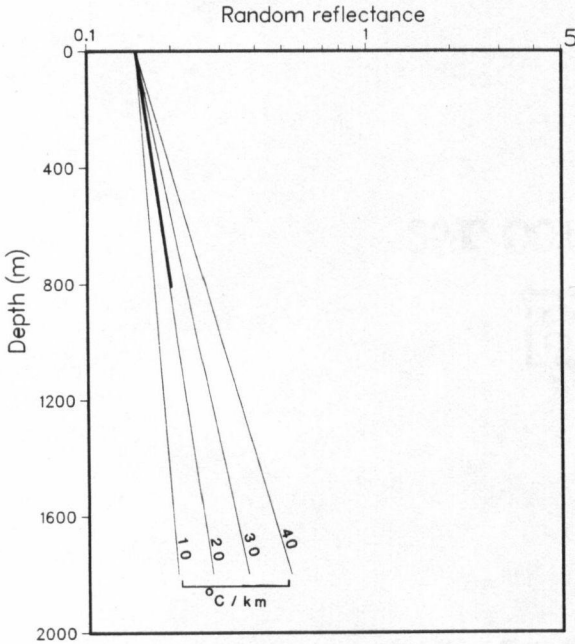
(a)



Socony Mobil WM N. Cathedral B-62.

Tatsieta Formation

(b)



(c)

Figures 19 a), b), c) Western Eagle Plain. Devonian (Tatsieta, Ogilvie, Canol and Imperial Formations) and Carboniferous (Ford Lake Shale) strata entered the window in Late Carboniferous time. The Devonian sequence exited the oil window in Permian time; Carboniferous strata left the oil window during the Late Cretaceous.

b. Thickness of Eroded Section

The thickness of eroded section can be calculated by extrapolating the measured maturation gradients to 0.15% Rorand. This value, 0.15% Rorand, is close to the lowest DOM measured in the Eagle Plain (0.16% Rorand) and is considered the 'zero DOM' (see also England and Bustin, 1986 and Bustin, 1986). An inherent assumption in calculating the amount of removed overburden is that the measured maturation gradient is representative of the maturation gradient of the eroded section. Inasmuch as the measured maturation gradients do not change across subsurface unconformities (erosional surfaces; Figs. 4d, e, h-k), such an assumption is reasonable in the study area.

The amount of eroded section at the I-50 well in western Peel Plateau (Fig. 4 c) is calculated by extrapolating the maturation gradient measured in Devonian strata; a maturation gradient could not be calculated for Lower Cretaceous strata due to a poor fit of reflectance data. A substantial increase in the DOM across the contact of Lower Cretaceous and Upper Devonian strata at the I-50 well (0.26% to 0.42% Rorand) indicates that maturation of pre-Aptian strata is mainly pre-Aptian, as discussed in Appendix C (on file in geology department, UBC).

The thickness of eroded section varies from 0.7 to 4.7 km based on interpretation of measured maturation gradients. In Peel Plateau, approximately 1.7 km of post-Upper Devonian section has been eroded. In eastern Eagle Plain, the amount of removed post-Carboniferous overburden is on the order of 2.6 to 2.8 km whereas in western Eagle Plain, up to 4.7 km of coeval strata have

been eroded. In northwestern Eagle Plain, about 3.5 km of post mid-Cretaceous section has been eroded which is almost three times the amount of coeval overburden which has been removed in southern Mackenzie Delta (1.1 km). Estimates of the eroded Upper Cretaceous section vary significantly from central to northern Eagle Plain (0.7 to 3.4 km) and thus help define Late Cretaceous depositional patterns.

(i) Consideration of Sedimentation and Denudation Rates

In order to determine if the amount of eroded section calculated by extrapolation of the measured maturation gradients is reasonable, the amount of section that could be deposited and eroded has been estimated by using sedimentation and denudation rates calculated from the preserved section in the study area. Appendix C (on file in geology department, UBC) summarizes the details of these calculations and discusses the implications of thickness of eroded section with respect to depositional patterns and paleogeothermal gradients. Table II summarizes the results of these calculations and shows that it is geologically reasonable to deposit and subsequently erode at least the amount of eroded section calculated by extrapolation of measured maturation gradients.

In Peel Plateau, sedimentation rates of 78 to 90 m/Ma during the Jurassic to Berriasian and 26 to 30 m/Ma in Barremian to Late Cretaceous time could deposit 1.5 to 2.4 km of sediment, which agrees with the amount of eroded section (1.7 km) calculated by extrapolating the measured maturation gradients (Figs. 4b and c). The amount of eroded post-Carboniferous section in Eagle Plain

(2.6 to 4.7 km) agrees with estimates of the missing section (4.1 to 5.9 km) derived from sedimentation rates of 30 to 35 m/Ma during the Permian, 13 to 15 m/Ma in the Jurassic to mid-Hauterivian, 72 to 83 m/Ma during late Hauterivian to Albian time and 98 to 113 m/Ma in Late Cretaceous time. Estimates of eroded Upper Cretaceous section (0.7 to 2.2 km) in Eagle Plain concur with the amount of eroded section (2 to 2.3 km) calculated from sedimentation rates of 98 to 113 m/Ma during the Late Cretaceous, except in northern Eagle Plain where 3.4 to 3.5 km of removed Upper Cretaceous overburden was calculated by extrapolation of measured maturation gradients. The amount of eroded section calculated for the A-37 well in southern Mackenzie Delta (1.1 km) is about half the amount of missing section (2.1 to 2.3 km) estimated from sedimentation rates of 46 to 53 m/Ma during the Late Cretaceous and 62 to 72 m/Ma in Late Cretaceous to Tertiary time.

Table II. Comparison of calculated thickness of eroded section using sedimentation rates based on the preserved section, to the amount of eroded section calculated by extrapolation of measured maturation gradients (see Appendix C for details, on file in geology department, UBC). The unconformity at each well represents the age of the strata in which the well was spudded. Calc. Thick and Sed. Thick. = amount of eroded section, calculated using measured maturation gradients and sedimentation rates respectively. Unconformities: mid-Cret=mid-Cretaceous; Carb=Carboniferous, which includes erosion of Jurassic to Albian and Upper Cretaceous strata at the D-77 well in addition to Permian strata at the B-62 and N-05 wells; Late Dev=Late Devonian in the Peel Plateau which includes erosion of Jurassic to Berriasian strata at the I-50 well, in addition to Barremian to Turonian strata at the H-57 well. The thickness of eroded section at the I-50 well includes the preserved Lower Cretaceous section (0.26 km; 1.2 to 1.4 km calculated from sedimentation rates, plus 0.26 km=1.5 to 1.7 km); pre-Apt=pre-Aptian; Upper Cret=Upper Cretaceous.

<u>Well location</u>	<u>Unconformity</u>	<u>Calc. Thick.</u> <u>(km)</u>	<u>Sed. Thick.</u> <u>(km)</u>
A-37	mid-Cret	1.1	2.1-2.3
B-62	Carb	4.7	5.0-5.9
N-05	"	2.6	5.0-5.9
D-77	Permian	2.8	4.1-4.8
C-18	Upper Cret	1.9	2.0-2.3
J-19	"	2.2	"
N-58	"	1.8	"
J-70	"	3.4	"
O-22	"	0.7	"
H-57	Late Dev	1.7	2.0-2.4
I-50	Late Dev to pre-Apt	1.7	1.5-1.7
N-53	mid-Cret	3.5	2.0-2.3

E. DISCUSSION

1. Interpretation of Paleogeothermal Gradients

The paleogeothermal gradients interpreted from modelling of the maturation gradients in the study area agree with the general geological setting of the deposits. The maturation gradients and calculated paleogeothermal gradients from Peel Plateau (0.32 log Rorand/km, 40 to 45°C/km), southern Mackenzie Delta (0.23 log Rorand/km, 30 to 35°C/km) and eastern, northwestern and north-central Eagle Plain (0.18 to 0.29 log Rorand/km, 20 to 35°C/km) fall within the limits of what is regarded as 'normal' gradients for intracratonic sedimentary basins (20 to 45°C/km; Gretener, 1981).

In the central, western and most northern portion of Eagle Plain, the maturation and interpreted paleogeothermal gradients (10 to 20°C/km) are relatively low but similar to present day gradients in parts of the study area (A.A.P.G., 1976). The low maturation gradients may reflect rapid sedimentation and uplift or, alternatively, low heat flow. Thermal conductivity contrasts cannot explain lower gradients because the gross thermal conductivity differences are small in interbedded sandstones, siltstones and shales comprising the Carboniferous to Upper Cretaceous sequence in Eagle Plain.

The low maturation gradients measured in the Western Canadian Sedimentary Basin (England and Bustin, 1986) and the Gippsland Basin (Shibaoka and Bennet, 1977) have been ascribed to rapid sedimentation and uplift such that an

equilibrium gradient may never have existed. Similarly, the low measured maturation gradients in parts of Eagle Plain may reflect rapid sedimentation and uplift or, alternatively, low paleoheat flow. Paleoheat flow calculated from the maturation gradients (assuming a constant thermal conductivity of $2 \text{ W/m}^\circ\text{C}$), although low (20 to 40 mW/m^2), are not uncommon and have been reported from parts of the Western Canadian Sedimentary Basin (A.A.P.G., 1976), from the Great Plains of the central United States and the Wyoming Basin (Sass et al., 1981). The Eagle Plain coincides in position with the Eagle Fold Belt which lies within a deep re-entrant in the Ogilvie Mountains (part of the Taiga-Nahoni Fold Belt, D.K. Norris, 1985) and has experienced less tectonism than adjacent mountainous areas. Maturation gradients increase from Eagle Plain towards the Richardson and Ogilvie Mountains where the tectonic framework is more complex than in Eagle Plain (D.K. Norris, 1985). Hence, low paleogeothermal gradients in the central, western and northern Eagle Plain may reflect low paleoheat flow associated with relative tectonic stability and/or rapid sedimentation and uplift in the Late Cretaceous.

2. Interpretation of Maturation Levels

The DOM of Upper Cambrian to Upper Cretaceous strata in the study area reflects both the paleogeothermal gradient and the maximum depth of burial. Time-temperature modelling indicates that the maturity level of Upper Cambrian to Upper Cretaceous strata increases from central and north-central to northwestern, western and northern Eagle Plain due to a corresponding increase in the depth of burial (Figs. 11a to 19a). A slight decrease in the DOM of

Lower and Upper Cretaceous strata from south-central to east-central portion of Eagle Plain (Figs. 7i and j) is interpreted to be an effect of deeper burial in the axis of the Upper Cretaceous to Tertiary Eagle Plain intermontane (Martin, 1973) basin. The increase in DOM of Upper Cambrian to Carboniferous strata (Road River Group, Ford Lake Shale, Tatsieta, Kutchin, Ogilvie, Hume, Hare Indian, Canol, Imperial and Hart River Formations), on the other hand, from central to eastern and southeastern Eagle Plain is due to corresponding higher maturation (0.26 to 0.29 log Rorand/km) and interpreted paleogeothermal (30 to 45°C/km) gradients (compare Figs. 15c, 16c and 17c to 13c and 14c).

In Peel Plateau, time-temperature modelling indicates that maturation of Middle to Upper Devonian strata (Hume, Canol and Imperial Formations) increases from east to west due to a corresponding deeper burial both in the Devonian and in Jurassic to Early Cretaceous time (Figs. 9a and 10a).

3. Anomalous Maturation Levels

a. Richardson Mountains

Maturity levels not consistent with regional trends were obtained from Upper Devonian to Lower Cretaceous strata on the west side of the Treeless Creek Fault in the central Richardson Mountains (see Figs. 7d, g-i). The Treeless Creek Fault is one of a series of near-vertical faults comprising the Richardson Fault array; the fault may be southern extension of the Cape Kellet Fault Zone (Norris and Yorath, 1981) which marks a hinge to the west and south of which

the dip and thickness of the Phanerozoic succession increases rapidly (Lerand, 1973). The Richardson Fault Array was active from the Late Proterozoic to Early Carboniferous and again in the Early Tertiary (Norris and Yorath, 1981); up to about 2500 m of vertical separation at the pre-Mesozoic level has been identified in the northern part of the array (Coté et al., 1974). Inasmuch as the DOM of Upper Devonian to Lower Cretaceous strata in the central Richardson Mountains reflects the stratigraphic level, the rapid increase in the DOM across the Treeless Creek Fault may be a result of deeper burial due to rapid subsidence caused by foundering of graben blocks within the Richardson Fault Array.

High paleoheat flow may explain the rapid increase in maturation levels towards the central Richardson Mountains from Peel Plateau and Eagle Plain. Although maturation gradients could not be measured in the Richardson Mountains due to poor exposure, high paleoheat flow associated with tectonism may have produced high paleogeothermal gradients (greater than $45^{\circ}\text{C}/\text{km}$). Maturation levels of Upper Cambrian to Lower Cretaceous strata in the Richardson Mountains and of Upper Cambrian to Carboniferous strata in the Ogilvie Mountains are generally higher than in Eagle Plain and Peel Plateau. Furthermore, measured maturation gradients in Eagle Plain increase both to the east ($0.26 \log \text{Rorand}/\text{km}$) and to the southeast ($0.29 \log \text{Rorand}/\text{km}$), in the directions of the Richardson and Ogilvie Mountains, respectively. Assuming a constant thermal conductivity of $2.0 \text{ W}/\text{m}^{\circ}\text{C}$, the paleoheat flow on the western flank of the Richardson Mountains is estimated at $70 \text{ mW}/\text{m}^2$ (paleogeothermal gradient= $35^{\circ}\text{C}/\text{km}$) and, on the northern margin of the Ogilvie Mountains, at $80 \text{ mW}/\text{m}^2$ (paleogeothermal

gradient=40°C/km). Such high heat flow is not uncommon in tectonically active areas (see summary by Sass et al., 1981 and Gretener, 1981) and, as discussed above, the Richardson Fault array has been active since late Proterozoic to Early Carboniferous time. Both the Richardson and Ogilvie Mountains are major Tertiary elements (Norris and Yorath, 1981), but high paleoheat flow must have existed prior to Tertiary time because maturation is considered pre-orogenic (pre-Tertiary, as discussed later). Additional regional study is required to resolve whether or not high paleoheat flow and/or deep burial on the downthrown side of normal faults in the Richardson Mountains is responsible for the higher maturation levels. It must also be noted that the pattern of maturation in the Richardson Mountains is probably much more complex than indicated by the present study because the Richardson Fault array consists of a number of blocks that were free to move up, down or laterally (Norris and Yorath, 1981) and consequently experienced different burial and thermal histories over small distances.

b. Campbell Uplift

Anomalously high paleoheat flow associated with basement uplift may explain the relatively high DOM (1.60% Rorand) in Lower Cretaceous strata on the Campbell Uplift and the progressive decrease in DOM away from (0.92% Rorand) the Uplift (Fig. 7i). The Campbell Uplift is one of several elements comprising the Aklavik Arch Complex in which many unconformities attest to prolonged and intermittent tectonic activity involving basement (Norris and Yorath, 1981). Inasmuch as the high calculated maturation gradient on the northwest limb of

the uplift (0.94 log Rorand/km, Fig. 5) suggests a high paleogeothermal gradient (greater than 45°C/km), the Campbell Uplift may represent basement uplift with paleoheat flow greater than 90 mW/m². Such high paleoheat flow is not uncommon in areas of active basement uplift (Gretener, 1981) and is required to attain a high DOM (up to 1.60% Rorand) during a 'cooking time' of about 110 Ma because Lower Cretaceous strata were never deeply buried in the area of the Campbell Uplift (see Young et al., 1976). The gradual decrease in the DOM away from the Campbell Uplift supports the suggestion of a broad, anticlinal feature associated with basement uplift and associated high heat flow.

4. Hydrocarbon Generation Models

a. Regional Variation in Maturation Levels with Respect to Hydrocarbon Generation

The regional variation in maturation levels with respect to hydrocarbon generation (immature, mature and overmature) are illustrated by projecting measured maturation levels (% Rorand and CAI; Fig. 6) onto a cross-section through part of the study area (Fig. 20). Maturation increases with structural complexity from the Interior Platform (Peel Plateau) and Eagle Fold Belt (Eagle Plain) towards the Richardson Anticlinorium (Richardson Mountains) and from the Eagle Fold Belt towards the Taiga-Nahoni Fold Belt (Ogilvie Mountains). Mesozoic strata are immature to marginally mature in the Interior Platform, Eagle Fold Belt and Taiga-Nahoni Fold Belt and mature to overmature in the Richardson Anticlinorium. Paleozoic and Mesozoic strata are overmature on the Campbell Uplift, in the northwestern corner of the Interior Platform. Upper Paleozoic strata

are immature to marginally mature in the central Eagle Fold Belt but are mature to overmature in all other areas of the study. Lower Paleozoic strata are overmature in all regions.

The regional maturity pattern in the study area is further illustrated with a map of the depth to the oil window (Fig. 21). The map was constructed by calculating the depth to the oil window (0.61% Rorand; Waples, 1980) at each well location using the regression line equations in figure 4 and by contouring surface control points. From east to west across Peel Plateau, the depth to the oil window increases slightly, due to the correspondingly thicker Lower Cretaceous fill, but intersects the surface (0 km) in the northeast corner of the study area (toward the Campbell Uplift). In southern Mackenzie Delta, the depth to the oil window increases to over 1 km and then reaches the surface (0 km) to the west, in the Cordilleran orogen. The depth to the oil window progressively decreases from over 1 km in the central Eagle Plain to 0 km in the eastern, western and southeastern Eagle Plain. In the northern and south-central Eagle Plain, the oil window is at depths over 2 km which corresponds to a present day thicker Upper Cretaceous fill and interpreted thicker eroded Upper Cretaceous section in northern Eagle Plain. One effect of the relatively low paleogeothermal gradients in the central Eagle Plain is the great thickness of Carboniferous to Upper Cretaceous strata which have never entered the oil window.

In the Richardson and Ogilvie Mountains, the depth to the oil window intersects the surface, or projects above the surface, which is interpreted to be a result of higher paleoheat flow. High maturation levels in the Richardson Mountains are

also a result of deeper burial due to rapid subsidence associated with the foundering of grabens in the Richardson Fault Array.

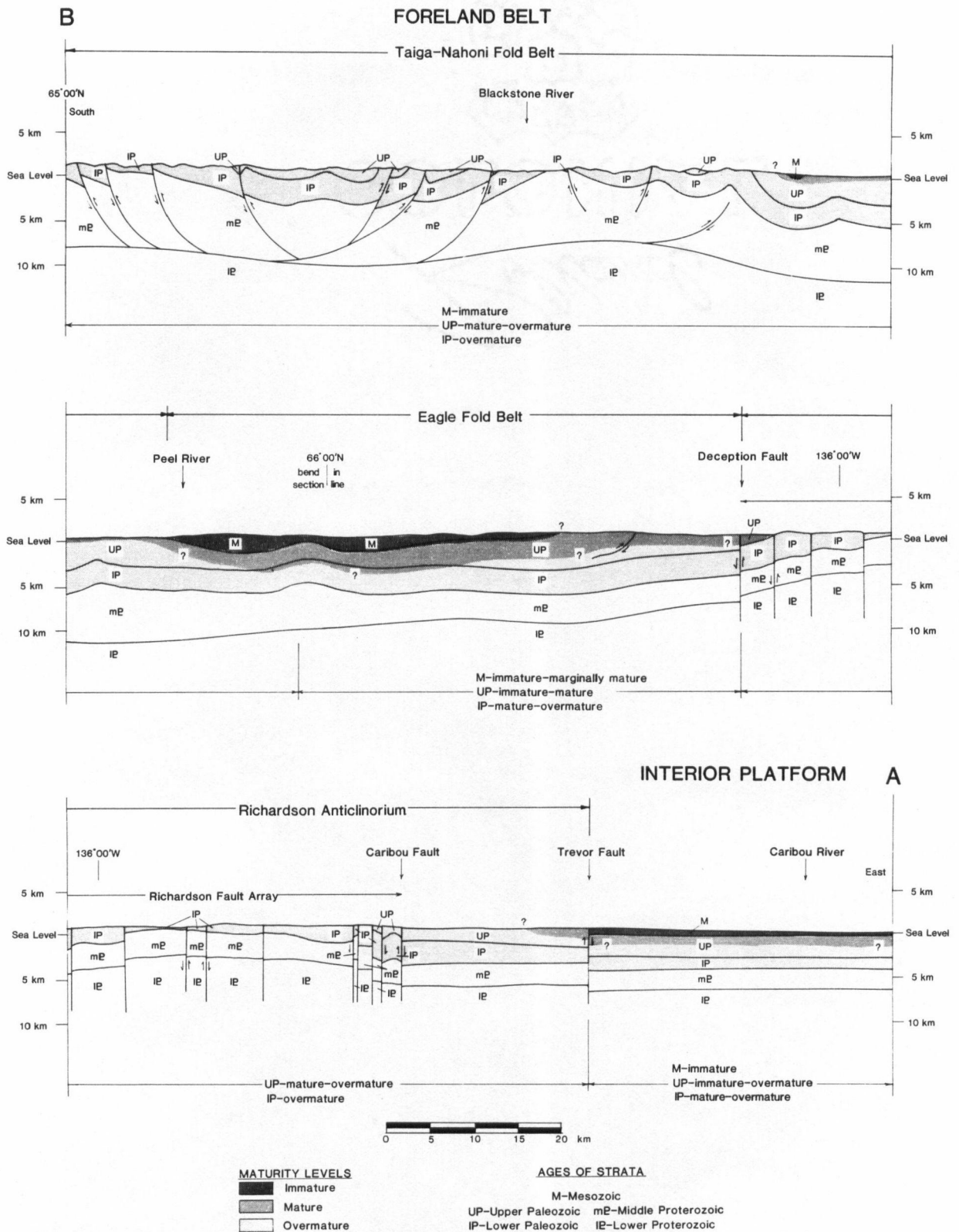


Figure 20. Cross-section through northern Yukon and northwestern District of Mackenzie showing regional maturation pattern with respect to hydrocarbon generation. A-B in figure 6 denotes line of section. Approximate maturation levels are plotted by projecting measured maturation values onto line of section. (Section modified from Norris, 1987, unpublished.)

b. Timing of Hydrocarbon Generation

Potential source rocks are composed mainly of type III OM (see part II of thesis). The timing of hydrocarbon generation has been estimated in the study area using the burial and thermal history plots (Figs. 8 to 19) and the limits of the oil window for type III organic matter (0.61% to 1.35% Rorand, Waples, 1980). In Eagle Plain, Devonian strata entered the oil window in the Late Carboniferous to Permian during deep burial (Figs. 11a to 14a and 19a). The Middle and Upper Devonian sequence exited the oil window in Permian to Late Cretaceous time in western and eastern Eagle Plain (Figs. 13a, 14a and 19a) but are presently within the oil window in northwestern Eagle Plain (Fig. 12a). Carboniferous and Permian strata in western Eagle Plain (Fig. 19a) entered the oil window in the Late Carboniferous but not until the Early Jurassic in southeastern Eagle Plain (Fig. 14a) and the Late Cretaceous to Early Tertiary in northwestern and eastern Eagle Plain (Figs. 12a and 13a). The earlier onset of HC generation in western Eagle Plain than in other parts of Eagle Plain can be explained by deeper burial during the Carboniferous and Permian in the western Eagle Plain. Most of the Carboniferous sequence exited the oil window during the Late Cretaceous in western Eagle Plain (Fig. 19a) but are presently mature in northwestern (Fig. 12a), eastern (Fig. 13a) and southeastern (Fig. 14a) Eagle Plain. Carboniferous, Permian and Lower Cretaceous strata in the central Eagle Plain have not entered the oil window due to a combined effect of shallow burial depths (Figs. 15a, 16a and 17a) and low maturation gradients (0.15 to 0.18 log Rorand/km). Only in the northwestern Eagle Plain (Fig. 12a) are Lower Cretaceous strata mature; here the DOM required for hydrocarbon generation was

attained just after deep burial in Late Cretaceous time.

In western Peel Plateau, the onset of hydrocarbon generation in Devonian strata occurred in Late Devonian to Early Carboniferous time, but not until the Late Jurassic to Early Cretaceous in eastern Peel Plateau as a result of shallower burial depths (Figs. 9a and 10a). The Devonian succession exited the oil window in Early Permian to Late Jurassic time in western Peel Plateau whereas the strata are presently mature in eastern Peel Plateau. Lower Cretaceous strata in western Peel Plateau are immature as a result of shallow burial (Fig. 10a).

In southern Mackenzie Delta, Jurassic strata (lower part of Bug Creek Group) entered the oil window during the Late Cretaceous to Early Tertiary when they reached their maximum burial depths. Strata younger than Middle Jurassic age are immature (Fig. 8a).

(i) Timing of Hydrocarbon Generation Relative to Structure

Inasmuch as Rorand values reflect the stratigraphic rather than structural level of the strata in almost all areas of the study, maturation is considered to be pre-tectonic and thus pre-date Laramide orogeny (Late Cretaceous to mid-Tertiary; D.K. Norris, 1985; Dixon, 1986). Thus, hydrocarbons could potentially have been generated from petroleum source rocks in the study area and hence were available for migration prior to formation of structural traps during Laramide orogenesis. The timing of hydrocarbon generation must also be considered with respect to major erosional episodes which can potentially erode

and/or degrade trapped hydrocarbons. Hydrocarbons generated during Devonian to Late Carboniferous time in western Peel Plateau and western Eagle Plain, and during Jurassic to Early Cretaceous time in southeastern Eagle Plain and eastern Peel Plateau may have been eroded and/or degraded accompanying Columbian (Hauterivian) and/or mid-Cretaceous (Aptian) orogenesis.

F. SUMMARY AND CONCLUSIONS

1. The DOM of Upper Cambrian to Upper Cretaceous strata in the northern Yukon and northwestern District of Mackenzie generally reflects the stratigraphy and maturation is considered to be pre-orogenic (pre-Laramide). The variation in DOM reflects a wide range of maturation gradients in Eagle Plain (0.10 to 0.29 log Rorand/km) and the effects of timing and magnitude of the maximum depths of burial.

2. Coeval strata are generally less mature in southern Mackenzie Delta, Peel Plateau and Eagle Plain than in the Richardson and Ogilvie Mountains. CAI values of 3.5 to 5 occur in Upper Cambrian to Middle Devonian strata. The DOM at the base of Middle Devonian (Givetian) strata varies from 0.79% to 3.75% Rorand whereas the regional variation in DOM at the base of Upper Devonian strata ranges from 0.80% to 2.13% Rorand. Reflectance values vary laterally from 0.50% to 1.69% Rorand at the base of Carboniferous strata and from 0.24% to 1.39% Rorand at the base of Lower Cretaceous strata. Upper Cretaceous strata have the lowest DOM with reflectance values at the base ranging laterally from 0.38% to 0.53% Rorand in Eagle Plain.

3. The DOM of all Upper Devonian to Lower Cretaceous strata increases rapidly from east to west across the Treeless Creek Fault in the central Richardson Mountains. The rapid increase in DOM is interpreted to be, at least in part, a result of deep burial due to rapid subsidence caused by the foundering of grabens within the Richardson Fault Array. Measured maturation gradients in Eagle Plain increase in the directions of the Richardson and northern Ogilvie Mountains. High paleoheat flow prior to Tertiary tectonism may also be responsible for the higher DOMs within strata of the same age in the Richardson and Ogilvie Mountains than in the adjacent areas (Eagle Plain and Peel Plateau).

4. Anomalously high reflectance values for Lower Cretaceous strata (1.60% Rorand) which occur on the Campbell Uplift are interpreted to be a result of high paleoheat flow associated with basement uplift.

5. In Peel Plateau and the southern Mackenzie Delta paleogeothermal gradients ranging from 20 to 45°C/km are interpreted from time-temperature modelling of the measured maturation gradients (0.23 to 0.32 log Rorand/km). Paleogeothermal gradients calculated from measured maturation gradients (0.10 to 0.27 log Rorand/km) increase from 10 to 20°C/km in western and central Eagle Plain to 20 to 45°C/km towards the Richardson and Ogilvie Mountains. The low maturation (0.10 to 0.18 log Rorand/km) and interpreted paleogeothermal (10 to 20°C/km) gradients reflect low paleoheat flow and/or rapid sedimentation and uplift in the Late Cretaceous. As a result of the low paleogeothermal gradients, a great thickness (and volume) of Carboniferous to Upper Cretaceous

strata in the subsurface of the central Eagle Plain are immature ($< 0.61\%$ Rorand).

6. Time-temperature modelling in the study area shows that for Devonian strata, the DOM required for hydrocarbon generation was attained in the Late Devonian to Early Carboniferous in the Peel Plateau but not until Late Carboniferous to Permian time in Eagle Plain. The Devonian sequence exited the oil window in Carboniferous to Early Tertiary time in most of the study area. Carboniferous and Permian strata in western Eagle Plain entered the oil window in the Late Carboniferous but not until Early Jurassic time in southeastern Eagle Plain and Late Cretaceous to Early Tertiary time in northwestern and eastern Eagle Plain, due to corresponding deeper burial during the Late Carboniferous to Permian in southern and western Eagle Plain. Most of the Carboniferous sequence left the oil window during the Late Cretaceous in western Eagle Plain but are still within the oil window in northwestern, eastern and southeastern Eagle Plain. In central Eagle Plain, Carboniferous and Permian strata are immature as a result of shallow burial depths and lower maturation (0.10 to 0.18 log Rorand/km) and thus paleogeothermal gradients (10 to 20°C/km). Lower and Upper Cretaceous strata in most of Eagle Plain have not entered the oil window due to low maturation and thus paleogeothermal gradients (10 to 20°C/km) in central Eagle Plain and shallow burial depths in north-central Eagle Plain. In Peel Plateau and southern Mackenzie Delta, Lower Cretaceous strata are immature as a result of shallow depths of burial whereas in northwestern Eagle Plain, these strata entered the oil window in Tertiary time just after maximum burial.

7. Calculated thicknesses of eroded section are consistent with approximated sedimentation and denudation rates. In Peel Plateau, approximately 1.7 km of post-Upper Devonian section has been eroded whereas the amount of removed post-Carboniferous overburden is on the order of 2.6 to 2.8 km in eastern Eagle Plain and up to 4.7 km in western Eagle Plain. In northwestern Eagle Plain, about 3.5 km of post mid-Cretaceous section has been eroded which is almost three times the amount of coeval overburden which has been removed in southern Mackenzie Delta (1.1 km), either because burial was deeper in the Eagle Plain during Late Cretaceous to Early Tertiary time, or because the calculated maturation gradient in southern Mackenzie Delta is not representative of the paleogeothermal gradient of the eroded section. Estimates of the amount of eroded Upper Cretaceous section vary significantly from central to northern Eagle Plain (0.7 to 3.4 km) and thus help define Late Cretaceous depositional patterns. Consideration of erosion and sedimentation rates calculated from the preserved section of various ages of strata in the study area indicates that it is geologically reasonable to deposit and subsequently erode at least the amount of eroded section calculated by extrapolation of the measured maturation gradients.

IV. REFERENCES

- American Association of Petroleum Geologists, 1976, Geothermal gradient map of North America, 1:5,000,000. American Association of Petroleum Geologists and United States Geological Survey.
- Balkwill, H.R., Cook, D.G., Detterman, R.L., Embry, A.F., Hakansson, E., Miall, A.D., Poulton, T.P. and Young, F.G., 1983. Arctic North America and northern Greenland; in Mesozoic of Arctic North America and Greenland. In: M. Moullade and A.E.M. Nairn, eds., Phanerozoic of the World II, Mesozoic A. Amersterdam: Elsevier, p. 1-31.
- Bamber, E.W. and Waterhouse, J.B., 1971. Carboniferous and Permian stratigraphy and paleontology, northern Yukon Territory, Canada. Bulletin of Canadian Petroleum Geology, 19, p. 29-250.
- Batten, D.J., 1981. Palynofacies, organic maturation and source rock potential for petroleum. In: J. Brooks, ed., Organic maturation studies and fossil fuel exploration. London: Academic Press, p. 201-224.
- Bostick, N.H., 1973. Time as a factor in thermal metamorphism of phytoclasts. Congrès International de Stratigraphie et de Géologie du Carbonifère Septième, Krefeld. August 23-28, 1971. Compte Rendu, 2, Illinois State Geological Survey reprint series 1974-H, p. 183-193.
- Bostick, N.H., 1979. Microscopic measurement of the level of catagenesis of solid organic matter in sedimentary rocks to aid exploration for petroleum and to determine former burial temperature - A review. Society of Economic Paleontologists and Mineralogists, Special Publication 26, p. 17-43.
- Bustin, R.M., 1984. Coalification levels and their significance in the Groundhog Coalfield, north central British Columbia. Coal Geology, 4, p. 21-44.
- Bustin, R.M., 1986. Organic maturity of Late Cretaceous and Tertiary coal measures, Canadian Arctic Archipelago. International Journal of Coal Geology, 6, p. 71- 106.
- Bustin, R.M., Barnes, M.A., and Barnes, W.C., 1985. Organic diagenesis 10. Quantification and modelling of organic diagenesis. Geoscience Canada, 12, p.

1-21.

- Cameron, A.R., Norris, D.K. and Pratt, K.C., 1986. Rank and compositional data on coals and carbonaceous shale of the Kayak Formation, northern Yukon Territory. Geological Survey of Canada, Paper 86-1B, p. 665-670.
- Castano, J.R. and Sparks, D.M., 1974. Interpretation of vitrinite reflectance measurements in sedimentary rocks and determination of burial history using vitrinite reflectance and authigenic minerals. In: R.R. Dutcher and others, eds., Carbonaceous materials as indicators of metamorphism. Geological Society of America, Special Paper 153, p. 31-52.
- Cecile, M.P., Cook, D.G. and Snowdon, L. R., 1982. Plateau overthrust and its hydrocarbon potential, Mackenzie Mountains, Northwest Territories. Geological Survey of Canada, Paper 82-1A, p. 89-94.
- Coté, R.P., Rector, R.J. and Lerand, M.M., 1974. Gulf describes geology of Parsons Lake gas field. Canadian Petroleum, 15, p. 72-78.
- Creaney, S., 1978. Spore fluorescence coloration - a rapid microscopic method of maturation assessment. Geological Survey of Canada, Paper 78-1C, p. 101-103.
- , 1980. The organic petrology of the Upper Cretaceous Boundary Creek Formation, Beaufort-Mackenzie Basin. Bulletin of Canadian Petroleum Geology, 28, p. 112-129.
- Davis, A., 1978. The reflectance of coal. In: C. Karr, ed., Analytical methods for coal and coal products. London: Academic Press, 1, p. 27-28.
- Dixon, J., 1982. Jurassic and Lower Cretaceous subsurface stratigraphy of the Mackenzie Delta-Tuktoyaktuk peninsula, N.W.T. Geological Survey of Canada, Bulletin 349, 52 p.
- , 1986. Cretaceous to Pleistocene stratigraphy and paleogeography, northern Yukon and northwestern District of Mackenzie. Bulletin of Canadian Petroleum Geology, 34, p. 49-70.
- , in press. Mesozoic stratigraphy, Eagle Plain area, northern Yukon. Geological Survey of Canada. Bulletin.

- England, T.D.J. and Bustin, R.M., 1986. Thermal maturation of the Western Canadian Sedimentary Basin, south of the Red Deer River: I) Alberta Plains. *Bulletin of Canadian Petroleum Geology*, 34 , p. 71-90.
- Epstein, A. G., Epstein, J.B. and Harris, L.D., 1977. Conodont color alteration - an index to organic metamorphism. *United States Geological Survey Professional Paper*, 995, p. 1-27.
- Graham, A.D., 1973. Carboniferous and Permian stratigraphy, southern Eagle Plain, Yukon Territory, Canada. *In*: J.D. Aitken and D.J. Glass, eds., *Symposium on geology of the Canadian Arctic*. Geological Association of Canada and Canadian Society of Petroleum Geologists, p. 159-180.
- Gretener, P.E., 1981. Geothermics: Using temperature in hydrocarbon exploration. *American Association of Petroleum Geologists Short Course Note Series* 17, p. 170.
- Gunther, P.R., 1976. A study employing methods to evaluate organic metamorphism of oil generative potential of sediments in the Mackenzie Delta area, District of Mackenzie. *Geological Survey of Canada, Paper* 76-1C, p. 143-152.
- and Meijer-Dress, N.C., 1977. Devonian coal in the subsurface of Great Slave Plain: A guide to exploration for oil and gas. *Geological Survey of Canada, Paper* 77-1A, p. 147-150.
- Hacquebrad, P.A. and Donaldson, J.R., 1974. Rank studies of coals in the Rocky Mountains and inner Foothills belt, Canada. *Geological Survey of Canada, Special Paper* 153, p. 75-94.
- Harris, A.G., 1979. Conodont color alteration, an organo-mineral metamorphic index and its application to Appalachian Basin geology. *Society of Economic Paleontologists and Mineralogists, Special Publication* 26, p. 3-16.
- Hea, J.P., Arcuri, J., Campbell, G.R., Fraser, I., Fuglem, M.O., O'Bertos, J.J., Smith, D.R. and Zayat, M., 1980. Post-Ellesmerian basins of Arctic Canada: Their depocentres, rates of sedimentation and petroleum potential. *In*: A.D. Miall, ed., *Facts and principles of world petroleum occurrence*. Canadian Society of Petroleum Geologists, *Memoir* 6, p. 447-488.
- Hood, A., Gutjahr, C.C.M. and Heacock, R.L., 1975. Organic metamorphism and

the generation of petroleum. American Association of Petroleum Geologists Bulletin, 59, p. 986-996.

- Hume, G.S., 1954. Lower Mackenzie River area, Northwest Territories and Yukon. Geological Survey of Canada, Memoir 273, 118 p.
- and Link, T.A., 1945. Canol investigations in the Mackenzie River area, Northwest Territories and Yukon. Geological Survey of Canada Paper, Paper 45-16, 87 p.
- Hunt, J.M., 1979. Petroleum geology and geochemistry. San Fransisco: W.H. Freeman, 617 p.
- International Committee for Coal Petrography (I.C.C.P.), 1971. International handbook for coal petrology, 1st supplement to 2nd edition. Centre National de la Recherche Scientifique, Paris.
- Jeletsky, J.A., 1958. Uppermost Jurassic and Cretaceous rocks of Aklavik Range, northeastern Richardson Mountains, Northwest Territories. Geological Survey of Canada, Paper 58-2, 84 p.
- , 1960. Uppermost Jurassic and Cretaceous rocks, east flank of Richardson Mountains between Stony Creek and lower Donna River, Northwest Territories. Geological Survey of Canada, Paper 59-14, 31 p.
- , 1961. Uppermost Jurassic and Lower Cretaceous rocks, west flank of Richardson Mountains between the headwaters of Blow River and Bell River, Yukon Territory. Geological Survey of Canada, Paper 61-9, 42 p.
- , 1967. Jurassic and (?)Triassic rocks of the eastern slopes of Richardson Mountains, northwestern District of Mackenzie. Geological Survey of Canada, Paper 66-50, 171 p.
- , 1972. Stratigraphy, facies and paleogeography of Mesozoic rocks of northern Yukon and northwest Mackenzie District, N.W.T. (NTS-197B, 106M, 117A, 116O N 1/2). Geological Survey of Canada, Paper 72-1A, p. 212-215.
- , 1974. Contribution to the Jurassic and Cretaceous geology of northern Yukon Territory and District of Mackenzie, N.W.T. Geological Survey of

Canada, Paper 74-10, 23 p.

- , 1975. Jurassic and Lower Cretaceous paleogeography and depositional tectonics of Porcupine Plateau, adjacent areas of northern Yukon and those of Mackenzie District. Geological Survey of Canada Paper, 74-16, 52 p.
- , 1980. Lower Cretaceous and Jurassic rocks of McDougall Pass area and some adjacent areas of north-central Richardson Mountains, northern Y.T. and northwestern District of Mackenzie, N.W.T. (NTS-116P/9 and 116P/10): a reappraisal. Geological Survey of Canada, Paper 78-22, 35 p.
- Karweil, J., 1956. The metamorphism of coals from the standpoint of physical chemistry. *Zeitschrift der Geologischen Gesellschaft*, 107, p. 132-139. (in German)
- Kunst, H., 1973. The Peel Plateau. In: R.G. McCrossan, ed., *The future petroleum provinces of Canada*. Canadian Society of Petroleum Geologists, Memoir 1, p. 213-244.
- Kalkreuth, W. and McMechan, M., 1984. Regional pattern of thermal maturation as determined from coal rank studies, Rocky Mountain foothills and Front Ranges north of Grande Cache, Alberta - Implication for petroleum exploration. *Bulletin of Canadian Petroleum Geology*, 32, p. 249-271.
- Miall, ed., *Facts and principles of world petroleum occurrence*. Canadian Society of Petroleum Geologists, Memoir 6, p. 523-534.
- Legall, F.D., Barnes, C.R. and Macqueen, R.W., 1981. Thermal maturation, burial history and hotspot development, Paleozoic strata of southern Ontario-Quebec, from conodont and acritarch alteration studies. *Bulletin of Canadian Petroleum Geology*, 29, p. 492-539.
- Lerand, M., 1973. Beaufort Sea. In: R.G. McCrossan, ed., *The future petroleum provinces of Canada*. Canadian Society Petroleum Geologists, Memoir 1, p. 315-386.
- Lopatin, N.V., 1971. Temperature and geologic time as factors in coalification: *Izvestiya Akademii Nauk USSR, Seriya Geologicheskaya*, 3, p. 95-106. (in Russian)

- Martin, H.L., 1972. Upper Paleozoic stratigraphy of the Eagle Plain basin, Yukon Territory. Geological Survey of Canada, Paper 71-14, 54 p.
- , 1973. Eagle Plain basin, Yukon Territory. In: R.G. McCrossan, The future petroleum provinces of Canada. Canadian Society of Petroleum Geologists, Memoir 1, p. 275-306.
- McKenzie, D.P., 1981. The variation of temperature with time and hydrocarbon maturation in sedimentary basins formed by extension. Earth and Planetary Science Letters, 55, p. 87-98.
- Miall, A.D., 1973. Regional geology of northern Yukon. Bulletin of Canadian Petroleum Geology, 21, p. 81-116.
- Mountjoy, E.W., 1967. Upper Cretaceous and Tertiary stratigraphy, northern Yukon and northwestern District of Mackenzie. Geological Survey of Canada, Paper 66-16, 70 p.
- and Chamney, T.P., 1969. Lower Cretaceous (Albian) of the Yukon: Stratigraphy and foraminiferal subdivisions, Snake and Peel rivers. Geological Survey of Canada, Paper 68-26, 71 p.
- Norford, B.S., Brideaux, W.W., Chamney, T.P., Copeland, M.J., Trebold, H., Hopkins, W.S., Jr., Jeletsky, J.A., Johnson, B., McGregor, D.C., Norris, A.W., Pedder, A.E.H., Tozer, E.T. and Uyeno, T.T., 1973. Biostratigraphic determinations of fossils from the subsurface of the Yukon Territory and the districts of Franklin, Keewatin and Mackenzie. Geological Survey of Canada, Paper 72-38, p. 5.
- Norris, A.W., 1985. Stratigraphy of Devonian outcrop belts in northern Yukon Territory and Northwest Territories, District of Mackenzie (Operation Porcupine Area). Geological Survey of Canada, Memoir 410, 81 p.
- Norris, D.K., 1963. Operation Porcupine. Geological Survey of Canada, Paper 63-1, p.1-70.
- , 1980. Bedrock geology of the Dempster Lateral. In: A.D. Miall, ed., Facts and principles of world oil occurrence. Canadian Society Petroleum Geologists, Memoir 6, p. 535-550.

- , 1981a. Geology: Fort McPerson, District of Mackenzie. Geological Survey of Canada, Map 1520A.
- , 1981b. Geology: Arctic Red River, District of Mackenzie. Geological Survey of Canada, Map 1521A.
- , 1981c. Geology: Bell River, Yukon Territory-Northwest Territories. Geological Survey of Canada, Map 1519A.
- , 1981d. Geology: Eagle Plain, Yukon Territory. Geological Survey of Canada, Map 1523A.
- , 1981e. Geology: Aklavik, District of Mackenzie. Geological Survey of Canada, Map 1517A.
- , 1981f. Geology: Porcupine River, Yukon Territory. Geological Survey of Canada, Map 1522A.
- , 1982a. Geology: Hart River, Yukon Territory. Geological Survey of Canada, Map 1527A.
- , 1982b. Geology: Ogilvie River, Yukon Territory. Geological Survey of Canada, Map 1526A.
- , 1983. Geotectonic correlation chart 1532A - Operation Porcupine Project area. Geological Survey of Canada.
- , 1985. Eastern Cordilleran foldbelt of northern Canada: Its structural geometry and hydrocarbon potential. *The American Association of Petroleum Geologists*, 69, p. 788-808.
- and Yorath, C.J., 1981. The North American plate from the Arctic Archipelago to the Romanzof Mountains. *In*: E.M. Nairn, M. Churkin, Jr. and F.G. Stehli, eds., *The ocean basins and margins*, 5, chap. 3, *The Arctic Ocean*. New York and London: Plenum Press, p. 37-103.
- and Cameron, A.R., 1986. An occurrence of bitumen in the Interior Platform near Rengleng River, District of Mackenzie. Geological Survey of Canada. Paper 86-1A, p. 645-648.

- Poulton, T.P., 1982. Paleogeographic and tectonic implications of the Lower and Middle Jurassic facies patterns in northern Yukon Territory and adjacent Northwest Territories. In: A.F. Embry and H.R. Balkwill, eds., Arctic Geology and Geophysics. Canadian Society of Petroleum Geologists, Memoir 8, p. 13-28.
- Pugh, D.C., 1983. Pre-Mesozoic geology in the subsurface of Peel River Map area, Yukon Territory and District of Mackenzie. Geological Survey of Canada, Memoir 401, 61 p.
- Read, P., in press. Metamorphic map of Western Canadian Cordillera.
- Ricketts, B.D., 1985. A coal index for Yukon Territory and District of Mackenzie. Geological Survey of Canada, Open File No. 1115.
- Sass, J.H., Blackwell, D.D., Chapman, D.S., Costain, J.K., Decker, E.R., Lawver, L.A. and Swanberg, C.A., 1981. Heat flow from the crust of the United States, Chap. 12. In: Y.S. Toulockian, W.R. Judd and R.F. Roy, eds., Physical Properties of Rocks and Minerals, Volum II-2, McGraw Hill/Cindas, Data Series on Material Properties, p. 503-548.
- Shiboaka, M. and Bennett, A.J.R., 1977. Patterns of diagenesis in some Australian sedimentary basins. Australian Petroleum Exploration Association Journal, 17, p. 58-63.
- Snowdon, L.R., 1987. Petroleum source potential and thermal maturation of Eagle Plain. Geological Survey of Canada, Open File No. 1720.
- Sweet, A.R., 1978. Palynology of the lower part, type section, Tent Island Formation, Yukon Territory. Geological Survey of Canada, Paper 78-1B, p. 31-37.
- Tassonyi, E.J., 1969. Subsurface geology, lower Mackenzie River and Anderson River area, District of Mackenzie. Geological Survey of Canada, Paper 68-25, 207 p.
- Teichmüller, M. and Wolf, M., 1977. Application of fluorescence microscopy in coal petrology and oil exploration. Journal of Microscopy, 109, p. 49-73.
- and Durand, B., 1983. Fluorescence microscopical rank studies of liptinites

and vitrinites in peat and coal, and comparison with results of the RockEval pyrolysis. *International Journal of Coal Geology*, 2, p. 197-230.

Tipper, H.W., Woodsworth, G.J. and Gabrielse, H., 1981. Tectonic assemblage map of the Canadian Cordillera and adjacent part of the United States of America. Geological Survey of Canada, Map 1505A.

Waples, D.W., 1980. Time and temperature in petroleum formation with application of Lopatin's method to petroleum exploration. *American Association of Petroleum Geologists Bulletin*, 64, p. 916-926.

Yorath, C.J. and Cook, D.G., 1981. Cretaceous and Tertiary stratigraphy and paleogeography, northern Interior Plains, District of Mackenzie. Geological Survey of Canada, Memoir 398, 76 p.

Young, F.G., 1971. Mesozoic stratigraphic studies, northern Yukon Territory and northeastern District of Mackenzie. Geological Survey of Canada, Paper 71-1A, p. 245-247.

-----, 1975a. Upper Cretaceous stratigraphy, Yukon Coastal Plain and northwestern Mackenzie Delta. Geological Survey of Canada, Bulletin 249, 83 p.

-----, 1975b. Stratigraphic and sedimentologic studies in northeastern Eagle Plain, Yukon Territory. Geological Survey of Canada, Paper 75-1B, p. 309-323.

-----, 1977. The mid-Cretaceous flysch and phosphatic ironstone sequence, northern Richardson Mountains, Yukon Territory. Geological Survey of Canada, Paper 77-1C, p. 67-74.

----- (ed.), 1978. Geological and Geographical Guide to the Mackenzie Delta Area. Canadian Society of Petroleum Geologists, 158 p.

-----, Myhr, D.W. and Yorath, C.J., 1976. Geology of the Beaufort Mackenzie Basin. Geological Survey of Canada, Paper 76-11, 63 p.

**V. PART II. PETROLEUM SOURCE POTENTIAL OF PHANEROZOIC
STRATA IN NORTHERN YUKON AND NORTHWESTERN DISTRICT OF
MACKENZIE**

A. ABSTRACT

Rock-Eval/TOC analysis and organic petrography have been used to evaluate the petroleum source rock potential of the Phanerozoic succession in the northern Yukon and northwestern District of Mackenzie. Average total organic carbon (TOC) contents are generally low to moderate (0.1 to 2.0%) but organic-rich intervals occur throughout the studied succession. TOC values of up to 14.5% are present in the Upper Cretaceous Eagle Plain Group, values up to 9.5% occur in the Middle Devonian Canol Formation and Upper Cambrian to Lower Devonian Road River Group and values up to 5.0% are present in the Lower Cretaceous map unit Kwr and Mount Goodenough Formation, the Lower Cretaceous and Jurassic Husky Formation, the Jurassic Porcupine River Formation and the Upper Carboniferous Blackie and Hart River Formations and the Ford Lake Shale. The organic matter (OM) is dominantly type III except for minor amounts of type I or II in Lower Paleozoic strata and locally a mixture of type II and III in Middle Devonian, Carboniferous, Jurassic and Lower Cretaceous strata.

The significant deviation in the quality of organic matter (QOM) is a result of variation in the level of organic maturity, the type of organic matter and, in some cases, migration. Average QOM values are generally low to moderate (0.01 to 1.5 mg HC/g Corg) and, along with low to moderate hydrogen indexes (HI,

<300 mg HC/g Corg), suggest poor to moderate petroleum source potential. Relatively few examples of potential oil prone source rocks (type I or type II OM) occur, but these include the upper and lower parts of the Road River Group and some intervals in the Hare Indian, Canol, Hart River, Blackie, Mount Goodenough and Arctic Red River Formations, the Ford Lake Shale, unnamed Carboniferous unit and the map unit Kwr. Gas prone (type III OM) source rocks comprise the Blackie, Husky, Mount Goodenough and Arctic Red River Formations and the Bug Creek Group and map unit Kwr. Carbonaceous samples from the Porcupine River Formation and the Eagle Plain Group also have some gas potential.

For some strata, the variation in source rock quality closely reflects the depositional environment. The distribution of TOC in the Road River Group closely parallels the sedimentology of the strata; graptolite-bearing and siliceous shales of the Loucheux and Vitreekwa Formations of deep water origin (Richardson and Blackstone Troughs) have the highest TOC content. Organic-rich shales containing a mixture of type II and III OM in the Canol Formation coincide with sediments deposited in upwelling zones during widespread transgression across the continental shelf during the Devonian. Variations in TOC content of the Imperial Formation may be related to differences in sedimentation rates between turbidite and deltaic deposition. Organic-rich shales of the Ford Lake Shale which contain a mixture of type II and III OM, are considered to have been deposited on the continental shelf during a transgression in the Early Carboniferous. Jurassic to Lower Cretaceous strata comprising the Bug Creek Group, Husky Formation and Parsons Group are characterized by marine shelf

sediments in which TOC closely mimics variable sediment supply and transgressive and regressive episodes. Terrestrial OM (type III) is abundant in samples with low TOC of the Murray Ridge, Aklavik, Martin Creek, Husky and McGuire Formations which are regressive sequences. High TOC values occur in transgressive desposits of the Richardson Mountain and Husky Formations. Deltaic sediments of the Porcupine River Formation, in part equivalent to the Husky Formation, contain mostly type III OM. The Mount Goodenough and Arctic Red River Formations and the map unit Kwr are low-energy shelf deposits with a wide range of TOC values. Type III OM is dominant in Lower Cretaceous strata; a mixture of type II and III OM in some samples is more typical of marine shale facies comprising parts of the succession. Variations in average TOC (1.4 to 4.9%) in the Eagle Plain Group may be related to local bathymetric highs and lows on the shelf or, alternatively, to significant input of terrestrial OM in a nearshore to inner shelf depositional environment.

B. INTRODUCTION

Organic geochemical evaluation of basins requires identification of potential petroleum source rocks, establishing the degree of organic maturation (DOM) and determining the regional extent of hydrocarbon source rocks and organic facies. The petroleum source rock potential of several organic-rich units in the northern Yukon and northwestern District of Mackenzie has been alluded to previously (Hume and Link, 1945; Tassonyi, 1969; Graham, 1973; Martin, 1973; Kunst, 1973; Coté et al., 1975; Pugh, 1983; A.W. Norris, 1985; and D.K. Norris, 1985) but little or no geochemical data have accompanied these discussions. The

present study is the first systematic attempt to determine the organic content and character, and the petroleum source potential of the Phanerozoic succession in the northern Yukon and northwestern District of Mackenzie.

Microscopic examination of samples combined with organic geochemical analysis can be utilized to assess the origin and hydrocarbon source potential of organic-rich sediments (Espatilié et al., 1977; Hunt, 1979; Durand, 1980; Waples, 1980; Tissot and Welte, 1984; Bustin et al., 1985; and many others). In this study, Rock-Eval pyrolysis and organic petrography are used to identify and quantify petroleum source rocks and to determine the degree of organic maturity (DOM). The regional extent of possible hydrocarbon source rocks and organic facies are documented and, combined with thermal maturity data, are used to delineate areas of potential hydrocarbon generation. The variation in source rock quality appears to closely reflect the interpreted depositional environment of some of the strata and thus help define the regional extent of potential hydrocarbon source rocks.

This research must be considered a reconnaissance because it is the first attempt to study the thermal maturation and petroleum source potential of Phanerozoic strata in the study area and, because of the large geographic area, complex geologic history and various tectonic elements. It is hoped that this paper will provide working models that can be modified as further study warrants.

C. METHODS

The petroleum source rock characteristics of 240 outcrop and 818 well cutting samples were determined by Rock-Eval pyrolysis (Espitalié et al., 1977) and organic petrography (I.C.C.P., 1971) using standard procedures. Cuttings samples were sieved and the < 2 mm (-10 mesh) portion was washed to remove water-soluble drilling mud contaminants prior to crushing. Outcrop and well cuttings samples were crushed and pulverized with a centrifugal grinding mill to approximately 170 μm (80 mesh) particles. A portion of the pulverized sample was used to prepare organic concentrates for vitrinite reflectance measurements. Sample sizes for Rock-Eval were 100 mg for samples with < about 3% total organic carbon (TOC) and 5 to 50 mg for samples with > about 3% TOC. Included in this study are some 4700 Rock-Eval analyses from Eagle Plain on open file with the Geological Survey of Canada (Snowdon, 1987a).

Interpretation of Rock-Eval data in this study is based on parameters and their experimental limits documented by Espitalié et al. (1985) and Peters (1986). Table III summarizes the measured and calculated parameters derived from Rock-Eval/TOC analysis. TOC is used to indicate organic richness; $(S_1 + S_2)$ indicates the hydrocarbon (HC) potential (genetic potential; Tissot and Welte, 1984, p. 218); $[(S_1 + S_2)/\text{TOC}]$ expresses the relative quality of organic matter (QOM) and the S_2/S_3 ratio is used to indicate the types of products (oil or gas) that will be generated from source rocks at a DOM equivalent to 0.6% (Peters, 1986). The QOM is a measure of the type of OM and thermal maturity; high ratios indicate immature to mature hydrogen-rich strata.

Table III. Measured and calculated parameters derived from Rock-Eval/TOC analysis. OM=Organic matter; HC's=hydrocarbons.

a. Measured parameters.

S₁: HC's generated at $\leq 300^{\circ}\text{C}$

S₂: HC's generated from $300^{\circ}\text{-}600^{\circ}\text{C}$

S₃: Organic CO₂ generated from $300^{\circ}\text{-}600^{\circ}\text{C}$

Tmax: Temperature of maximum rate of evolution of pyrolysis HC's

TOC: Total Organic Carbon = (S₁ + S₂) plus (Organic CO₂ generated from combustion of OM at 600°C after pyrolysis)

b. Calculated parameters.

S₁ + S₂: HC potential or Genetic potential

S₁/(S₁ + S₂): Production Index (PI) or Transformation Ratio; maturity indicator

S₂/S₃: Organic typing parameter; high value = hydrogen-rich OM.

HI: Hydrogen Index = (S₂*100)/TOC; organic typing parameter

OI: Oxygen Index = (S₃*100)/TOC; organic typing parameter

QOM: Quality of Organic Matter = (S₁ + S₂)/TOC; organic typing & maturity indicator, subject to migration effects

A significant spread in the QOM which cannot be related to variations in the DOM or type of organic matter (OM) is considered to reflect the effects of migration of hydrocarbons into or out of the strata (Espitalié et al., 1985). Depletion of S_1 and S_2 values is common in outcrop samples as a result of oxidation of OM (Peters, 1986) and was evident in some field samples collected in the study area. Similarly, oxidation of OM could potentially occur during erosional episodes which are represented by various unconformities in the studied succession. Thus, the QOM of some samples does not closely reflect the regional variation in petroleum potential of a particular horizon.

The Hydrogen Index (HI) and Oxygen Index (OI; Table III) when interpreted in concert with maturation data can be used to define the type of organic matter (Espitalié et al., 1985). Type I refers to kerogen with an HI > 600 mg HC/g Corg whereas type II kerogen is defined by HI values which range from 300 to 600 mg HC/g Corg, assuming a DOM equivalent to about 0.6% Rorand (Espitalié et al., 1985). Relatively low HI values (< 300 mg HC/g Corg) define type III OM (Espitalié et al., 1985). Type I and II OM comprise oil and gas prone kerogen whereas type III kerogen is mostly gas prone (Tissot and Welte, 1984, p. 151-154). Although some recent studies suggest type III OM can contain 10 to 20% liptinite or resinite in a vitrinite matrix and thus may act as effective oil prone source rocks (Snowdon, 1980; Powell and Snowdon, 1983; Snowdon, 1987b), others (Lewan and Williams, 1987) argue that resinites contribute only minor components to conventionally sourced crude oils and are not likely sources of commercial oil deposits. In the present study, liptinite was observed petrographically in some samples from the Eagle Plain Group but it

never comprises a substantial portion of the OM.

The DOM can be approximated from the production index (PI or Transformation Ratio; Tissot and Welte, 1984, p. 218)) and temperature of maximum HC evolution (Tmax; Table III). In general, PI and Tmax values < 0.1 and 435°C , respectively, indicate immature OM (Peters, 1986). The oil zone starts at 435°C for both type II and III OM whereas the wet gas zone begins at about 450°C for type II OM but not until about 465°C for type III OM (Espitalié et al., 1985). Overmature OM is defined by Tmax values $> 465^{\circ}\text{C}$ for type III OM and > 450 to 455°C for type II OM. The Tmax of type I OM is, for the most part, independent of the DOM, and generally ranges from 460 to 470°C (Snowdon, pers. comm., 1987).

PI values between about 0.1 and 0.4 define the oil zone and the PI increases to 1.0 when the HC generation capacity of the kerogen is exhausted, for all types of OM (Peters, 1986). The PI best illustrates the DOM by plotting PI vs. depth (Espitalié et al., 1977; 1985). Anomalously high PI values may indicate HC accumulation whereas anomalously low values indicate depletion (Espitalié et al., 1985). In general, Tmax values can not be determined as accurately if S_2 yields are < 0.2 mg HC/g rock (Espitalié et al., 1985). In the present study, the boundaries of maturity relative to HC generation (immature, marginally mature, mature and overmature) were interpreted based on the correlation and limits of DOM indicators summarized in Bustin et al. (1985) and figure 2 of Macauley et al. (1985).

In order to assess the potential of petroleum source rocks, the regional distribution of organic richness and type, and maturity were examined. Organic richness is best determined as the average TOC content across the thickness of a potential source horizon rather than considering organic richness as a measure of OM concentrated in a discrete sample. Because the smallest thickness determined in the present study is formation thickness, average TOC content, HC potential ($S_1 + S_2$) and QOM [$(S_1 + S_2)/\text{TOC}$] have herein been calculated across the thickness of each formation at different locations. In this way, regional evaluation of each mapped unit can be discussed by considering individual parameters and their combined effects on source rock potential.

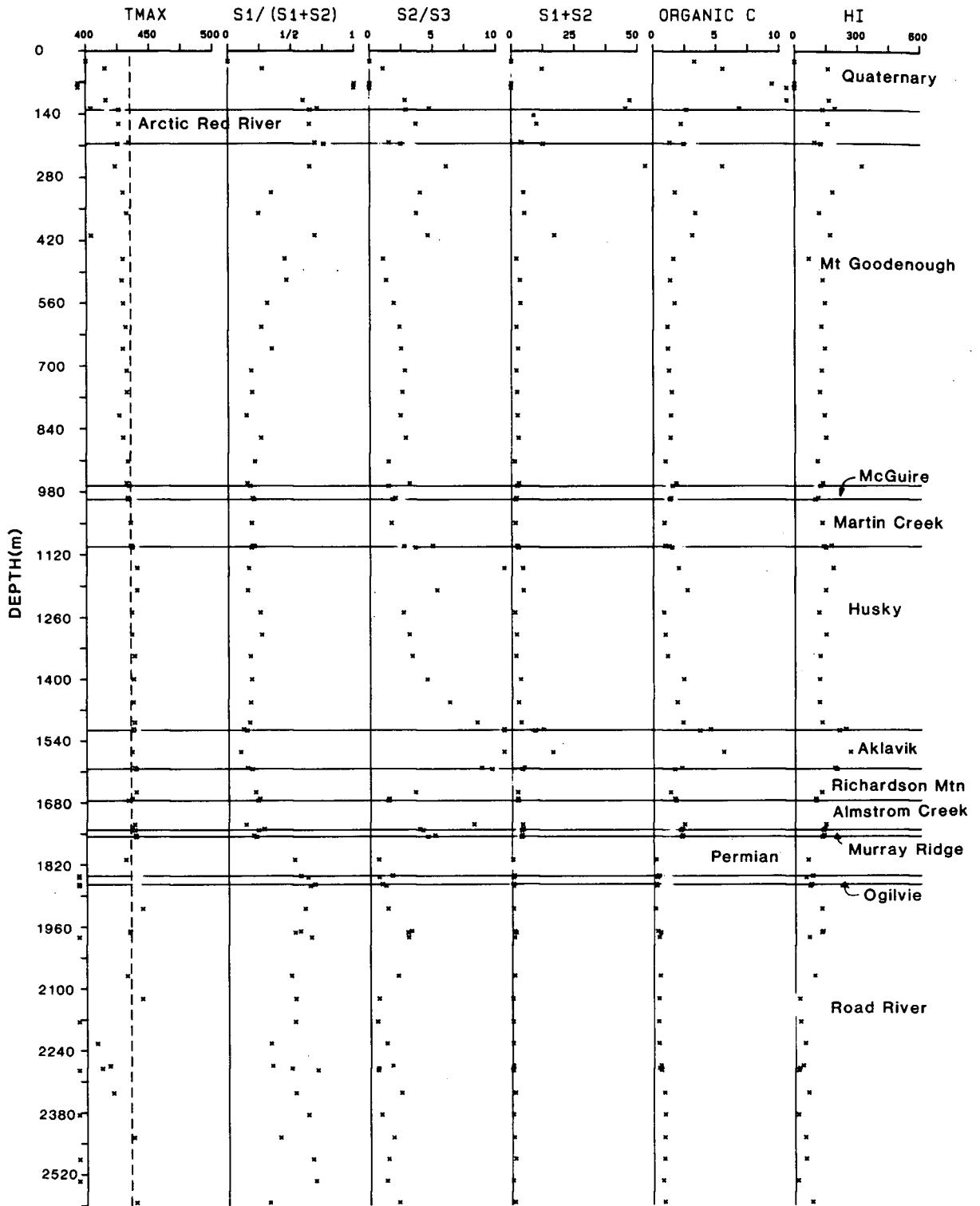
D. RESULTS

Rock-Eval logs, histograms of TOC content and modified van Krevelen diagrams (HI versus OI plots) are plotted in figures 22, 23 and 24 respectively. Appendix D (on file in geology department, UBC) contains Rock-Eval data for individual samples. Table IV summarizes the classification and maturation of specific stratigraphic units. In figures 25 to 34 inclusive, the lateral variation in organic richness (TOC), type (QOM) and maturity ($\% R_{o_{rand}}$) and conodont alteration index; CAI) for specific stratigraphic horizons are plotted.

Figure 22. Rock-Eval logs for 12 wells examined in study area. Location of wells is shown in figure 35 and well names are identified on each log. Tmax, S₁, S₂, S₃, HI (Hydrogen Index) and organic C (total organic carbon) are all standard Rock-Eval parameters (Espatilié et al., 1977).



SHELL AKLAVIK A-37

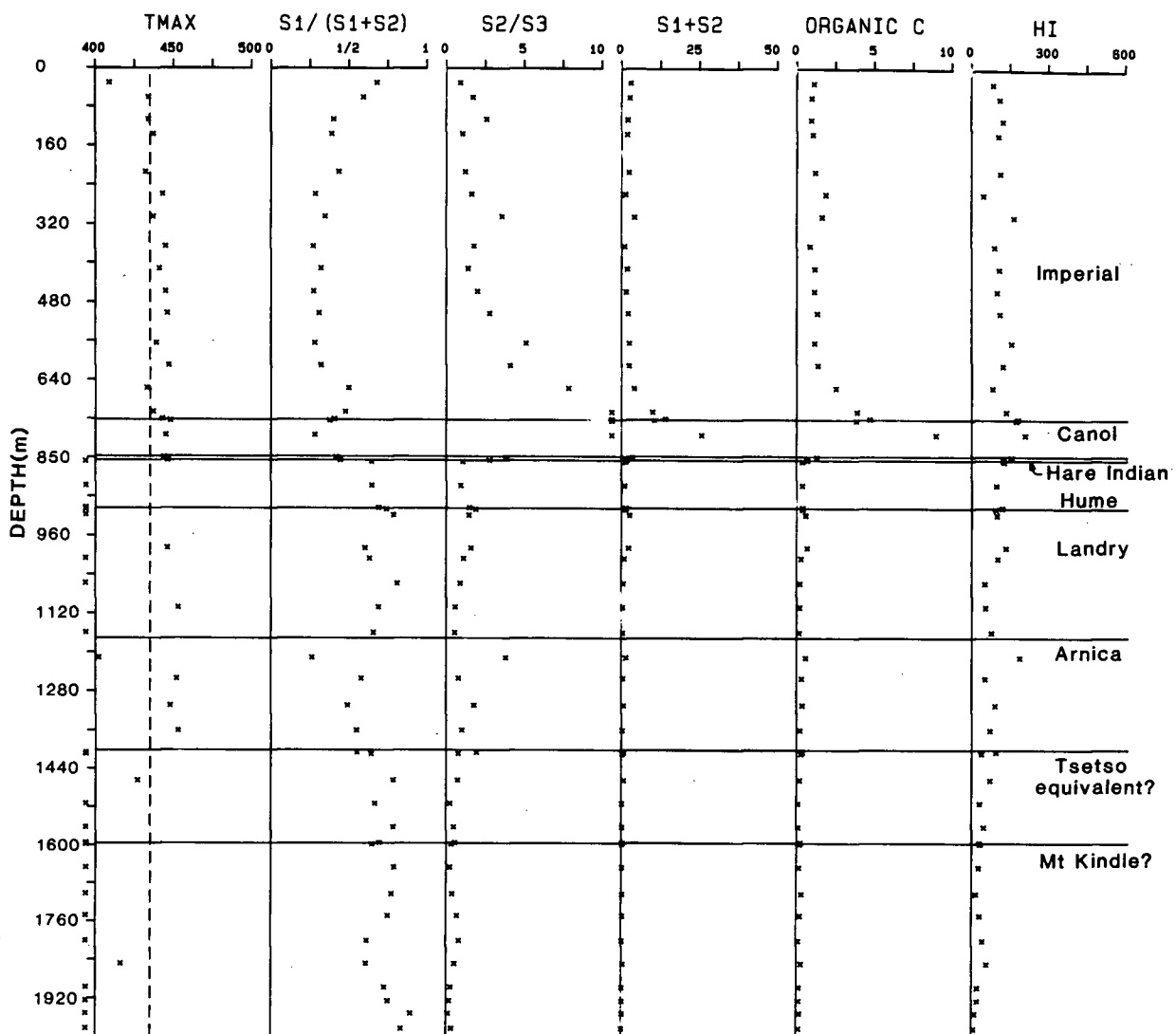


(a)

a) Southern Mackenzie Delta.

*

SHELL TREE RIVER E. H-57

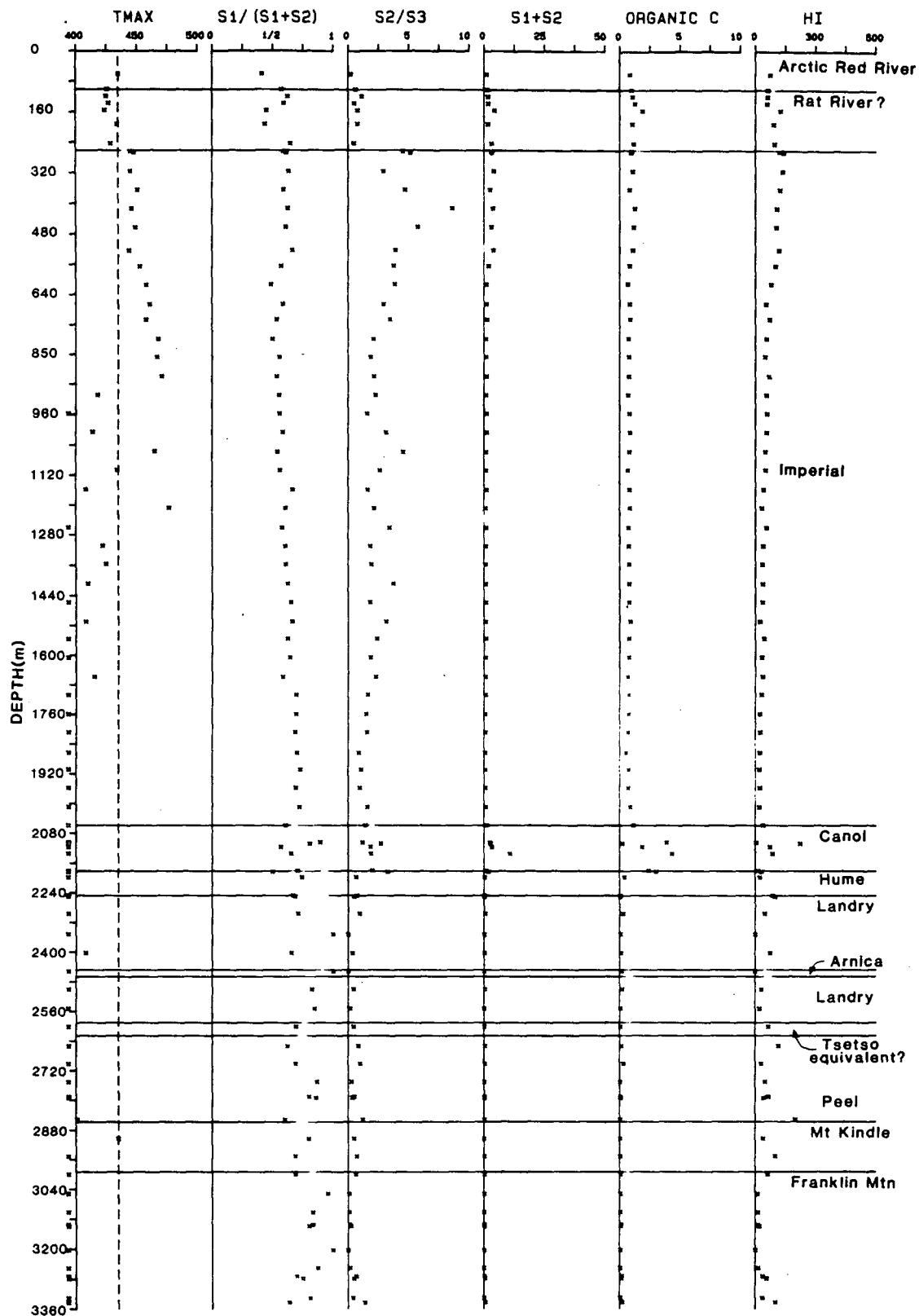


(b)

b) Eastern Peel Plateau.



IOE STONY I-50

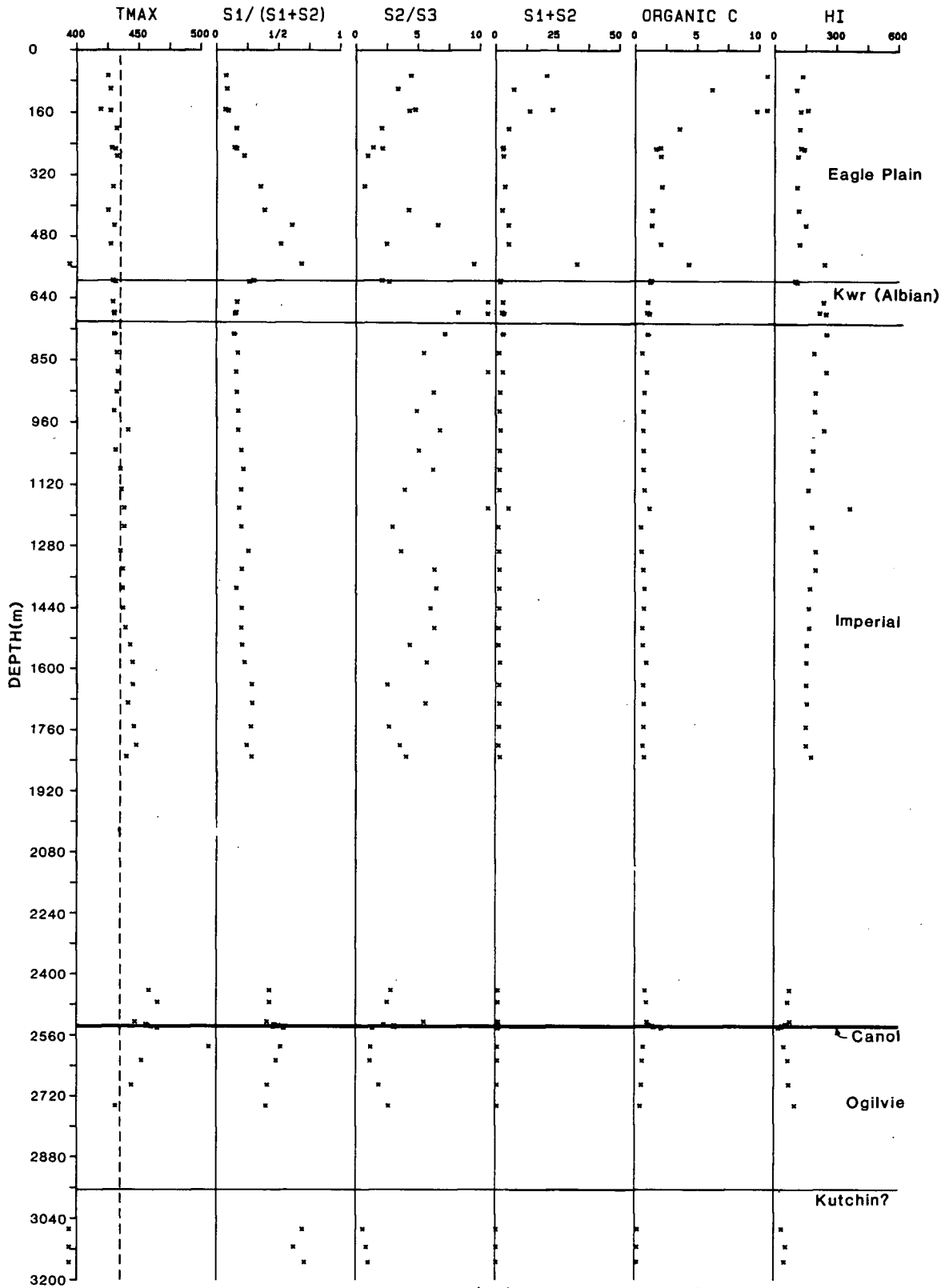


(c)

c) Western Peel Plateau.



SHAEFFER CREEK 0-22

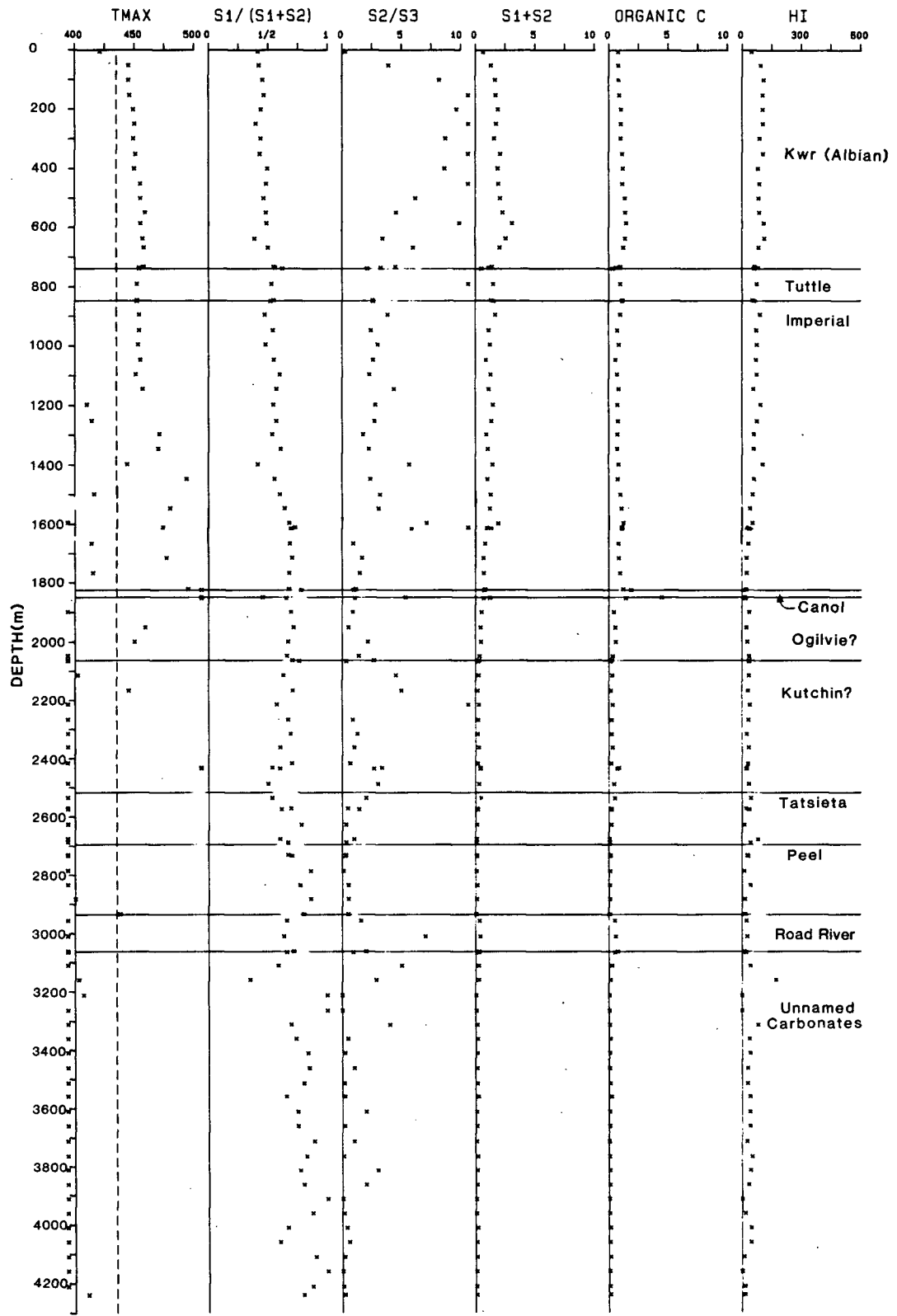


(d)

d) North-central Eagle Plain.



WESTERN MINERALS N. HOPE N-53

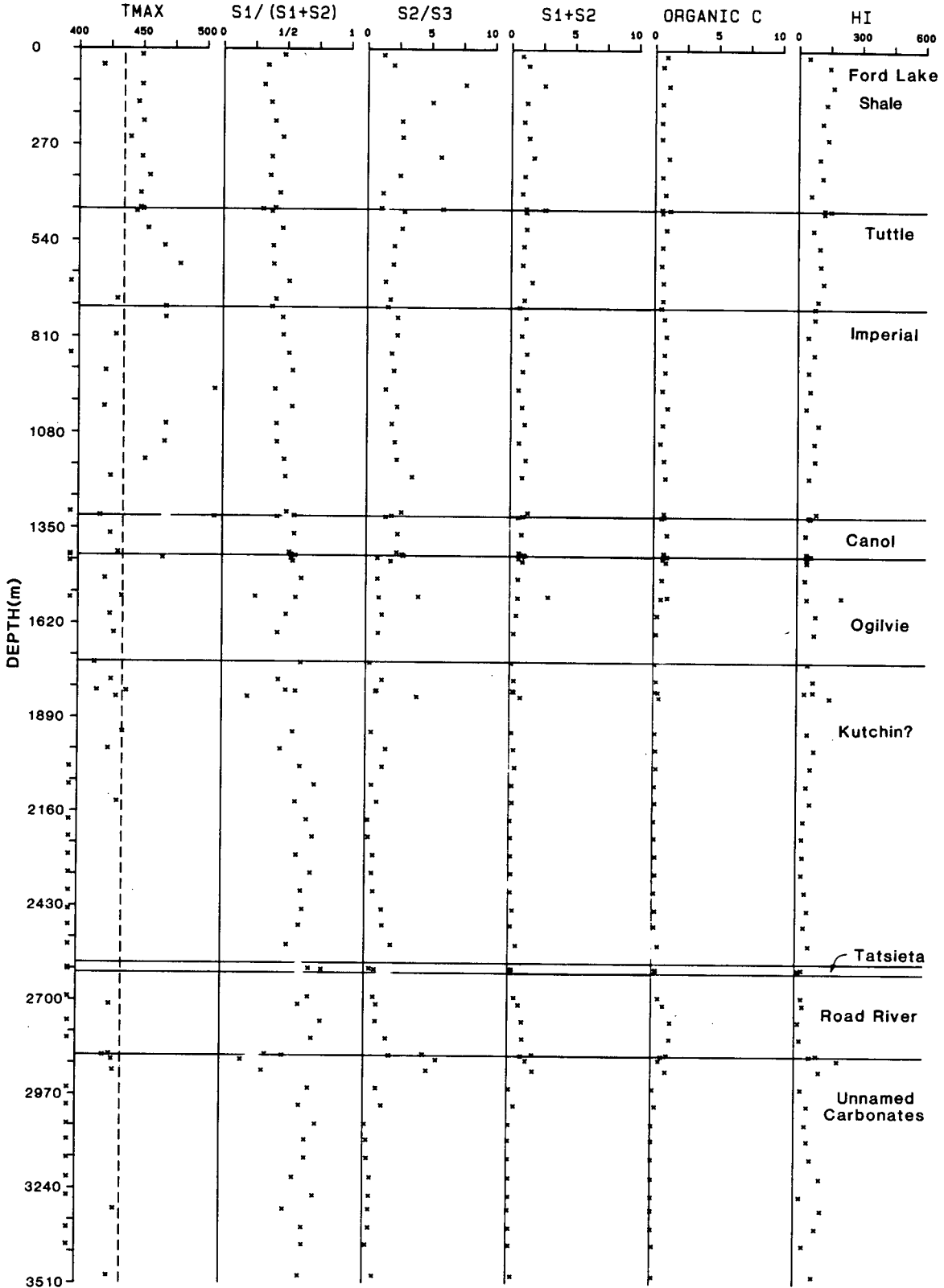


(e)

e) Northwestern Eagle Plain.



SOCONY MOBIL WM S. TUTTLE N-05

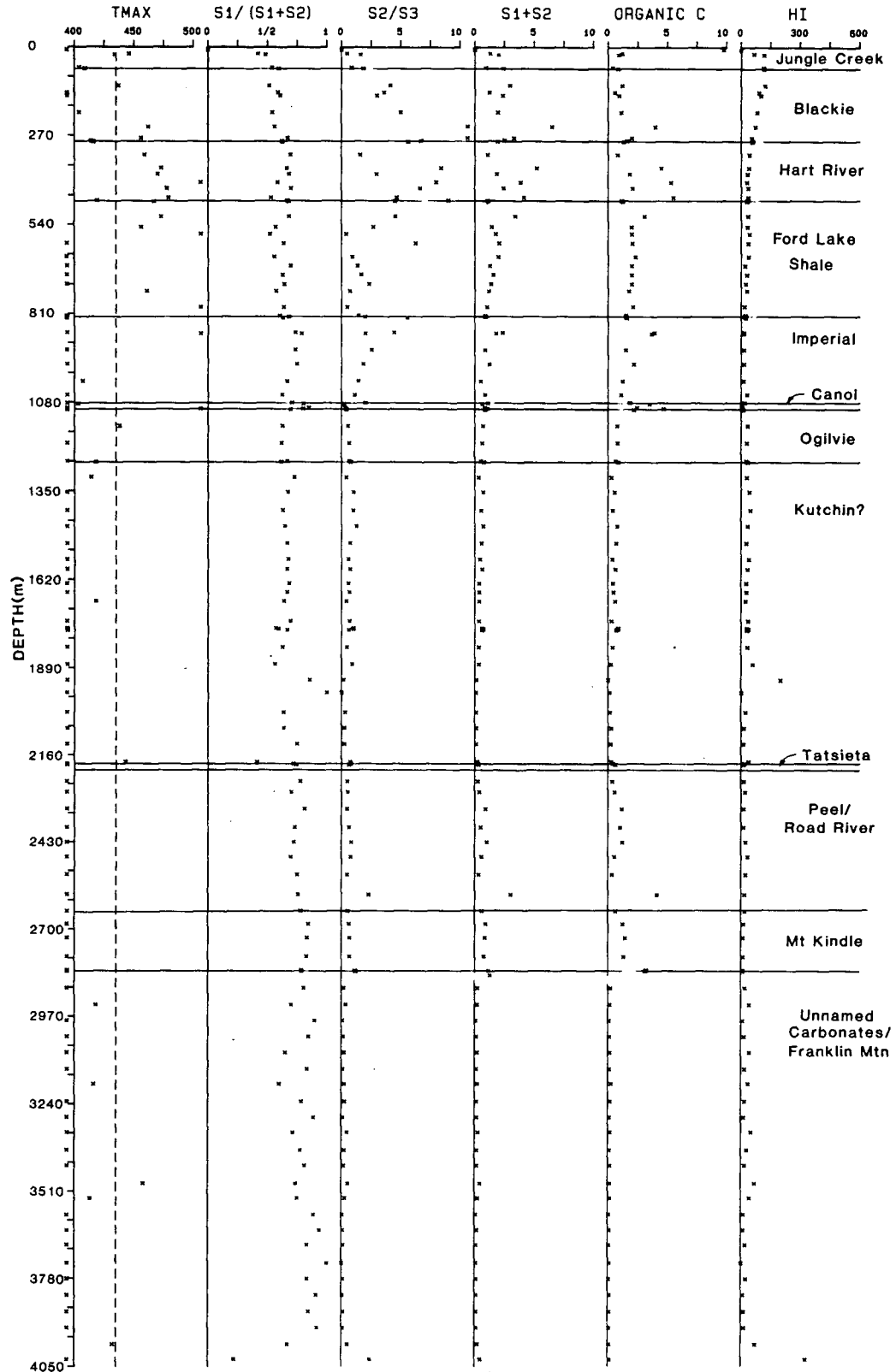


(f)

f) Eastern Eagle Plain. The interval indicated by the Ford Lake Shale and Tuttle Formation is now considered to be part of the Imperial Formation (Snowdon, 1987a).



SOBC BLACKSTONE YT D-77

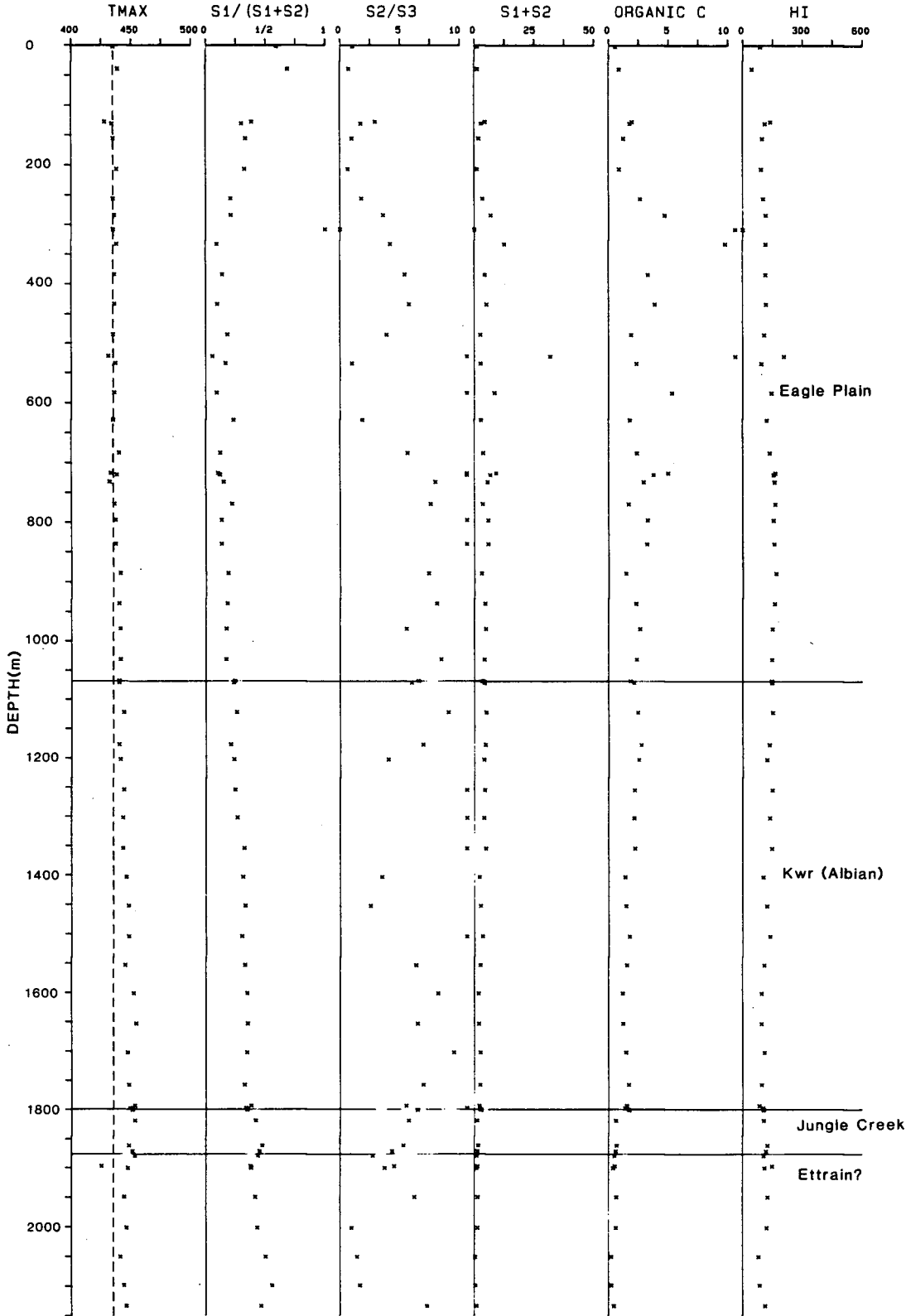


(g)

g) Southeastern Eagle Plain.



MURPHY MESA BP S. WHITESTONE N-58

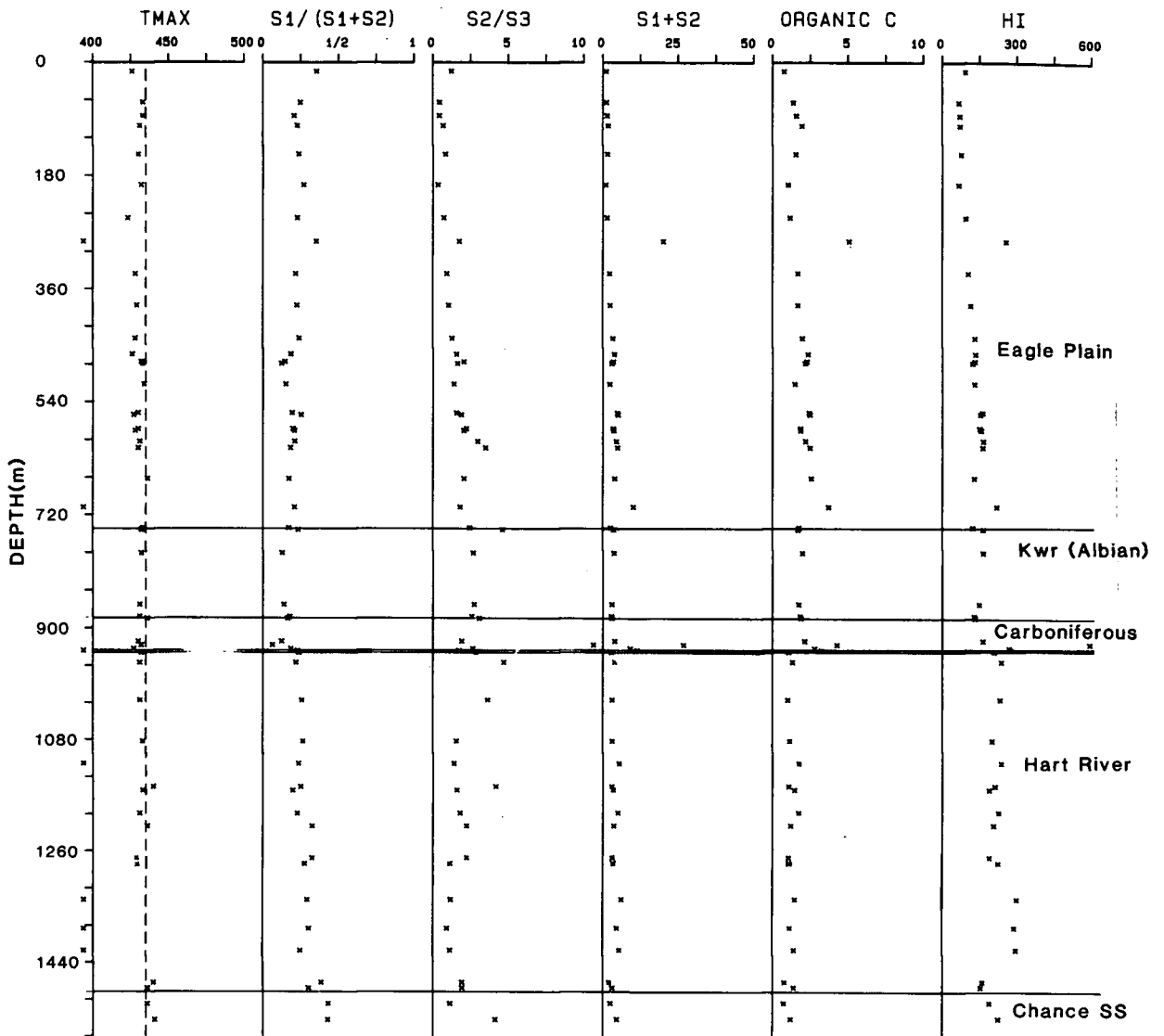


(h)

h) Central Eagle Plain.



CANOE RIVER E. CHANCE C-18

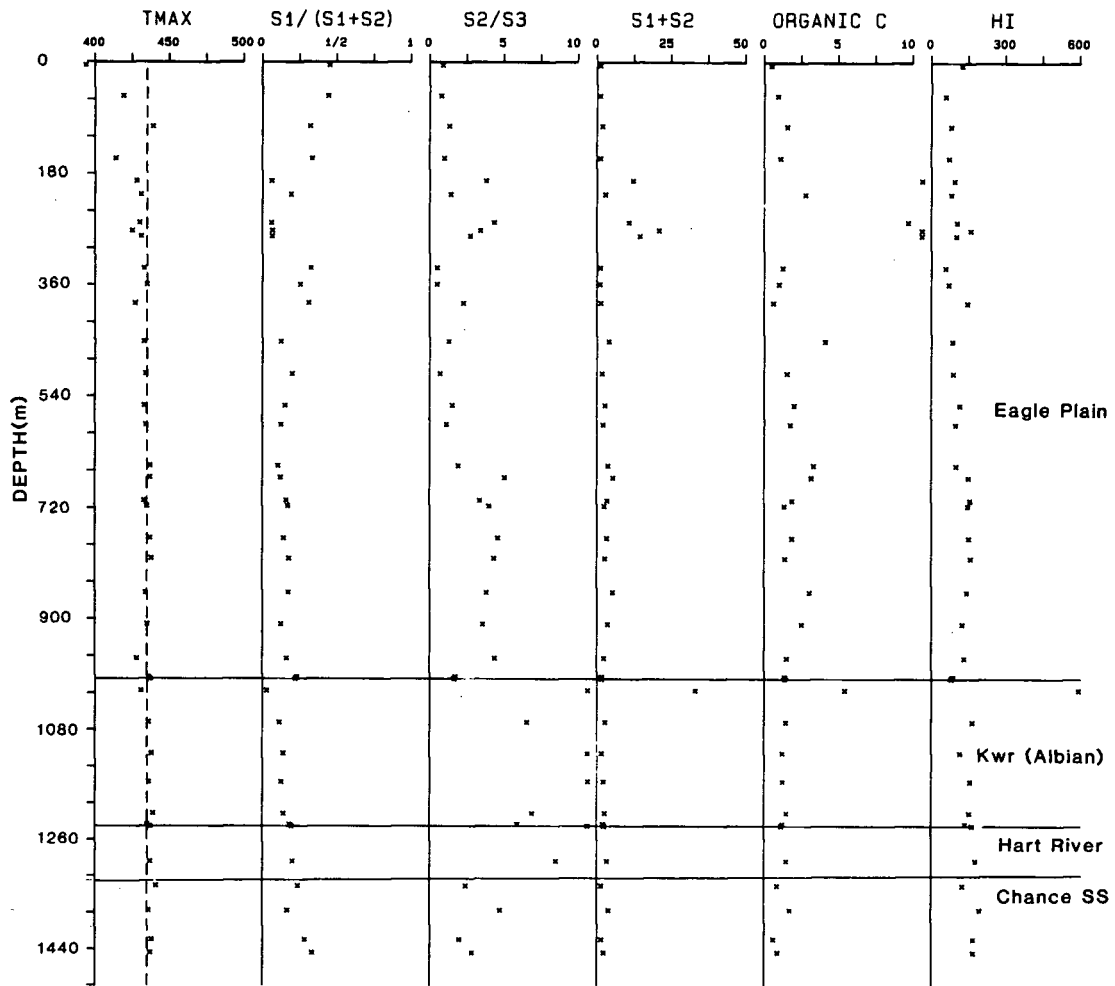


(i)

i) Central Eagle Plain.



CANOE RIVER CHANCE J-19

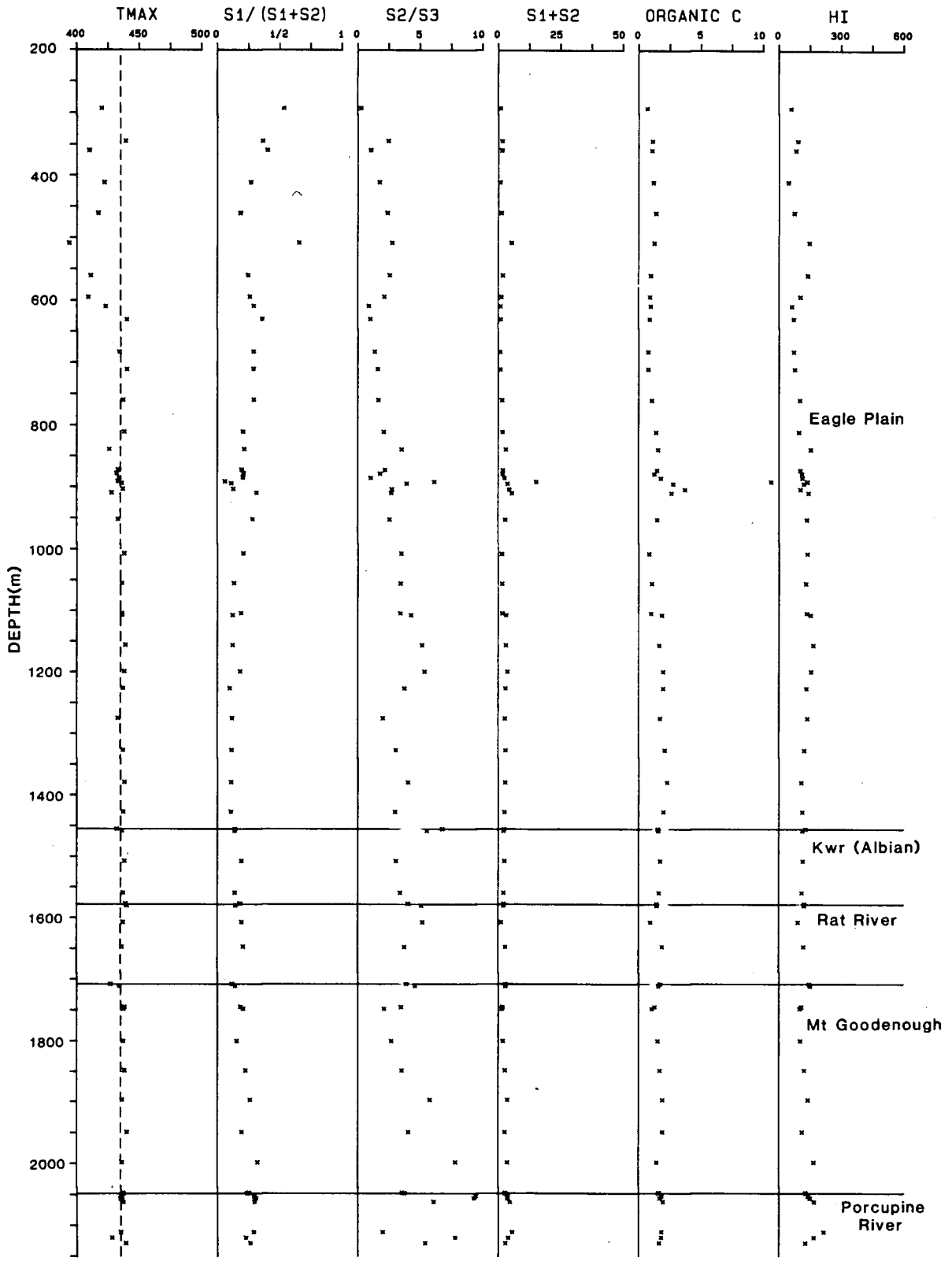


(j)

j) Central Eagle Plain.



CHEVRON SOBC WM WHITEFISH J-70

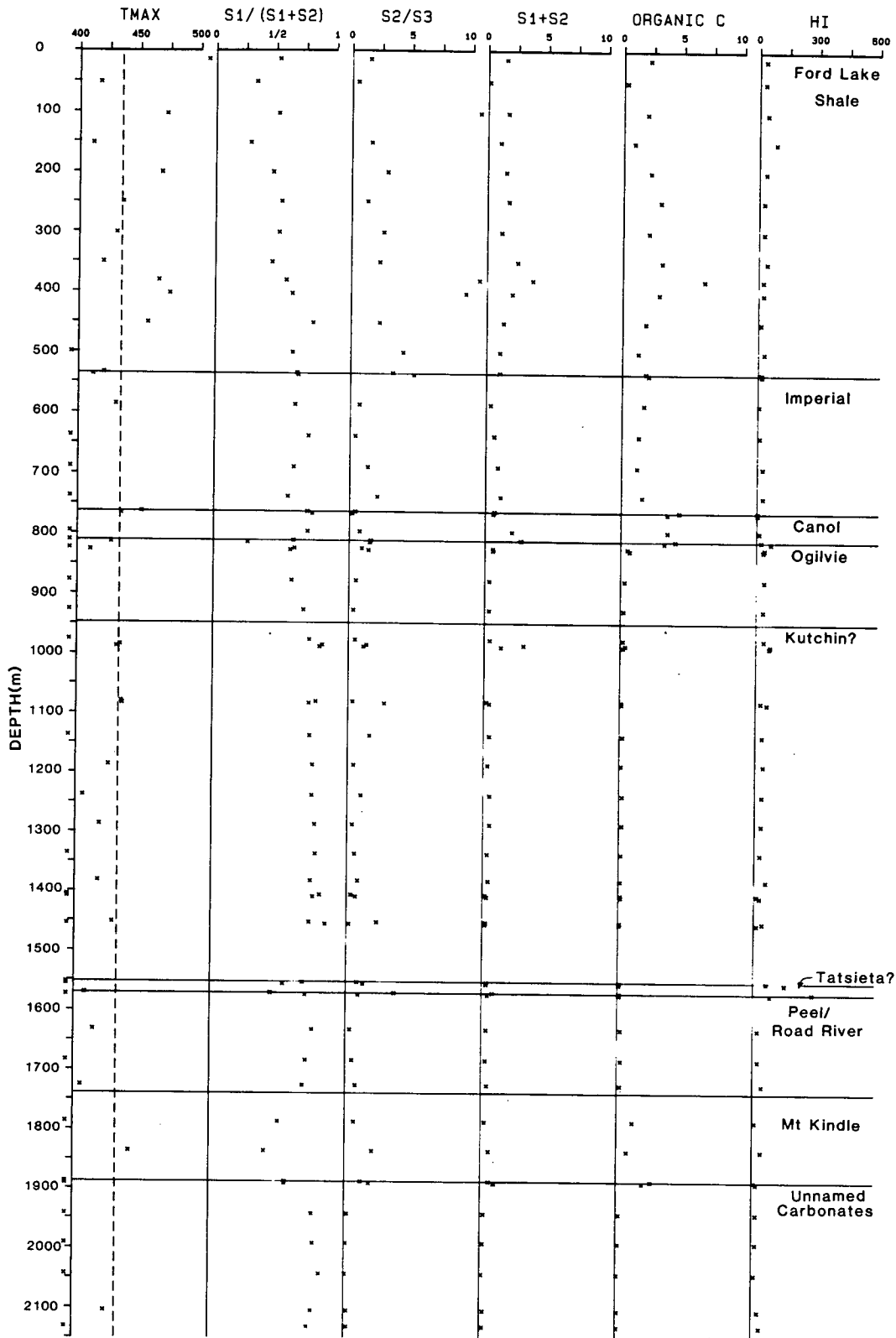


(k)

k) Northern Eagle Plain.



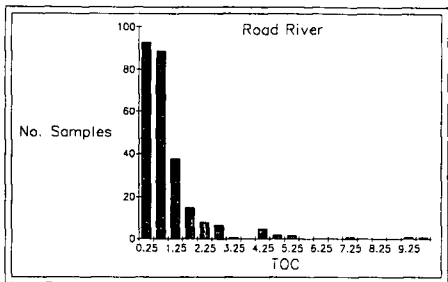
SOCONY MOBIL WM N. CATHEDRAL B-62



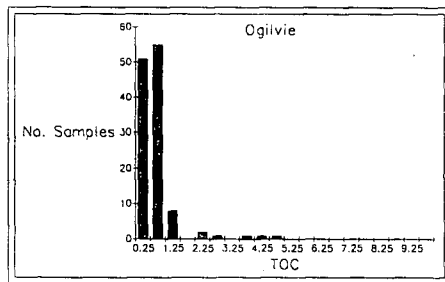
(1)

1) Western Eagle Plain.

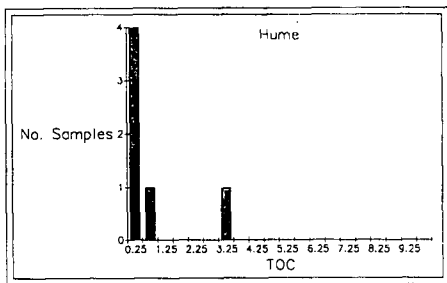
Figure 23. Histograms of total organic carbon (TOC) content of some formations and groups examined in study area. Data includes outcrop and well cuttings samples. Individual TOC values are tabulated in Appendix D. TOC is expressed as weight per cent. Formation, group and unit names are indicated on individual plots.



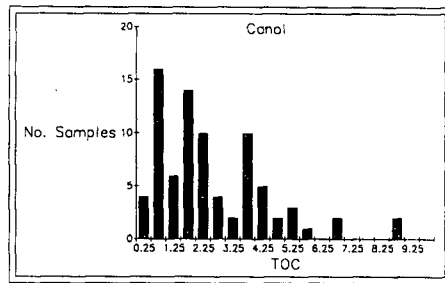
(a)



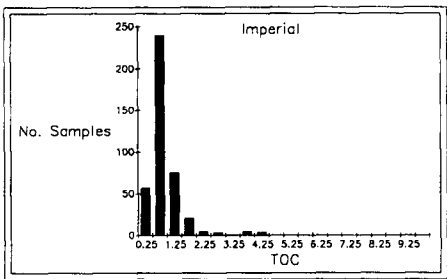
(b)



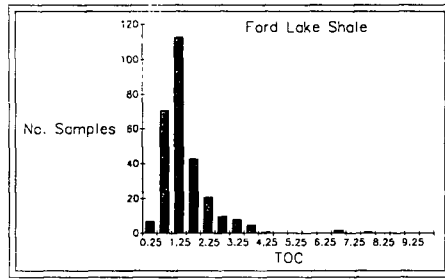
(c)



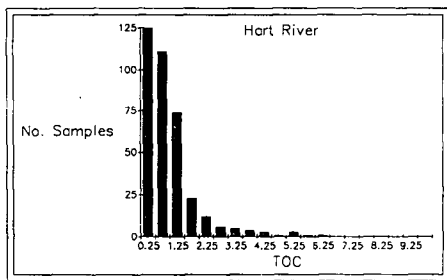
(d)



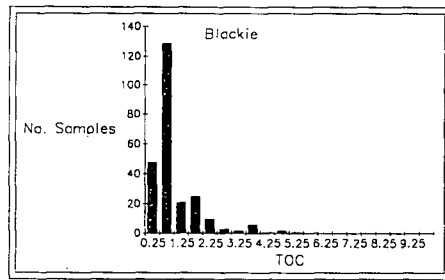
(e)



(f)

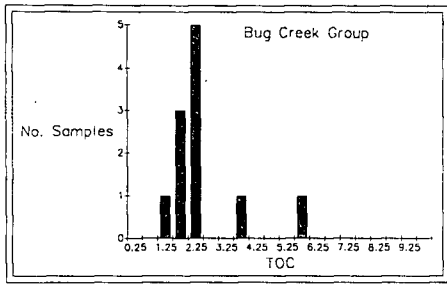


(g)

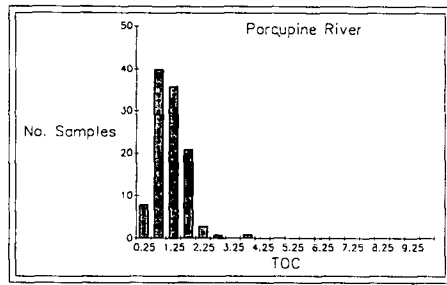


(h)

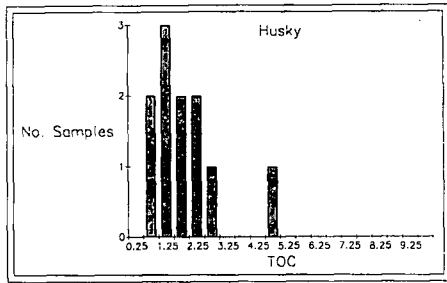
Figure 23



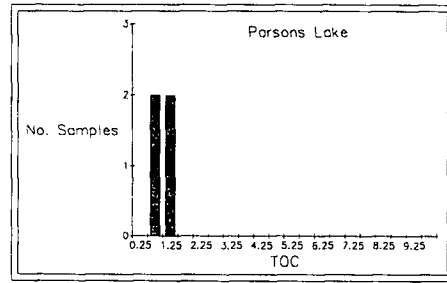
(i)



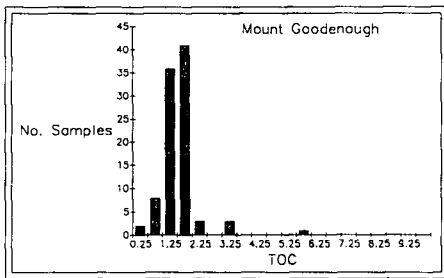
(j)



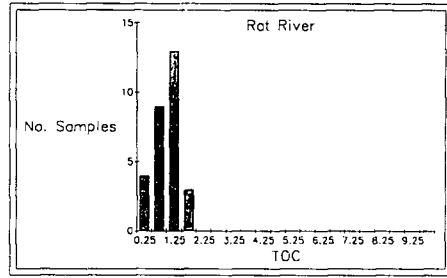
(k)



(l)

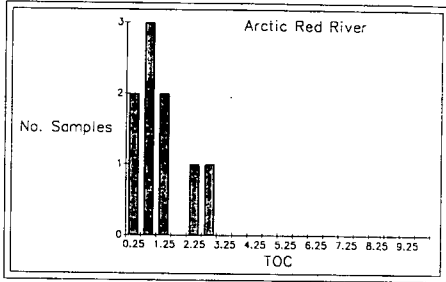


(m)

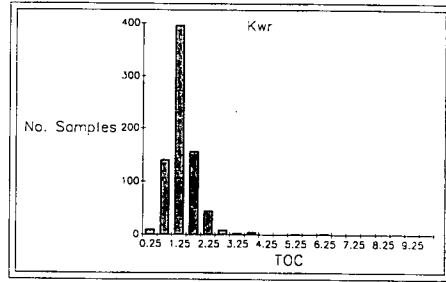


(n)

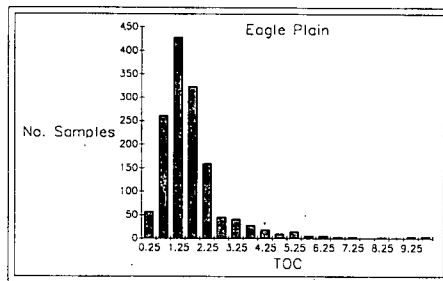
Figure 23 cont'd.



(o)



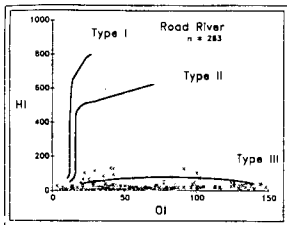
(p)



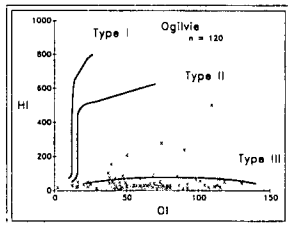
(q)

Figure 23 cont'd.

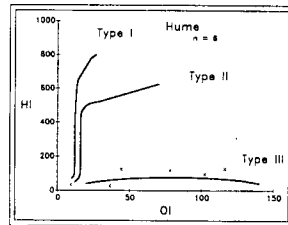
Figure 24. Modified van Krevelen diagrams (Hydrogen Index (HI) versus Oxygen Index (OI)) for some formations and groups examined in study area. Data includes outcrop and well cuttings samples. Individual HI and OI values are tabulated in Appendix D. HI units=mg HC/g Corg; OI units=mg CO/g Corg. Formation, group and unit names are indicated on individual plots. 'n'=number of samples.



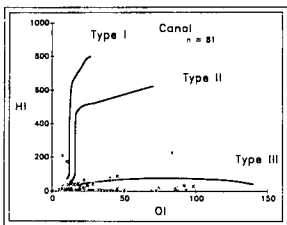
(a)



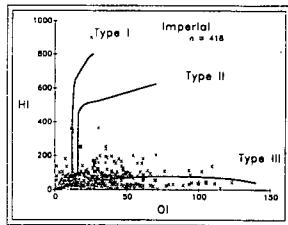
(b)



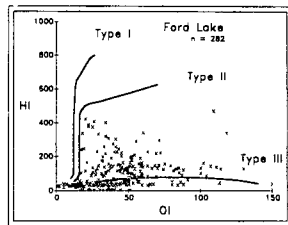
(c)



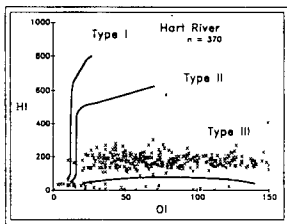
(d)



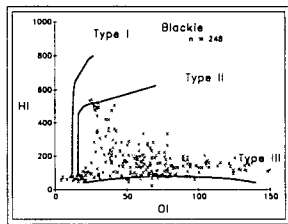
(e)



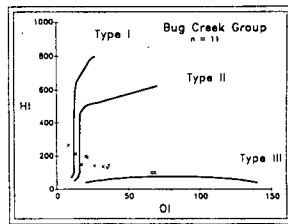
(f)



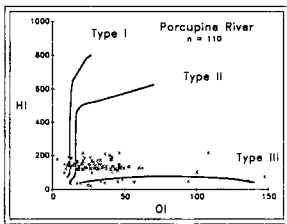
(g)



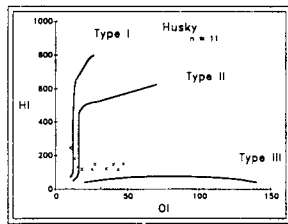
(h)



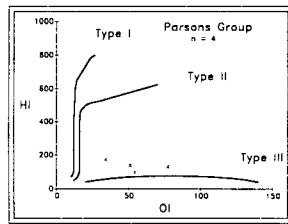
(i)



(j)

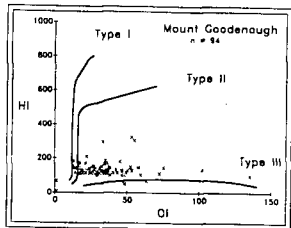


(k)

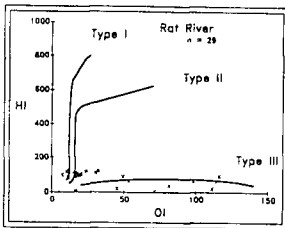


(l)

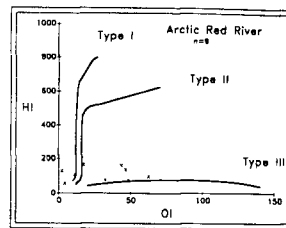
Figure 24



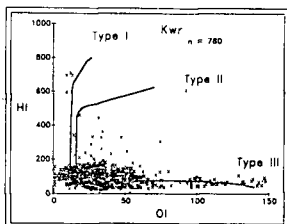
(m)



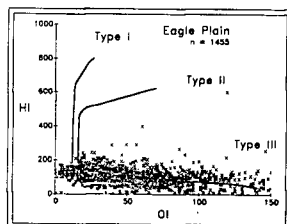
(n)



(o)



(p)



(q)

Figure 24 cont'd.

Table IV. Classification and maturation of various stratigraphic units in the study area. TOC, Tmax, HI, PI, HC potential and QOM are averaged values calculated across the thickness of the unit at one well or sample locality. '-' denotes a range of values for outcrop samples from different localities in the indicated area. Refl= vitrinite reflectance (Rorand), which represents the level of maturity at or near the base of the unit, measured or calculated (Δ) from the line of best fit (see Fig. 4, Part I). CAI=conodont alteration index. # Spl=Number of samples. Well=well location. See table III for explanation of Rock-Eval parameters and figures 25 to 35 for well and sample localities. Loc=Location: MD=Mackenzie Delta; PP=Peel Plateau; RM=Richardson Mountains; EP=Eagle Plain; OM=Ogilvie Mountains; O/C=outcrop samples; W=western; E=eastern; N=northern; C=central; SE=southeastern; NW=northwestern; N-C=north-central.

a. Road River Group.

<u>Loc</u>	<u>Well</u>	<u># Spl</u>	<u>TOC</u>	<u>Tmax</u>	<u>HI</u>	<u>PI</u>	<u>HC</u>	<u>QOM</u>	<u>Refl</u>	<u>CAI</u>
							pot		(Δ)	
MD	A-37	19	0.5	403	59	0.5	0.6	1.4	1.0	
RM	O/C	29	0.2- 9.6	218- 534	0-9	0-1	≤	≤		5
NW	N-53	2	0.5	380	24	0.7	0.4	0.7	2.2	
EP										
E EP	N-05	5	1.1	399	26	0.6	1.1	1.0	3.3	
SE	D-77	204	0.8	305	17	0.7	0.5	0.6	6.0	
EP										
W EP	B-62	2	1.1	401	26	0.5	0.5	0.5	2.3	
OM	O/C	3	0.1- 5.0	270- 597	0-9	0-1	≤	≤		4.5 5

c. Hare Indian Formation.

<u>Loc</u>	<u>Well</u>	<u>#</u>	<u>Spl</u>	<u>TOC</u>	<u>Tmax</u>	<u>HI</u>	<u>PI</u>	<u>HC</u>	<u>pot</u>	<u>QOM</u>	<u>Refl</u>
E PP	H-57	1		1.3	444	153	0.4	3.4		2.6	1.0

d. Hume Formation.

<u>Loc</u>	<u>Well</u>	<u>#</u>	<u>Spl</u>	<u>TOC</u>	<u>Tmax</u>	<u>HI</u>	<u>PI</u>	<u>HC</u>	<u>pot</u>	<u>QOM</u>	<u>Refl</u>
E PP	H-57	4		0.5	392	114	0.6	1.3		3.0	1.1
W PP	I-50	2		1.7	366	28	0.6	1.2		0.8	2.3

e. Canol Formation.

<u>Loc</u>	<u>Well</u>	<u># Spl</u>	<u>TOC</u>	<u>Tmax</u>	<u>HI</u>	<u>PI</u>	<u>HC</u>	<u>QOM</u>	<u>Refl</u>	<u>CAI</u>
							<u>pot</u>			
E PP	H-57	2	6.4	447	189	0.3	18.1	2.8	0.8	
W PP	I-50	6	2.3	360	74	0.7	3.6	3.0	2.2	
RM	O/C	6	1.5-	284-	0-5	0-	≤	≤	2.4-	5
			8.6	386		0.1			3.4	
N-C	O-22	2	1.5	460	40	0.5	1.2	0.8	0.9	
EP										
NW	N-53	2	1.5	512	15	0.7	0.8	0.5	1.1	
EP										
E EP	N-05	17	2.4	411	21	0.6	1.4	0.6	1.4	
SE	D-77	17	1.6	283	13	0.7	0.6	1.2	2.1	
EP									(Δ)	
W EP	B-62	3	4.2	410	6	0.8	1.2	0.3	1.6	
OM	O/C	4	0.7-	306-	0-	0-	≤	<0.01	2.3-	5
			6.8	522	17	0.1			3.8	

f. Imperial Formation. (b) denotes samples containing bitumen (albertite).

<u>Loc</u>	<u>Well</u>	<u># Spl</u>	<u>TOC</u>	<u>Tmax</u>	<u>HI</u>	<u>PI</u>	<u>HC pot</u>	<u>QOM</u>	<u>Refl</u>
PP	O/C	8	0.5-	275-	1-	0-	0.01-	0.1-	0.5
			1.6	466	135	0.2	1.8	1.5	0.7
PP	O/C	3	4.3-	456-	66-	0.5	3.7-	0.7-	0.7
	(b)		95.7	479	360		363.5	3.8	0.8
E PP	H-57	16	1.7	438	113	0.4	3.5	1.9	0.8
W PP	I-50	37	0.8	414	59	0.6	1.3	1.5	2.1
RM	O/C	6	0.2-	306-	2-	0-	0.01-	0.01	1.8
			1.2	458	33	0.3	0.1	0.3	2.1
EP	O/C	6	0.4-	364-	10-	0-	0.02-	0.2-	1.0
			0.5	497	60	0.3	0.3	0.6	
N EP	F-48	38	0.8	450	103	0.3	1.0	1.6	
N EP	P-34	35	1.2	431	30	0.5	0.7	0.6	
N-C	O-22	28	0.8	440	176	0.2	1.8	2.6	1.1
EP									
NW	N-53	25	0.9	447	58	0.6	1.2	1.4	1.2
EP									
E EP	N-05	88	0.6	388	238	0.5	0.7	4.8	1.3
SE	D-77	87	1.4	317	24	0.6	0.8	0.8	1.7
EP									
W EP	B-62	5	1.7	388	18	0.7	0.9	0.6	1.4

g. Ford Lake Shale.

<u>Loc</u>	<u>Well</u>	<u># Spl</u>	<u>TOC</u>	<u>Tmax</u>	<u>HI</u>	<u>PI</u>	<u>HC</u>	<u>pot</u>	<u>QOM</u>	<u>Refl</u>
EP	O/C	8	0.5-	426-	51-	0.1-	0.5-	0.6-	0.7	
			7.9	466	467	0.3	19.0	5.3	0.9	
E EP	N-05	10	0.7	445	113	0.4	1.3	1.9	0.9	
SE	B-34	11	2.6	323	152	0.2	5.3	1.9		
EP										
SE	D-77	134	1.2	344	37	0.5	1.0	0.9	1.7	
EP										
W EP	B-62	13	2.4	441	32	0.5	1.6	0.7	1.6	
C EP	L-08	105	1.5	451	163	0.2	3.5	2.1		

h. Hart River Formation.

<u>Loc</u>	<u>Well</u>	<u># Spl</u>	<u>TOC</u>	<u>Tmax</u>	<u>HI</u>	<u>PI</u>	<u>HC</u>	<u>pot</u>	<u>QOM</u>	<u>Refl</u>
EP	O/C	2	0.4-	418-	318-	0.1-	1.5-	3.8-		
			1.3	431	572	0.2	7.8	6.1		
SE	B-34	148	1.2	431	178	0.2	2.8	4.6		
EP										
SE	D-77	34	1.6	457	129	0.6	1.8	3.7	1.2	
EP										
C EP	C-18	19	1.3	413	221	0.3	4.2	3.1	0.6	
C EP	F-18	20	0.8	444	146	0.3	1.7	2.3		
C EP	J-19	6	1.1	438	166	0.2	2.5	2.2	0.5	
C EP	L-08	133	0.5	442	167	0.3	1.3	2.4		
OM	O/C	8	0.4-	433-	0-	0.2-	0.01-	0.01-	0.9	
			4.9	563	34	0.3	0.1	0.3	1.4	

i. Blackie Formation and unnamed Carboniferous unit.

<u>Loc</u>	<u>Well</u>	<u># Spl</u>	<u>TOC</u>	<u>Tmax</u>	<u>HI</u>	<u>PI</u>	<u>HC pot</u>	<u>QOM</u>	<u>Refl</u>
SE	B-34	170	0.9	432	242	0.1	3.1	2.8	
EP									
SE	D-77	77	1.2	424	85	0.6	2.2	1.9	1.2
EP									
C EP	C-18	4	2.8	431	286	0.1	10.7	3.2	0.4

j. Bug Creek Group, A-37 well. Form=Formation; Akl=Aklavik; R Mtn=Richardson Mountain; Al Ck=Almstrom Creek; M Rg=Murray Ridge Formations.

<u>Loc</u>	<u>Form</u>	<u>#</u>	<u>Spl</u>	<u>TOC</u>	<u>Tmax</u>	<u>HI</u>	<u>PI</u>	<u>HC</u>	<u>pot</u>	<u>QOM</u>	<u>Refl</u>
MD	Akl	3		3.0	437	221	0.1	7.1		2.4	0.5
MD	R Mtn	3		1.6	438	140	0.2	2.8		1.8	0.6
MD	Al Ck	2		2.2	436	126	0.2	3.6		1.7	0.7
MD	M Rg	3		2.2	439	136	0.2	3.9		1.7	0.7

k. Porcupine River Formation.

<u>Loc</u>	<u>Well</u>	<u>#</u>	<u>Spl</u>	<u>TOC</u>	<u>Tmax</u>	<u>HI</u>	<u>PI</u>	<u>HC</u>	<u>pot</u>	<u>QOM</u>	<u>Refl</u>
N EP	F-48	74		0.9	445	137	0.3	1.6		1.9	
N EP	P-34	18		1.6	385	54	0.5	1.9		1.1	
N EP	J-70	18		1.8	440	167	0.3	4.3		2.4	0.5

l. Husky Formation.

<u>Loc</u>	<u>Well</u>	<u>#</u>	<u>Spl</u>	<u>TOC</u>	<u>Tmax</u>	<u>HI</u>	<u>PI</u>	<u>HC</u>	<u>pot</u>	<u>QOM</u>	<u>Refl</u>
MD	A-37	10		2.0	438	146	0.2	3.9		1.9	0.5

m. Parsons Group, A-37 well. Form=Formation; McG=McGuire; M Ck=Martin Creek Formations.

<u>Loc</u>	<u>Form</u>	<u>#</u>	<u>Spl</u>	<u>TOC</u>	<u>Tmax</u>	<u>HI</u>	<u>PI</u>	<u>HC</u>	<u>pot</u>	<u>QOM</u>	<u>Refl</u>
MD	McG	2		1.5	434	116	0.2	2.1		1.4	0.4
MD	M Ck	4		1.1	435	134	0.2	1.8		1.7	

n. Mount Goodenough Formation.

<u>Loc</u>	<u>Well</u>	<u># Spl</u>	<u>TOC</u>	<u>Tmax</u>	<u>HI</u>	<u>PI</u>	<u>HC</u>	<u>pot</u>	<u>QOM</u>	<u>Refl</u>
MD	A-37	16	2.0	428	143	0.4	7.3	2.7	0.4	
PP	O/C	3	0.6-	310-	1-	0-	0.1-	0.1-	0.4	
			0.8	444	65	0.07	0.7	1.7	0.7	
RM	O/C	1	0.7	513	8	0	0.1	0.1	1.3	
N EP	J-70	75	1.5	440	141	0.2	2.6	1.9	0.5	

o. Rat River Formation.

<u>Loc</u>	<u>Well</u>	<u># Spl</u>	<u>TOC</u>	<u>Tmax</u>	<u>HI</u>	<u>PI</u>	<u>HC</u>	<u>pot</u>	<u>QOM</u>	<u>Refl</u>
PP	O/C	4	0.3-	439-	3-	0-	0.01-	0.03-	0.4	
			0.9	444	46	0.1	0.4	0.4	0.5	
W PP	I-50	6	1.2	428	82	0.6	2.4	1.9	0.3	
RM	O/C	3	0.3-	383-	5-	0-	0.1	0.1-	1.3	
			0.9	548	48	0.01		0.5	1.4	
N EP	J-70	15	1.2	442	103	0.2	1.5	1.3	0.5	

p. Albian strata: Arctic Red River Formation in Mackenzie Delta and Peel Plateau areas; Horton River Formation on Campbell Uplift; Kwr unit (Whitestone River Formation) in Eagle Plain area. CU=Campbell Uplift.

<u>Loc</u>	<u>Well</u>	<u>#</u>	<u>Spl</u>	<u>TOC</u>	<u>Tmax</u>	<u>HI</u>	<u>PI</u>	<u>HC</u>	<u>pot</u>	<u>QOM</u>	<u>Refl</u>
MD	A-37	3		2.1	439	129	0.7	8.1		3.8	0.3
CU	O/C	12		0.5-	262-	0-	0-	0.01-		0.01-	0.9
				2.0	493	67	0.2	0.5		0.6	1.6
PP	O/C	5		0.5-	436-	54-	0.1-	0.5-		1.0-	0.6
				1.1	451	103	0.3	2.1		2.0	
W PP	I-50	1		0.9	435	74	0.4	1.1		1.3	0.2
RM	O/C	1		1.3	518	20	0.1	0.3		0.2	1.1
EP	O/C	3		0.6-	435-	109-	0.1	0.8-		1.2-	0.3
				2.4	438	134		3.0		1.6	
N EP	F-48	198		1.3	427	94	0.2	1.6		1.2	
N EP	P-34	256		1.2	452	64	0.4	1.3		1.1	
N EP	J-70	29		1.6	443	111	0.2	2.1		1.3	0.5
N-C	O-22	4		1.1	430	166	0.2	2.3		2.1	0.4
EP											
NW	N-53	17		1.1	450	91	0.5	1.8		1.7	1.1
EP											
SE	B-34	57		1.4	448	185	0.1	2.5		2.1	
EP											
C EP	C-18	4		1.8	432	127	0.2	3.2		1.8	0.5
C EP	C-24	103		2.1	437	154	0.1	5.3		1.7	

Table IV p continued.

<u>Loc</u>	<u>Well</u>	<u># Spl</u>	<u>TOC</u>	<u>Tmax</u>	<u>HI</u>	<u>PI</u>	<u>HC</u>	<u>pot</u>	<u>QOM</u>	<u>Refl</u>
C EP	F-18	44	1.6	438	116	0.1	2.2	1.4		
C EP	J-19	7	1.9	436	200	0.1	6.5	2.2	0.5	
C EP	L-08	38	1.0	441	127	0.1	1.5	1.4		
C EP	N-58	18	1.8	446	122	0.3	3.2	1.7	0.6	

q. Eagle Plain Group.

<u>Loc</u>	<u>Well</u>	<u># Spl</u>	<u>TOC</u>	<u>Tmax</u>	<u>HI</u>	<u>PI</u>	<u>HC</u>	<u>pot</u>	<u>QOM</u>	<u>Refl</u>
EP	O/C	27	0.3-	358	6-	0-	0.02-	0.1-	0.2	
			1.2	489	208	0.2	1.9	1.9	0.4	
N EP	P-34	128	1.5	450	111	0.3	2.4	1.7		
N EP	J-70	263	1.4	430	118	0.3	2.3	1.8	0.4	
N-C	O-22	13	4.9	423	136	0.3	9.8	2.3	0.3	
EP										
SE	B-34	37	1.1	447	134	0.2	1.9	1.6		
EP										
C EP	C-18	24	2.1	423	127	0.2	3.9	1.6	0.4	
C EP	C-24	306	2.7	431	108	0.2	3.6	1.3		
C EP	F-18	120	1.5	438	79	0.1	1.5	0.9		
C EP	J-19	26	3.4	430	110	0.2	4.4	1.4	0.5	
C EP	L-08	167	1.4	431	78	0.2	1.4	0.9		
C EP	N-58	343	2.1	446	145	0.3	3.8	2.0	0.4	

Figures 25 to 34. Regional distribution of average TOC content, average HC potential, quality of organic matter (QOM), and the degree of organic maturity (DOM) for some formations and groups examined in the study area. Erosional edges modified from Geological Survey of Canada, Map 1505A, Tipper et al. (1981). a) Average organic carbon content map of the formation(s) or group(s). Values plotted are average TOC content calculated across the thickness of the formation/group at each well or outcrop location. b) Average HC potential ($S_1 + S_2$) and average QOM [$(S_1 + S_2)/\text{TOC}$] plotted with the DOM (measured by vitrinite reflectance and/or CAI) for the formation or group. The average HC potential and QOM (to the left and right of ', ' respectively) are calculated across the thickness of the formation/group. HC-potential units= mg HC/g rock; QOM units=mg HC/g Corg. Legend: '◇' =calculated vitrinite reflectance (from regression line in Fig. 4 of part I); '◆' = measured vitrinite reflectance (% Rorand); '■' =conodont alteration index (CAI). % Rorand values are plotted near or at the base of the formation/group. DOM contours are dashed lines; QOM contours are solid lines. Scale is the same as figure 5.

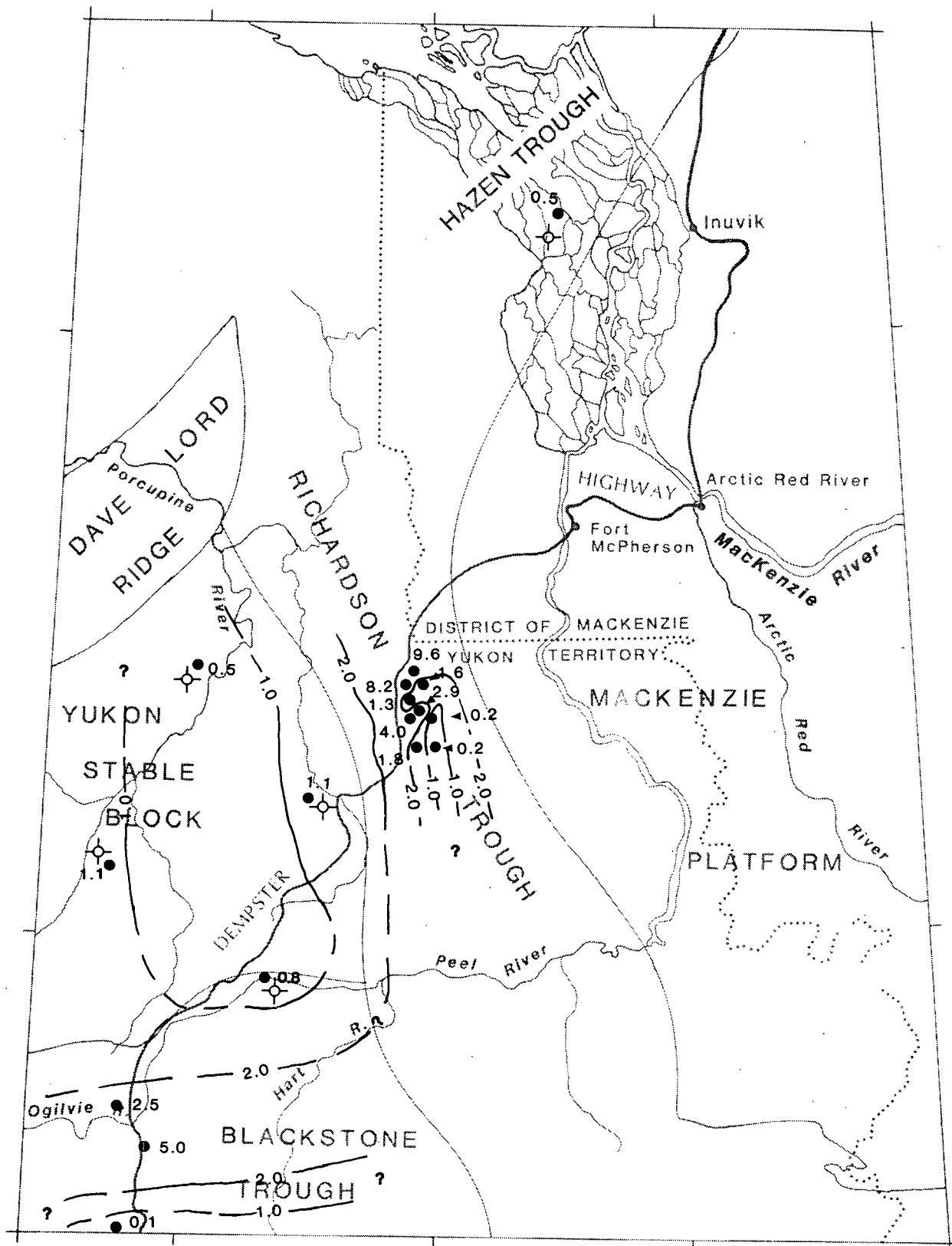
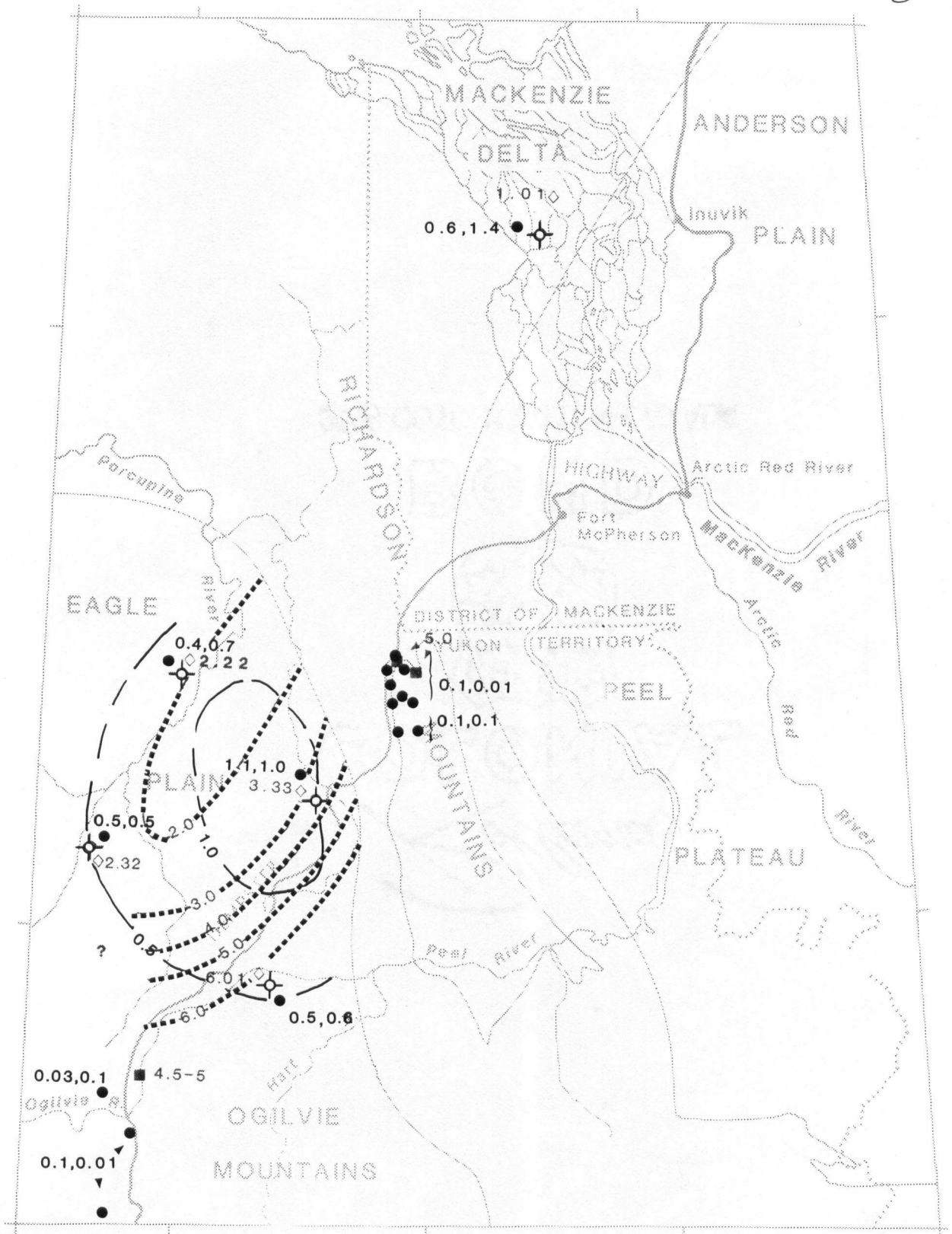


Figure 25. Road River Group. Boundaries of paleogeographic divisions (after A.W. Norris, 1985) and the erosional edge of the EDM assemblage in the Richardson Mountains are shown.

a) Regional distribution in TOC. Contour interval=1.0% TOC.



b) Regional distribution of DOM, HC potential and QOM. Contour interval for DOM=1.0% Rorand; contour interval for QOM=0.5 mg HC/g Corg.

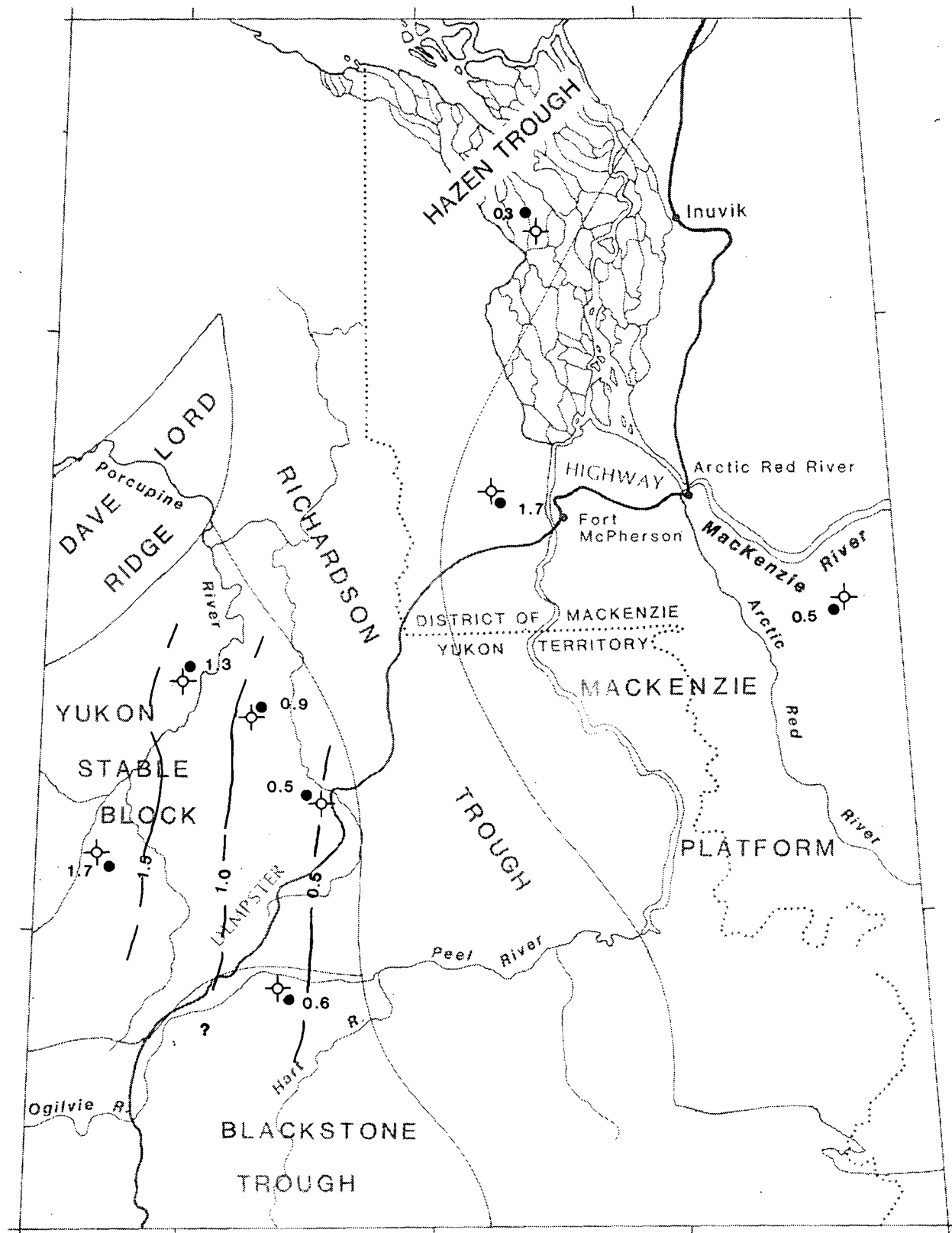
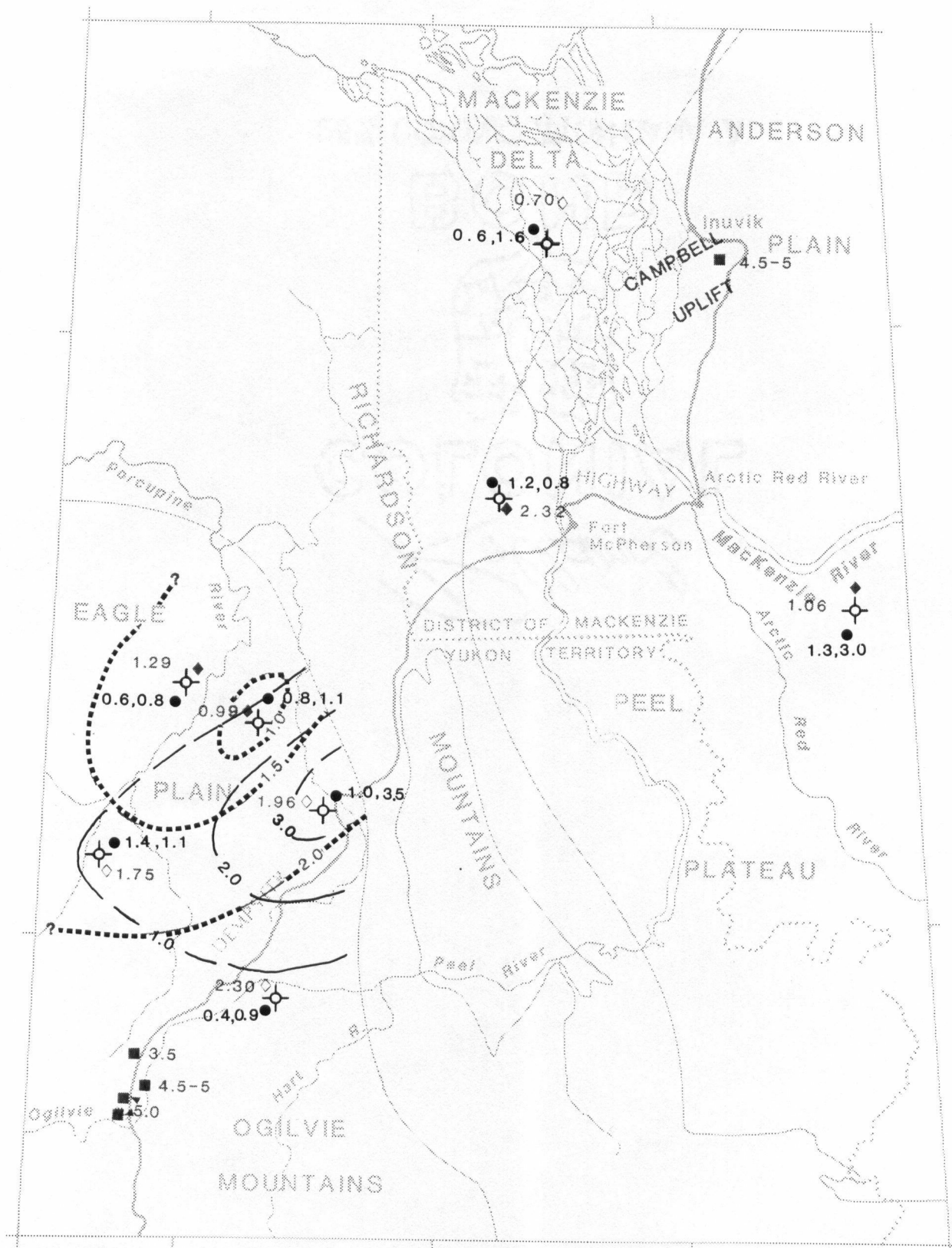


Figure 26. Ogilvie Formation (Yukon Stable Block and Hazen Trough) and Hume Formation (Mackenzie Platform). Boundaries of paleogeographic divisions (after A.W. Norris, 1985) and the erosional edge of the EDM assemblage in the Richardson Mountains are shown.

a) Regional distribution in TOC. Contour interval=0.5% TOC.



b) Regional distribution of DOM, HC potential and QOM. Contour interval for DOM=0.5% Rorand; contour interval for QOM=1.0 mg HC/g Corg.

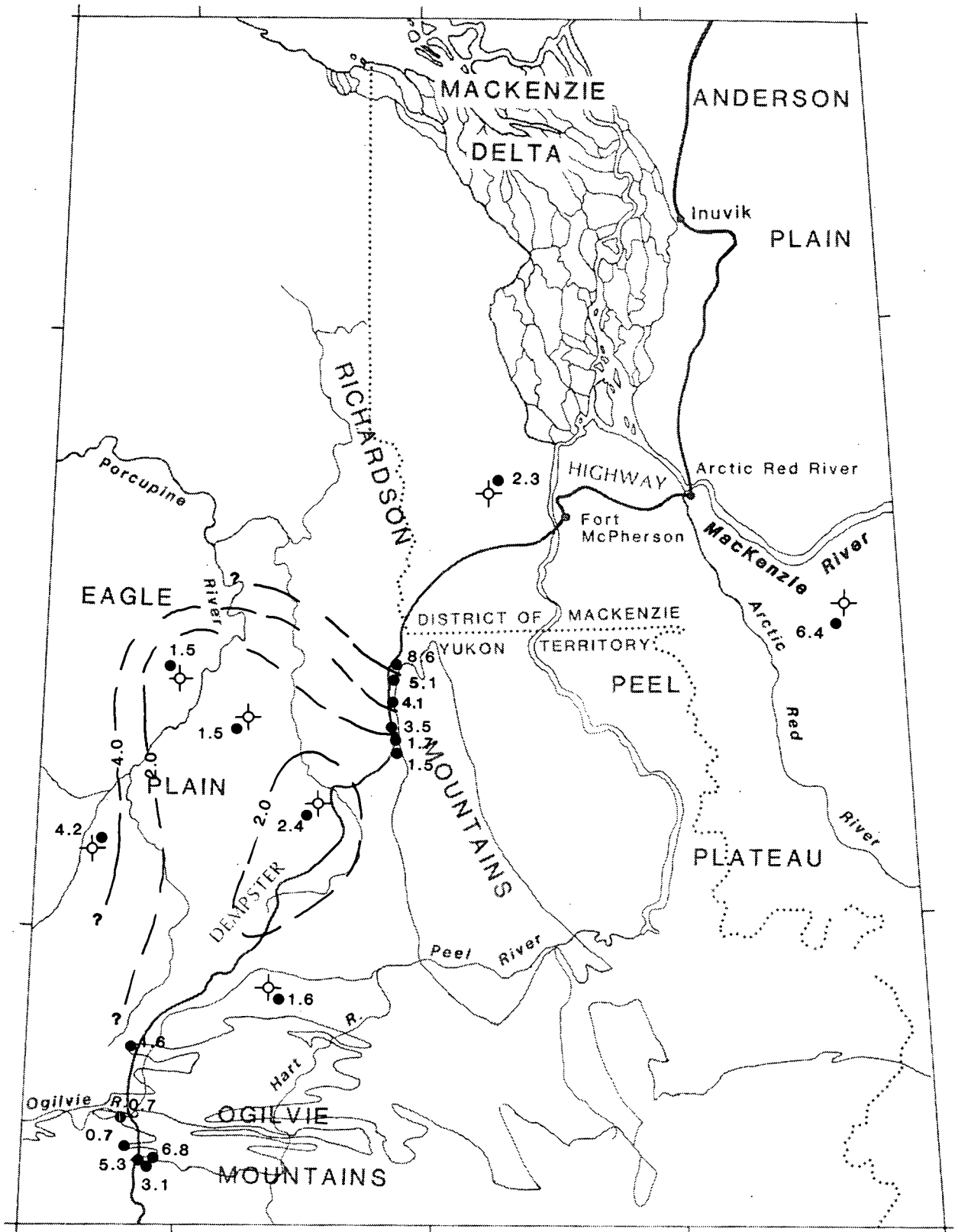
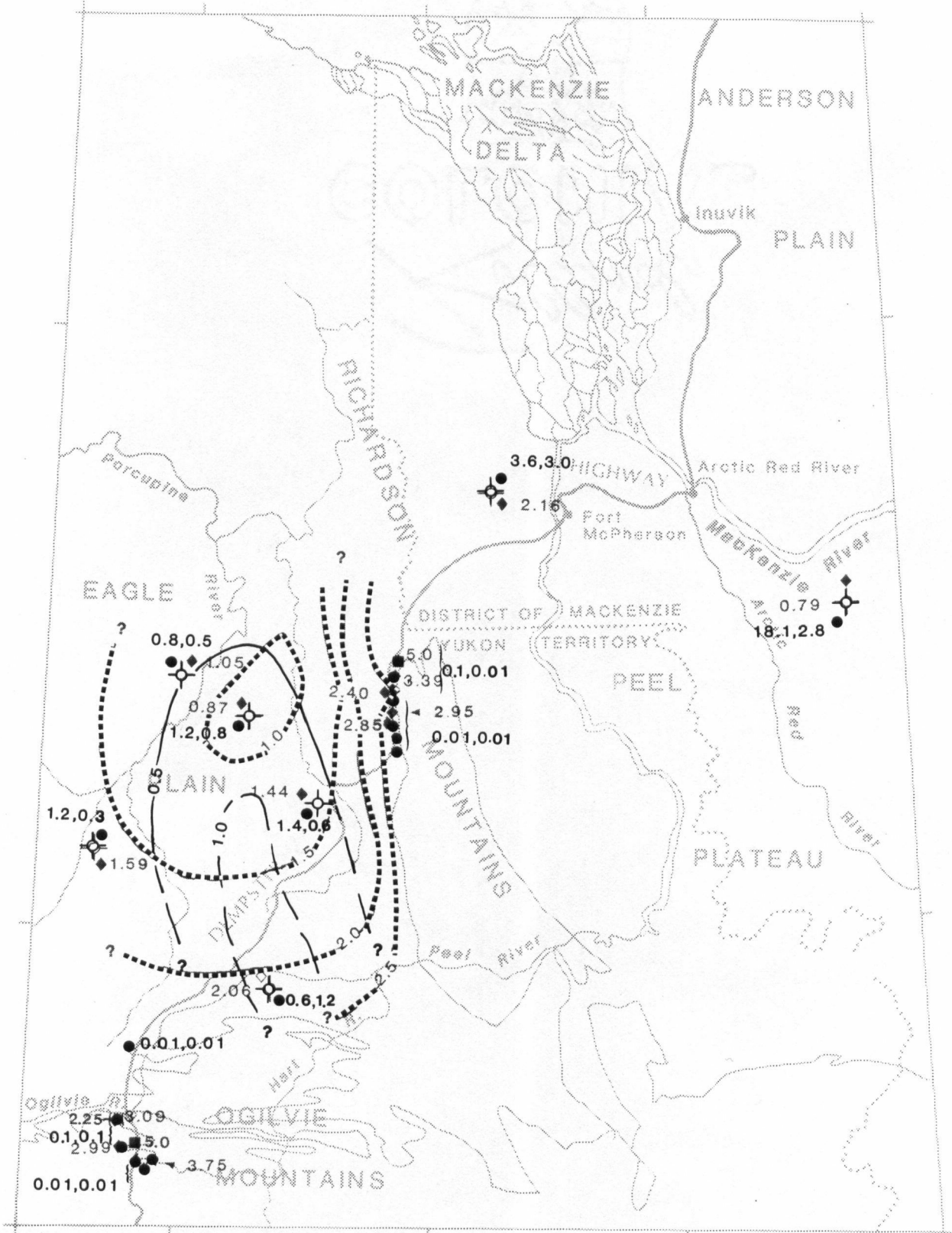


Figure 27. Canol Formation. The erosional and/or depositional edge of the DJF assemblage is shown.

a) Regional distribution of TOC. Contour interval=2% TOC.



b) Regional distribution of DOM, HC potential and QOM. Contour interval for DOM=0.5% Rorand; contour interval for QOM=1.0 mg HC/g Corg.

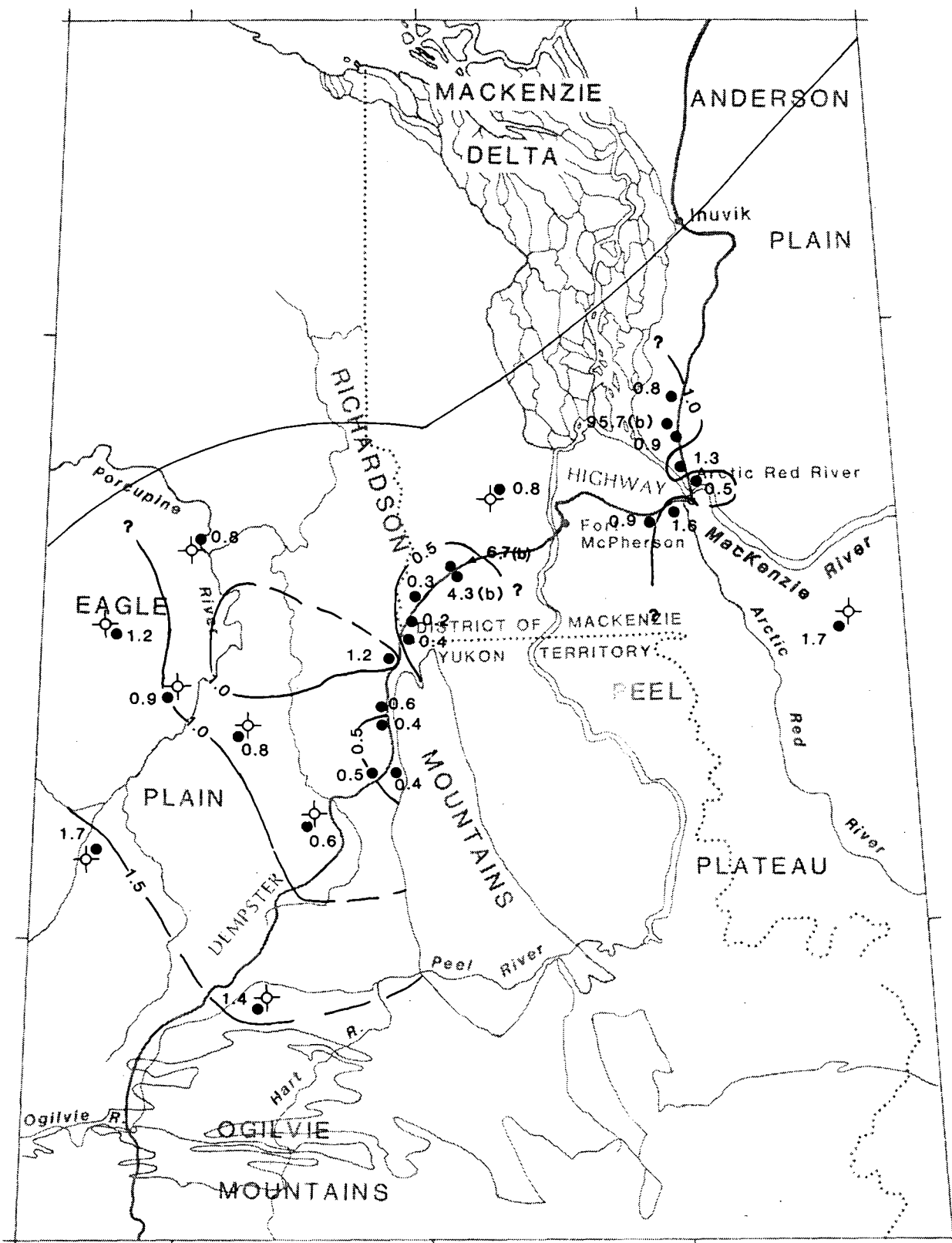
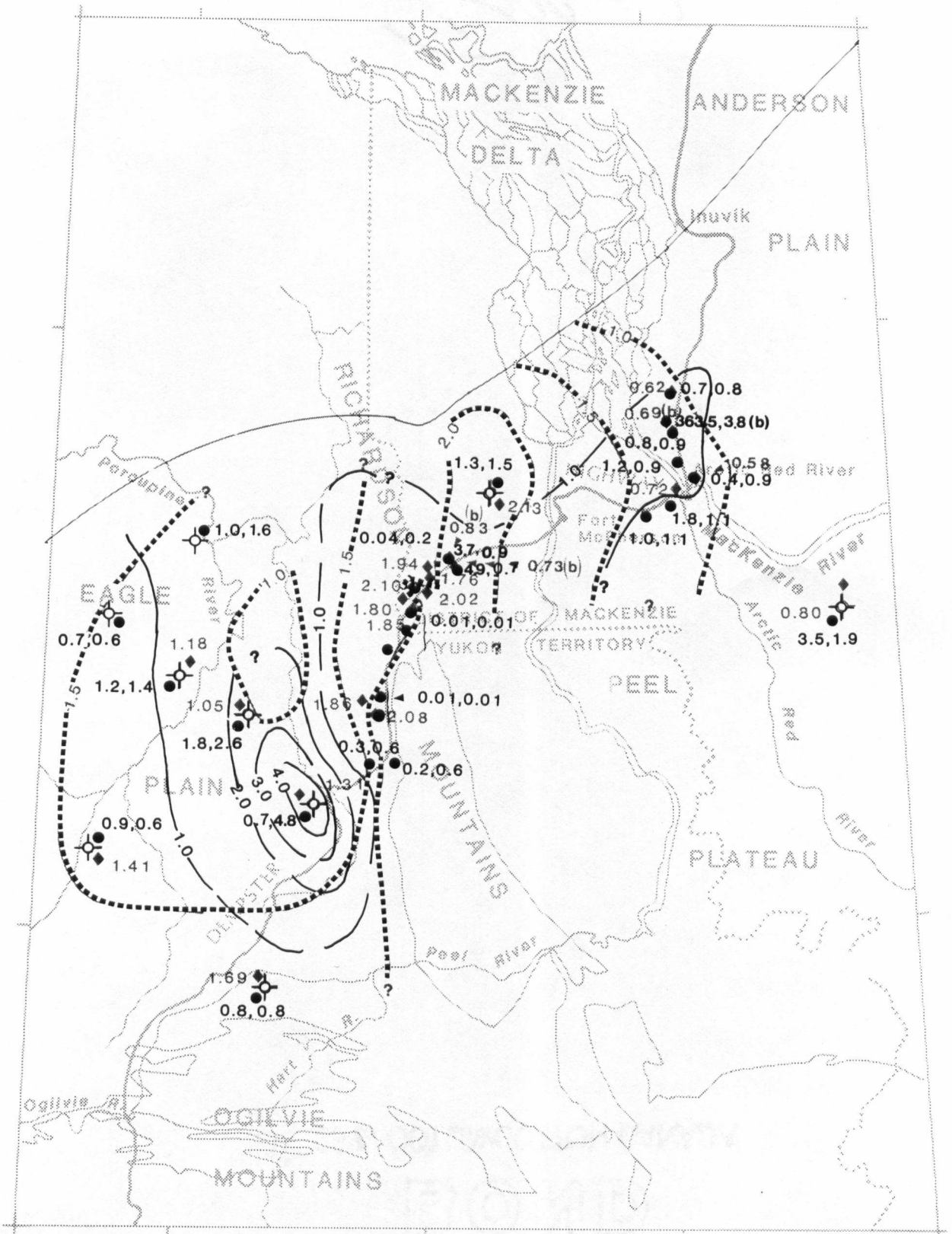


Figure 28. Imperial Formation. The erosional and/or depositional edge of the DJF assemblage is shown. Northern erosional edge modified from Pugh (1983).
 a) Regional distribution of TOC. Contour interval=0.5% TOC. '(b)' denotes TOC content of samples containing bitumen (not used to contour TOC data).



b) Regional distribution of DOM, HC potential and QOM. Contour interval for DOM=0.5% Rorand; contour interval for QOM=1.0 mg HC/g Corg.

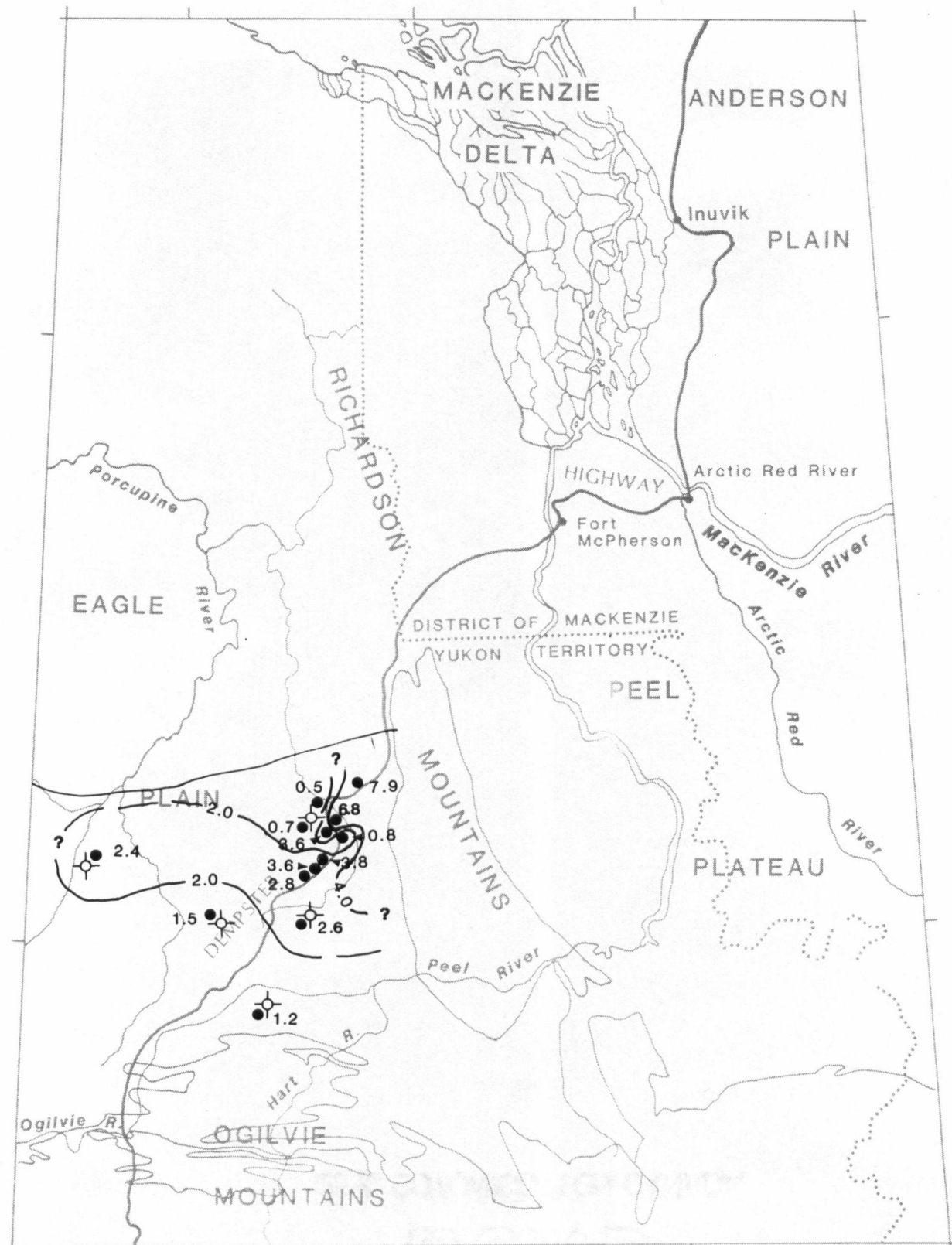
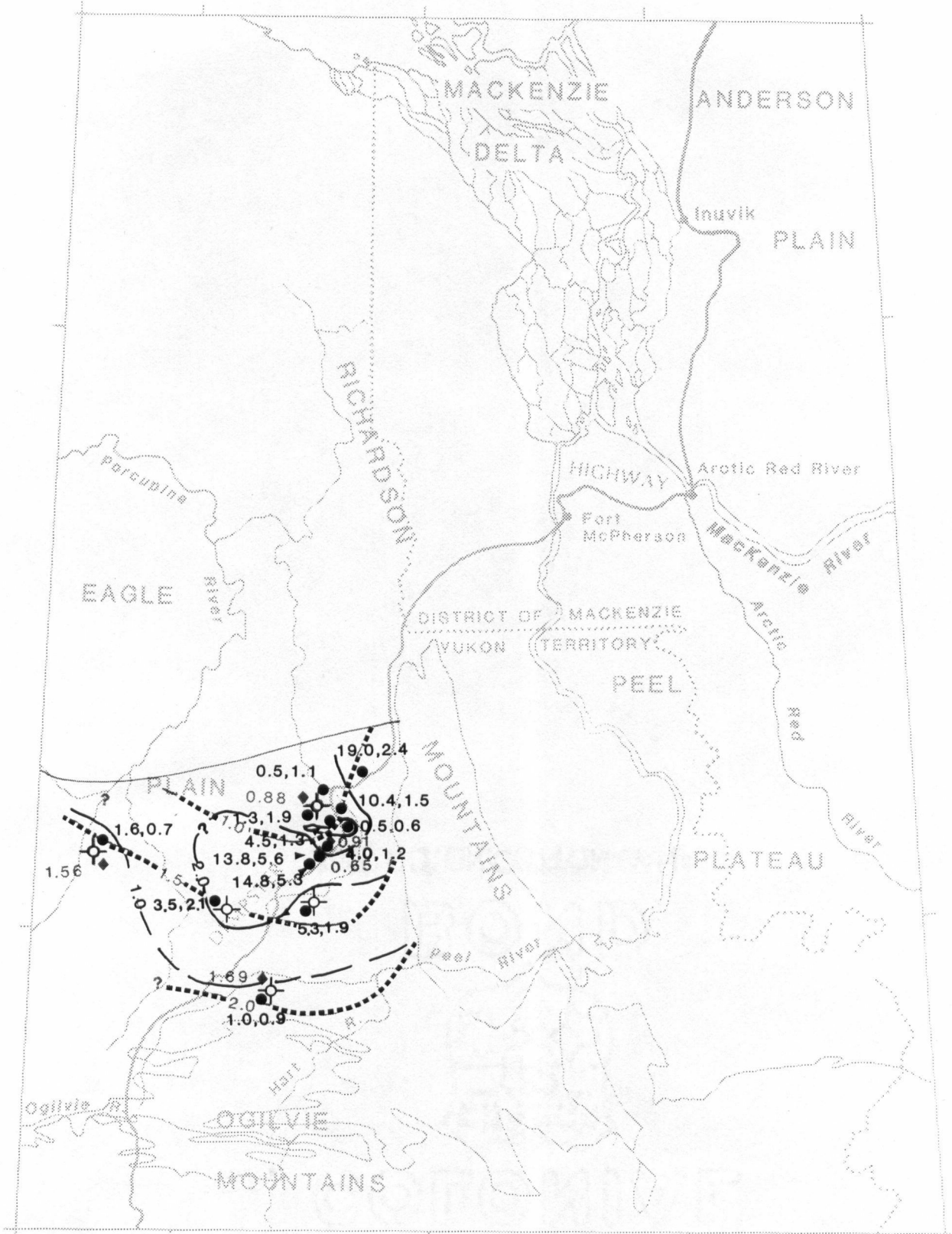


Figure 29. Ford Lake Shale. The erosional and/or depositional edge of the DJF assemblage is shown. Northern erosional edge modified from Pugh (1983).
a) Regional distribution of TOC. Contour interval=2.0% TOC.



b) Regional distribution of DOM, HC potential and QOM. Contour interval for DOM=0.5% Rorand; contour interval for QOM=1.0 mg HC/g Corg.

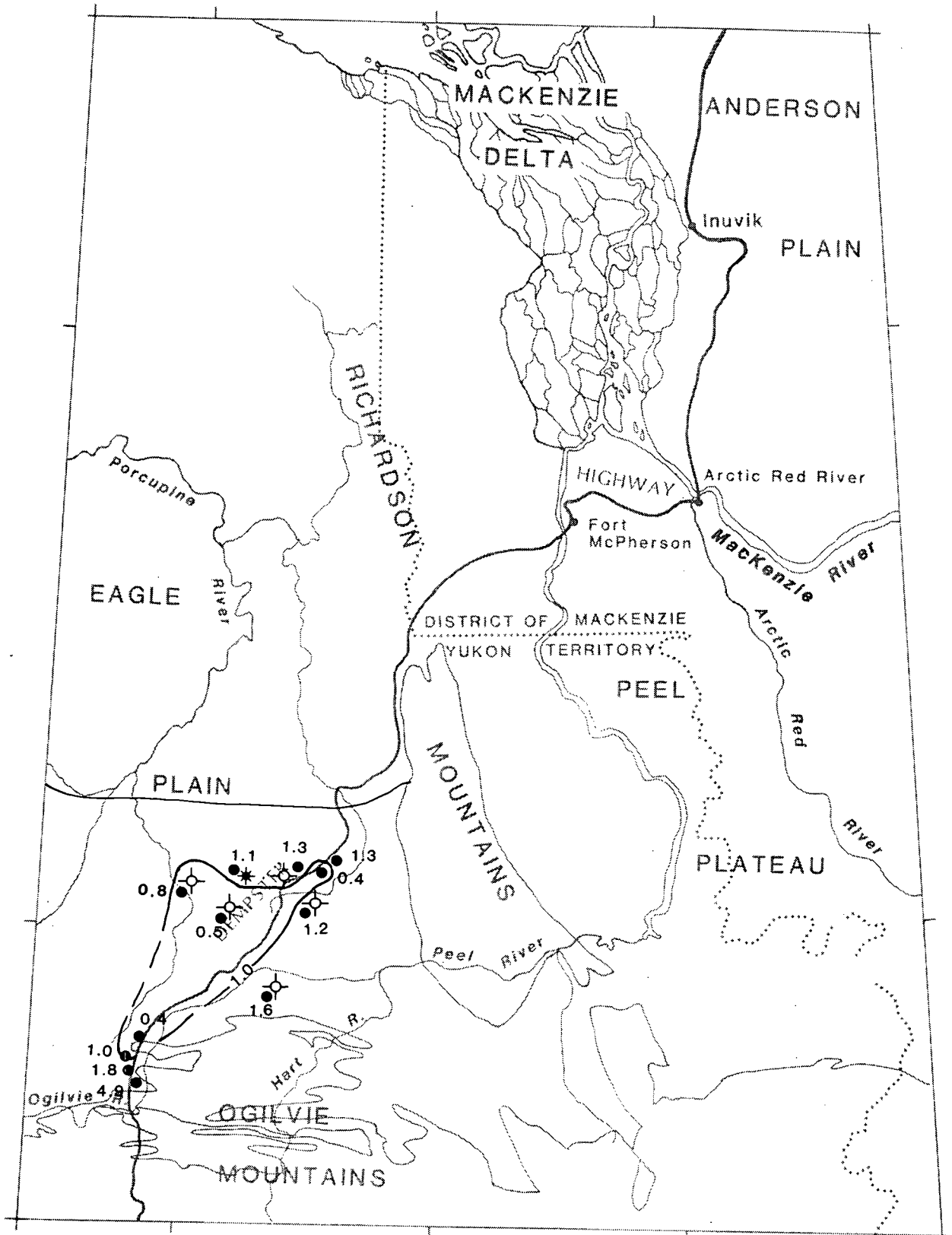
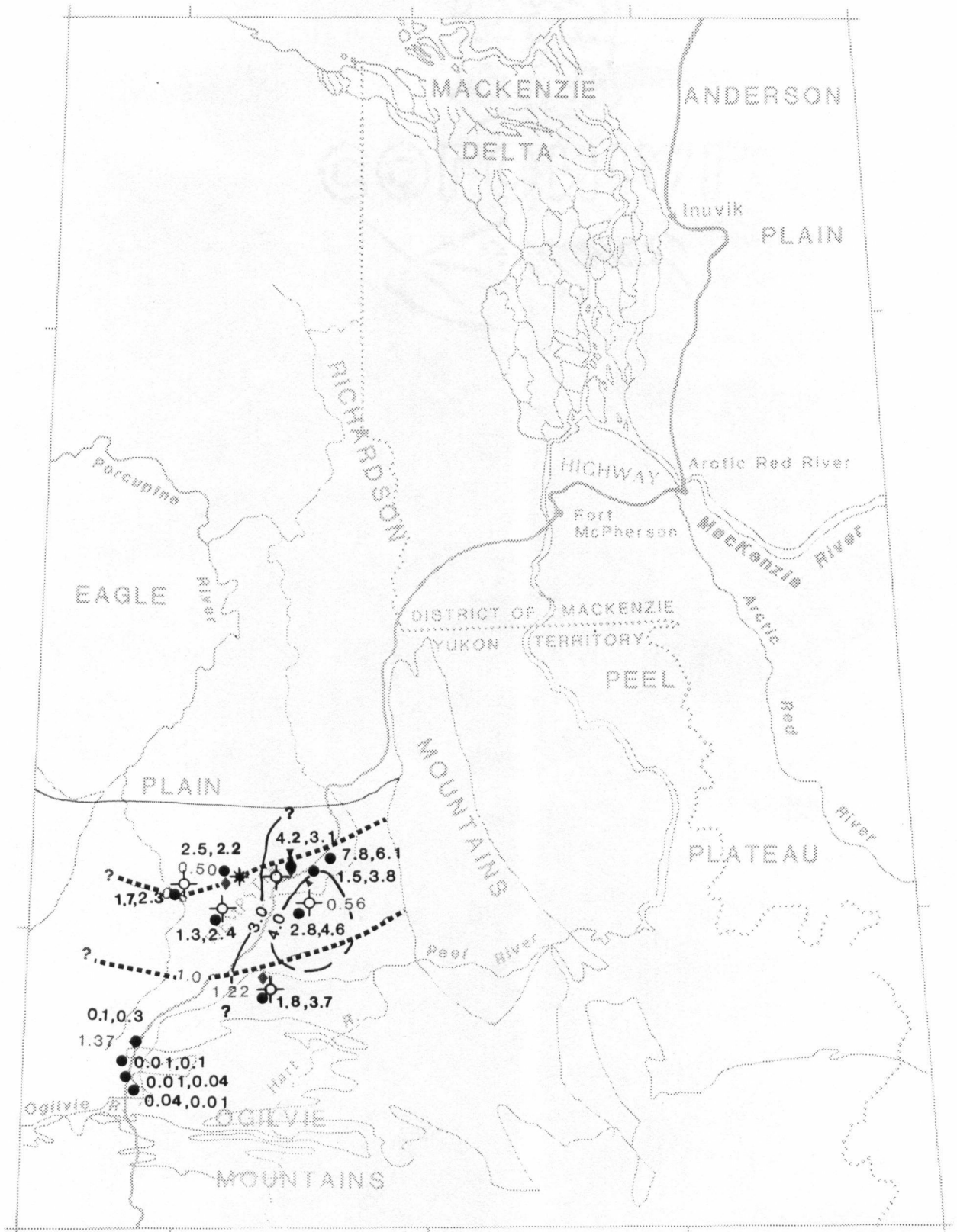


Figure 30. Hart River Formation. The erosional and/or depositional edge of the DJF assemblage is shown. Northern erosional edge modified from Pugh (1983).

a) Regional distribution of TOC. The 1% TOC contour is shown.



b) Regional distribution of DOM, HC potential and QOM. Contour interval for DOM=0.5% Rorand; contour interval for QOM=1.0 mg HC/g Corg.

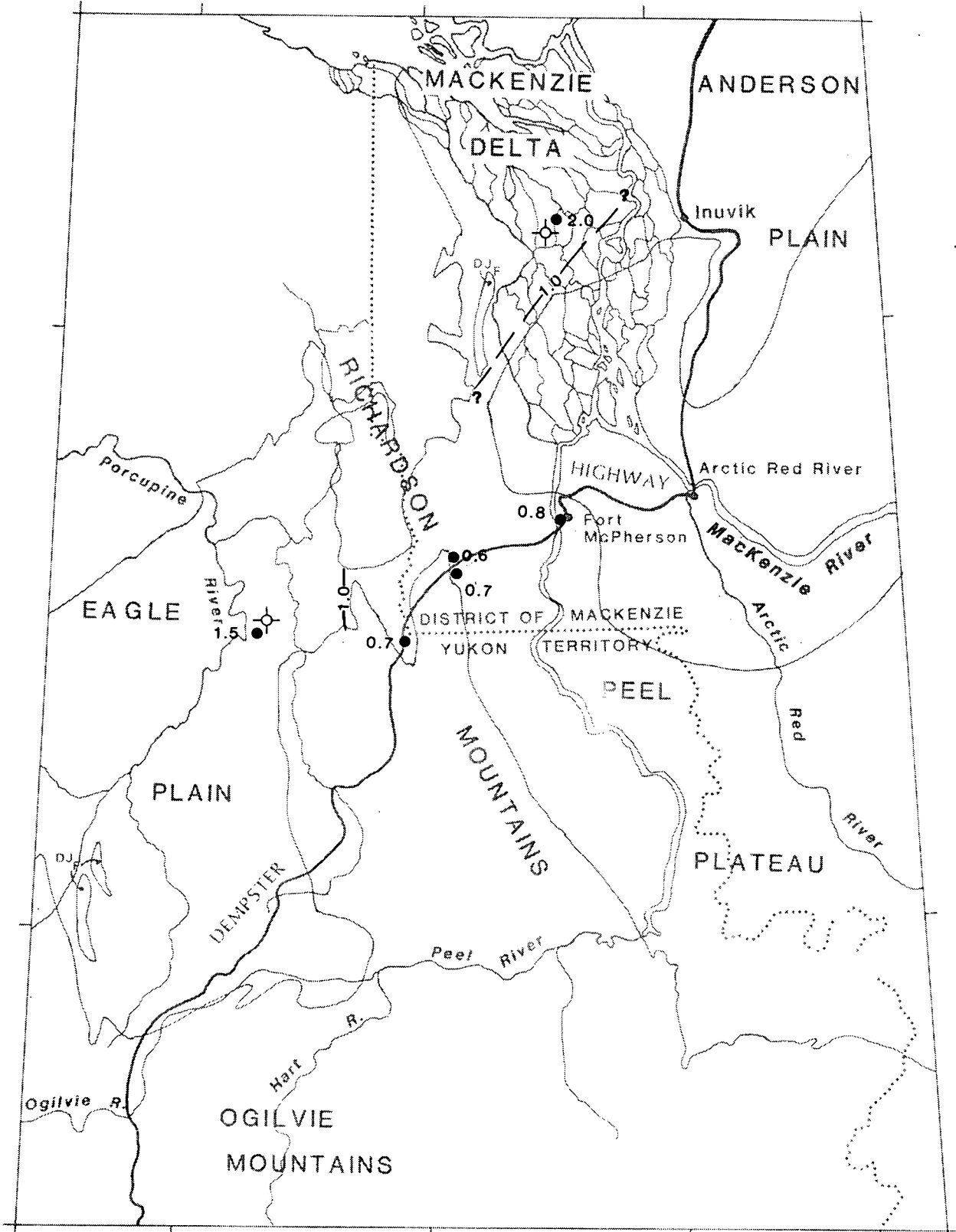
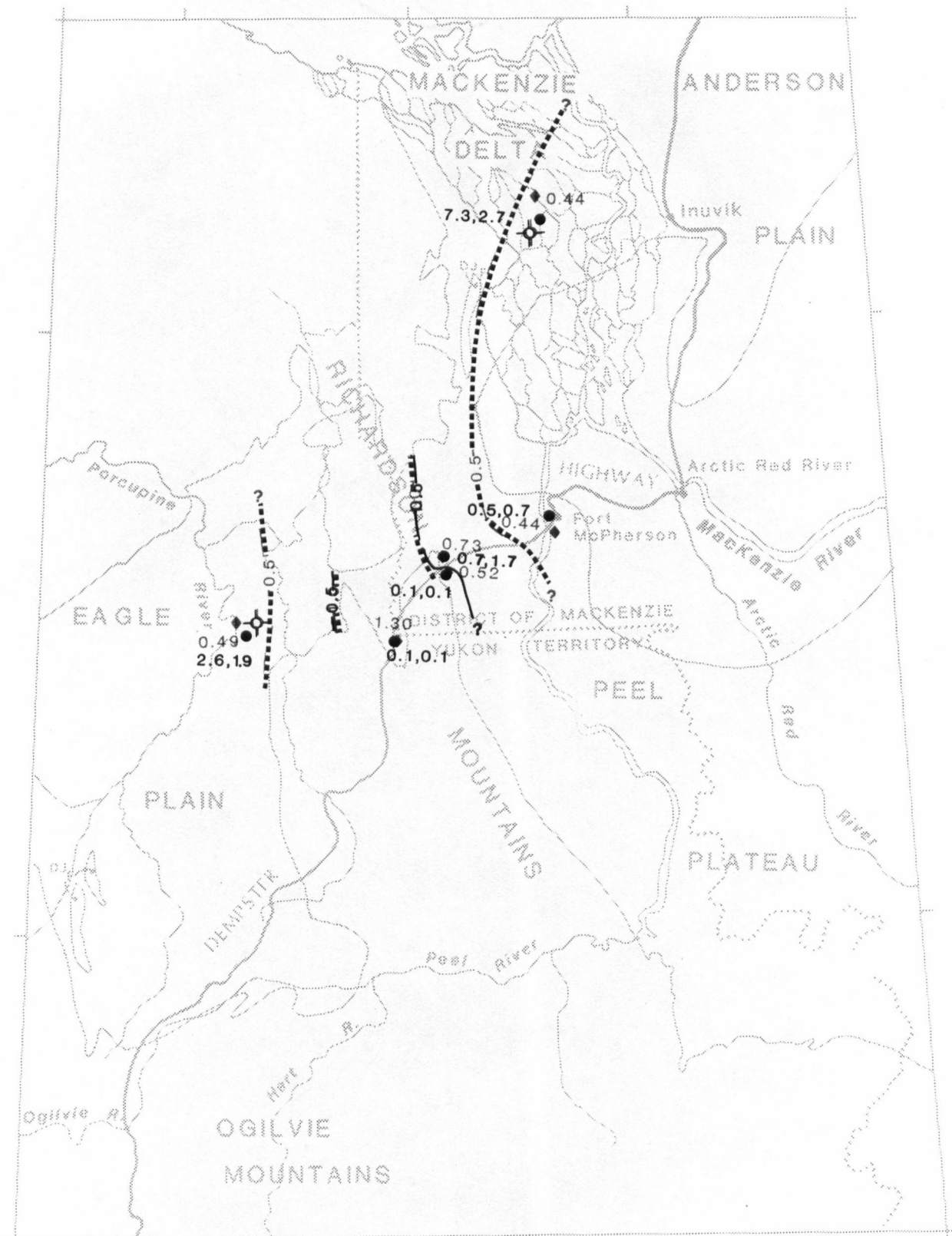


Figure 31. Mount Goodenough Formation. The erosional and/or depositional edge of the JKK assemblage is shown.

a) Regional distribution of TOC. The 1% TOC contour is shown.



b) Regional distribution of DOM, HC potential and QOM. Contour interval for DOM=0.5% Rorand. The 0.5 mg HC/g Corg contour is shown for QOM. (Outcrop samples from near the top of the Formation in Peel Plateau are included for control points.)

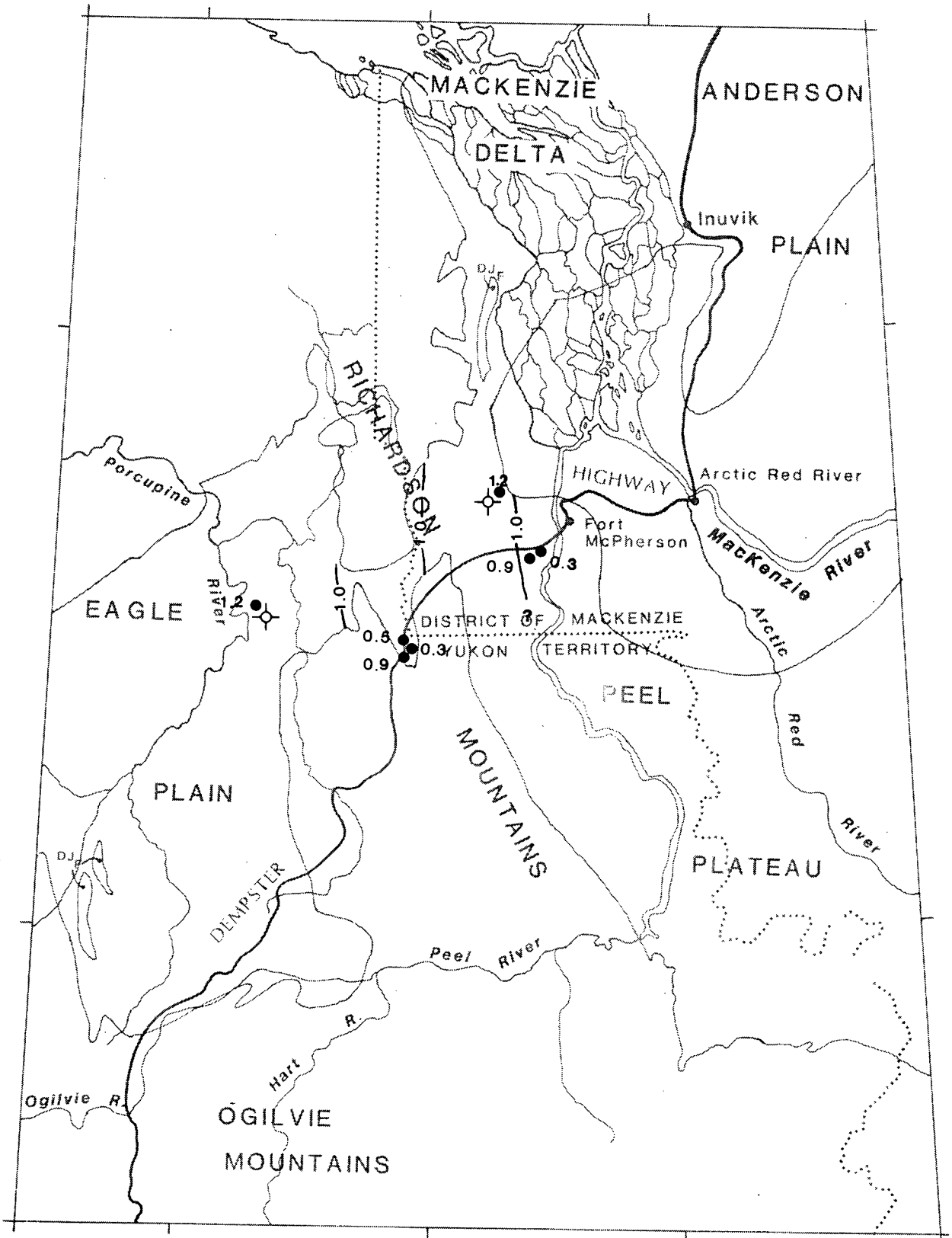
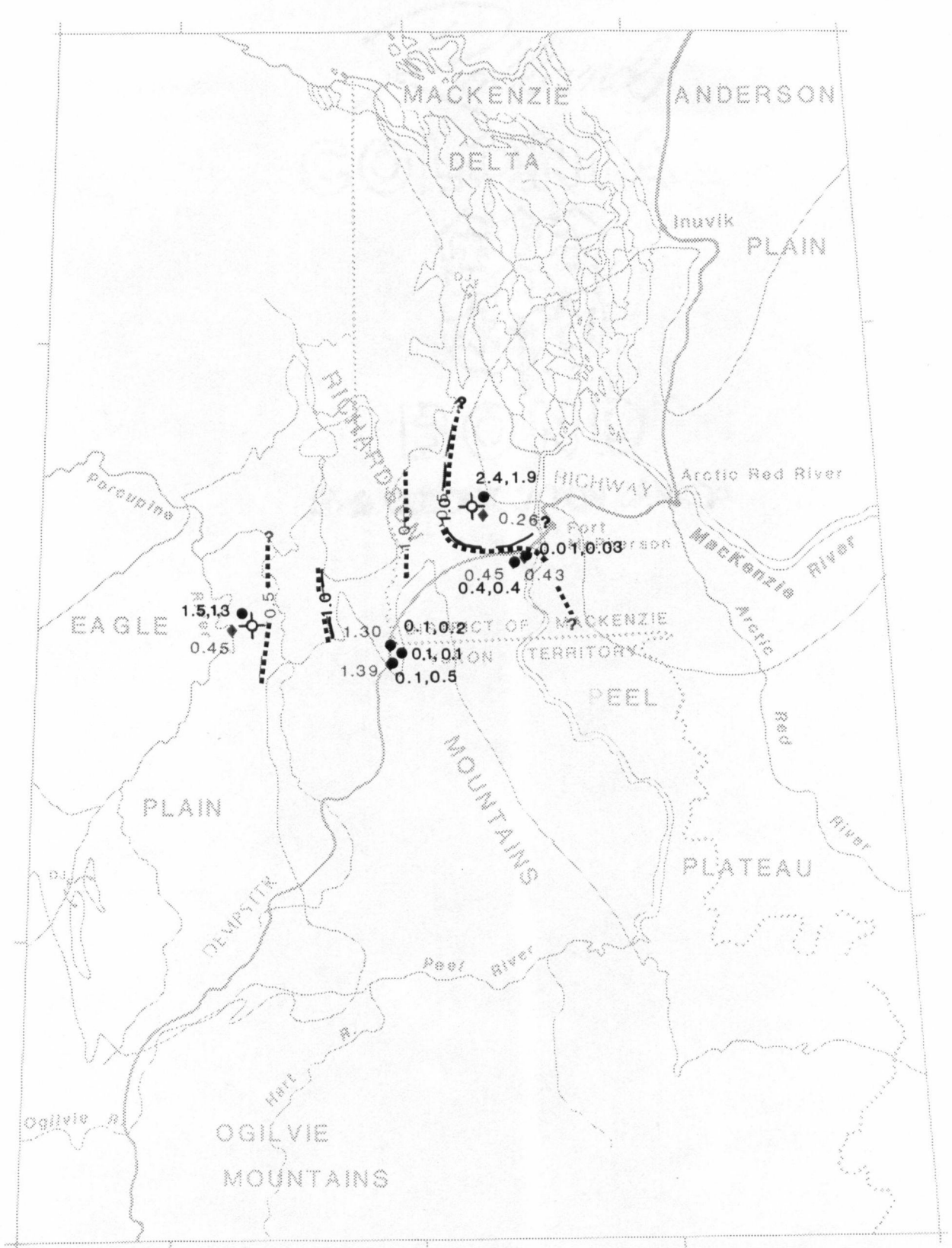


Figure 32. Rat River Formation. The erosional and/or depositional edge of the JKK assemblage is shown.

a) Regional distribution of TOC. The 1% TOC contour is shown.



b) Regional distribution of DOM, HC potential and QOM. Contour for DOM = 0.5% Rorand. The 1.0 mg HC/g Corg contour is shown for QOM. (Outcrop samples from near the top of the Formation in Peel Plateau are included for control points.)

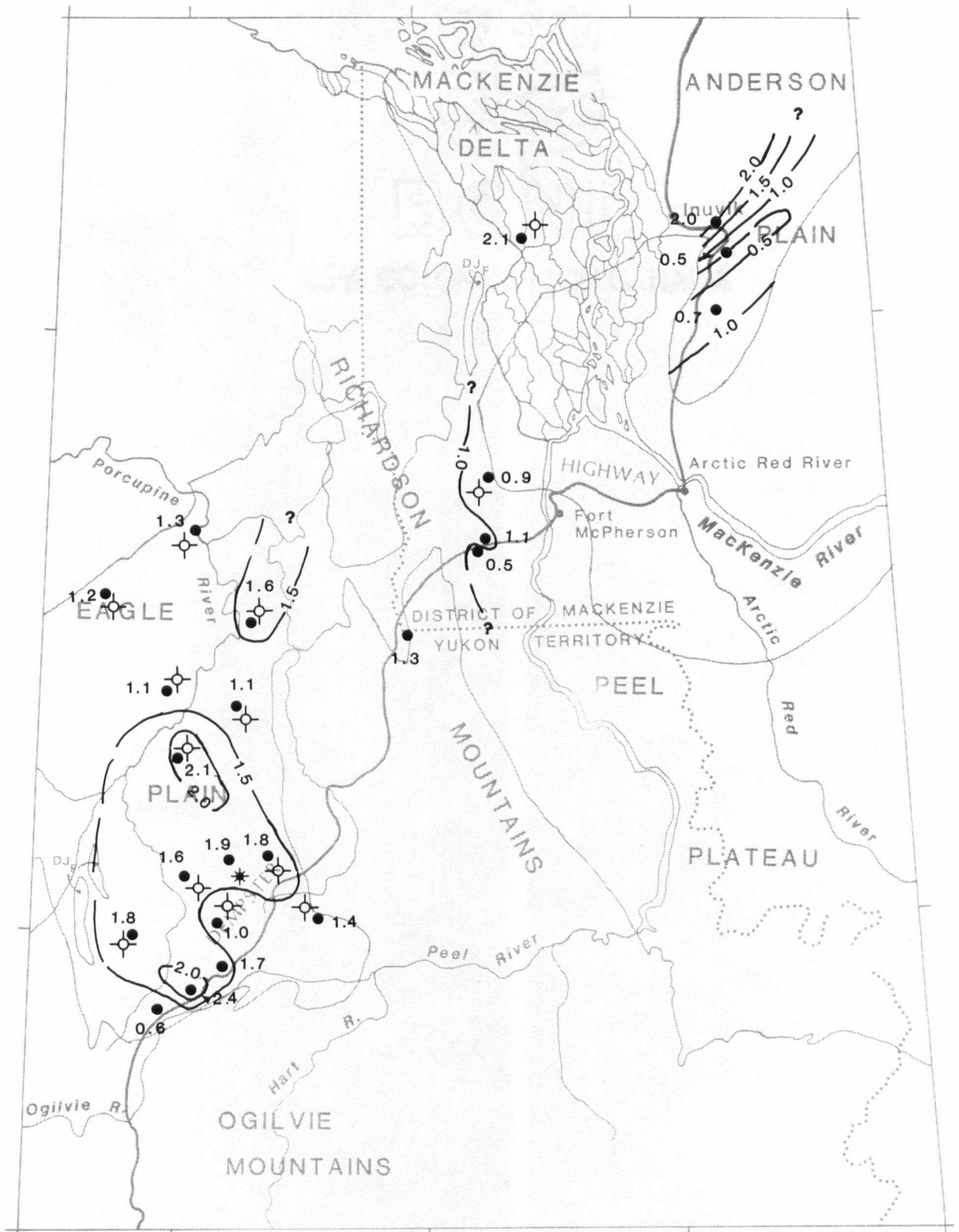


Figure 33. Albian strata (Arctic Red River and Horton River Formations and map unit Kwr). The erosional and/or depositional edge of the JKK assemblage is shown.

a) Regional distribution of TOC. Contour interval=0.5% TOC.

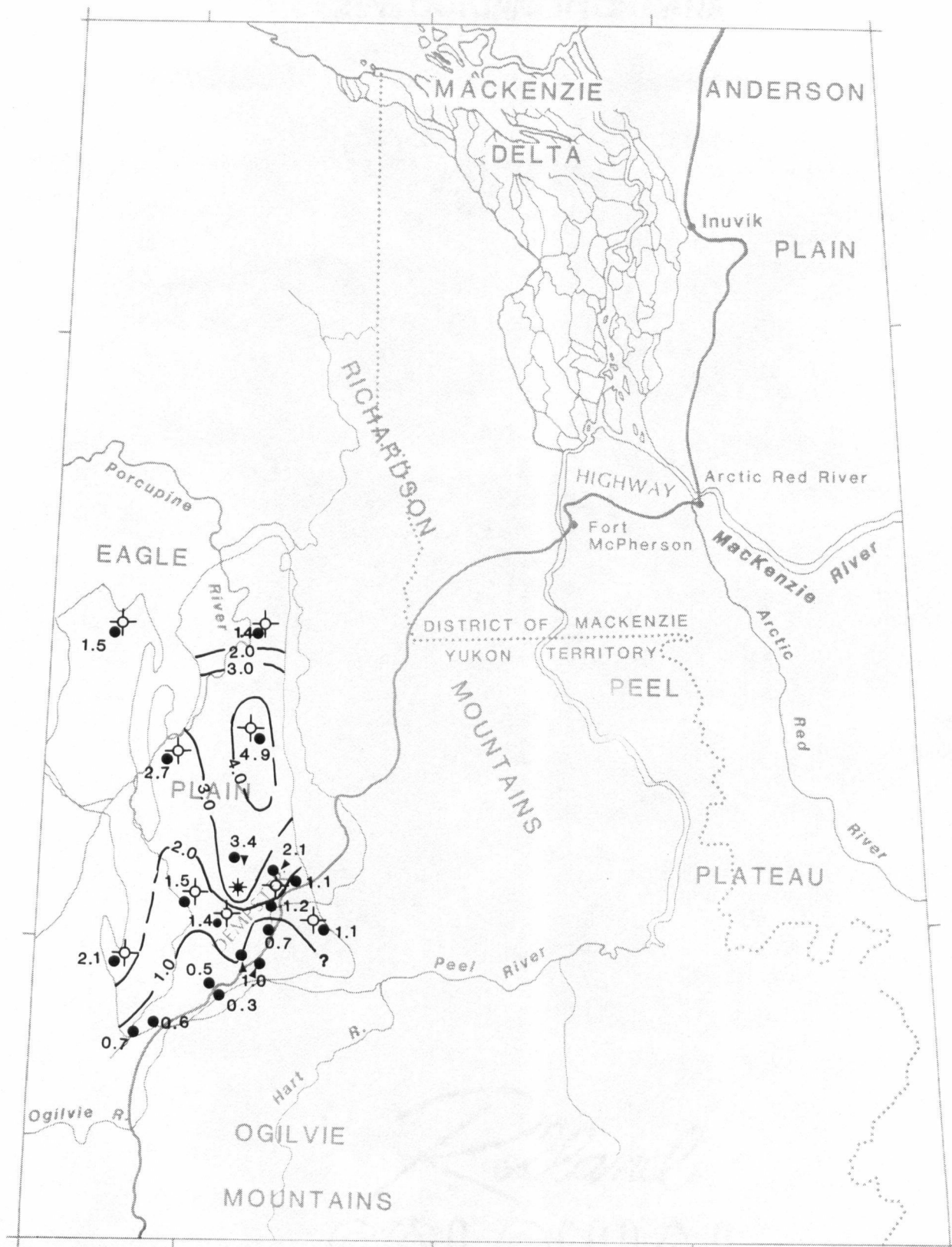
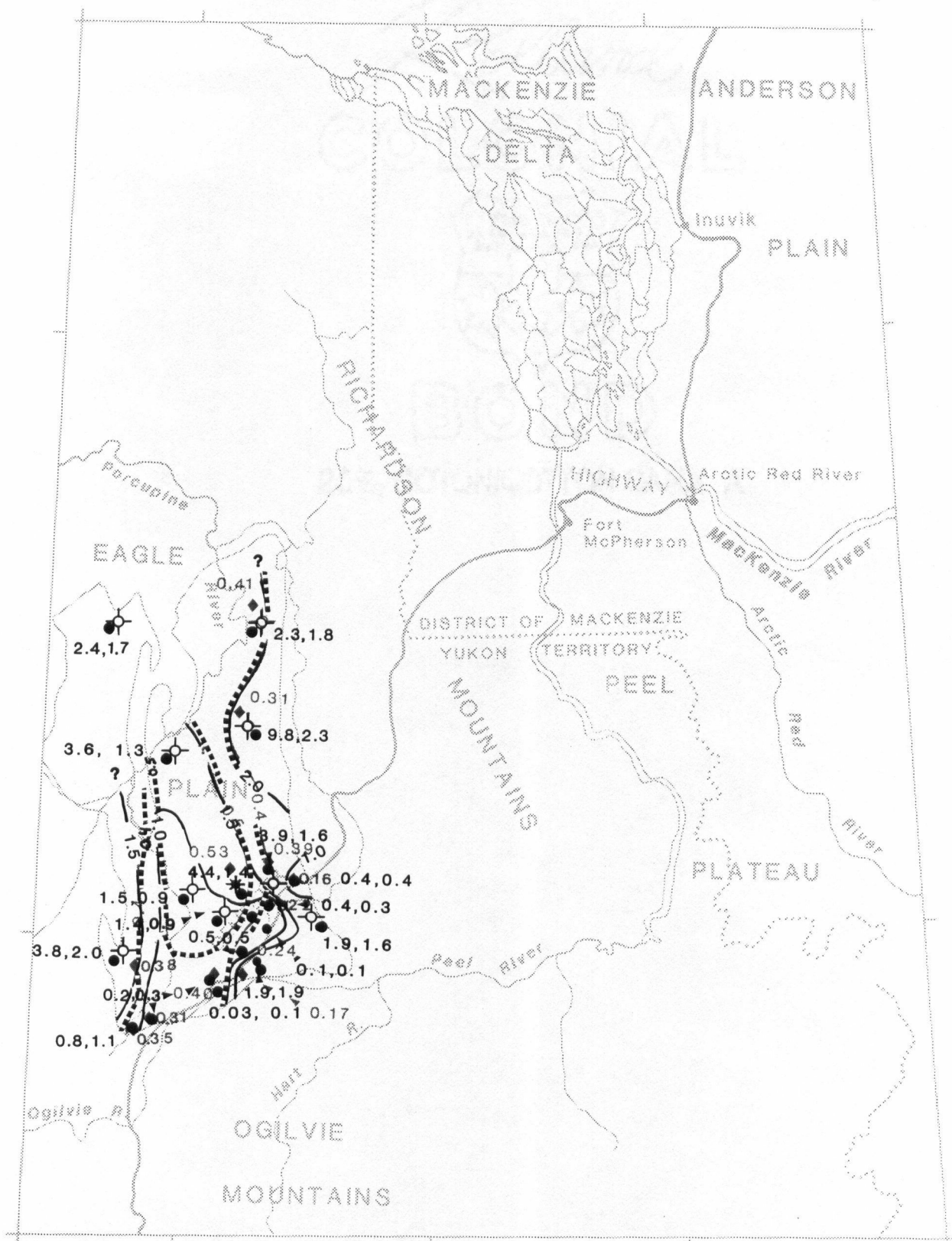


Figure 34. Eagle Plain Group. The erosional and/or depositional edge of the KA assemblage is shown.

a) Regional distribution of TOC. Contour interval=1% TOC.



b) Regional distribution of DOM, HC potential and QOM. Contour interval for DOM=0.1% Rorand; contour interval for QOM=0.5 mg HC/g Corg. (Outcrop samples from near the top of the Group are included for control points.)

E. DISCUSSION

It is difficult to interpret organic richness and maturation patterns laterally over any distance, especially where sample density is low, because the northern Cordilleran Orogen is characterized by a limited lateral continuity of stratigraphic units. Thus it must be emphasized that the interpretations presented here are based on limited data and the organic richness and isomaturity lines may ultimately change as more data become available.

1. Petroleum Source Rock Potential

a. Organic Maturation and Hydrocarbon Generation

A potential petroleum source rock is a stratigraphic interval or facies unit which has sufficient hydrocarbon generating capability to generate economic hydrocarbon reserves. It is well documented that the petroleum source potential of a unit is controlled by the quantity, quality and maturity of the organic matter (Dow, 1977; Hunt, 1979; Durand, 1980; Waples, 1980; Powell and Snowdon, 1983; Barnes et al., 1984; Tissot and Welte, 1984 and many others). In this study, the level of organic maturity of Phanerozoic strata was determined from vitrinite reflectance, CAI (see part I also) and Rock-Eval pyrolysis (Tmax data). Interpretation of maturation levels and paleogeothermal gradients are discussed in detail in part I and are briefly summarized here. In figure 35, the regional variation in level of organic maturity with respect to hydrocarbon generation is plotted.

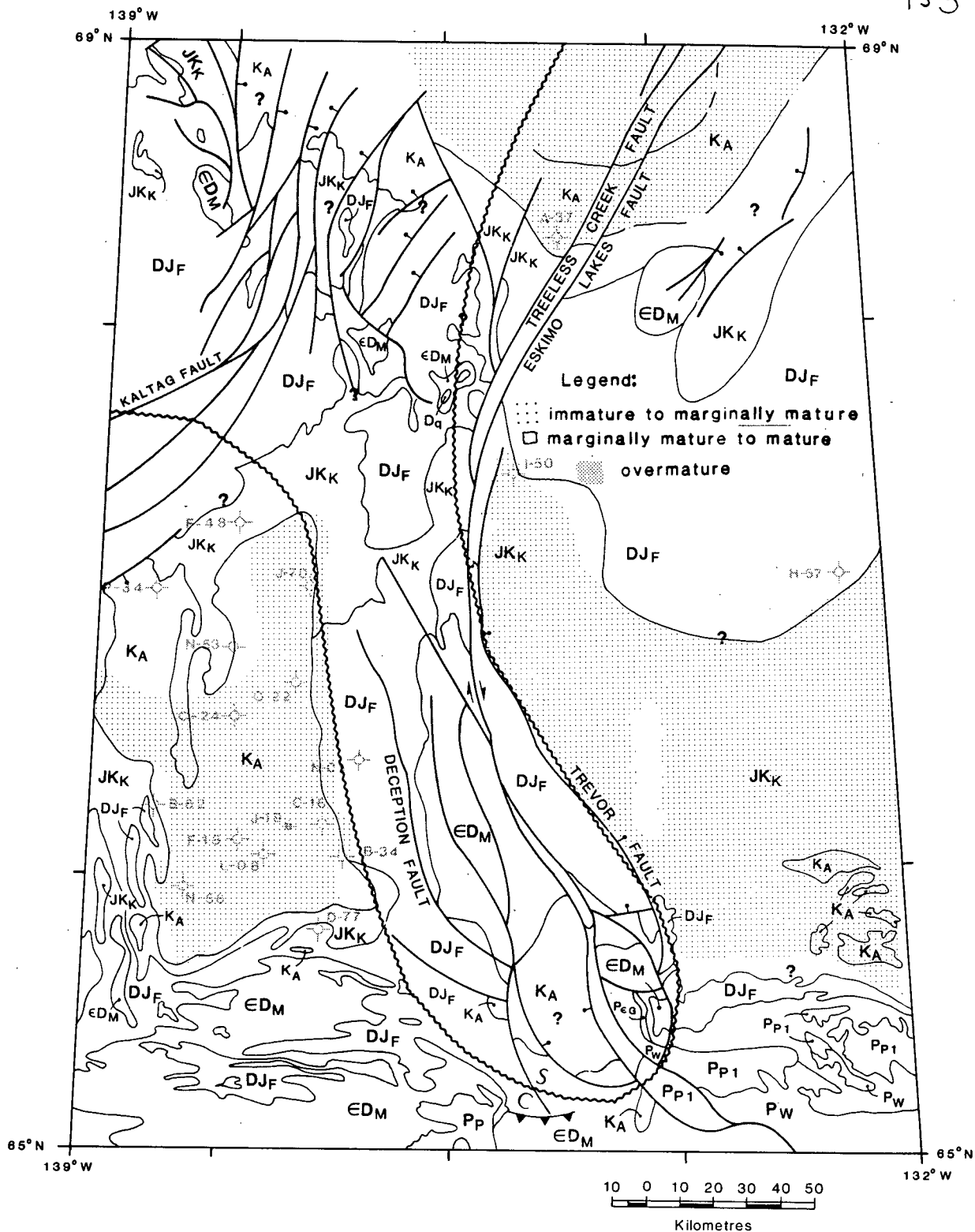


Figure 35. Present day maturity map of Phanerozoic strata in the study area. (modified from part I.)

Maturation increases with structural complexity from the Interior Platform (Peel Plateau) and Eagle Fold Belt (Eagle Plain) towards the Richardson Anticlinorium (Richardson Mountains) and from the Eagle Fold Belt towards the Taiga-Nahoni Fold Belt (Ogilvie Mountains). Mesozoic strata are immature to marginally mature in the Interior Platform, the Eagle Fold Belt and Taiga-Nahoni Fold Belt and mature to overmature in the Richardson Anticlinorium. Paleozoic and Mesozoic strata are overmature on the Campbell Uplift, in the northwestern corner of the Interior Platform. Upper Paleozoic strata are immature to marginally mature in central Eagle Fold Belt but are mature to overmature in all other areas of the study. Lower Paleozoic strata are overmature in all regions.

b. Source Rock Properties

In order to characterize a petroleum source rock, the quality of organic matter and the level of organic maturity must be assessed simultaneously, because of the strong interrelation of these two parameters (Tissot and Welte, 1984, p. 547). Several potential petroleum source rocks have been identified in the study area, based on evaluation of Rock-Eval data and maturation levels discussed above, using the experimental limits defined by Espatilié et al. (1985) and Peters (1986). The details of timing of hydrocarbon generation for different source rocks are discussed in part I.

(i) *Upper Cambrian to Lower Devonian*

Road River Group (Cronin, Loucheux, Dempster, Vitreekwa Formations)

(Figs. 23a, 24a, 25; Table IV a)

Road River strata have poor petroleum source potential, as evident from low QOM (< 1.4 mg HC/g Corg). TOC values up to 9.6% and type I or II organic matter indicate the Vitreekwa and Loucheux Formations were excellent oil prone source rocks in the former areas of the Richardson and Blackstone Troughs. However, hydrocarbons generated from Road River strata were available for migration in the Devonian to Carboniferous (see Figs. 10a, 13a, 14a and 19a of part I). In southern Mackenzie Delta, mature strata have moderate QOM (1.4 mg HC/g Corg) but poor petroleum source potential (HC potential=0.6 mg HC/g rock) as a result of low TOC content (0.5%).

The Hazen Trough is considered a northern extension of the Richardson Trough (Miall, 1976) and if the Hazen Trough had a similar deep-water depositional environment to the Richardson and Blackstone Troughs, then organic-rich shales equivalent to Road River strata may be found in the subsurface of the Mackenzie Delta.

(ii) *Middle Devonian*

Ogilvie Formation

(Figs. 23b, 24b, 26; Table IV b)

Middle Devonian carbonates have generally poor petroleum source potential, as

evident from low QOM (< 1.4 mg HC/g Corg) where strata are overmature. In southern Mackenzie Delta, mature strata have poor petroleum source potential (HC potential= 0.6 mg HC/g rock) due to low TOC (0.6%). The QOM is high (3.5 mg HC/g Corg) in overmature strata in eastern Eagle Plain (N-05 well), probably due to the presence of pyrobitumen ($T_{max}=405^{\circ}\text{C}$, $S_2=2.9$ mg HC/g rock, $HI=277$ mg HC/g Corg). The source of the pyrobitumen is uncertain but hydrocarbons generated from oil prone kerogen (type I or II) in the Road River Group and/or the Canol Formation could have migrated into porous reef carbonates of the Ogilvie Formation.

Hare Indian Formation

(Fig. 22b; Table IV c)

In the eastern Peel Plateau, a calcareous shale sample has fair gas and some oil source ($S_2/S_3=4$) potential (QOM= 2.6 mg HC/g Corg; HC potential= 3.4 mg HC/g rock) and is still within the oil window.

Hume Formation

(Figs. 23c, 24c, 26; Table IV d)

Petroleum source potential of the Hume Formation is generally poor. A TOC of 1.7% in overmature strata in western Peel Plateau indicates residual kerogen with a low QOM (0.8 mg HC/g Corg) or, alternatively, may represent cavings from the overlying Canol Formation. In eastern Peel Plateau, the sequence has poor petroleum potential (HC potential= 1.3 mg HC/g rock) but high QOM (3.0

mg HC/g Corg) because strata have a moderate level of organic maturity (1.1% Rorand; also see part I).

Canol Formation

(Figs. 23d, 24d, 27; Table IV e)

Black bituminous shales of the Canol Formation have fair to good gas and some oil potential in eastern Peel Plateau where they are mature (QOM=2.8 mg HC/g Corg; HC potential=18.1 mg HC/g rock). In western Peel Plateau, high QOM (3.0 mg HC/g Corg) in overmature strata reflects the presence of bitumen which is considered to have migrated into fracture zones in Canol shales. The strata are overmature in the Eagle Plain and Richardson and Ogilvie Mountains. Here, residual kerogen (2.4 to 8.6% TOC) suggests sufficient organic carbon was present to generate hydrocarbons when Canol strata entered the oil window in Devonian to Carboniferous time (see Figs. 9a to 19a of part I).

Regional mapping and further geochemical studies may prove the Canol Formation has sourced hydrocarbon reserves in Peel Plateau, Anderson Plain and Eagle Plain areas. The Canol Formation is considered to be the source rock for the Norman Wells oil field (Hume and Link, 1945) located on the eastern margin of the Cordillera, south of the study area.

(iii) *Upper Devonian*

Imperial Formation

(Figs. 23e, 24e, 28; Table IV f)

The Imperial Formation generally has insufficient amounts of organic carbon to be considered a possible source rock (TOC < 1%; HC potential < 2 mg HC/g rock). Notable exceptions occur in southern Eagle Plain where overmature strata contain residual kerogen (1.2 to 1.7% TOC) and in eastern Peel Plateau where mature strata in the lower part of the section have fair to good gas source potential and the QOM is moderate (1.9 mg HC/g Corg). In eastern and north-central Eagle Plain, a high QOM (4.8 and 2.6 mg HC/g Corg) reflects the presence of pyrobitumen or drilling mud contaminants. Solid bitumen (albertite, 0.69% $R_{o_{rand}}$, also see part I) which commonly occurs in outcrop samples and as a bituminous sill in Peel Plateau has excellent oil source potential (HC potential up to 363 mg HC/g rock). Norris and Cameron (1986) believe the bitumen represents mobilized, highly biodegraded hydrocarbons derived from the Canol Formation. As discussed above, Canol shales have some oil source potential in the area of Peel Plateau. Furthermore, time-temperature modelling (see part I) suggests that hydrocarbons generated from the Canol Formation were available for migration in Late Carboniferous to Early Cretaceous time in the Peel Plateau and therefore could have migrated into the Imperial Formation. Exposure at the pre-Mesozoic unconformity could subsequently have biodegraded the hydrocarbons.

(iv) *Carboniferous*

Ford Lake Shale

(Figs. 23f, 24f, 29; Table IV g)

Black and gray bituminous shales contain significant amounts of overmature organic matter (1.2 to 2.6% TOC) in the southeastern (D-77 well) and western (B-62 well) Eagle Plain. Mature organic matter in eastern (N-05 well and outcrop samples), southeastern (B-34 well) and central (L-08 well) Eagle Plain (0.7 to 7.9% TOC; QOM=1.9 to 5.3 mg HC/g Corg; HC potential=2.0 to 19 mg HC/g rock) have fair to good gas and some oil potential (type II and III organic matter). Erosional breaching of both source and reservoir rocks at the surface would have destroyed any hydrocarbon accumulations generated by the Ford Lake Shale where it crops out in eastern Eagle Plain but mature to overmature organic matter in the subsurface is considered the source of hydrocarbons in Carboniferous and Permian reservoir rocks (Graham, 1973) in Eagle Plain.

Hart River Formation

(Figs. 23g, 24g, 30; Table IV h)

Immature to marginally mature strata have fair to good gas and some oil potential (type II and III organic matter) in central (C-18 well) and southeastern (B-34 well) Eagle Plain (QOM=2.2 to 6.1 mg HC/g Corg and HC potential=1.5 to 7.8 mg HC/g rock). Overmature strata in the Ogilvie Mountains contain residual kerogen (3.7 to 4.9% TOC) which suggests sufficient organic carbon was present to consider the strata potential source rocks. Free hydrocarbons are

common throughout the section in southeastern (D-77, B-34 wells) and central (C-18, L-08 wells) Eagle Plain and may represent bitumen which migrated into the mature section. Alternatively, bitumen may have been generated from kerogen in Hart River strata (HC potential up to 7.8 mg HC/g rock). PI values which increase from 0.1 in the Ford Lake Shale to 0.6 in the Hart River Formation indicate a hydrocarbon depleted zone (Ford Lake Shale) and hydrocarbon accumulation zone in the immediately overlying Chance sandstone member of the Hart River Formation at the L-08 well (Snowdon, 1987a) and suggest the Ford Lake Shale acted as the source of hydrocarbons in the Chance sandstone.

Unnamed Carboniferous unit

(Fig. 22i; Table IV i)

Immature strata overlying the Hart River Formation in central (C-18 well) Eagle Plain have fair to good gas and some oil potential (type II and III organic matter; QOM=3.2 mg HC/g Corg; HC potential=10.7 mg HC/g rock). Free hydrocarbons (S_1 values up to 1.7 mg HC/g rock) suggest migration of hydrocarbons into immature (0.44% Rorand; see also part I) strata.

Blackie Formation

(Figs. 22g, 23h, 24h; Table IV i)

Basinal shales contain sufficient amounts of organic carbon (0.9 to 1.2% TOC) to consider the strata possible source rocks. Anomalously high HI (1050 mg HC/g Corg) and S_2/S_3 (> 5) values in the uppermost 30 to 45 m at the B-34 well

indicate type II OM (Snowdon, 1987a). Free hydrocarbons occur in parts of the section (S_1 values > 0.5 mg HC/g rock) and may represent hydrocarbons generated from mature kerogen in the Blackie Formation (HC potential=6.5 mg HC/g rock).

(v) *Jurassic*

Bug Creek Group (Murray Ridge, Almstrom Creek, Manuel Creek, Richardson Mountain, Aklavik Formations)

(Figs. 23i, 24i; Table IV j)

Organic-rich intervals indicate some petroleum source potential in southern Mackenzie Delta area. These include an 88 m section near the base of the Aklavik Formation and the top of the Richardson Mountain Formation and a 28 m section at the base of the Almstrom Creek Formation and the top of the Murray Ridge Formation. Fair to good gas source potential is interpreted for the upper zone (QOM=1.8 to 2.4 mg HC/g Corg; HC potential up to 16.2 mg HC/g rock) whereas the lower zone has fair gas potential (QOM=1.7 mg HC/g Corg; HC potential ranging from 2 to 5 mg HC/g rock).

Porcupine River Formation

(Figs. 23j, 24j; Table IV k)

Marginally mature to mature carbonaceous sandstones indicate fair gas source potential (QOM=2.4 mg HC/g Corg; HC potential=4.3 mg HC/g rock) in northern Eagle Plain (J-70 well). Free hydrocarbons which occur throughout the section at

the J-70 and F-48 wells reflect the onset of hydrocarbon generation, or may represent hydrocarbons which migrated into sandstones. The QOM (1.1 mg HC/g Corg) indicates that there is little or no petroleum generation potential left in the overmature section at the P-34 well in northern Eagle Plain.

(vi) Jurassic and Lower Cretaceous

Husky Formation and Parsons Group (Martin Creek, McGuire, Kamik Formations)

(Figs. 23k, l, 24k, l; Tables IV l, m)

The petroleum source potential of the Husky Formation and Parsons Group varies stratigraphically in southern Mackenzie Delta. The basal and upper 100 m of the Husky Formation have fair gas source potential (QOM=2.8 mg HC/g Corg and HC potential ranges from 2.6 to 12.5 mg HC/g rock) whereas the middle 200 m section has moderate TOC (0.9%) but poor petroleum source potential due to low QOM (< 1.5 mg HC/g Corg). TOC content decreases upwards from the Husky Formation to the Martin Creek Formation and petroleum source potential of the latter is poor (HC potential=1.8 mg HC/g rock; QOM=1.7 mg HC/g Corg). Moderate TOC (1.5%) and hydrocarbon potential (2.1 mg HC/g rock) indicate the overlying McGuire Formation could be an effective gas source. The Husky Formation is mature (0.53% Rorand; see also part I) in southern Mackenzie Delta and is considered to be the source for Parsons/Siku gas and condensate but the restricted areal distribution (Dixon et al., 1985) of the source units limits the overall source potential of the Husky Formation.

Mount Goodenough, Rat River and Arctic Red River Formations

(Figs. 23m-o, 24m-o, 31, 32, 33; Tables IV n-p)

Marine shale facies of the Mount Goodenough and Arctic Red River Formations contain organic-rich intervals which are potential gas source rocks. In northern Eagle Plain (J-70 well), the Mount Goodenough Formation has fair gas source potential (HC potential=2.6 mg HC/g rock; QOM=1.9 mg HC/g Corg). Immature strata from the upper 200 m of the Mount Goodenough Formation (HC potential=4.7 to 50 mg HC/g rock) and from the overlying Arctic Red River Formation (HC potential=3.8 mg HC/g rock; QOM=8.1 mg HC/g Corg) in southern Mackenzie Delta area have fair to excellent gas with minor oil source (HI up to 321 mg HC/g Corg) potential. Free hydrocarbons detected in immature strata in southern Mackenzie Delta are interpreted to represent hydrocarbons which have migrated into the section or, alternatively, may be contaminants from the drilling mud. In Peel Plateau and Richardson Mountains, the Mount Goodenough and Rat River Formations have poor petroleum source potential (QOM < 0.4 mg HC/g Corg) as a result of low TOC content (0.3% to 0.7%). Anomalously high hydrocarbon potential (2.4 mg HC/g rock) and QOM (1.9 mg HC/g Corg) in the Rat River Formation in western Peel Plateau (I-50 well) reflects the presence of migrated hydrocarbons in the immature section (PI=0.6; S₁=0.7 to 2.0 mg HC/g rock).

map unit Kur (Whitestone River Formation; Dixon, in press)

(Figs. 23p, 24p, 34; Table IV p)

Hydrocarbon potential ranging from 2.3 to 5.3 mg HC/g rock and QOM which varies from 1.3 to 2.2 mg HC/g Corg indicate fair to good gas source potential in central (C-18 and J-19 wells), north-central (O-22 well), southeastern (B-34 well) and northern (J-70 well) Eagle Plain. Liptinite observed petrographically in some samples, along with the HI vs OI plot indicate that type I and II oil prone organic matter is present in certain samples from southeastern (B-34 well), central (C-24, J-19 wells) and northern (P-34, F-48 wells) Eagle Plain. The high HI values (590 to 1140 mg HC/g rock) may represent drilling mud contaminants.

Strata are immature at all locations where they were examined except in the Richardson Mountains and northwestern (N-53 well) Eagle Plain where strata are mature but have poor petroleum source potential (QOM=0.2 to 1.7 mg HC/g Corg; HC potential=0.3 to 1.8 mg HC/g rock).

(vii) Upper Cretaceous

Eagle Plain Group (Cody Creek, Burnthill Creek, Fishing Branch and Parkin Formations; Dixon, in press)

(Figs. 23q, 24q, 16, Table IV q)

Carbonaceous strata of the Eagle Plain Group have fair to excellent gas source potential in parts (see Table IV p) of central Eagle Plain (QOM=1.3 to 2.3 mg HC/g Corg; HC potential=2.3 to 9.8 mg HC/g rock) but are immature, except at

the P-34 well where the strata are mature. Petrographically, vitrinite and varying proportions of liptinite and inertinite comprise most of the organic matter in carbonaceous samples. Variations in the amount of hydrogen-rich organic matter (liptinite) is reflected in the wide spread of the QOM (0.1 to 2.3 mg HC/g Corg). The high hydrocarbon potential (3.6 mg HC/g rock) and TOC (2.7%) at the C-24 well may be a result of drilling mud additives (Snowdon, 1987a) or, alternatively, may be correlative with carbonaceous samples (HC potential=3.9 mg HC/g rock; TOC=2.1%) at the C-18 well nearby.

2. Relationship of Type and Abundance of Organic Matter to Depositional Environment

The factors affecting the quality and quantity of organic matter in sediments has recently received considerable attention. In particular, studies by Dow (1977), Tourtelot (1979), Demaison and Moore (1980), McKirdy and Cook (1980), Tissot et al. (1980), Barron (1985) and Dembicki et al. (1985) have documented the importance of depositional environment in evaluating petroleum source potential. The chemical composition of immature kerogen varies with the original biomass and with the physical, chemical and biochemical conditions of deposition. Three or four types of kerogen are traditionally recognized, based on the atomic composition of 3 major elements (C, H, O; Van Krevelen, 1961). Type I kerogen comprises mainly lipids and results from the accumulation of algal organic material and/or from biodegradation of non-lipid organic matter during deposition in a marine or lacustrine environment (Tissot and Welte, 1984, p. 151). Type II organic matter is usually related to marine sediments where anoxic conditions in

the water column are critical for enhanced preservation of marine planktonic and microbial remains (Demaison and Moore, 1980; Tissot and Welte, 1984, p. 151). Terrestrial plants comprise type III organic matter, which is commonly associated with detrital sedimentation along continental margins (Tissot and Welte, 1984, p. 154) where an oxic water column suppresses the deposition of planktonic remains (Tissot et al., 1980). A mixture of type II and III kerogen is generally considered a result of significant terrestrial input into anoxic marine basins (Tissot et al., 1980).

In this study, where there is no obvious indication for a different depositional environment or for migration phenomena, HI values > 400 mg HC/g Corg which occur in several samples are interpreted to represent drilling mud contaminants. TOC, S_2 and S_3 tend to decrease as the DOM increases and the S_2/S_3 ratio and the HI become less meaningful at higher levels of organic maturity (Snowdon, 1987b). Thus, low and/or scattered HI values and S_2/S_3 ratios may not be related to processes operating in the depositional environment.

In this reconnaissance study, too few data are available to rigorously interpret the distribution of organic matter, however, for at least some stratigraphic units there appears to be a good correlation between depositional environment and organic richness and type as summarized below.

(i) *Upper Cambrian to Lower Devonian*

Road River Group (Cronin, Loucheux, Dempster, Vitreekwa Formations)

(Figs. 23a, 24a, 7; Table IV a)

Road River strata have the highest TOC content in the Richardson (2.9 to 9.6% TOC) and Ogilvie (2.5 to 5.0% TOC) Mountains, which mark the former position of the Richardson and Blackstone Troughs. These troughs were fault-bounded intracratonic depressions which dissected a regional shelf that extended across the Mackenzie Platform and Yukon Stable Block (Porcupine Platform) from Cambrian until Early to Middle Devonian time (A.W. Norris, 1985). The distribution of TOC in the Road River Group closely reflects a four-fold lithological division. The lower and upper graptolite-bearing and siliceous shale units of deep water origin (Blackstone and Richardson Troughs) have TOC values up to 9.6%. Low TOC values (< 1% TOC) correspond to limestones which were deposited during shallowing of the troughs and on neighboring platforms (A.W. Norris, 1985).

Kerogen is dominantly type III but tasmanites was observed petrographically in the Vitreekwa Formation (see also part III) indicating the presence of hydrogen-rich (type I or II) organic matter.

(ii) *Middle Devonian*

Ogilvie and Hume Formations

(Figs. 23b, c, 24b, c, 8; Tables IV b, d)

Limestones of the Ogilvie and Hume Formations with low TOC (0.5%) were deposited on platforms to the west and east, respectively, of the Richardson Trough shale basin (A.W. Norris, 1985). A single organic-rich sample from the Hume Formation (3% TOC) in western Peel Plateau may correspond to a transition from carbonate platform to basinal shale deposition (A.W. Norris, 1985) or, alternatively, may represent cavings from the overlying Canol Formation. High TOC (up to 4.5%) in the Ogilvie Formation in eastern Eagle Plain reflects the presence of pyrobitumen (see discussion above, Source Rock Properties) rather than processes operating in the depositional environment. Although the organic matter in carbonates is commonly sapropelic (type I or II; Hunt, 1974, p. 278), HI vs OI plots (Figs. 24b and c) suggest organic matter in the Hume and Ogilvie Formations is primarily type III. Relatively low HI values are, for the most part, due to the high degree of organic maturity (1.0 to 2.3% Rorand; see also part I).

Canol Formation

(Figs. 23d, 24d, 27; Table IV e)

The variation in TOC of the Canol Formation (Table IV e) is, for the most part, independent of the level of organic maturity and reflects both migration phenomena (see discussion above, Source Rock Properties) and lithofacies patterns.

A low TOC (0.7%) occurs in calcareous mudstones of the DCU unit (Norris, 1981e) whereas moderate to high (1.5 to 8.6%) TOC values occur in black siliceous shales. Bituminous, transgressive shales of the Canol Formation are believed to be products of slow sedimentation (Snowdon et al., 1987) and the absence of bioturbation, and thin, evenly-bedded shales suggest a deep-water anoxic environment of deposition (A.W. Norris, 1985). Modelling of sea level changes and global atmospheric circulation patterns has shown that northwestern Canada lay in a coastal upwelling zone in Devonian time, which may account for the organic-rich units of the Canol Formation (Parrish, 1982). Significant variation in organic enrichment (1.5 to 8.6% TOC) and type III and a mixture of type II and III organic matter are considered to represent variations in the degree of upwelling. The richest sources may represent sediments of deeper water origin whereas shales with lower TOC and which contain a mixture of type II and III organic matter are consistent with deposits near highlands where upwelling was less vigorous and/or there was a nearby source of terrestrial organic matter.

HI vs OI plots (Fig. 24d) indicate a large proportion of type III organic matter whereas other studies (Snowdon et al., 1987) suggest the organic matter is primarily type II in the Norman Wells area. Canol strata in the present study are less mature (mature to overmature, Table IV f; see also part I) than coeval strata in the Norman Wells area. Low HI values (and resulting type III classification) in Canol strata in the study area are interpreted to be a result of the high degree of organic maturity.

*(iii) Upper Devonian**Imperial Formation**(Figs. 23e, 24e, 28; Table IV f)*

The Canol provided the base during Late Devonian time for thick marine turbidite and deltaic deposits (Pugh, 1983) of the Imperial Formation. Sandstones and siltstones of the upper part of the Formation are interpreted as deposits of a rapidly prograding deltaic system (Pugh, 1983) in which low to moderate TOC (0.2 to 1.5%), composed of plant fragments and spores, occur. High sedimentation rates in the Devonian (up to 100 m/Ma; Hea et al., 1980) would tend to dilute the organic matter content of clastic deposits. Turbidite deposits (A.W. Norris, 1985) of the lower member of the Imperial Formation have moderate TOC (1.2%). Rapid sedimentation (up to 40 m/Ma; Ibach, 1982) associated with turbidite depositional environment would tend to dilute the organic matter on one hand, but preserve it on the other, due to limited diffusion of oxygen into the underlying sediments (Dow, 1977). Moderate to high sedimentation rates tend to reduce the residence time of organic matter on the sediment surface, where aerobic processes decompose the organic matter (Didyk et al., 1978), thereby enhancing the preservation of organic matter. The highest TOC values (1.4 to 1.7%) correspond to the black shale facies of Pugh (1983), located in southern Eagle Plain and eastern Peel Plateau areas, and may represent deposition of organic-rich muds in a marine basin where anoxic conditions were favorable for preservation of organic matter. Samples with TOC values ranging from 4.3 to 95.7% contain bitumen (albertite, 0.6% Rorand; see also part I) which is interpreted to be a result of migration (see discussion above, Source Rock

Properties'), rather than organic enrichment due to processes operating in the depositional environment.

(iv) Carboniferous

Ford Lake Shale and Hart River Formation

(Figs. 23f, g, 24f, g, 29, 30; Tables IV g, h)

Clastic sediments of Carboniferous age consist of transitional marine facies and marine limestone and calcareous shale facies of the Hart River Formation and the basinal transgressive facies of the Ford Lake Shale (Pugh, 1983). The variation in TOC of Carboniferous strata in Eagle Plain (Tables IV g and h) reflects increasing maturation to the southeast, but is otherwise independent of the level of organic maturity. Moderate to high TOC (1.2 to 7.9%) comprising a mixture of type II and III organic matter in the Ford Lake Shale and in shales of the Hart River Formation suggest significant input of terrestrial organic matter into a marine basin in central Eagle Plain. Low TOC values (0.5 to 0.8%) in shoreline sandstones and siltstones near the northern erosional edge of the Ford Lake Shale may be a result of poor preservation of organic matter in a high energy shoreface (oxygenated waters) depositional environment or, alternatively, may be due to oxidation of organic matter where strata are exposed at the pre-Mesozoic unconformity. The increase in TOC of the Hart River Formation towards southeastern Eagle Plain does not reflect the depositional environment but is a result of migrated bitumen.

(v) *Jurassic and Lower Cretaceous*

Bug Creek Group (Murray Ridge, Almstrom Creek, Manuel Creek, Richardson Mountain, Aklavik Formations)

Porcupine River and Husky Formations, Parsons Group (Martin Creek, McGuire, Kamik Formations)

(Figs. 23i-l, 24i-l; Tables IV j-l)

The lateral variation in organic-richness and maturity could not be determined for Jurassic to mid-Hauterivian strata because they have been eroded from most parts of the study area (Jeletsky, 1974, 1980). However, where preserved, the vertical variation in Rock-Eval data appears to be closely related to the depositional environment of the strata. Strata of the Bug Creek Group, Husky Formation and Parsons Group consist of marine shelf sediments oscillating between fine and coarse clastic deposits as a result of variable sediment supply, erosional episodes and transgressive and regressive phases (Dixon, 1982; Poulton et al., 1982). At the base of the succession, in southern Mackenzie Delta, moderate TOC content (2.2%) and type III organic matter with abundant spores and pollen (Poulton et al., 1982) are consistent with shoreface to offshore open marine sediments of the Murray Ridge Formation and shallow marine shelf deposits of the Almstrom Creek Formation. Declining TOC content (1.6%) in younger strata of the Richardson Mountain Formation coincide with local sands deposited on an otherwise muddy, open shelf regime (Poulton et al., 1982). TOC values which increase upwards from 2.2 to 3.7% in overlying carbonaceous (type III organic matter) sandstones of the Aklavik Formation attest to proximity to a shoreline (Dixon, 1982) where a significant input of terrestrial organic matter

occurred. A shale sample with high TOC (5.6%), in the middle of the Aklavik Formation, may represent a shale tongue of the Richardson Mountain Formation which extends into sandstones of the Aklavik Formation (see also Dixon, 1982). Basin-margin expansion (Dixon, 1982) resulted in deposition of low energy marine shales of the Husky Formation and corresponding increase in TOC (3.7 to 4.5%), followed by a basin-wide regression (Dixon, 1982), which correlates with TOC values which decrease upward from the base to the middle of the Husky Formation (4.5 to 0.8%). A short-lived transgression followed, which led to a reduction of sediment supply basinward (Dixon, 1982) and is reflected in TOC values which increase from 1.5% in the middle to 2.7% at the top of the Husky Formation. Progradation and basin-filling resulted in deposition of a thick coarsening-upward cycle representing an offshore-barrier island succession (Dixon, 1982) in which TOC values decrease upwards from the Husky to Martin Creek Formation (2.7 to 0.9%). TOC content which increases upwards (0.9 to 1.5%) in carbonaceous sandstones and shales of the overlying McGuire Formation is consistent with a change to a low energy nearshore to inner shelf depositional environment (lagoonal or upper coastal plain; Dixon, 1982) where significant terrestrial input occurred and/or preservation of marine organic matter was enhanced.

The Porcupine River Formation represents a minor phase of deltaic sedimentation (Jeletsky, 1980) in Eagle Plain area. Total organic carbon content is lower (0.9 to 1.8%) in carbonaceous sandstones of the Porcupine River Formation than in laterally equivalent marine shales of the Husky Formation (2.0%) and organic matter is primarily type III in both Formations.

Mount Goodenough Formation

(Figs. 23m, 24m, 31; Table IV m)

The Mount Goodenough Formation consists of basal transgressive strata overlain by a generally regressive complex of marine shales and siltstones deposited on the slope to inner shelf (Dixon, 1986). Although the variation in TOC (Table IV m), in part, reflects increasing maturation towards the Richardson Mountains, the regional TOC distribution appears to be related to the depositional environment. In southern Mackenzie Delta, TOC content (1.0 to 5.5%) and HI values (120 to 321 mg HC/g Corg) increase upwards in regressive deposits (nearshore to inner shelf; Dixon, 1982). An increase in HI (type II organic matter) has been related to enhanced marine organic productivity and/or physical controls such as reduced circulation of oxygenated water or an oxygen-minimum zone controlled by water depth (Snowdon, 1980). Shallow waters in a nearshore to inner shelf setting would enhance marine productivity and create an oxygen-minimum zone favorable to the preservation of marine (type II) organic matter. Alternatively, an increase in HI may represent liptinite-rich terrestrial organic matter derived from deposition and preservation of allochthonous spores and pollen in a nearshore environment. Lipids associated with water-insoluble waxes and cutins from higher plants are less easily hydrolyzed by bacteria than proteins and carbohydrates (Barnes et al., 1984.)

Low to moderate TOC (0.6 to 1.5%) and HI values (< 150 mg HC/g Corg) in Peel Plateau and Eagle Plain areas occur in sediments deposited on the continental shelf and slope. Low HI values may represent input of terrestrial

organic matter into oxygenated waters on the shelf and slope where marine (type II) organic matter would be chemically and/or biologically degraded.

*Arctic Red River and Horton River Formations and map unit Kwr
(Whitestone River Formation)*

(Figs. 23o, p, 24o, p, 33; Table IV o)

Albian strata of the Arctic Red River and Horton River Formations and map unit Kwr are low energy shelf deposits (Dixon, 1986) which generally contain 1 to 2% TOC in mainly terrestrial (type III) kerogen. A mixture of type II and III organic matter in some samples of the Arctic Red River Formation and map unit Kwr suggests input of terrestrial organic matter into anoxic marine waters on the continental shelf. The regional variation in TOC (Table IV o) is independent of maturity levels and may reflect local bathymetric lows and highs on the shelf. TOC values up to 5.4% and HIs ranging from 590 to 1140 mg HC/g Corg in the map unit Kwr suggest significant enrichment in marine-type (type II or I) organic matter or, alternatively, contaminants added to the drilling mud. In southern Mackenzie Delta, TOC contents up to 2.5% reflect the presence of free hydrocarbons rather than factors controlling organic richness in the depositional environment.

(vi) *Upper Cretaceous*

Eagle Plain Group (Cody Creek, Burnthill Creek, Fishing Branch and Parkin Formations)

(Figs. 23q, 24q, 34, Table IV p)

In most of the Eagle Plain area, the Upper Cretaceous part of the Eagle Plain Group (map units Kfb, Kb and Kcc of Norris, 1981g) consists of marine sandstones, siltstones and shales interpreted as nearshore to inner shelf deposits (Dixon, 1986). TOC content exceeds 4% in several samples in map units Kb and Kfb, in which carbonaceous and coaly debris was observed petrographically. Local bathymetric lows and highs probably existed on the shelf (Dixon, 1986) and may have controlled variations in organic richness by influencing water circulation patterns and/or water depths. Alternatively, high TOC values in carbonaceous samples containing varying proportions of vitrinite, liptinite and inertinite suggest significant input of terrestrial organic matter in a nearshore to inner shelf depositional environment. Anomalously high TOC (13%) and HI values (600 to 1000 mg HC/g Corg) at the P-34 and C-24 wells are considered a product of the presence of drilling mud additives (Snowdon, 1987a) rather than processes operating in the depositional environment.

F. SUMMARY AND CONCLUSIONS

1. Organic-rich units with mostly gas and some oil source potential occur throughout the Phanerozoic succession in the northern Yukon and northwestern District of Mackenzie.

- a. TOC content of the Upper Cambrian to Lower Devonian Road River Group and Middle Devonian strata (Hare Indian and Canol Formations) ranges from 0.1 to 9.6%; generally low QOM (< 1.5 mg HC/g Corg) indicates poor petroleum source potential. Notable exceptions occur in Peel Plateau where the Hare Indian (1.3% TOC) and Canol Formations have fair to good gas and some oil potential (QOM=2.6 to 3.0 mg HC/g Corg). Residual kerogen in overmature Road River and Canol strata indicate sufficient organic matter was present to consider the strata potential petroleum source rocks in the Eagle Plain (Canol Formation only) and Richardson and Ogilvie Mountains.
- b. Petroleum source potential of the Upper Devonian Imperial Formation is poor because TOC content is generally $< 1\%$ and QOM is < 1.5 mg HC/g Corg. Notable exceptions occur in southern Eagle Plain where overmature strata contain residual kerogen and eastern Eagle Plain where mature strata have some gas potential.
- c. Carboniferous strata of the Ford Lake Shale and Hart River and Blackie Formations and unnamed strata overlying the Hart River Formation have mean TOC values which vary from 0.4 to 7.9%. A significant spread in the QOM (0.4 to 6.1 mg HC/g Corg) is a result of variations in the level of organic maturity, the type of organic matter and, in some cases, migration. Carboniferous strata have fair to good gas source potential and

parts of the section have some oil potential (type II OM). The Ford Lake Shale is considered the source of hydrocarbons in the Chance sandstone member of the Hart River Formation.

- d. TOC content of the Jurassic Bug Creek Group generally falls between 1% and 2% with values up to 5.6% in the Richardson Mountain Formation. A moderate QOM (1.8 to 2.4 mg HC/g Corg) suggests fair to good gas potential in certain horizons (base of Aklavik and top of Richardson Mountain Formations and the base of Almstrom Creek and top of Murray Ridge Formations).
- e. TOC content generally ranges from 1 to 2% in the Jurassic to Lower Cretaceous Husky Formation in southern Mackenzie Delta and is lower (0.9 to 1.8% TOC) in Jurassic strata of the Porcupine River Formation which are in part equivalent. Some shale samples from the Husky Formation show significant organic enrichment (up to 4.5% TOC) and fair to good gas source potential (1.8 mg HC/g Corg). Moderate QOM of the Porcupine River Formation (1.9 to 2.4 mg HC/g Corg) in northern Eagle Plain indicates fair gas source potential whereas no potential petroleum generation remains in overmature strata further to the northwest (P-34 well) in Eagle Plain area.

f. Lower Cretaceous strata of the Parsons Group, Mount Goodenough and Arctic Red River Formations and map unit Kwr have TOC values which commonly fall between 0.5% and 1.5%; organic-rich units (up to 5.4%) occur in parts of the map unit Kwr and the Mount Goodenough Formation. Portions of the Parsons Group (McGuire Formation) have fair gas potential (QOM=1.4 mg HC/g Corg) in southern Mackenzie Delta. Significant variation in the QOM of the Mount Goodenough Formation (0.1 to 2.7 mg HC/g Corg) and Albian strata (0.01 to 3.8 mg HC/g Corg) reflects differences in the type of organic matter (hydrogen-rich versus hydrogen-poor) and in the regional variation in the level of organic maturity. In Eagle Plain, parts of the Mount Goodenough Formation and map unit Kwr have fair gas potential whereas fair to good gas and some oil potential is interpreted for the Arctic Red River Formation in southern Mackenzie Delta. Anomalously high HI values in some samples from the map unit Kwr suggest some oil source potential or, alternatively, may represent mud contaminants.

g. The Upper Cretaceous Eagle Plain Group has average TOC values generally ranging from 0.3 to 2.7% and carbonaceous samples contain up to 14.5% TOC. Organic-rich units (QOM=1.3 to 2.3 mg HC/g Corg) in central Eagle Plain have fair to excellent gas source potential but all strata are immature except in northern (P-34 well) Eagle Plain where the section is mature.

2. The organic matter is dominantly type III in all strata with minor amounts of type I or II in the Road River Group and a mixture of type II and III in parts of the Ford Lake Shale, the Hare Indian, Canol, Hart River, Blackie, Husky, Mount Goodenough and Arctic Red River Formations, the map unit Kwr and the unnamed Carboniferous unit.

3. There appears to be a good correlation between depositional environment and organic richness and kerogen type for at least some stratigraphic units.

a. Organic-rich graptolite-bearing and siliceous shales from the lower and upper parts of the Road River Group coincide with sediments of deep-water origin deposited in the ancient Richardson and Blackstone Troughs. Tasmanites, observed petrographically suggest type I or II organic matter in the Vitreekwa Formation.

b. Limestones with low TOC values of the Ogilvie and Hume Formations were deposited on the platforms to the west and east, respectively of the Richardson Trough shale basin.

c. A mixture of type II and III organic matter in transgressive bituminous shales of the Canol Formation corresponds to sediments deposited on a continental shelf where upwelling resulted in organic-rich marine shales

with variable amounts of terrestrial organic matter. The absence of bioturbation and thin, evenly bedded shales suggest a deep-water anoxic environment of deposition.

- d. Sandstones and siltstones of the upper part of the Imperial Formation are interpreted as deposits of a rapidly prograding deltaic system (Pugh, 1983) in which low to moderate TOC (0.2 to 1.5%), composed of plant fragments and spores, occur. Turbidite deposits of the lower member of the Formation have moderate TOC (1.2%). Variations in TOC content of the Imperial Formation may be related to differences in sedimentation rates between turbidite and deltaic deposition.
- e. Organic-rich marine shales of the Ford Lake Shale were deposited during a transgression in Early Carboniferous. A mixture of type II and III organic matter in the Ford Lake Shale and basinal shales of the overlying Hart River Formation may signify input of terrestrial organic matter into an anoxic marine basin.
- f. Variations in TOC content of Jurassic to Lower Cretaceous strata of the Bug Creek Group, Husky Formation and Parsons Group reflect variable sediment supply and to transgressive and regressive episodes. Terrestrial organic matter in the Murray Ridge Formation (abundant spores and

pollen) and the Aklavik and McGuire Formations (carbonaceous woody material) correspond to sediments deposited in close proximity to a shoreline during a regression. Organic-rich marine shales which were deposited in a low energy environment occur in the Richardson Mountain Formation and in the lower part of the Husky Formation; although these shales have been deposited in a marine setting, the organic matter is mainly type III. Low TOC values occur in strata which represent regressive episodes during sedimentation of the Martin Creek Formation and the middle part of the Husky Formation.

g. Deltaic deposits of the Jurassic Porcupine River Formation have moderate TOC values (0.9 to 1.2%) in mainly type III organic matter.

h. Lower Cretaceous strata of the Mount Goodenough and Arctic Red River Formations and unit Kwr comprise, in part, marine shale facies deposited in a low energy shelf environment. Type III organic matter is predominant in Lower Cretaceous strata but a mixture of type II and III organic matter occurs in some samples and is more typical of marine shale facies. Significant organic enrichment and hydrogen-rich organic matter in some samples may be related to enhanced marine organic productivity and/or physical controls such as water circulation or depth. Alternatively, hydrogen-rich organic matter may indicate liptinite-rich terrestrial organic matter derived from allocthonous spores and pollen

deposited in a nearshore to inner shelf environment. Drilling mud contamination may also explain anomalously high TOC and Hydroden Index values.

- i. TOC content exceeds 4% in several samples in map units Kb and Kfb of the Eagle Plain Group, in which carbonaceous and coaly debris was observed petrographically. Variations in average TOC (1.4 to 4.9%) in the Eagle Plain Group may be related to local bathymetric highs and lows on the shelf or, alternatively, to significant input of terrestrial OM in a nearshore to inner shelf depositional environment.

VI. REFERENCES

- Balkwill, H.R., Cook, D.G., Detterman, R.L., Embry, A.F., Hakansson, E., Miall, A.D., Poulton, T.P. and Young, F.G., 1983. Arctic North America and northern Greenland; in Mesozoic of Arctic North America and Greenland. In: M. Moullade and A.E.M. Nairn, eds., Phanerozoic of the World II, Mesozoic A. Amsterdam: Elsevier, p. 1-31.
- Bamber, E.W. and Waterhouse, J.B., 1971. Carboniferous and Permian stratigraphy and paleontology, northern Yukon Territory, Canada. Bulletin of Canadian Petroleum Geology, 19, p. 29-250.
- Bamber, E.W., Macqueen, R.W. and Richards, B.C., 1980. Facies relationships at the Mississippian carbonate platform margin, Western Canada. Geological Survey of Canada, Open File No. 674.
- Barnes, M.A., Barnes, W.C. and Bustin, R.M., 1984. Diagenesis 8. Chemistry and evolution of organic matter. Geoscience Canada, 11, p. 103-114.
- Barron, E.F., 1985. Numerical climate modelling, a frontier in petroleum source rock prediction: Results based on Cretaceous sediments. American Association of Petroleum Geologists Bulletin, 69, p. 448-459.
- Bustin, R.M., Barnes, M.A., and Barnes, W.C., 1985. Organic diagenesis 10. Quantification and modelling of organic diagenesis. Geoscience Canada, 12, p. 1-21.
- Coté, R.P., Lerand, M.M. and Rector, R.J., 1975. Geology of the Lower Cretaceous Parsons Lake gas field, Mackenzie Delta, Northwest Territories. In: C.J. Yorath, E.R. Parker and D.J. Glass, eds., Canada's continental margins and offshore petroleum exploration. Canadian Society of Petroleum Geologists; Memoir 4, p. 613-632.
- Demaison, G.J. and Moore, G.T., 1980. Anoxic environments and oil source bed genesis. American Association of Petroleum Geologists Bulletin, 64, p. 1179-1209.
- Dembicki, H., Jr. and Pirkle, F.L., 1985. Regional source rock mapping using a source potential rating index. American Association of Petroleum Geologists

Bulletin, 69, p. 567-581.

Didky, B.M., Simoneit, B.R.T., Brassell, S.C. and Eglinton, G., 1978. Organic geochemical indicators of paleoenvironmental conditions of sedimentation. *Nature*, 272, p. 216-222.

Dixon, J., 1982. Jurassic and Lower Cretaceous subsurface stratigraphy of the Mackenzie Delta-Tuktoyaktuk peninsula, N.W.T. Geological Survey of Canada, Bulletin 349, 52 p.

-----, 1986. Cretaceous to Pleistocene stratigraphy and paleogeography, northern Yukon and northwestern District of Mackenzie. *Bulletin of Canadian Petroleum Geology*, 34, p. 49-70.

-----, Dietrich, J.R., McNeil, D.H., McIntyre, D.J., Snowdon, L.R. and Brooks, P., 1985. Geology, biostratigraphy and organic geochemistry of Jurassic to Pleistocene strata, Beaufort-Mackenzie area, northwest Canada. *Canadian Society of Petroleum Geologists, Course Notes*, 65 p.

-----, in press. Mesozoic stratigraphy, Eagle Plain area, northern Yukon. Geological Survey of Canada, Bulletin.

Dow, W.G., 1977. Petroleum source beds on continental slopes and rises. *American Association of Petroleum Geologists Continuing Education Course Notes Series*, No. 5, p. D1-D37.

Durand, B., ed., 1980. *Kerogen: Insoluble organic matter from sedimentary rocks*. Paris: Technip, 622 p.

Espitalié, R., Madec, M. and Tissot, B., 1977. Source rock characterization method for petroleum exploration. 9th Annual Offshore Technology Conference, Houston, Texas, p. 439-444.

-----, Deroo, G. and Marquis, F., 1985. RockEval pyrolysis and its applications. *Institut Francais du Petrole*, reprint No. 27299, 132 p.

Graham, A.D., 1973. Carboniferous and Permian stratigraphy, southern Eagle Plain, Yukon Territory, Canada. *In: J.D. Aitken and D.J. Glass, eds., Symposium on geology of the Canadian Arctic*. Geological Association of Canada and Canadian Society of Petroleum Geologists, p. 159-180.

- Hea, J.P., Arcuri, J., Campbell, G.R., Fraser, I., Fuglem, M.O., O'Bertos, J.J., Smith, D.R. and Zayat, M., 1980. Post-Ellesmerian basins of Arctic Canada: Their depocentres, rates of sedimentation and petroleum potential. In: A.D. Miall, ed., Facts and principles of world petroleum occurrence. Canadian Society of Petroleum Geologists, Memoir 6, p. 447-488.
- Hume, G.S., 1954. Lower Mackenzie River area, Northwest Territories and Yukon. Geological Survey of Canada, Memoir 273, 118 p.
- and Link, T.A., 1945. Canol investigations in the Mackenzie River area, Northwest Territories and Yukon. Geological Survey of Canada Paper, Paper 45-16, 87 p.
- Hunt, J.M., 1979. Petroleum geology and geochemistry. San Francisco: W.H. Freeman, 617 p.
- Ibach, L.E., 1982. Relationship between sedimentation rate and total organic carbon content in ancient marine sediments. American Association of Petroleum Geologists Bulletin, 66, p. 170-180.
- International Committee for Coal Petrography (I.C.C.P.), 1971. International handbook for coal petrology, 1st supplement to 2nd edition. Centre National de la Recherche Scientifique, Paris.
- Jeletsky, J.A., 1958. Uppermost Jurassic and Cretaceous rocks of Aklavik Range, northeastern Richardson Mountains, Northwest Territories. Geological Survey of Canada, Paper 58-2, 84 p.
- , 1960. Uppermost Jurassic and Cretaceous rocks, east flank of Richardson Mountains between Stony Creek and lower Donna River, Northwest Territories. Geological Survey of Canada, Paper 59-14, 31 p.
- , 1961. Uppermost Jurassic and Lower Cretaceous rocks, west flank of Richardson Mountains between the headwaters of Blow River and Bell River, Yukon Territory. Geological Survey of Canada, Paper 61-9, 42 p.
- , 1967. Jurassic and (?)Triassic rocks of the eastern slopes of Richardson Mountains, northwestern District of Mackenzie. Geological Survey of Canada, Paper 66-50, 171 p.

- , 1972. Stratigraphy, facies and paleogeography of Mesozoic rocks of northern Yukon and northwest Mackenzie District, N.W.T. (NTS-197B, 106M, 117A, 116O N 1/2). Geological Survey of Canada, Paper 72-1A, p. 212-215.
- , 1974. Contribution to the Jurassic and Cretaceous geology of northern Yukon Territory and District of Mackenzie, N.W.T. Geological Survey of Canada, Paper 74-10, 23 p.
- , 1975. Jurassic and Lower Cretaceous paleogeography and depositional tectonics of Porcupine Plateau, adjacent areas of northern Yukon and those of Mackenzie District. Geological Survey of Canada Paper, 74-16, 52 p.
- , 1980. Lower Cretaceous and Jurassic rocks of McDougall Pass area and some adjacent areas of north-central Richardson Mountains, northern Y.T. and northwestern District of Mackenzie, N.W.T. (NTS-116P/9 and 116P/10): a reappraisal. Geological Survey of Canada, Paper 78-22, 35 p.
- Kunst, H., 1973. The Peel Plateau. In: R.G. McCrossan, ed., The future petroleum provinces of Canada. Canadian Society of Petroleum Geologists, Memoir 1, p. 213-244.
- Lerand, M., 1973. Beaufort Sea. In: R.G. McCrossan, ed., The future petroleum provinces of Canada. Canadian Society Petroleum Geologists, Memoir 1, p. 315-386.
- Lewan, M.D. and Williams, J.A., 1987. Evaluation of petroleum generation from resinites by hydrous pyrolysis. American Association of Petroleum Geologists Bulletin, 71, p. 207-214.
- Macauley, G., Snowdon, L.R. and Ball, F.D., 1985. Geochemistry and geological factors governing exploitation of selected Canadian oil shale deposits. Geological Survey of Canada, Paper 85-13, 65 p.
- Martin, H.L., 1972. Upper Paleozoic stratigraphy of the Eagle Plain basin, Yukon Territory. Geological Survey of Canada, Paper 71-14, 54 p.
- , 1973. Eagle Plain basin, Yukon Territory. In: R.G. McCrossan, The future petroleum provinces of Canada. Canadian Society of Petroleum Geologists, Memoir 1, p. 275-306.

- McKirdy, D.M. and Cook, P.J., 1980. Organic geochemistry of Pliocene - Pleistocene calcareous sediments, DSDP Site 262, Timar Trough. American Association of Petroleum Geologists Bulletin, 64, p. 2118-2138.
- Miall, A.D., 1973. Regional geology of northern Yukon. Bulletin of Canadian Petroleum Geology, 21, p. 81-116.
- , 1976. Proterozoic and Paleozoic geology of Banks Island, Arctic Canada. Geological Survey of Canada, Bulletin 258, 77 p.
- Mountjoy, E.W., 1967. Upper Cretaceous and Tertiary stratigraphy, northern Yukon and northwestern District of Mackenzie. Geological Survey of Canada, Paper 66-16, 70 p.
- and Chamney, T.P., 1969. Lower Cretaceous (Albian) of the Yukon: Stratigraphy and foraminiferal subdivisions, Snake and Peel rivers. Geological Survey of Canada, Paper 68-26, 71 p.
- Norris, A.W., 1985. Stratigraphy of Devonian outcrop belts in northern Yukon Territory and Northwest Territories, District of Mackenzie (Operation Porcupine Area). Geological Survey of Canada, Memoir 410, 81 p.
- Norris, D.K., 1980. Bedrock geology of the Dempster Lateral. In: A.D. Miall, ed., Facts and principles of world oil occurrence. Canadian Society Petroleum Geologists, Memoir 6, p. 535-550.
- , 1981a. Geology: Fort McPerson, District of Mackenzie. Geological Survey of Canada, Map 1520A.
- , 1981b. Geology: Arctic Red River, District of Mackenzie. Geological Survey of Canada, Map 1521A.
- , 1981c. Geology: Bell River, Yukon Territory-Northwest Territories. Geological Survey of Canada, Map 1519A.
- , 1981d. Geology: Eagle Plain, Yukon Territory. Geological Survey of Canada, Map 1523A.
- , 1981e. Geology: Aklavik, District of Mackenzie. Geological Survey of

- Canada, Map 1517A.
- , 1981f. Geology: Porcupine River, Yukon Territory. Geological Survey of Canada, Map 1522A.
- , 1982a. Geology: Hart River, Yukon Territory. Geological Survey of Canada, Map 1527A.
- , 1982b. Geology: Ogilvie River, Yukon Territory. Geological Survey of Canada, Map 1526A.
- , 1983. Geotectonic correlation chart 1532A - Operation Porcupine Project area. Geological Survey of Canada.
- , 1985. Eastern Cordilleran foldbelt of northern Canada: Its structural geometry and hydrocarbon potential. *The American Association of Petroleum Geologists*, 69, p. 788-808.
- and Yorath, C.J., 1981. The North American plate from the Arctic Archipelago to the Romanzof Mountains. *In*: E.M. Nairn, M. Churkin, Jr. and F.G. Stehli, eds., *The ocean basins and margins*, 5, chap. 3, The Arctic Ocean. New York and London: Plenum Press, p. 37-103.
- and Cameron, A.R., 1986. An occurrence of bitumen in the Interior Platform near Rengleng River, District of Mackenzie. Geological Survey of Canada, Paper 86-1A, p. 645-648.
- Parrish, J.T., 1982. Upwelling and petroleum source beds, with reference to Paleozoic. *American Association of Petroleum Geologists Bulletin*, 66, p. 750-774.
- Peters, K.E., 1986. Guidelines for evaluating petroleum source rocks using programmed pyrolysis. *American Association of Petroleum Geologists*, 70, p. 318-329.
- Poulton, T.P., Leskiw, K. and Audretsch, A., 1982. Stratigraphy and microfossils of the Jurassic Bug Creek Group of northern Richardson Mountains, northern Yukon and adjacent Northwest Territories. Geological Survey of Canada, Bulletin 325, 137 p.

- Powell, T.G. and Snowdon, L.R., 1983. A composite hydrocarbon generation model: Implications for evaluation of basins of oil and gas. *Erdol and Kohle Erdgas. Petrochemie*, 36, p. 163-170.
- Pugh, D.C., 1983. Pre-Mesozoic geology in the subsurface of Peel River Map area, Yukon Territory and District of Mackenzie. Geological Survey of Canada, Memoir 401, 61 p.
- Snowdon, L.R., 1980. Resinite - A potential petroleum source in the Upper Cretaceous/Tertiary of the Beaufort-Mackenzie basin. In: A.D. Miall, ed., Facts and principles of world petroleum occurrence. Canadian Society of Petroleum Geologists, Memoir 6, p. 421-446.
- , 1987a. Petroleum source potential and thermal maturation of Eagle Plain. Geological Survey of Canada, Open File No. 1720.
- , 1987b. Organic properties and source rock potential of two Early Tertiary shales, Beaufort-Mackenzie Basin. Canadian Society of Petroleum Geologists Bulletin, 35, p. 212-232.
- , Brooks, P.W., Williams, G.K. and Goodarzi, F., 1987. Correlation of the Canol Formation source rock with oil from Norman Wells. *Organic Geochemistry*, 11, p. 529-548.
- Sweet, A.R., 1978. Palynology of the lower part, type section, Tent Island Formation, Yukon Territory. Geological Survey of Canada, Paper 78-1B, p. 31-37.
- Tassonyi, E.J., 1969. Subsurface geology, lower Mackenzie River and Anderson River area, District of Mackenzie. Geological Survey of Canada, Paper 68-25, 207 p.
- Tipper, H.W., Woodsworth, G.J. and Gabrielse, H., 1981. Tectonic assemblage map of the Canadian Cordillera and adjacent part of the United States of America. Geological Survey of Canada, Map 1505A.
- Tissot, B., Durand, B., Espitalié, J. and Combaz, A., 1974. Influence of nature and diagenesis of organic matter in formation of petroleum. *American Association of Petroleum Geologists Bulletin*, 58, p. 499-506.

- , Demaison, G., Masson, P., Deltail, J.R. and Combaz, A., 1980. Paleoenvironment and petroleum potential of Middle Cretaceous black shales in Atlantic basins. American Association of Petroleum Geologists Bulletin, 64, p. 2051-2063.
- and Welte, D.H., 1984. Petroleum formation and occurrence. New York: Spinger-Verlag, 699 p.
- Tourtelot, H.A., 1979. Black shale - its deposition and diagenesis. Clays and Clay Minerals, 27, p. 313-333.
- van Krevelen, D.W., 1971. Coal: Typology, chemistry, physics, constitutions. New York: Elsevier, 514 p.
- Waples, D., 1980. Organic geochemistry for exploration geologists. New York: Burgess, 141 p.
- Yorath, C.J. and Cook, D.G., 1981. Cretaceous and Tertiary stratigraphy and paleogeography, northern Interior Plains, District of Mackenzie. Geological Survey of Canada, Memoir 398, 76 p.
- Young, F.G., 1971. Mesozoic stratigraphic studies, northern Yukon Territory and northeastern District of Mackenzie. Geological Survey of Canada, Paper 71-1A, p. 245-247.
- , 1975a. Upper Cretaceous stratigraphy, Yukon Coastal Plain and northwestern Mackenzie Delta. Geological Survey of Canada, Bulletin 249, 83 p.
- , 1975b. Stratigraphic and sedimentologic studies in northeastern Eagle Plain, Yukon Territory. Geological Survey of Canada, Paper 75-1B, p. 309-323.
- , 1977. The mid-Cretaceous flysch and phosphatic ironstone sequence, northern Richardson Mountains, Yukon Territory. Geological Survey of Canada, Paper 77-1C, p. 67-74.
- (ed.), 1978. Geological and Geographical Guide to the Mackenzie Delta Area. Canadian Society of Petroleum Geologists, 158 p.

-----, Myhr, D.W. and Yorath, C.J., 1976. Geology of the Beaufort Mackenzie Basin. Geological Survey of Canada, Paper 76-11, 63 p.

VII. PART III. OPTICAL CHARACTERISTICS OF GRAPTOLITES AND THEIR UTILITY AS INDICES OF THERMAL MATURITY IN LOWER PALEOZOIC STRATA IN NORTHERN YUKON

A. ABSTRACT

The utility of graptolites as a measure of thermal maturity in the Lower Paleozoic Road River Group in northern Yukon has been evaluated by measuring maximum, minimum and random reflectance. The progressive changes in optical properties of graptolites produced by increasing depth of burial, are correlated to other organic matter (conodonts and bitumen) in the same sample. Maximum reflectance is the most reliable method of assessing the level of thermal maturity of graptolites because of the anisotropic and biaxial nature of their optical properties.

In the Road River Group, the mean maximum reflectance of graptolites ranges laterally from 4.0% to 6.5% R_{max} . R_{max} of graptolites increases with increasing depth of burial and the relationship between reflectance and depth fits a log (reflectance) linear (depth) relationship. The vertical variation of the maximum reflectance of graptolites through an 800 m section ranges from 4.2% R_{max} at the top to 6.5% R_{max} at the bottom yielding a maturation gradient of 0.39 log R_{max} /km.

A correlation of graptolite reflectance calibrated by conodonts with vitrinite reflectance shows that a graptolite reflectance of 5% R_{max} ($\text{CAI}=5$) corresponds

to temperature of approximately 320°C whereas a vitrinite reflectance of 5% Romax agrees with a temperature of about 190°C, using a burial time of 70 Ma. Graptolite organic remains appear to behave similar to bitumen with increasing depth of burial; at higher levels of thermal maturity, graptolite reflectance increases more rapidly than vitrinite reflectance. A CAI of 5 corresponds to a vitrinite reflectance of about 4.0% Romax and a graptolite reflectance range of 5.0% to 6.5% Romax.

B. INTRODUCTION

It is important in hydrocarbon exploration to accurately determine the thermal maturation of potential petroleum source rocks. Standard petroleum and coal industry techniques for assessing thermal maturity include vitrinite reflectance (Castano and Sparks, 1974; Davis, 1978; Bostick, 1979 and others), fluorescence and reflectance of bitumen and kerogen (Teichmüller and Wolf, 1977; Creaney, 1978; Robert, 1980; Teichmüller and Durand, 1983), palynomorph color (Batten, 1981; Rovnina, 1981) and conodont alteration index (CAI) (Epstein et al., 1977; Legall et al., 1981). With the exception of CAI, no petrographic techniques exist for quantifying the thermal maturity of Lower Paleozoic rocks because pre-Upper Silurian rocks generally do not contain vitrinite or spores (used for Thermal Alteration Index, TAI). A new index, graptolite reflectance, has recently been suggested as an indicator of thermal maturity (Kurylowicz et al., 1976; Teichmüller, 1978; Clausen and Teichmüller, 1982; Goodarzi, 1984; Goodarzi and Norford, 1985; Bertrand and Hérroux, 1987) but no good correlation exists as yet between graptolite reflectance and other conventionally measured maturation

parameters.

This study reviews the literature and provides background information on graptolites and their use as a thermal maturation index. The utility of graptolite reflectance as an indicator of organic maturation in Lower Paleozoic strata of northern Yukon is evaluated by examining the progressive changes in optical properties of graptolites with increasing level of thermal maturity. Organic matter in 19 samples collected from the Road River Group and Canol Formation were examined petrographically (Figs. 36 and 37 and Table V) from measurements of maximum (Romax), minimum (Romin) and random (Rorand) reflectance on polished whole-rock specimens. Progressive changes in reflectance of graptolites with increasing depth of burial is compared to other organic matter (bitumen and conodonts) in the same sample and an attempt is made to correlate graptolite and vitrinite reflectance, calibrated by CAI.

1. Previous Work

Only recently have graptolites been utilized to evaluate the level of organic maturation of sedimentary rocks. Early studies of Kurylowicz et al. (1976) demonstrated that graptolite optical properties are similar to vitrinite. Subsequently, Teichmüller (1978) and Clausen and Teichmüller (1982) reported maximum reflectances of graptolites ranging from 0.36% to 12.0% Romax. Goodarzi (1984) examined details of the internal structure and optical properties of graptolites from drillhole samples and described maximum graptolite reflectance values from 2.72% to 4.61% Romax, corresponding to present burial depths of

approximately 500 to 1500 metres. More recently, Goodarzi and Norford (1985) described optical properties of graptolites with maximum reflectance in oil ranging from 0.64% to 11.90% and calibrated these values with CAI's ranging from 1 to 5.

Studies to date indicate the maximum reflectance in oil and bireflectance (RoB) are the most diagnostic characteristics for assessing thermal maturity of graptolites. Correlation of Romax and RoB of graptolites with CAI indicates that Romax and RoB of graptolites increases slowly at low levels of CAI (Goodarzi and Norford, 1985) whereas at CAI values greater than 3, Romax of graptolites increases more rapidly with increasing thermal maturity than CAI. Goodarzi and Norford (1985) correlated graptolite reflectance, calibrated by conodonts, with vitrinite reflectance and reported a graptolite reflectance of 2.5% Romax indicates a temperature of about 100°C whereas a vitrinite reflectance of 2.5% corresponds to temperatures greater than 130°C.

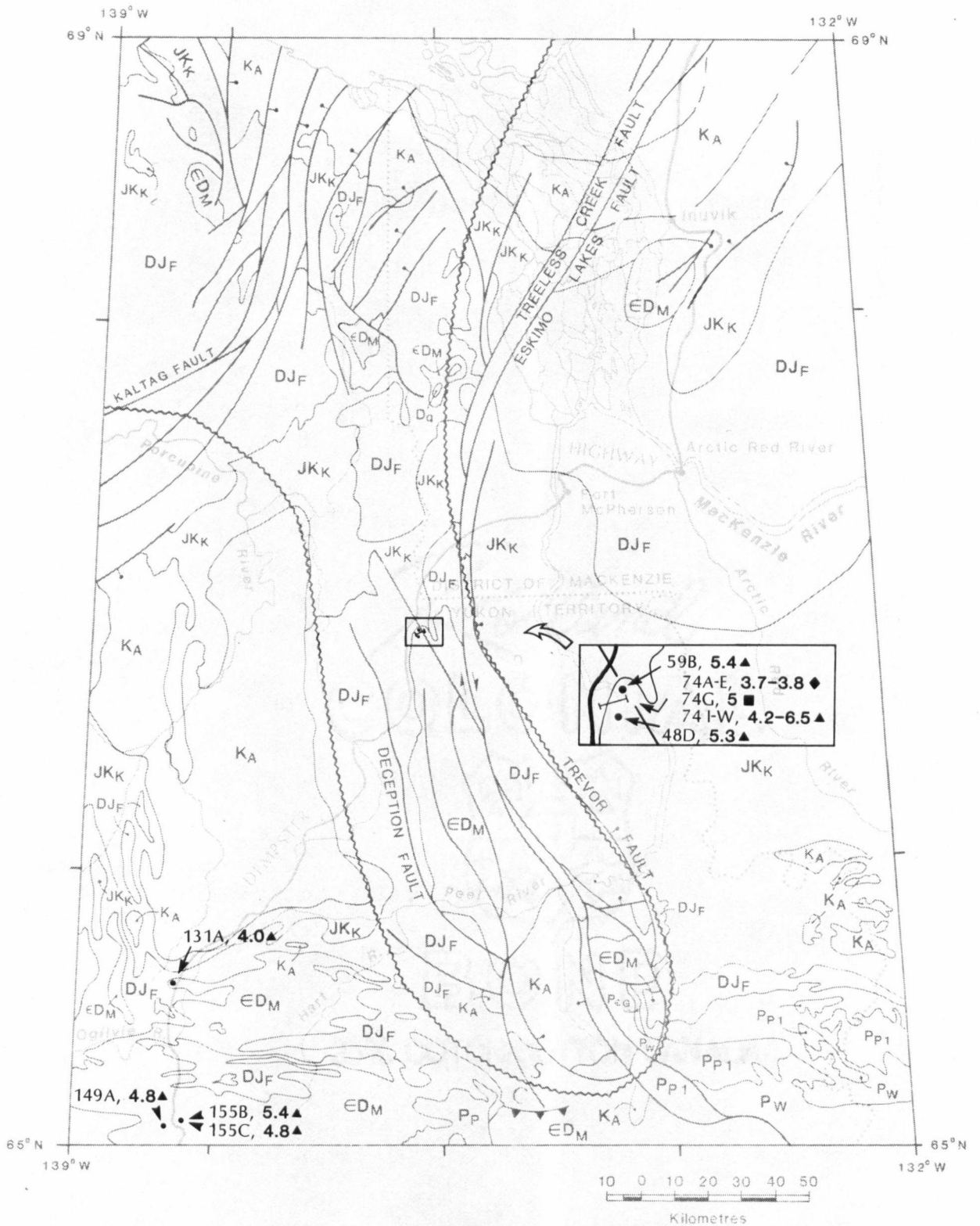


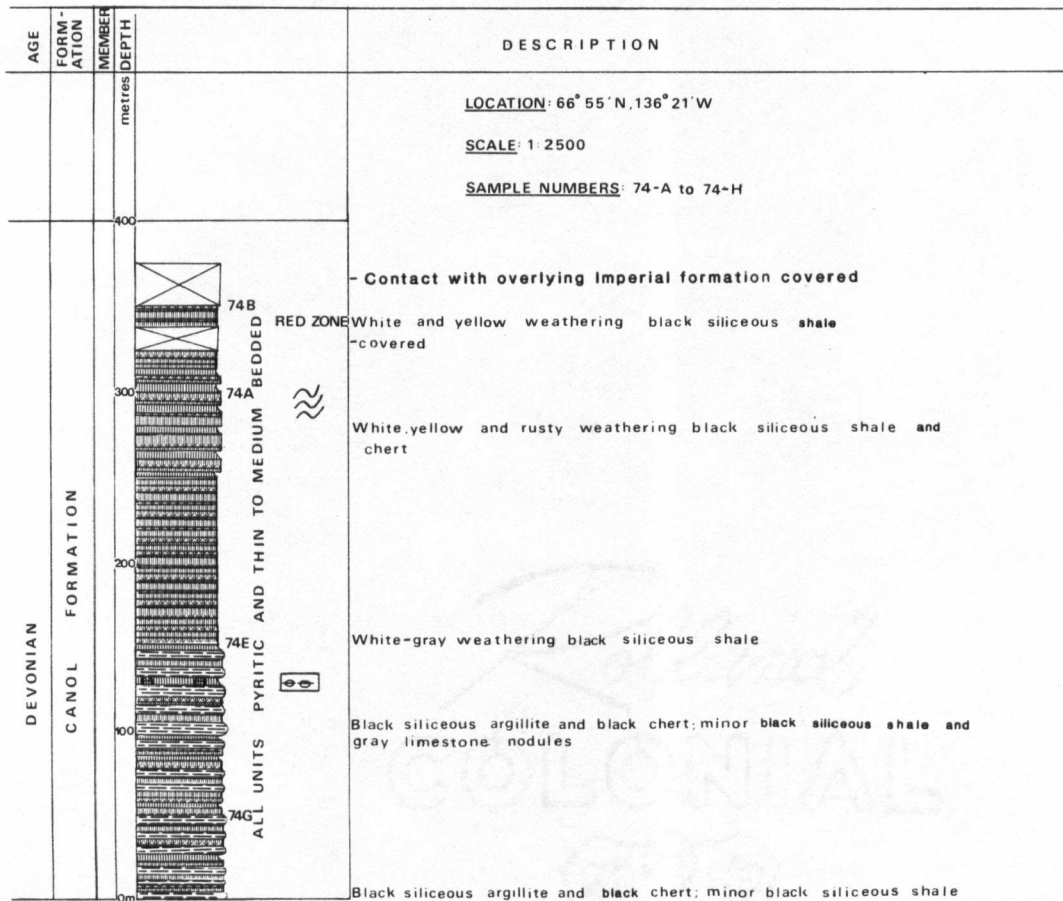
Figure 36. Locality map, Romax values of graptolites, vitrinite and CAI values of the Road River Group and Canol Formation.

(◆)=vitrinite reflectance, % Romax. (▲)=graptolite reflectance, %Romax, (■)=CAI.

Base map modified from Tipper et al. (1981). See table I for explanation of tectono-stratigraphic assemblages.

<u>LEGEND</u>	
<u>SYMBOL</u>	<u>LITHOLOGY AND DESCRIPTION</u>
	BLACK CHERT
	SILICEOUS LIMESTONE
	CALCAREOUS SHALE or DOLOMITIC SHALE
	SILICEOUS SHALE
	SHALEY LIMESTONE
	ARGILLITE
	FOLDS
	GRAPTOLITES

SECTION 1. CANOL FORMATION



(a)

Figure 37. Measured section along James River, Yukon Territory, 66°55 N, 136°15 W.
A. Stratigraphy of the Canol Formation.

SECTION 2. ROAD RIVER GROUP



(b)

B. Stratigraphy of the Road River Group. Formation names adopted from Cecile et al. (1982).

Table V. Graptolite-bearing samples collected from northern Yukon. See figure 1 for sample locations. Sil. = Silurian; Dev. = Devonian; Calc. = calcareous; Arg. = argillaceous; sh. = shale; ls. = limestone; weath. = weathered.

<u>Sample</u>	<u>Depth</u>	<u>Formation</u>	<u>Age</u>	<u>Lithology</u>
48D	--	Vitreekwa	Sil. to Dev.?	Arg. ls.
59B	--	Vitreekwa	Sil. to Dev.?	Calc. sh.
131A	--	Road Group	River Ord. to Dev.?	Calc. sh., weath.
149A	--	Road Group	River Ord. to Dev.?	Calc. sh.
155B	--	Road Group	River Ord. to Dev.?	Calc. sh.
155C	--	Road Group	River Ord. to Dev.?	Calc. sh.

2. Morphology and Optical Properties of Graptolites

'Graptolites' is a colloquial term for members of Class Graptolithina (Phylum Hemichordata; Clarkson, 1981, p. 238). Graptolites are colonial marine invertebrates with a planktonic habitat that occur in Lower Paleozoic marine rocks. Since the early 1900's, graptolites have been used for biostratigraphy and correlation of shaly facies of Lower Paleozoic rocks. There are several orders within Class Graptolithina but only two are of importance: the Graptoloidea (Early Ordovician to Upper Silurian) and Dendroidea (Cambrian to Lower Carboniferous; Clarkson, 1981, p. 245). Graptolites examined in this study belong to the order Graptoloidea and include species primarily of *Monograptus* with minor examples of *Bohemograptus*, *Climactograptus*, *Dicellograptus*, *Orthograptus*, *Amplexograptus* and *Didymograptus* (Cecile et al., 1982).

The graptolite rhabdosome (skeleton of colony; Fig. 38) consists of: 1) thecae - compartments once occupied by zooids; 2) apertures - the external openings of each tube in the skeleton; 3) common canal - the cavity round the virgula into which thecae open; 4) a virgula - a continuous central structure that extends as a spine projecting from the thecae; and 5) a periderm - the substance composing the rhabdosome, which consists of an inner layer (fusellar tissue) with growth bands and lines, and an outer layer (cortical tissue) of laminated material (Crowther, 1981). Microstructures visible in reflected light include the cortical tissue, common canal and layered walls of the periderm (Figs. 39 and 40).

Initially, it was believed that the graptolite periderm was constructed of a

chitinous substance (Kozłowski, 1949) but more recent work indicates a collagen-like nature of the component fibrils composing the fusellar and cortical tissue of the periderm (Towe and Urbanek, 1972; Crowther and Rickards, 1977).

Graptolite skeletal material has optical properties similar to that of vitrinite but graptolites have distinct morphological features. Graptolite fragments show anisotropy, segmented structure and the surface may be granular or non-granular. Granular fragments comprise a mosaic of very fine 'grains' composing the exoskeleton or common canal and have weaker anisotropy and lower reflectance than non-granular fragments; the latter are usually hard and brittle (Goodarzi and Norford, 1985).

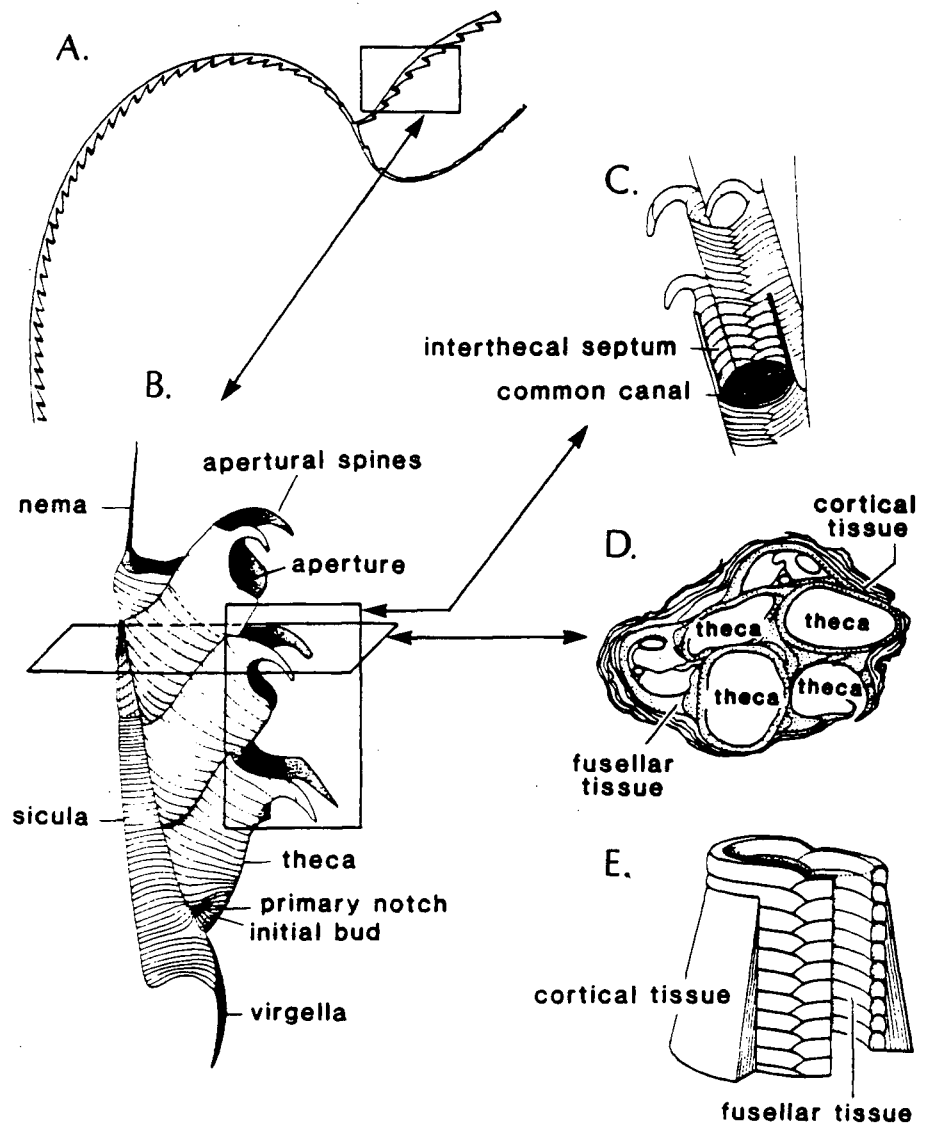


Figure 38. Structural features of the graptolite rhabdosome.

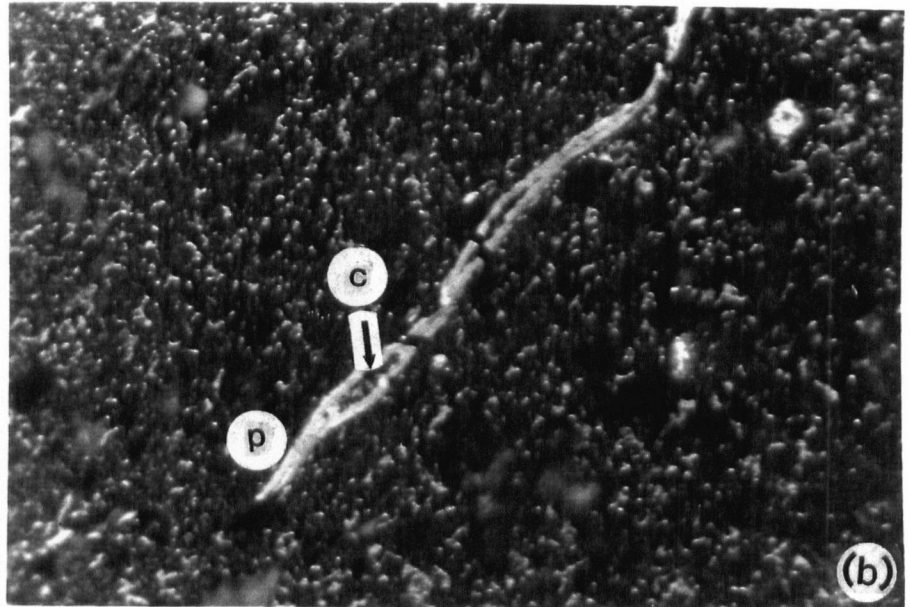
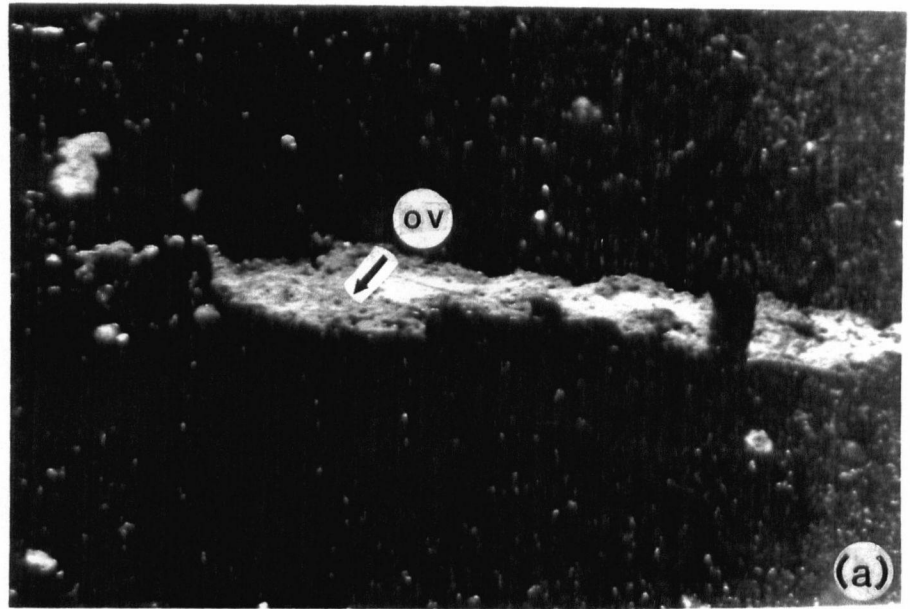
A. Graptolite rhabdosome (colony).

B. Enlarged lateral view of one stipe.

C. Structure of theca and common canal with part removed.

D. Transverse section of a stipe showing cortical tissue surrounding fusellar tissue (stipled), which has the form of complete or split tubes for thecae.

E. Diagram of periderm showing fusellar tissue laid down in alternating half-rings, surrounded by laminated cortical tissue. A to C modified from Clarkson (1981, p. 239); D to E modified from Moore (1955, p. 22).



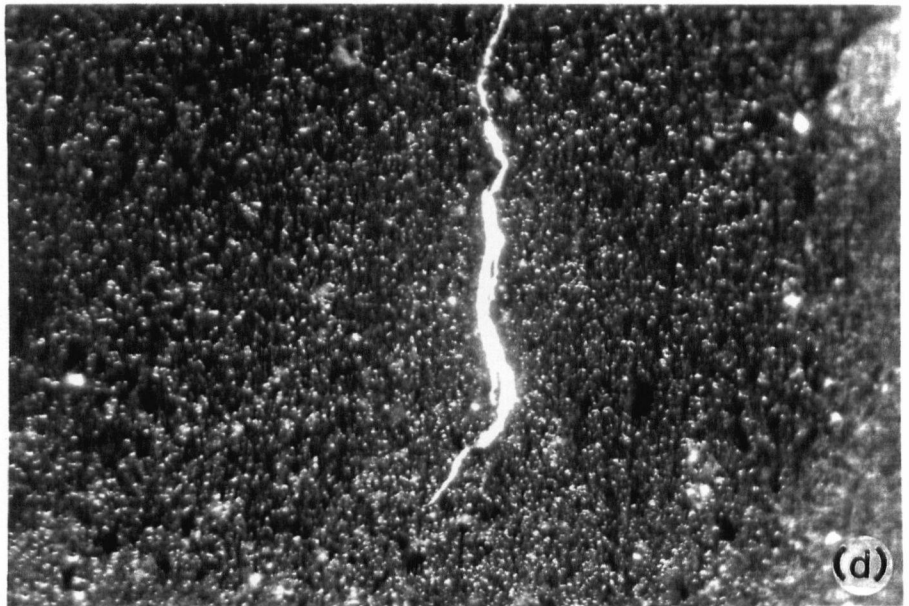
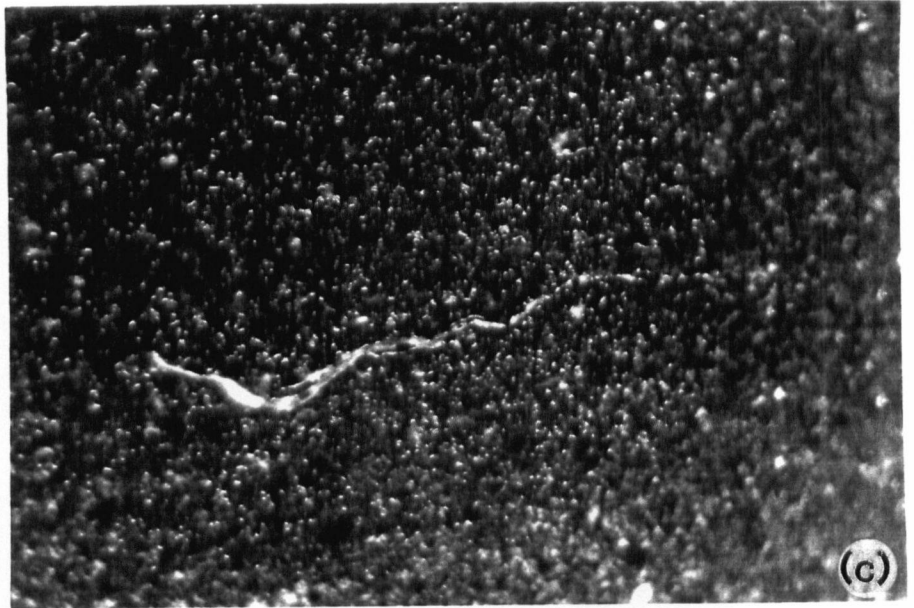
50 microns



Figure 39. Fragments of graptolites in Road River Group samples, polished surfaces, oil immersion. Sections cut normal to bedding, plane polarized light.

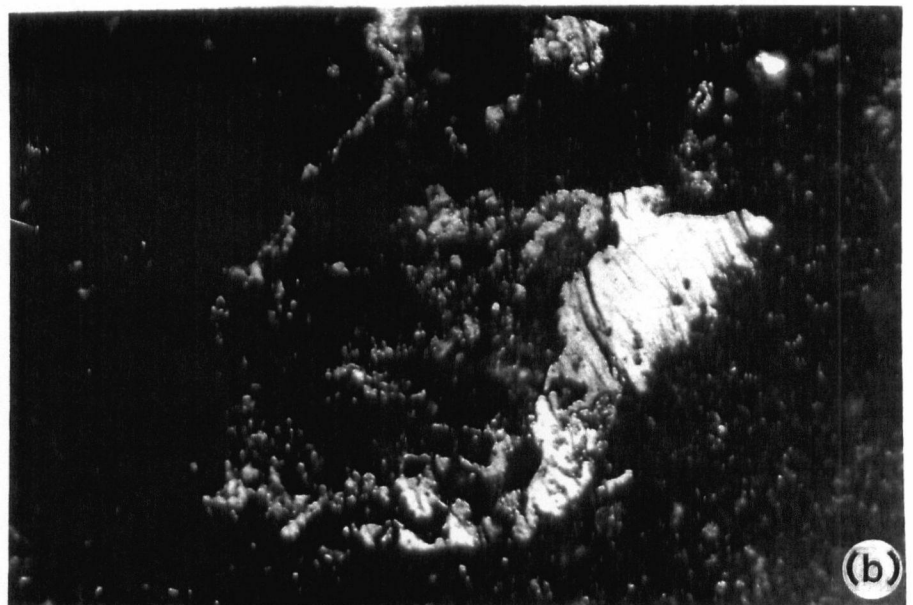
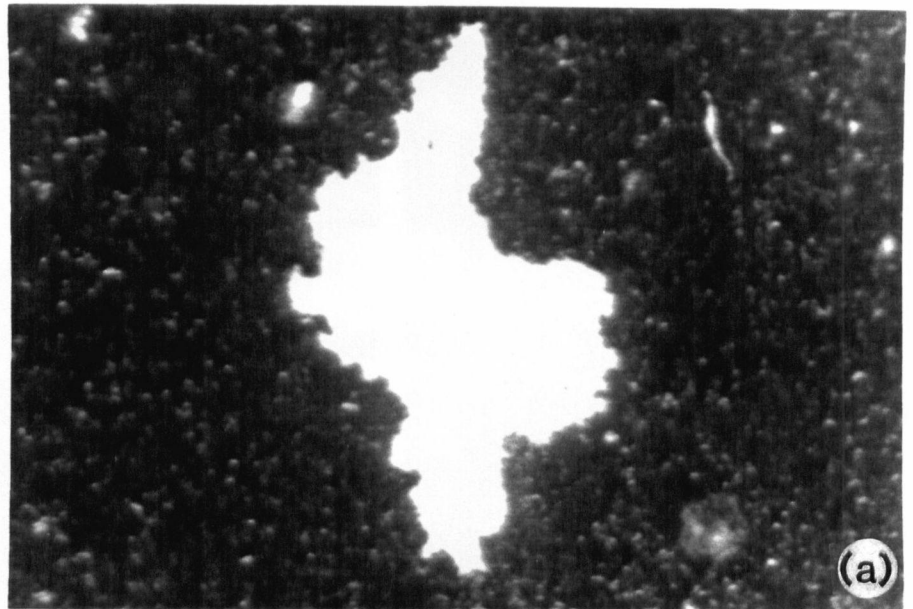
A. Granular, lath-shaped graptolite fragment from sample 74I. Note lower reflectance than fragment in 'C' and oval-shaped pits (ov).

B. Non-granular fragments from sample 74U. Note the periderm (P) and common canal (C) filled with carbonate and clay minerals.



50 microns

Figure 39 cont'd. C. Non-granular fragments from sample 74V showing higher reflectance than fragment in 'A' and stipe-like morphology.
D. Same as 'C', with specimen rotated to show anisotropy.

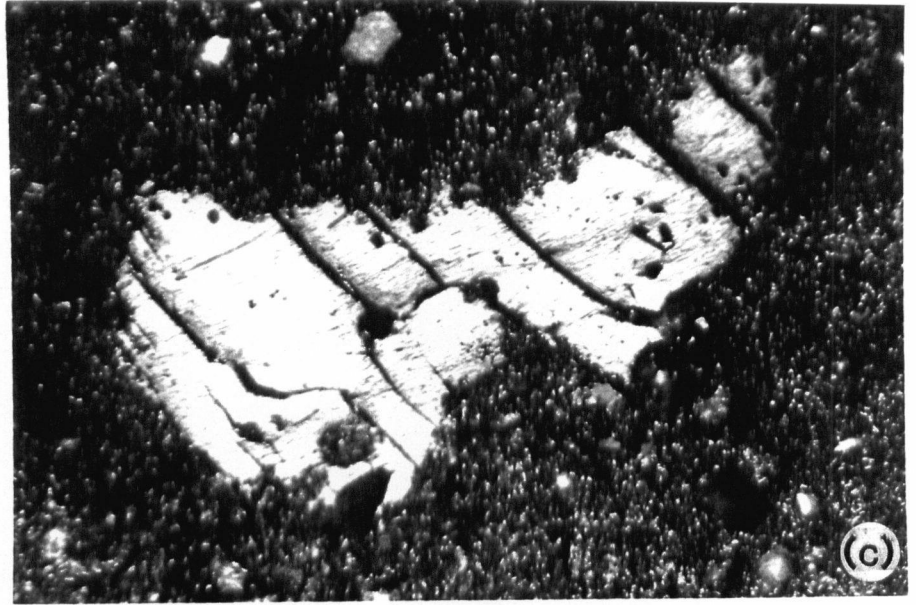


50 microns

Figure 40. Fragments of graptolites from the Road River Group in sections cut and polished parallel to bedding. Same conditions as figure 39.

A. Cortical tissue showing non-granular morphology in sample 74U.

B. Non-granular fragments from sample 74I showing traces of cortical bandages.



50 microns

Figure 40 cont'd. C. Non-granular fragments from sample 741 showing blocky morphology.

C. METHODS

Graptolite reflectance and CAI were determined from 14 outcrop samples collected from a measured section of the Road River Group (Fig. 37) and from nearby locations (Fig. 36). Graptolites were observed on bedding surfaces in hand specimens of most samples and thus ensured graptolites were examined (as opposed to other zooclasts, e.g., scolecodonts and chitinizoans). In order to correlate graptolite and vitrinite reflectance, calibrated by CAI, vitrinite reflectance and CAI was determined from 4 samples of the Canol Formation (Fig. 37).

The level of organic maturity (rank) of all samples was determined utilizing a technique similar to vitrinite reflectance methods (I.C.C.P., 1971). Whole rock specimens were mounted in cold-setting polyester resin pellets. The whole-rock specimen was placed in a 3 cm diameter plastic mold and enough epoxy added to cover the sample. A series of samples were then placed under a vacuum. The pressure was released, more epoxy added and then reapplied to eliminate air bubbles in the resin. Samples were left to set overnight and cured in a 30°C oven for 8 to 10 hours. Samples from the measured section (74 I-W) were cut and polished along a plane perpendicular to bedding and a plane parallel to bedding. The remaining samples were cut and polished perpendicular to bedding. The mean maximum and minimum reflectance values in oil ($n=1.518$ at 546 nm) were determined for some samples by rotating the microscope stage through 360° as the reflectance was recorded with a computerized Leitz® microscope (orthoplan M.P.V. II). The mean random reflectance (Rorand, polarizer out) was measured for comparison on samples 74 A-W.

All samples were examined for conodonts. Samples ranging in weight from 70 to 2000 grams were dissolved in dilute (10%) acetic, formic or hydrofluoric acid, depending on lithology. Conodonts dissolved in acetic or formic acid were then isolated from the 74 to 2000 μm (-10 to +200 mesh) fraction of the residues by standard tetrabromoethane heavy-liquid and hand picking techniques. Conodonts dissolved in hydrofluoric acid were hand picked from the 74 to 177 μm (-80 to +200 mesh) portion, with no prior heavy liquid separation. The 177 to 2000 μm (-10 to + 80 mesh) portion was also examined for samples processed in this manner. The conodont color was then established by using a standard binocular microscope in conjunction with a visual color comparison (Epstein et al., 1977) and a set of standards compiled from field collections with CAI's ranging from 1 to 5.

D. RESULTS

1. Microscopic Morphology of Graptolites

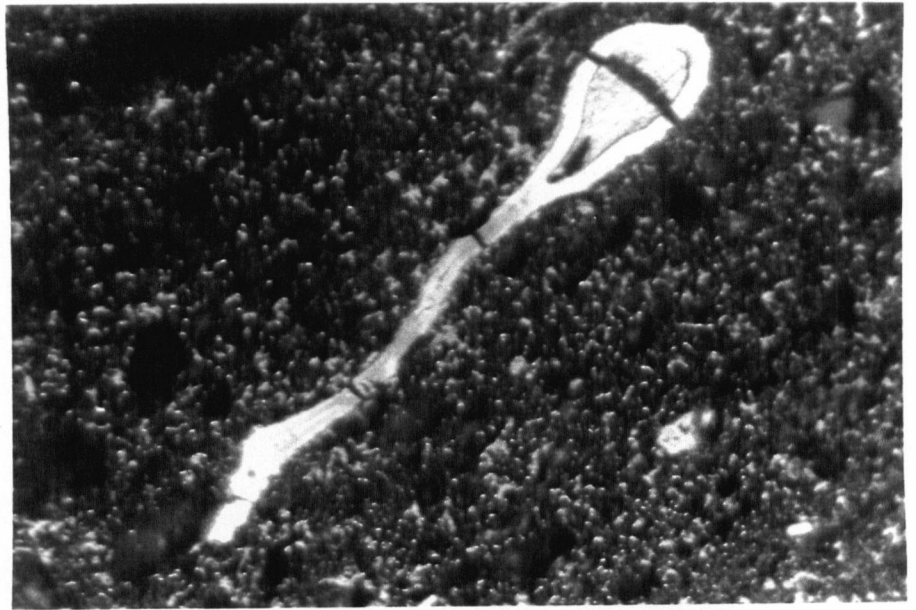
Features which are characteristic of graptolite fragments and distinguish them from bitumen and other fossil organic matter in the samples examined in this study include: 1) morphological aspects such as a periderm, thecae and common canal; 2) weak to strong anisotropy; 3) granular and non-granular fragments; 4) oval-shaped pits, which may represent irregularly spaced vesicles that form pits in the cortical tissue (see Crowther, 1981, p. 13 and 52); and 5) cortical tissue (outer layer of the periderm wall) with cortical bandages often visible (Figs. 39 and 40).

All graptolites examined contained non-granular, white (in reflected light), brittle (fractured) fragments with weak to strong anisotropy. Sample 74I contained both granular and non-granular particles with maximum reflectance values of 2.7% and 4.0% Romax, respectively (Table VI and figure 39). The granular material is commonly lath-shaped and has lower reflectance values than non-granular fragments. Non-granular material exhibits blocky morphology on sections cut parallel to the plane of bedding but appear as thin blades in sections normal to bedding (Fig. 39). Sample 74J contains non-granular fragments, exhibiting weak (RoB=0.7) and strong (RoB=1.7) anisotropy (Tables VIa and VIb), which may represent different species of graptolites or perhaps fragments of other organic matter (e.g., tasmanites observed in sample 74I, Fig. 41, or chitinozoans). No distinguishing morphological features are evident.

Bitumen was observed in several samples and is distinguished by its lack of a definitive morphology, devolatilization vacuoles and its common occurrence in cavities, lenses and veins or dispersed throughout the matrix (Fig. 42).

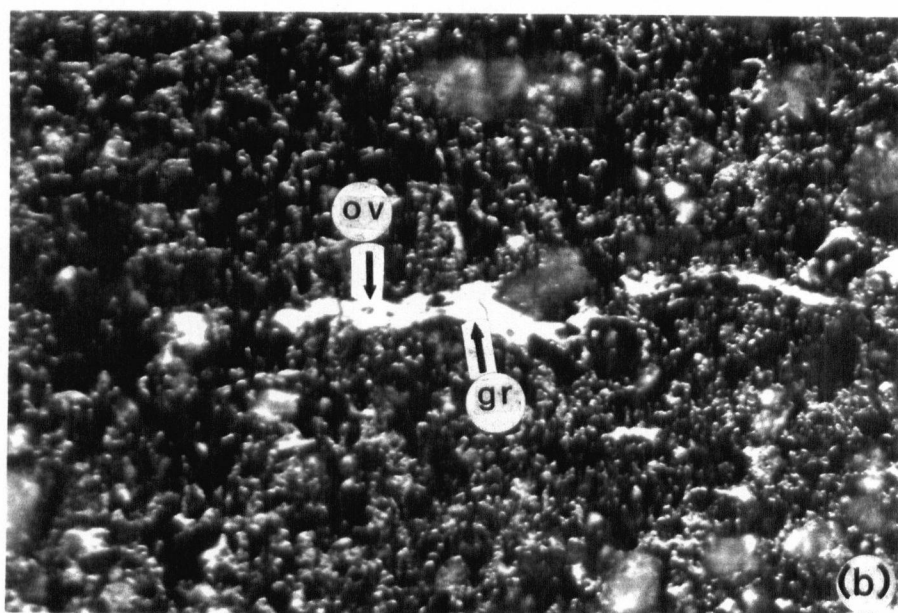
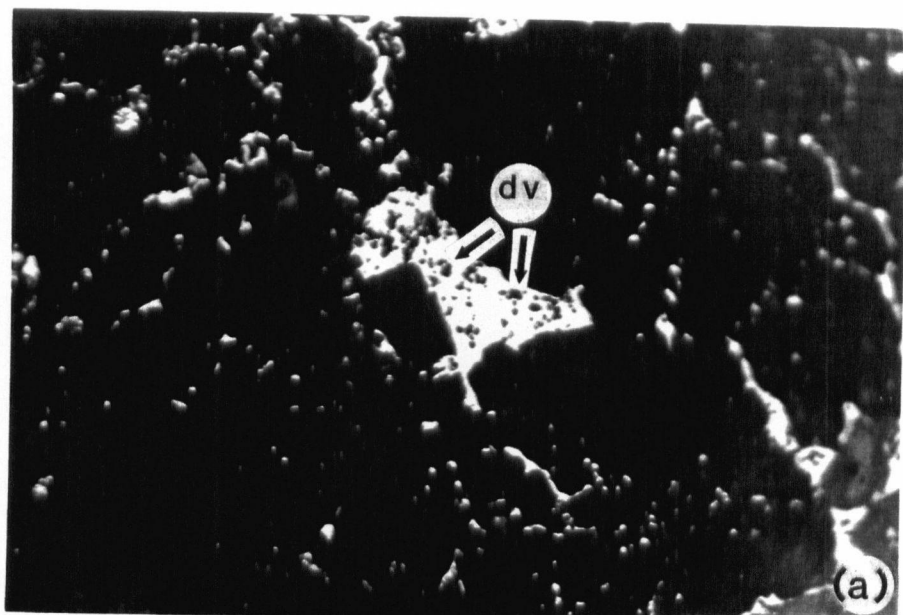
2. Reflectance Data

The reflectance data of graptolites, vitrinite and bitumen are summarized in tables VI, VII, VIII and IX.



50 microns

Figure 41. Fragments of Tasmanites in section cut and polished normal to bedding. Same conditions as in figure 39. Note strong anisotropy of Tasmanites and cavity filled with granular organic matter.



50 microns

Figure 42. Bitumen in sections cut and polished parallel to bedding. Same conditions as in figure 39.

A. Pyrobitumen in sample 74M. Note devolatilization vacuoles (dv) and non-granular texture.

B. Bitumen in sample 59B. Bitumen is yellow, granular and dispersed throughout the matrix. Note granular graptolite fragment (gr) with oval-shaped pits (ov).

Table VI. Measured graptolite reflectance in samples collected from measured section of Road River Group, along James River, northern Yukon. Figure 36 shows sample locations and figure 37 summarizes the stratigraphy and present depths of burial. ng= non-granular, gr= granular graptolites, Romax= maximum reflectance, BRO= bireflectance, Rorand= random reflectance, Romin= minimum reflectance, N= number of graptolite fragments measured.

a. Sections cut and polished perpendicular to bedding.*' denotes sections in which bedding was not well-defined.

<u>Sample</u>	<u>Romax</u>	<u>σ</u>	<u>Romin</u>	<u>σ</u>	<u>BRO</u>	<u>Rorand</u>	<u>σ</u>	<u>N</u>
74I	2.66	0.04	2.01	0.08	0.65	--	--	2
	(gr)							
	4.04	0.37	3.21	0.30	0.83	2.42	0.19	6
	(ng)							
74J	4.30	0.13	2.84	0.83	1.16	--	--	11
	(ng)							
	5.28	0.29	2.38	0.97	2.90	2.51	0.13	13
	(ng)							
74N*	4.50	0.16	2.87	0.16	1.63	2.47	0.14	2
	(ng)							
74O*	4.60	0.36	1.96	0.06	2.64	2.96	0.57	2
	(ng)							
74U*	4.69	0.31	3.06	0.57	1.63	2.23	0.01	4
	(ng)							
74V	5.74	0.87	1.00	0.40	4.74	2.88	0.42	5
	(ng)							

Table VI b. Sections cut and polished parallel to bedding. '*' denotes samples in which bedding was not well-defined.

<u>Sample</u>	<u>R_{max}</u>	<u>σ</u>	<u>R_{min}</u>	<u>σ</u>	<u>BRO</u>	<u>R_{orand}</u>	<u>σ</u>	<u>N</u>
74I	2.51	0.16	1.92	0.23	0.59	--	--	5
	(gr)							
	4.15	0.52	3.41	0.41	0.74	2.09	0.78	7
	(ng)							
74J	4.17	0.34	3.51	0.36	0.66	--	--	6
	(ng)							
	5.98	0.46	4.54	0.64	1.44	2.59	0.41	11
	(ng)							
74N*	4.38	0.37	2.90	0.87	1.48	2.75	0.32	10
	(ng)							
74O*	4.86	0.00	2.29	0.00	2.57	2.84	0.00	1
	(ng)							
74U*	5.03	0.00	3.35	0.00	1.68	2.98	0.00	1
	(ng)							
74V	6.45	0.42	5.35	0.37	1.09	3.01	0.52	6
	(ng)							

Table VII. Measured graptolite reflectance in samples collected from Road River Group in northern Yukon. Figure 36 shows sample locations and table V describes the age and lithology of samples. Abbreviations are explained in table V. Sections are cut and polished approximately normal to bedding.

<u>Sample</u>	<u>Romax</u>	<u>σ</u>	<u>Romin</u>	<u>σ</u>	<u>BRO</u>	<u>N</u>
48D	5.28 (ng)	0.73	3.61	1.03	1.67	3
59B	5.44 (ng)	0.59	2.99	0.40	2.45	26
131A	3.99 (ng)	0.42	3.07	0.34	0.92	43
149A	4.81 (ng)	0.56	3.75	0.66	1.14	27
155B	5.39 (ng)	0.73	3.23	0.53	2.16	4
155C	4.75 (ng)	0.50	4.02	0.41	0.75	19

Table VIII. Measured bitumen reflectance in sections cut perpendicular to bedding. Romax= maximum reflectance, BRO= bireflectance, Rorand= random reflectance, N= number of fragments of bitumen measured.

<u>Sample</u>	<u>Romax</u>	<u>σ</u>	<u>BRO</u>	<u>Rorand</u>	<u>σ</u>	<u>N</u>
74G	----	----	----	1.18	0.67	67
74I	1.74 2.96	0.24 0.48	0.78 1.40	1.76 2.45	0.52 0.48	8 16
74M	3.01	0.29	1.18	3.06	0.24	3
74N	3.38	0.00	2.01	2.62	0.00	1
74O	2.69	0.42	0.98	1.98	0.57	15
74V	1.93	0.38	0.72	1.56	0.54	15
59B	3.95	0.47	1.71	--	--	6
149A	3.10	0.47	0.50	--	--	8

Table IX. Measured vitrinite reflectance in samples collected from measured section of Canol Formation, along James River in northern Yukon. Figure 36 shows sample locations and figure 37 summarizes the stratigraphy and present depths of burial. Abbreviations are explained in table V.

<u>Sample</u>	<u>R_{max}</u>	<u>σ</u>	<u>R_{min}</u>	<u>σ</u>	<u>BRO</u>	<u>R_{rand}</u>	<u>σ</u>	<u>N</u>
74B	3.62	0.00	2.99	0.00	0.63	3.39	0.01	1
74A	3.72	0.03	3.02	0.36	0.70	2.96	0.00	2
74E	3.82	0.03	2.75	0.42	1.07	3.17	0.04	3

a. Optical Properties of Graptolites

All graptolite specimens from the Road River Group have biaxial negative optical properties with the maximum and intermediate reflectance values located in (or close to) the plane of bedding and the minimum reflectance normal to bedding. Similar results have been obtained for graptolites (Goodarzi, 1984) and for vitrinite (Bustin et al., 1986). It is important to note the indicatrix serves to illustrate how the refractive index varies according to the vibration direction of a light wave in a transparent crystal, whereas the reflectance indicatrix (optical indicating surface) is used to denote the principal vibrating directions, refractive indices and absorption coefficients for an absorbing material (e.g., vitrinite or graptolites; Hallimond, 1972, p. 122). For biaxial substances, the optical indicating surface (reflectance indicatrix) of reflectivity has 3 planes of symmetry (Hevia and Virgos, 1977). Figure 43 illustrates the reflectance indicatrix and principal reflectance axes, of the biaxial indicating surface of graptolites, measured in different orientations.

b. Maximum Reflectance and Bireflectance of Graptolites

In sections cut normal to bedding, maximum reflectance of non-granular graptolites ranges from 4.0% to 5.7% (Tables VIa and VII) whereas in sections cut parallel to bedding, maximum reflectance values from 4.2% to 6.5% (Table VIb) were obtained for non-granular graptolites.

The degree of anisotropy (bireflectance) in non-granular fragments ranges from 0.75 to 4.7 (Tables VIa and VII) and from 0.7 to 2.6 (Table VIb) for sections cut normal and parallel to bedding, respectively.

Laterally, the level of organic maturity, measured from graptolite organic matter, near the top of the Road River Group varies from 4.0% to 5.4% Romax. Romax values increase from 4.0% to 5.4% in sections cut perpendicular to bedding whereas in sections cut parallel to bedding, Romax values increase from 4.2% at the top to 6.5% at the bottom through an 800 m section.

The vertical (stratigraphic) variation in maturity (maturation gradient) through the Road River Group was determined from the 800 m section. The measured maturation gradient fits a log (Romax) linear (depth) relationship (Fig. 44) although insufficient data is available to confidently define the relationship. Maturation gradients based on coal show a similar log-linear relationship between vitrinite reflectance and depth of burial (e.g., Bustin, 1986). The maturation gradient calculated for graptolite reflectance data ranges from 0.36 to 0.39 log Romax/km for Romax measured normal and parallel to bedding respectively (Figs. 44a and b). Inasmuch as Romax measured on plane parallel to bedding should equal Romax measured perpendicular to bedding, for biaxial negative substances (Fig. 43), the difference in maturation gradients measured parallel and perpendicular to bedding (0.03 log Romax/km) is insignificant. Hence the maturation gradient measured parallel to bedding (0.39 log Romax/km) will be used to describe the vertical variation in maturity of the Road River Group in this study.

c. Maximum Reflectance and Bireflectance of Bitumen

The maximum reflectance of bitumen ranges from 1.7% to 4.0% and RoB varies from 0.5 to 2.0 (Table VIII). Bitumen reflectance is consistently lower than graptolite reflectance in all samples which contain both types of organic matter (Tables VI, VII and VIII). Sample 74I contains 2 phases of bitumen and the reflectance of the white, non-granular phase (3.0% Romax) is almost twice that of the yellow, granular phase (1.7% Romax).

d. Random Reflectance of Graptolites and Bitumen

Random and maximum reflectance measurements of graptolites and bitumen are summarized in tables VI and VIII. Random reflectance values of graptolites ranges from 2.2% to 3.0% and from 2.1% to 3.0% for sections cut normal and parallel to bedding respectively (Tables VIa and VIb). Random reflectance values of bitumen varied from 1.6% to 3.1% (Table VIII). There is a larger standard deviation for random reflectance determinations than for maximum reflectance, making Romax the preferred measurement for reflectance of graptolites and bitumen. Similar results have been reported for vitrinite reflectance measurements (Davis, 1978).

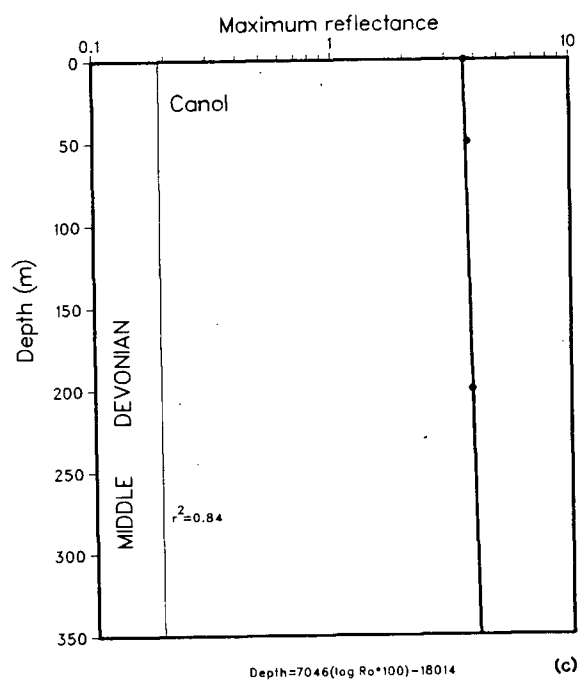
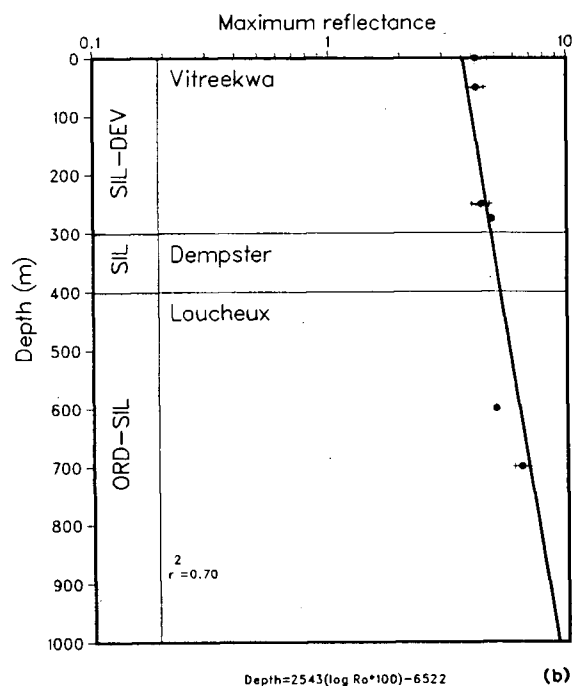
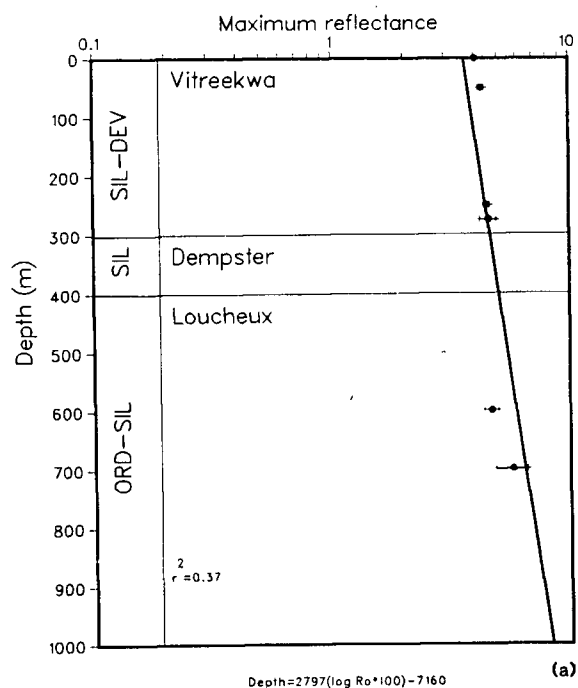


Figure 44. Maturation gradients for stratigraphic sections through the Road River Group and Canol Formation. Location and stratigraphy of the sections are shown in figures 36 and 37. Regression line: $\log(\text{Romax})$, linear (depth). r^2 is goodness of fit of regression line. Standard deviation bar is shown for samples for which more than one reflectance measurement was made.

A. Romax of graptolites measured normal to bedding of Road River samples. Maturation gradient = 0.36 log Ro/km.

B. Romax of graptolites measured in the plane of bedding of Road River samples. Maturation gradient = 0.39 log Ro/km.

C. Romax of vitrinite measured in samples from the Canol Formation. Maturation gradient = 0.14 log Ro/km.

The poor correlation ($r^2=0.15$) between Rorand and Romax for graptolites is a result of Romax increasing at a different rate than Romin with increasing thermal maturity. Teichmüller and Teichmüller (1982, p.52) report similar results for vitrinite; the degree of anisotropy (bireflectance; difference between maximum and minimum reflectance) increases with increasing maturation and shows considerable scatter between 4% and 6% Romax. Random reflectance is the mean of the maximum and apparent minimum reflectances (Davis, 1978) and therefore will not increase in a predictable and progressive manner at high levels of organic maturity (e.g., $>> 1.4\%$ Romax; Davis, 1978). Romax is thus the preferred measurement of both graptolites and bitumen examined in this study.

e. Vitrinite Reflectance Data

The reflectance data for vitrinite in the Canol Formation is summarized in table IX. Reflectance of vitrinite ranges from 3.6% to 3.8% Romax and 3.0% to 3.4% Rorand. RoB of vitrinite varies from 0.6 to 1.1 and a poor correlation ($r^2=0.26$) exists between Rorand and Romax for vitrinite.

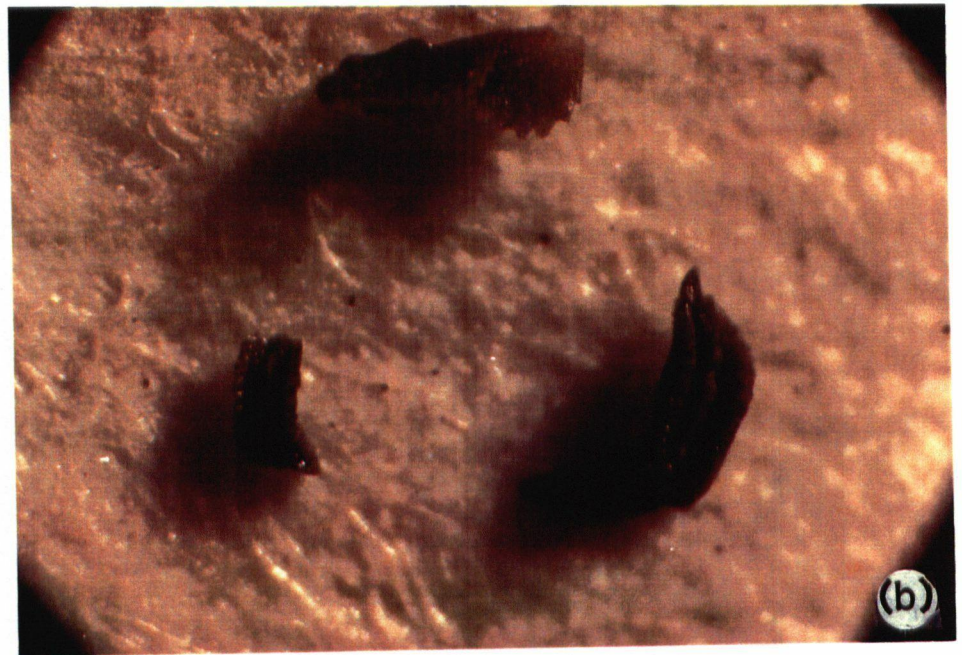
In figure 44c, the vertical variation in vitrinite maturity (maturation gradient) of a 300 m section of the Canol Formation indicates a maturation gradient of 0.14 log Romax/km.

3. Conodont Alteration Index

CAI values of the few samples which produced conodonts upon extraction are summarized in table X and illustrated in figure 45. The CAI is constant at a value of 5 for all samples examined. Conodonts which have a CAI of 4.5 or higher often show changes in surface texture from smooth and vitreous to pitted and grainy (Epstein et al., 1977), as evident in some conodont fragments of this study (Fig. 45). Subtle changes in the CAI at such a high level of maturity are difficult to ascertain as a result of genetic and structural differences between different conodont species and the shape, size, stage of growth, maturity and/or robustness of individual conodont elements (Epstein et al., 1977).

Table X. Conodont alteration index (CAI) determined for samples collected from Road River Group and Canol Formation. Refer to figure 37 for summary of sample descriptions. Romax=mean maximum reflectance: (g) denotes Romax of graptolite fragments measured on the plane of bedding for samples 74U and V; Romax for sample 74T was calculated from the line of best fit in figure 44b; (v) denotes Romax of vitrinite in sample 74G, calculated from the line of best fit in figure 44c.

<u>Sample</u>	<u>CAI</u>	<u>Romax</u>
74G	5	3.97(v)
74T	5	5.77(g)
74U	5	5.03(g)
74W	5	6.45(g)



200 microns

Figure 45. Conodonts recovered from the Road River Group, CAI of 5.
A. Sample 74T.
B. Sample 74U.



200 microns

Figure 45 cont'd. C. Sample 74W.

a. Calibration of Graptolite Reflectance with CAI

In figure 46, graptolite reflectance is plotted with CAI and indicates graptolite reflectance increases slowly with low levels of CAI. Graptolite reflectance increases more rapidly than the CAI at high levels of maturity and thus is a more sensitive indicator of thermal maturity at CAI values greater than about 3. Separate curves are plotted for graptolites from shales and graptolites from carbonates because, in a given sample, graptolite reflectance is higher in shales than in carbonates.

E. DISCUSSION

1. Granular and Non-granular Graptolite Fragments

Granular fragments of graptolites are differentiated from non-granular shapes by lower reflectance, lath-like morphology and the appearance of a mosaic of very fine 'grains'. Goodarzi and Norford (1985) consider the granular fragments to be part of the common canal. Hence, the granular fragments may consist of the remains of zooids which once occupied individual thecae and were interconnected via the common canal. Alternatively, granular particles may represent granular cortical tissue composing the outer layer of the periderm. Cortical bandages (ribbon-like increments of the cortical tissue) are enveloped by a bounding granular sheet fabric (Crowther, 1981, p. 13) which may appear granular in reflected light. Similarly, granular particles may depict fusellar tissue of the periderm. Fusellar tissue is the primary component of all graptolite thecal walls

but is often masked by ectocortex (cortical tissue; Crowther, 1981, p. 11). A packet of loosely anastomosing fibrils comprises each fusellum (Crowther, 1981, p. 11); fusellar fabric exposed along fracture surfaces of broken periderm (Crowther, 1981, p. 11) may also appear granular in reflected light. If the granular fragments represent one layer (fusellar or cortical) of the periderm, then non-granular fragments may be the manifestation of an intact periderm where both fusellar and cortical tissue are seen.

Another possible explanation for granular graptolite fragments might be that different genera or species show different optical properties and morphology. However, the type of paleontological classification required to determine the relationship between granular versus non-granular fragments and graptolite species or genera type is absent at present.

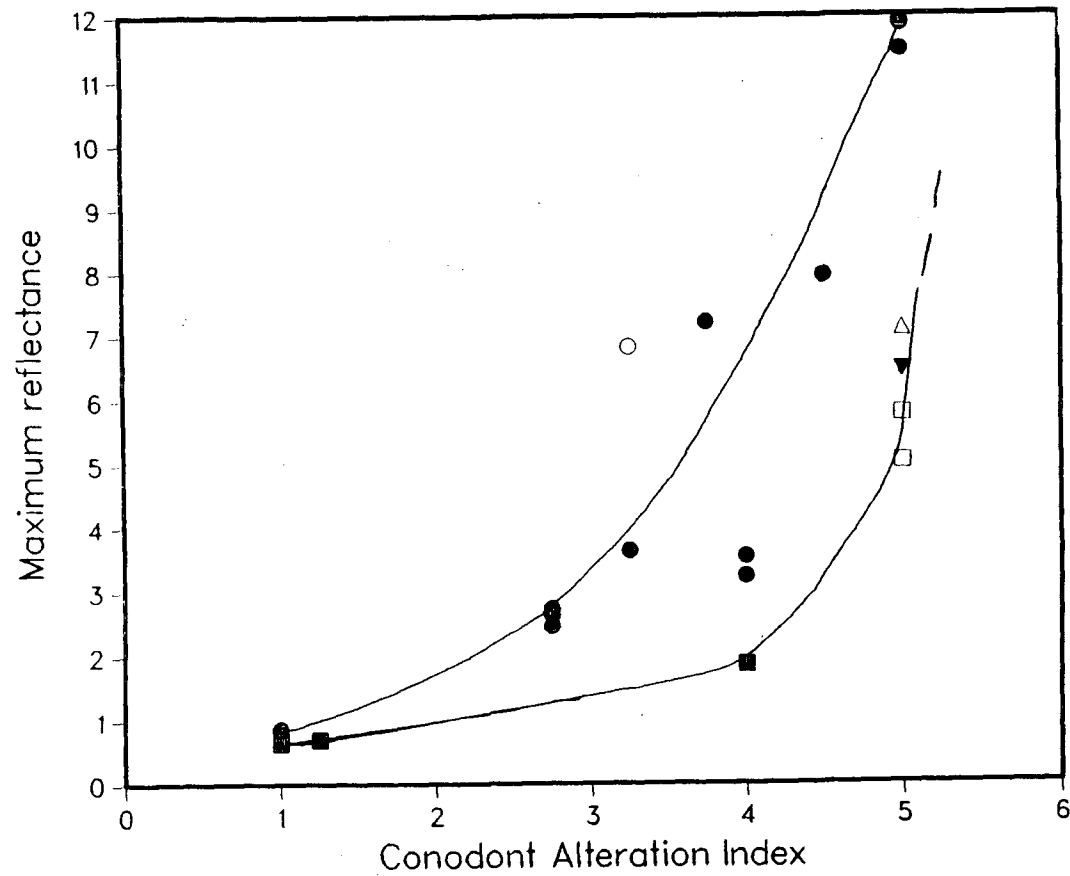


Figure 46. Maximum reflectance in oil of graptolites versus CAI. Goodarzi and Norford's (1985) data: (●), graptolite in shale; (○), weathered graptolite; (■), graptolite in limestone and calcareous shale; and (△), graptolite in sedimentary lead-zinc deposit. Data from the present study: (▼), graptolite in shale; (□), argillaceous limestone. See table X for specific Romax and CAI values from the present study.

2. Biaxial Nature of Graptolites

Graptolites examined in this study with Romax values of 4.0% to 6.5% have biaxial negative optical properties. Preliminary studies involving laboratory-induced maturation of graptolites (Bustin and Link, unpublished) suggest that significant changes in graptolite reflectance with increasing temperature can result and that a deviatoric stress field is not necessary to produce biaxial optical properties in graptolites. Preferred 'crystal' growth may be the major mechanism for producing preferred orientation of the aromatic graphite-like lamellae in coals (Levine and Davis, 1984) and may be responsible for the biaxial nature of graptolites even with maturation under hydrostatic conditions. Fossil organic matter is usually considered as a colloidal substance, but the term crystal growth is used here to express the relative increase in the proportion of carbon atoms in an aromatic structure which yields aromatic graphite-like lamellae.

As discussed previously, graptolite periderm may be composed of a chitinous (N-acetyl glucosamine) or collagen-like (proteinaceous) substance; neither of these compounds contain an aromatic structure. It is important to note, therefore, that the graptolite periderm may not contain an aromatic structure at low levels of organic maturity. Chitin is probably not responsible for high reflectivity in graptolites because chitin also composes light-colored (low reflectivity) fungal cells in certain coals (Teichmüller, 1982, p. 280). However, thermal maturation of chitin could produce an aromatic structure (which would show an increase in reflectivity due to preferred orientation of graphite-like lamellae) as a result of diagenetic reactions such as dehydration and deamination (Hunt, 1979, p.

114-115). If, however, the graptolite periderm comprises a collagen-like substance, then preferred orientation of aromatic graphite-like lamellae is not responsible for high reflectivity of graptolites. Rather, high reflectivity from a collagen-like substance may be a result of the highly-ordered 3 dimensional helix shape (Leninger, 1975, p. 135). Clearly, detailed analysis of the graptolite periderm is required in order to elucidate its chemical and structural framework and relate this to the optical properties of graptolites in reflected light.

a. Variations in Romax

In specimens which exhibit biaxially negative properties, the measured values of Romax on the plane normal to bedding (Ra in Fig. 43B(iii)) should be approximately equal to Romax values measured on the plane parallel to bedding (Ra in Fig. 43B(i); if the measurements are made on different planes with the polarizer in the same position (parallel to Romax). Several factors may explain the observed differences in Romax measured parallel to, and normal to bedding (compare Tables VIa and VIb). A t-test of the hypothesis that the orientation of the section (normal or parallel to bedding) does not affect the measured value of Romax shows that the difference between Romax measured normal to and parallel to bedding is not significant (95% confidence level); hence the orientation does not have an effect on the measured Romax. Alternatively, the principal reflectance axes of graptolites may not always lie exactly parallel or perpendicular to bedding perhaps because the maximum stress was oriented non-perpendicular to bedding (e.g., see Bustin, et al., 1986). Thus, the plane containing the trace of Romax (the Ra-Rb and Ra-Rc planes in figure 43B) may

make a small angle with the bedding plane. Furthermore, differences in the quality of polish may arise on different surfaces and errors may be made in cutting the sections so they are not perfectly normal or parallel to bedding. At the microscopic level, the bedding of the limestone is difficult to ascertain (samples 74N, -O, -U) so that the measured surface may not be perfectly parallel to bedding.

3. Lateral and Stratigraphic Variation in Reflectance

Laterally, the mean R_{max} values of graptolites in the Road River Group range from 4.0% to 6.5% R_{max} and the highest values occur near the base of the Group (Loucheux Formation) in the central Richardson Mountains. The Richardson Mountains mark the former position of the Richardson Trough (A.W. Norris, 1985) and deep burial in the trough sometime before the Carboniferous (see Figs. 10a and 13c, part I) is responsible for high R_{max} values of graptolites in the Road River Group. Because of structural complexity in the Ogilvie and Richardson Mountains, it is not possible to provide definitive stratigraphic correlation between the maturation levels of the Group.

The higher maturation gradient (0.39 log R_{max} /km) calculated from the older (Ordovician to Early Devonian) graptolite-bearing strata than the gradient (0.14 log R_{max} /km) calculated from younger (Middle Devonian) vitrinite-bearing strata may signify a higher paleogeothermal gradient during maturation of graptolite-bearing strata. The Richardson Trough represents a Paleozoic aulacogen (failed arm) whose genesis may lie in a heat plume-generated triple junction

(Pugh, 1983). High paleoheat flow ($> 70 \text{ mW/m}^2$; Sclater and Francheteau, 1973, p. 487) associated with evolution of the aulacogen during the Proterozoic (Young et al., 1979) could therefore be responsible for high paleogeothermal gradients ($> 35^\circ\text{C/km}$) during burial of Road River strata. Such high heat flow however, probably also existed during burial of Canol strata. Also, because the decrease in heat flow during the interval of time representing the end of Road River deposition and the start of Canol sedimentation (24 Ma) would be insignificant (see Sclater and Francheteau, 1973, Fig. 38-9, p. 482). Therefore, it seems unlikely that a higher paleogeothermal gradient existed during burial of Road River than Canol strata. Alternatively, as will be discussed later, the maturation gradient calculated from graptolite reflectance data is greater than the gradient calculated from vitrinite reflectance data because graptolite reflectance increases more rapidly than vitrinite reflectance at higher levels of maturity.

A maturation gradient was not calculated for the bitumen reflectance data because of the presence of different phases with different reflectance values within one sample and between samples (Table VIII) which could represent multiple hydrocarbon generation or multiple oil migration episodes (Robert, 1980).

a. Variation in Bireflectance

Bireflectance (RoB) of graptolites does not show any relationship to the depth of burial nor to the thermal maturity (Tables VI and VII). Similar results have been observed in vitrinite at Romax values between 4% and 6% where there is a large scatter in the RoB of vitrinite (Teichmüller, 1982, p. 49). In coals, a

progressive increase in the RoB of vitrinite is a measure of the increasing order achieved by the aromatic lamellae. The organic matter comprising the graptolite exoskeleton may have a variable degree of ordering in the range 4% to 6.5% Romax; thus a relationship between RoB of graptolites and thermal maturity may not exist. Alternatively, the relationship between RoB and depth of burial may not be obvious due to errors in measuring Romin and therefore RoB. For example, the measured surface containing Romin may not be cut precisely normal to bedding, or Romin may not lie exactly normal to bedding, both of which would affect the calculated RoB. Measurement of Romin is difficult on sections cut perpendicular to bedding as a result of the generally small particle size exposed in this orientation (thin, lath-like shapes as opposed to blocky morphology in sections cut parallel to bedding).

4. Influence of Host-rock Lithology on Graptolite Reflectance

Graptolites in limestone samples have lower reflectance values than predicted by the line of best fit in figure 44. Goodarzi and Nordord (1985) similarly noted lower reflectance values for graptolites in limestones than in shales and vitrinite in carbonates has been shown to have lower reflectances than in coals (Epstein et al., 1977). Factors which might explain the relationship between host-rock lithology and graptolite reflectance include polishing techniques, thermal conductivity contrasts of different lithologies, varying graptolite species with facies, and dissolution of carbonates. Recent studies (Goodarzi and Stasiuk, 1987) suggest that negative relief due to polishing fragments which are softer than the imbedding media may result in a decrease of the true reflectance. If graptolites

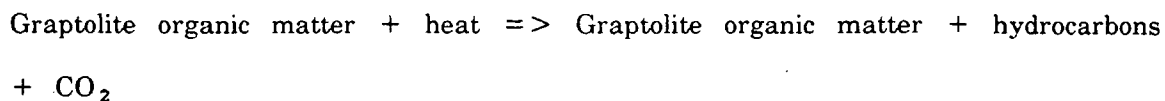
are softer than the carbonate host-rock (imbedding media in whole-rock specimens), then negative relief could decrease the measured reflectance of graptolites in carbonates. Carbonates are harder than shales and therefore more negative relief of the graptolite surface, and hence lower reflectivity, may occur in carbonates than in shales. No obvious difference in the polished graptolite surface in carbonates and shales was observed in this study and resolving whether lower graptolite reflectance in carbonates as compared to shales is a result of polishing techniques requires further study.

Thermal conductivity contrast between carbonates and shales cannot explain lower reflectance values in carbonates because it is unlikely that a significant difference in thermal history would exist between thinly interbedded limestones and shales of the Road River Group.

Graptolite species with a lower reflectance might preferentially be associated with limestones but this seems unlikely because graptolites are not associated ecologically with any particular type of sedimentary environment due to their planktonic nature (Moore, 1955, p. 16).

The most likely explanation for lower graptolite reflectance values in limestones appears to be related to dissolution of the carbonates. All of the limestone samples examined in this study are weathered, and the carbonates show signs of dissolution, which increases their porosity and permeability. Oxidation of graptolites could thus be enhanced by exposure to the atmosphere at or near the surface, or by oxygenated groundwater percolating through the permeable

limestone. Naturally oxidized vitrinite is reported to have lower reflectance values (Bustin et al., 1985) and graptolites could react in the same manner. Alternatively, release of CO_2 during the dissolution of carbonates in the subsurface would increase the pressure of CO_2 (PCO_2) in limestones. High PCO_2 could inhibit the reaction:



The net effect would be to slow the rate of thermal maturation of graptolites in limestones.

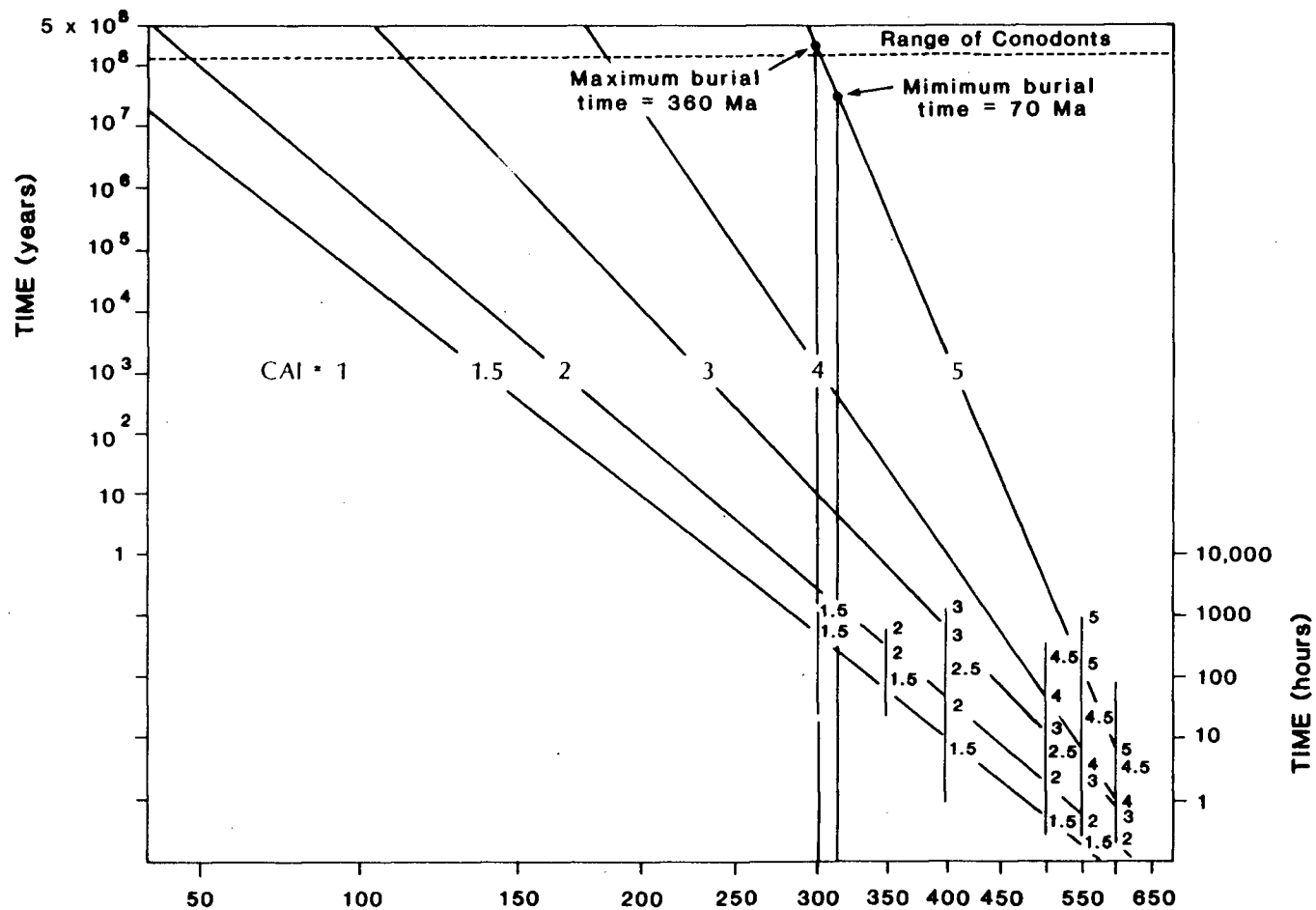
5. Correlation of Graptolite and Vitrinite Reflectance using CAI

a. Calibration of Graptolite Reflectance with Time and Temperature

Time, temperature and tectonics are controlling parameters of maturity and an assessment of their effects on graptolite and vitrinite reflectance and CAI should help in establishing a correlation between the thermal maturation indices. The Arrhenius plot presented in figure 47 illustrates the relationship between temperature, duration of burial and CAI. These experimental data are used to estimate the maximum and minimum temperatures which Road River strata experienced. Conodonts recovered from the Road River strata in this study have a CAI of 5 and are approximately 430 Ma old (Orchard, pers. comm., 1986). The minimum possible time for burial and heating of the strata is on the order

of 70 Ma if unloading by erosion began at the end of the Devonian during the Ellesmerian orogeny (which occurred about 360 Ma; Pugh, 1983). If however, uplift and erosion did not begin until Late Cretaceous to Early Tertiary time (Laramide orogeny, about 70 Ma; Dixon, 1986) then the maximum possible burial time for the Road River strata could be as long as 360 Ma. Using the Arrhenius plot of conodont data (Fig. 47), the temperature required to produce a CAI of 5 for a burial time of 360 Ma is about 310°C whereas a temperature of about 320° C would result in a CAI of 5 for a burial time of 70 Ma. Thus, graptolite reflectances of 5% to 6.5% Romax (correlated to a CAI of 5) represent temperatures of 310 to 320°C for maximum and minimum burial times of 360 and 70 Ma, respectively.

The burial history of the Road River Group is probably much more complex than suggested by estimates denoted above (see part I of thesis). However, the maximum and minimum durations of burial time used in the present study facilitate approximation of the minimum and maximum temperatures attained during burial of Road River strata. Neither the precision of the Arrhenius plot nor the maturation measurements warrant consideration of a more complex burial history at this time.



RECIPROCAL OF ABSOLUTE TEMPERATURE RECALIBRATED IN °C

Figure 47. Arrhenius plot of the experimental data of Epstein et al. (1977) and maximum and minimum temperature ranges of conodont samples from the Road River Group in the study area. The maximum temperature is determined by plotting the minimum burial time (70 Ma) on the line corresponding to a CAI of 5. This point is extrapolated to 320°C on the temperature axis. Similarly, the minimum temperature indicated by a CAI of 5 is found by extrapolating the maximum burial time of the Road River Group (360 Ma) to 310°C.

(i) Calibration of Graptolite and Vitrinite Reflectance with Time and Temperature

Because graptolites and vitrinite do not occur in the same strata in this study, calibration of graptolite with vitrinite reflectance is achieved by correlation of graptolite reflectance with CAI. In this study, only 2 samples which contained graptolites also yielded conodonts whereas none of the vitrinite-bearing samples included conodonts. Therefore, in order to calibrate graptolite and vitrinite reflectance, calibrated by CAI, a graptolite or vitrinite reflectance was calculated from the line of best fit in figure 44b (graptolite reflectance for sample 74T) and in figure 44c (vitrinite reflectance in sample 74G). Graptolite reflectance values of 5% to 6.5% Romax and a vitrinite reflectance of 4.0% Romax correspond to CAI values of 5 in this study (Table X).

If graptolite reflectance reacts to time-temperature changes in the same manner as vitrinite reflectance, then the maximum and minimum temperatures estimated from graptolite reflectance indirectly by CAI should approximate those estimated from similar plots of vitrinite reflectance data. Figure 48 is a plot of thermal history calibrated with vitrinite reflectance. Maximum and minimum temperatures represented by vitrinite reflectance values (equal to the measured graptolite reflectance values of 5% to 6.5% Romax) can be determined by plotting the minimum and maximum burial times of Road River strata (70 and 360 Ma, respectively) on isorefectance lines in figure 48. Vitrinite reflectances of 5% to 6.5% Romax indicate a temperature range of 120 to 150°C for the maximum burial time of 360 Ma whereas temperatures from 190 to 230°C are suggested

by vitrinite reflectances of 5% to 6.5% Romax for a minimum burial time of 70 Ma. Thus, for a minimum burial time of 70 Ma, graptolite reflectances of 5% to 6.5% Romax (CAI=5) correspond to a temperature of about 320° C whereas vitrinite reflectances of 5% to 6.5% Romax represent temperatures of about 190° to 230° C. Taken at face value, this suggests that graptolite organic matter, conodont material and vitrinite do not react to increasing temperature in the same manner.

b. Correlation of Graptolite and Vitrinite Reflectance

Goodarzi and Norford (1985) suggest that graptolite organic matter behaves similarly to bitumen with increasing depth of burial. Figure 49 demonstrates that reflectance data from graptolites examined in the present study plot close to the bitumen line. Bitumen which has experienced the same burial and thermal history as vitrinite has a lower reflectance value than vitrinite, up to a level of thermal maturity of about 1.0% vitrinite reflectance. At vitrinite reflectance values greater than about 1.0%, bitumen reflectance increases more rapidly than vitrinite reflectance (Jacob et al., 1985). If graptolite organic matter reacts in the same manner as bitumen, then a graptolite reflectance of 5.0% should correspond to a vitrinite reflectance less than 5.0%, for the same thermal history. Evidence for higher graptolite than vitrinite reflectance in a given sample is seen in vitrinite data obtained from the Canol Formation where a CAI of 5 corresponds to a vitrinite reflectance of about 4.0% Romax whereas a CAI of 5 in samples from the Road River Group corresponds to a graptolite reflectance values from 5% to 6.5% Romax. Furthermore, the higher maturation gradient calculated from

graptolite reflectance data (up to 3 times higher) than that calculated from vitrinite reflectance data suggests that graptolite reflectance increases more rapidly than vitrinite reflectance with increasing depth of burial.

Successful maturation modelling can only be obtained with an accurate model of the thermal history and an accurate knowledge of the reaction parameters comprising the system." The first-order reaction theory commonly used in time-temperature plots may not apply to graptolite organic matter. Also, the assumption of temperature independence of the constants in the Arrhenius equation is valid only over a short temperature range and thus estimation of geologic temperatures from laboratory-induced maturation data is not entirely accurate. The dependence of graptolite reflectance on time and temperature should be calibrated like that for vitrinite reflectance (e.g., Fig. 48) so that a direct comparison between graptolite and vitrinite reflectance can be made without indirectly correlating to CAI.

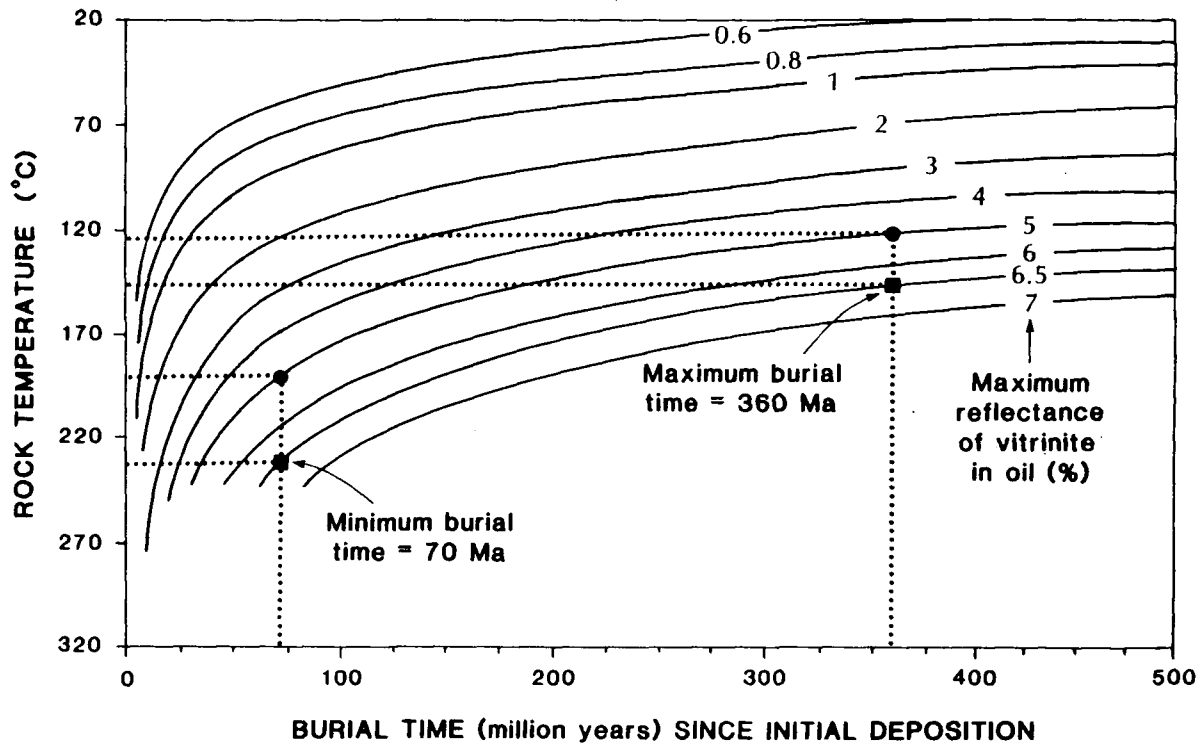


Figure 48. Diagram of thermal history calibrated with maximum vitrinite reflectance in oil. The maximum and minimum temperature ranges of graptolite reflectance values in the range of 5.0 to 6.5% Romax are determined by plotting a maximum burial time of 360 Ma and a minimum burial time of 70 Ma on isorefectance lines of 5% (●) and 6.5% (■) Romax. (modified from Wright, 1980).

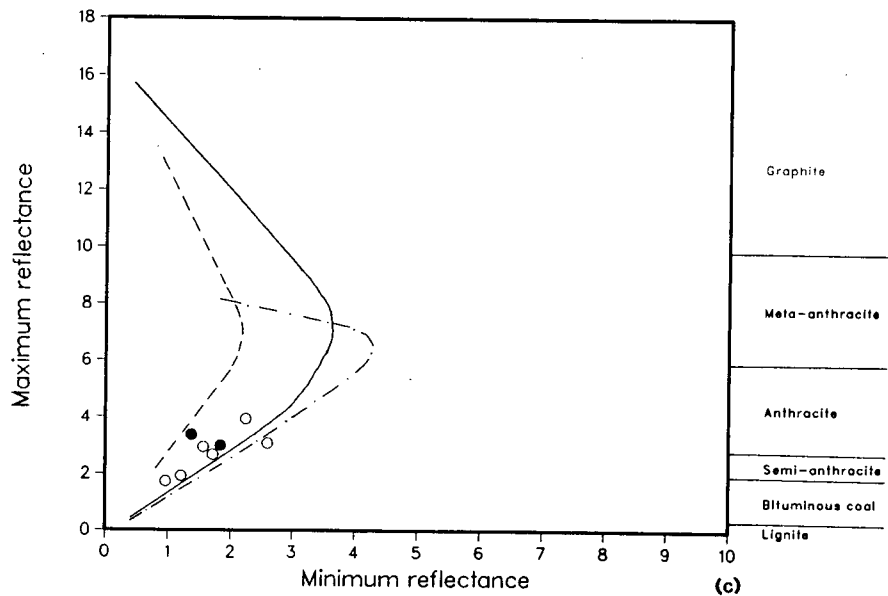
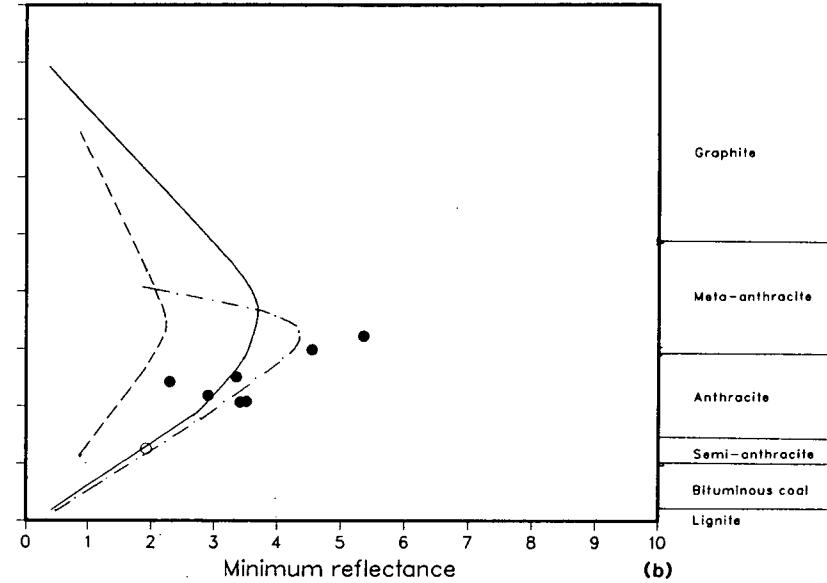
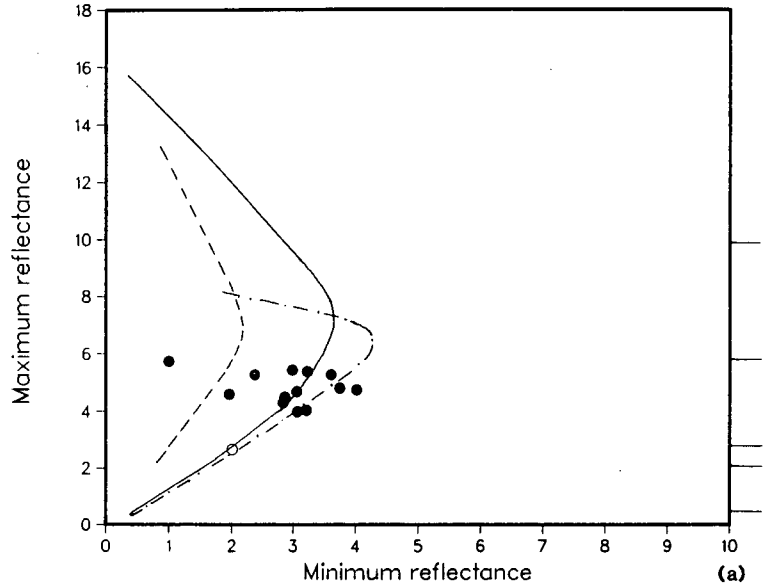


Figure 49. Plot of maximum versus minimum reflectance in oil for —, coal to graphite (after Teichmüller et al., 1979); ---, heat affected coal (after Brown and Taylor, 1961 and Chandra, 1963); -.-.-, bitumen (after Khavari-Khoransani, 1975). Graptolite and bitumen data from present study is superimposed on these curves: (●)=non-granular fragments; (○)=granular fragments.
 A. Graptolite data from surfaces cut and polished normal to bedding.
 B. Graptolite data from surfaces cut and polished parallel to bedding.
 C. Bitumen data from surfaces cut and polished normal to bedding.

742

F. SUMMARY AND CONCLUSIONS

1. Graptolite reflectance is a useful tool for assessing the level of thermal maturity of Lower Paleozoic marine strata in which vitrinite and spores are absent.

2. Graptolite fragments are easily recognized in reflected light microscopy because they have distinct features such as: a) weak to strong anisotropy; b) rough, granular fragments which are commonly lath-shaped; c) smooth, non-granular higher reflecting fragments which have blocky or stipe-like morphology; d) oval-shaped pits; and e) cortical bandages.

3. Maximum reflectance is the most reliable method of assessing the level of thermal maturity of graptolites. Graptolites with Romax values as low as 4% are anisotropic and have biaxial negative properties. The measured maximum graptolite reflectance is parallel to bedding and the measured minimum graptolite reflectance is normal to bedding. Depending on the orientation of the surface, the measured Romax will vary from the true Romax to an intermediate value. Random reflectance is not a reliable method of determining the reflectance of graptolites because of their anisotropic and biaxial nature.

4. The mean maximum reflectance of graptolites appears to increase with increasing depth of burial. The increase in Romax with depth fits a log (Romax) linear (depth) relationship although insufficient data is available to confidently define the relationship.

5. Graptolites in limestones have lower reflectance values than graptolites in shales from the same stratigraphic level, possibly as a result of the more permeable nature of the limestones which enhances the effects of weathering and oxidation. Alternatively, increased PCO_2 as a result of carbonate dissolution during maturation in the subsurface might slow the rate of thermal maturation of graptolites in limestones.

6. Graptolite reflectance is the more sensitive indicator of thermal maturity at CAI values greater than about 3 whereas graptolite reflectance increases more slowly at low levels of CAI. Subtle changes in the CAI at high levels of maturity (CAI=5) are difficult to ascertain as a result of genetic and structural differences between different conodont species and the shape, size, stage of growth, maturity and/or robustness of individual conodont elements (Epstein et al., 1977). Hence, the level of organic maturity determined by CAI is less quantitative and represents a wider range than the level of maturity measured by reflectance methods.

7. An attempt to correlate graptolite reflectance calibrated by CAI with vitrinite reflectance using a burial time of 70 Ma shows that graptolite reflectances of 5% to 6.5 % R_{max} indicate a temperature of about 320° C whereas a vitrinite reflectance of 5% corresponds to a temperature of about 190° C. Taken at face value, this suggests that graptolite, vitrinite and conodont organic matter do not react to increasing temperature in the same manner.

8. Graptolite organic matter may respond to increasing depth of burial (and

therefore increasing temperature) in the same manner as bitumen i.e., graptolite reflectance increases more rapidly than vitrinite reflectance at high levels of thermal maturity. In the present study, vitrinite reflectance (4.0% Romax) is less than graptolite reflectance (5.0% to 6.5% Romax) in strata which have approximately the same level of thermal maturity, calibrated by -CAI of 5. Furthermore, the maturation gradient calculated from graptolite reflectance data (0.39 log Romax/km) is almost 3 times the maturation gradient calculated from vitrinite reflectance data (0.14 log Romax/km). The higher maturation gradient calculated from graptolite reflectance data may represent a higher paleogeothermal gradient during burial of older (Ordovician to Early Devonian) graptolite-bearing strata than younger (Middle Devonian) vitrinite-bearing strata. Consideration of the age of the thermal event caused by the formation of the Richardson aulacogen and the difference in time (24 Ma) between deposition of Road River and Canol strata indicates the paleogeothermal gradient was not significantly greater during burial of Road River than Canol strata. Alternatively, graptolite reflectance may increase more rapidly than vitrinite reflectance at higher levels of maturity; hence, a maturation gradient from graptolite reflectance data would be higher than a gradient calculated from vitrinite reflectance data.

9. Future studies involving graptolite reflectance should address: a) the relationship between host-rock lithology and graptolite reflectance; b) the lateral and vertical variation of graptolite reflectance, especially through a thick section containing graptolites at various stratigraphic levels; c) the chemical and structural nature of the chitinous or collagen-like material comprising the graptolite periderm and differentiate between granular and non-granular

fragments; and d) the relationship between temperature, duration of burial and graptolite reflectance.

VIII. REFERENCES

- Balkwill, H.R., Cook, D.G., Detterman, R.L., Embry, A.F., Hakansson, E., Miall, A.D., Poulton, T.P. and Young, F.G., 1983. Arctic North America and northern Greenland; in Mesozoic of Arctic North America and Greenland. *In*: M. Moullade and A.E.M. Nairn, eds., *Phanerozoic of the World II, Mesozoic A*. Amsterdam: Elsevier, p. 1-31.
- Batten, D.J., 1981. Palynofacies, organic maturation and source rock potential for petroleum. *In*: J. Brooks, ed., *Organic maturation studies and fossil fuel exploration*. London: Academic Press, p. 201-224.
- Bertrand, R. and Héroux, Y., 1987. Chitinozoan, graptolite and scoleodont reflectance as an alternative to vitrinite and pyrobitumen reflectance in Ordovician and Silurian strata, Anticosti Island, Quebec, Canada. *American Association of Petroleum Geologists Bulletin*, 71, p. 951-957.
- Bloss, F.D., 1971. *Crystallography and crystal chemistry*. New York: Holt, Rinehart and Winston Inc., 545 p.
- Bostick, N.H., 1979. Microscopic measurement of the level of catagenesis of solid organic matter in sedimentary rocks to aid exploration for petroleum and to determine former burial temperature - a review. *Society of Economic Paleontologists and Mineralogists, Special Publication 26*, p. 17-43.
- Brown, H.R. and Taylor, G.H., 1961. Some remarkable Antarctic coals. *Fuel*, 40, p. 211-224.
- Bustin, R.M., Cameron, A.R., Grieve, D.A. and Kalkreuth, W.D., 1985. Coal petrology. Its principles, methods and application. *Geological Association of Canada Short Course Notes*, 3, 273 p.
- Bustin, R.M., 1986. Organic maturity of late Cretaceous and Tertiary coal measures, Canadian Arctic Archipelago. *International Journal of Coal Geology*, 6, p. 71- 106.
- Bustin, R.M., Ross, J.V. and Moffat, I., 1986. Vitrinite anisotropy under differential stress and high confining pressure and temperature: Preliminary observations. *Coal Geology*, 6, p. 343- 352.

- Castano, J.R. and Sparks, D.M., 1974. Interpretation of vitrinite reflectance measurements in sedimentary rocks and determination of burial history using vitrinite reflectance and authigenic minerals. In: R.R. Dutcher and others, eds., Carbonaceous materials as indicators of metamorphism. Geological Society of America, Special Paper 153, p. 31-52.
- Cecile, M.P., Hutcheon, I.E. and Gardner, V., 1982. Geology of the northern Richardson anticlinorium (map areas 106 L/12, 13, 116 I/9, 16). Geological Survey of Canada, Open File Report No. 875.
- Chandra, D., 1963. Reflectance of thermally metamorphosed coals. *Fuel*, 42, p. 69-74.
- Clarkson, E.N.K., 1981. Invertebrate paleontology and evolution. Boston: George Allen and Unwin. 323 p.
- Clausen, C.D. and Teichmüller, M., 1982. Die Bedeutung der graptolithen Fragmente im paläozoikum von Soest Erwitte für Stratigraphie und Inkohlung. *Fortschritte Geologie Rheinland und Westfalen*, 30, p. 145-167.
- Creaney, S., 1978. Spore fluorescence coloration - a rapid microscopic method of maturation assessment. Geological Survey of Canada, Paper 78-1C, p. 101-103.
- Crowther, P.R., 1981. The fine structure of graptolite periderm. Special papers in palaeontology, 26, The Palaeontological Association, London.
- Davis, A., 1978. The reflectance of coal. In: C. Karr, ed., Analytical methods for coal and coal products. London: Academic Press, 1, p. 27-28.
- Dixon, J., 1986. Cretaceous to Pleistocene stratigraphy and paleogeography, northern Yukon and northwest District of Mackenzie. *Bulletin of Canadian Petroleum Geology*, 34, p. 49-70.
- Durand, B., 1985. Diagenetic modification of kerogens. *Philosophical Transactions of the Royal Society of London*, 315, p. 77-90.
- Epstein, A. G., Epstein, J.B. and Harris, L.D., 1977. Conodont color alteration - an index to organic metamorphism. United States Geological Survey Professional Paper, 995, 27 p.

- Goodarzi, F., 1984. Organic petrography of graptolite fragments from Turkey. *Marine and Petroleum Geology*, 1, p. 202-210.
- Goodarzi, F. and Norford, B.S., 1985. Graptolites as indicators of the temperature histories of rocks. *Journal of the Geological Society of London*, 142, p. 1089-1099.
- Goodarzi, F. and Stasiuk, L.D., 1987. Graptolite preparation for reflected light microscopy - A technical note. Geological Survey of Canada, Paper 87-1A.
- Gretener, P.E., 1981. Geothermics: Using temperature in hydrocarbon exploration. American Association of Petroleum Geologists Short Course Note Series 17, p. 170.
- Hallimond, A.F., 1970. The polarizing microscope, Third edition. York: Vickers Ltd., 302 p.
- Hevia, V. and Virgos, J.M., 1977. The rank and anisotropy of anthracites: the indicating surface of reflectivity in uniaxial and biaxial substances. *Journal of Microscopy*, 109, p. 23-28.
- Hower, J.C. and Davis, A., 1981. Vitrinite reflectance anisotropy as a tectonic fabric element. *Geology*, 9, p. 165-168.
- Hunt, J.M., 1979. Petroleum geology and geochemistry. San Fransisco: W.H. Freeman, 617 p.
- International Committee for Coal Petrography (I.C.C.P.), 1971. International handbook for coal petrology, 1st supplement to 2nd edition. Centre National de la Recherche Scientifique, Paris.
- Jacob, H., Hiltmann, W., Wehner, H., Raschka, H. and Weiser, T., 1985. Microscopic-photometric analysis of dispersed solid bitumen in sediments. German Association for Petroleum Sciences and Coal Chemistry, Project 232.
- Khavari-Khoransani, G., 1975. The properties of structural ordering of some fossil bitumen. Ph. D. Thesis, University of Newcastle-Upon-Tyne, UK.
- Kurylowicz, L.E., Ozimic, O., Mckirdy, D.M., Kantsler, A.J. and Cook, A.C.,

1976. Reservoir and source rock potential of the Larapinta Group, Amadeus Basin, Central Australia. *Journal of Australian Petroleum Exploration Association*, 16, p. 44-65.
- Legall, F.D., Barnes, C.R. and Macqueen, R.W., 1981. Thermal maturation, burial history and hotspot development, Paleozoic strata of southern Ontario-Quebec, from conodont and acritarch alteration studies. *Bulletin of Canadian Petroleum Geology*, 29, p. 492-539.
- Leninger, A.L., 1975. *Biochemistry*. New York: Worth Publishers, Inc., 1104 p.
- Lerand, M., 1973. Beaufort Sea. *In*: R.G. McCrossan, ed., *The future petroleum provinces of Canada*. Canadian Society Petroleum Geologists, *Memoir 1*, p. 315-386.
- Levine, J.R. and Davis, A., 1984. Optical anisotropy of coals as an indicator of tectonic deformation, Broad Top Coal Field, Pennsylvania. *Geological Society of America Bulletin*, 95, p. 100-108.
- Miall, A.D., 1973. Regional geology of northern Yukon. *Bulletin of Canadian Petroleum Geology*, 21, p. 81-116.
- Moore, R.C., 1955. *Treatise on invertebrate paleontology*. Part V, Graptolithina. Geological Society of America. Kansas: University of Kansas Press, 101 p.
- Norris, A.W., 1985. Stratigraphy of Devonian outcrop belts in northern Yukon Territory and Northwest Territories, District of Mackenzie (Operation Porcupine Area). Geological Survey of Canada, *Memoir 410*, 81 p.
- Norris, D.K., 1981a. Geology: Fort McPerson, District of Mackenzie. Geological Survey of Canada, *Map 1520A*.
- , 1981b. Geology: Arctic Red River, District of Mackenzie. Geological Survey of Canada, *Map 1521A*.
- , 1981c. Geology: Bell River, Yukon Territory-Northwest Territories. Geological Survey of Canada, *Map 1519A*.
- , 1981d. Geology: Eagle Plain, Yukon Territory. Geological Survey of

Canada, Map 1523A.

-----, 1981e. Geology: Aklavik, District of Mackenzie. Geological Survey of Canada, Map 1517A.

-----, 1981f. Geology: Porcupine River, Yukon Territory. Geological Survey of Canada, Map 1522A.

-----, 1982a. Geology: Hart River, Yukon Territory. Geological Survey of Canada, Map 1527A.

-----, 1982b. Geology: Ogilvie River, Yukon Territory. Geological Survey of Canada, Map 1526A.

-----, 1985. Eastern Cordilleran foldbelt of northern Canada: Its structural geometry and hydrocarbon potential. *The American Association of Petroleum Geologists*, 69, p. 788-808.

Pugh, D.C., 1983. Pre-Mesozoic geology in the subsurface of Peel River Map area, Yukon Territory and District of Mackenzie. Geological Survey of Canada, Memoir 401, 61 p.

Robert, P., 1980. The optical evolution of kerogen and geothermal histories applied to oil and gas exploration. In: B. Durand, ed., *Kerogen*. Paris: Technips, p. 385-414.

Rovnina, L.V., 1981. Palynological method to determine the level of catagenesis of organic matter by using Jurassic deposits of Western Siberia. In: J. Brooks, ed., *Organic maturation studies and fossil fuel exploration*. London: Academic Press, p.427-432.

Sclater, J.G. and Francheteau, J., 1970. The implications of terrestrial heat flow: Observations on current tectonic and geochemical models of the crust and upper mantle of the earth. *Geophysical Journal of the Royal Astronomical Society*, 20, p. 509-542.

Teichmüller, M., 1978. Nachweis von Graptolithen - Periderm in geschieferten Gesteinen mit Hilfe Kohlenpetrologischer Methoden. *Monatshefte Neues Jahrbuch fuer Mineralogie, Geologie, und Palaeontologie*, 7, p. 430-447.

- and Wolf, M., 1977. Application of fluorescence microscopy in coal petrology and oil exploration. *Journal of Microscopy*, 109, p. 49-73.
- , Teichmüller, R. and Bartenstein, H., 1979. Inkohlung und Erdgas in Nordwestdeutschland. Eine Inkohlungskarte der oberfläche des oberkarbons. *Fortschritte Geologie Rheinland and Westfalen*, 27, p. 137-170.
- and Durand, B., 1983. Fluorescence microscopical rank studies of liptinites and vitrinites in peat and coal, and comparison with results of the Rock-Eval pyrolysis. *International Journal of Coal Geology*, 2, p. 197-230.
- Teichmüller, M., 1982. Origin of the petrographic constituents of coal. In: Stach, E., Mackowsky, M.-Th., Teichmüller, M., Taylor, G.H., Chandra, D. and Teichmüller, R., eds., *Stach's textbook of coal petrology*, 3rd edition. Berlin: Gebrüder Borntraeger, 535 p.
- and Teichmüller R., 1982. The geological basis of coal formation. In: Stach, E., Mackowsky, M.-Th., Teichmüller, M., Taylor, G.H., Chandra, D. and Teichmüller, R., eds., *Stach's textbook of coal petrology*, 3rd edition. Berlin: Gebrüder Borntraeger, 535 p.
- Tipper, H.W., Woodsworth, G.J. and Gabrielse, H., 1981. Tectonic assemblage map of the Canadian Cordillera and adjacent part of the United States of America. *Geological Survey of Canada*, Map 1505A.
- Wright, N.J.R., 1980. Time, temperature and organic maturation - the evolution of rank in a sedimentary pile. *Journal of Petroleum Geology*, 2, p. 411-435.
- Young, G.M., Jefferson, C.W., Delany, G.D. and Yeo, G.M., 1979. Middle and late Proterozoic evolution of the northern Canadian Cordillera and Shield. *Geology*, 7, p. 125-128.

SUMMARY AND CONCLUSIONS

1. The DOM of Upper Cambrian to Upper Cretaceous strata in the northern Yukon and northwestern District of Mackenzie generally reflects the stratigraphy and maturation is considered to be pre-orogenic (pre-Laramide). The variation in DOM reflects a wide range of maturation gradients in Eagle Plain (0.10 to 0.29 log Rorand/km) and the effects of timing and magnitude of the maximum depths of burial.

2. Graptolite reflectance values from 4.0% to 6.5% Romax and CAI values of 3.5 to 5 occur in Upper Cambrian to Lower Devonian strata. The degree of organic maturity (DOM) at the base of Middle Devonian (Givetian) strata varies laterally from 0.79% to 3.75% Rorand whereas the regional variation in DOM at the base of Upper Devonian strata ranges from 0.80% to 2.13% Rorand. Reflectance values vary laterally from 0.50% to 1.69% Rorand at the base of Carboniferous strata and ranges from 0.24% to 1.39% Rorand at the base of Lower Cretaceous strata. In Eagle Plain, the DOM of Upper Cretaceous strata ranges regionally from 0.38% to 0.53% Rorand. Maturity in coeval strata is generally lower in southern Mackenzie Delta, Peel Plateau and Eagle Plain than in the Richardson and Ogilvie Mountains.

3. A correlation of graptolite and vitrinite reflectance, calibrated by conodonts, shows that a graptolite reflectance range of 5% to 6.5% Romax (CAI=5) corresponds to a vitrinite reflectance of 4.0% Romax. Graptolite organic remains appear to behave similar to bitumen with increasing depth of burial; at higher

levels of thermal maturity, graptolite reflectance increases more rapidly than vitrinite reflectance.

4. Time-averaged numerical modelling of the measured maturation gradients (0.10 to 0.32 log Rorand/km) suggest paleogeothermal gradients on the order of 20 to 45°C/km in southern Mackenzie Delta and Peel Plateau and paleogeothermal gradients which increase from 10 to 20°C/km in central Eagle Plain to 20 to 45°C/km towards the Richardson and Ogilvie Mountains. The higher maturity levels in mountainous areas reflect higher maturation gradients and, in the Richardson Mountains, deeper burial due to rapid subsidence caused by the foundering of grabens within the Richardson Fault Array. Anomalously high maturation values (0.92% to 1.60% Rorand) measured in Lower Cretaceous strata on the Campbell Uplift are interpreted to reflect high paleoheat flow associated with basement uplift.

5. The thickness of eroded section in the study area varies from 0.7 to 4.7 km based on interpretation of measured maturation gradients. Such values are consistent with rates of subsidence and uplift estimated from the ages and thicknesses of preserved section in the study area. In Peel Plateau, approximately 1.7 km of post-Upper Devonian section has been eroded. In eastern Eagle Plain, 2.6 to 2.8 km of post-Carboniferous overburden has been removed whereas in western Eagle Plain, up to 4.7 km of coeval strata has been eroded. In northwestern Eagle Plain, about 3.5 km of post mid-Cretaceous section has been eroded which is almost three times the amount of post mid-Cretaceous overburden which has been removed in southern Mackenzie Delta (1.1 km). Estimates of the

eroded Upper Cretaceous section vary significantly from central to northern Eagle Plain (0.7 to 3.4 km) and thus help define Late Cretaceous depositional patterns.

6. Average TOC contents are generally low to moderate (0.1 to 2.0%) but organic-rich intervals occur throughout the studied succession. TOC values of up to 14.5% are present in the Upper Cretaceous Eagle Plain Group, values up to 9.5% occur in the Middle Devonian Canol Formation and Upper Cambrian to Lower Devonian Road River Group and values up to 5.0% are present in the Lower Cretaceous map unit Kwr and Mount Goodenough Formation, the Lower Cretaceous and Jurassic Husky Formation, the Jurassic Porcupine River Formation and the Upper Carboniferous Blackie and Hart River Formations and the Ford Lake Shale.

7. The organic matter (OM) is dominantly type III except for minor amounts of type I and II in Lower Paleozoic strata and a mixture of type II and III in parts of Middle Devonian, Carboniferous, Jurassic and Lower Cretaceous strata.

8. The significant variation in the quality of organic matter (QOM; 0.01 to 6.1 mg HC/g Corg) is a result of spread in the level of organic maturity, the type of OM and, in some cases, migration. Average QOM values are generally low to moderate (0.01 to 1.5 mg HC/g Corg) and, along with low to moderate Hydrogen Index values (<300 mg HC/g Corg), suggest poor to moderate petroleum source potential. Relatively few examples of potential oil prone source rocks occur, but these include parts of the Road River Group, the Hare Indian, Canol, Hart River, Blackie, Mount Goodenough and Arctic Red River Formations, the Ford

Lake Shale, unnamed Carboniferous unit and map unit Kwr. Gas prone source rocks comprise parts of the Blackie, Porcupine River, Husky, Mount Goodenough and Arctic Red River Formations and the Bug Creek and Eagle Plain Groups and map unit Kwr.

9. Tmax values from Rock-Eval pyrolysis and other maturation indexes indicate that Upper Cretaceous strata are generally immature, Lower Cretaceous to Permian strata are immature to mature, Carboniferous strata are immature to overmature, and Devonian and older rocks are mature to overmature (with respect to petroleum generation). The timing of hydrocarbon generation from source rocks in the study area varied substantially both laterally and stratigraphically as a result of variations in the timing and magnitude of the maximum depths of burial.

10. The variation in source rock quality reflects the depositional environment of some of the strata.

a. The distribution of TOC in the Road River Group closely parallels the sedimentology of the strata; graptolite-bearing and siliceous shales of the Loucheux and Vitreekwa Formations of deep water origin (Richardson and Blackstone Troughs) have the highest TOC content.

b. Organic-rich shales containing a mixture of type II and III OM in the Canol Formation coincide with sediments deposited in upwelling zones during

widespread transgression across the continental shelf during the Devonian.

- c. Variations in TOC content of the Imperial Formation may be related to differences in sedimentation rates between turbidite and deltaic deposition.

- d. Organic-rich shales of the Ford Lake Shale which contain a mixture of type II and III OM, are considered to reflect continental shelf sedimentation during a transgression in the Early Carboniferous.

- e. Jurassic to Lower Cretaceous strata comprising the Bug Creek Group, Husky Formation and Parsons Group are characterized by marine shelf sediments in which TOC closely mimics variable sediment supply and transgressive and regressive episodes. Terrestrial OM (type III) is abundant in samples with low TOC of the Murray Ridge, Aklavik, Martin Creek, Husky and McGuire Formations which are regressive sequences. High TOC values occur in transgressive deposits of the Richardson Mountain and Husky Formations. Deltaic sediments of the Porcupine River Formation, in part equivalent to the Husky Formation, contain mostly type III OM.

- f. The Mount Goodenough and Arctic Red River Formations and the map unit

Kwr are low-energy shelf deposits with a wide range of TOC values. Type III OM is dominant in Lower Cretaceous strata; a mixture of type II and III OM in some samples is more typical of marine shale facies comprising parts of the succession.

- g. Variations in average TOC (1.4 to 4.9%) in the Eagle Plain Group may be related to local bathymetric highs and lows on the shelf or, alternatively, to significant input of terrestrial OM in a nearshore to inner shelf depositional environment.